The characterisation of low temperature tolerance in legumes.

James William Cooper

Submitted in accordance with the requirements for the degree of Doctor of Philosophy

The University of Leeds
School of Biology
Centre for Plant Sciences

August 2016

Declaration and Publications

The candidate confirms that the work submitted is their own, except where work which has formed part of jointly authored publications has been included. The contribution of the candidate to this work has been explicitly indicated below. The candidate confirms that appropriate credit has been given with the thesis where reference has been made to the work of others.

Chapter 1:

Foyer, C. H., Lam, H-M., Nguyen, H. T., Siddique, K. H. M., Varshney, R. K., Colmer, T. D., Cowling, W., Bramley, H., Mori, T. A., Hodgson, J. M., **Cooper, J. W**., Miller, A. J., Kunert, K. J., Vorster, J., Cullis, C., Ozga, J. A., Wahlqvist, M. L., Liang, Y., Shou, H., Shi, K., Yu, J., Fodor, N., Kaiser, B. N., Wong, F. L., Valliyodan, B., Considine, M. J. (2016). Neglecting legumes has compromised human health and sustainable food production. Nature Plants, 2. DOI:10.1038/nplants.2016.112

The candidate was responsible for the generation of figure 3 and contributed to the body of the review text.

Quain M. D., Makgopa, E. M., **Cooper, J. W.,** Kunert, K. J., Foyer, C. H. (2015). Ectopic phytocystatin expression increases nodule numbers and influences the responses of soybean (Glycine max) to nitrogen deficiency. Phytochemistry, 112, 179-187. DOI:10.1016/j.phytochem.2014.12.027

The candidate was responsible for the generation of the graphical abstract and contributed to the writing of the text.

Chapter 3:

Marquez-Garcia, B., Shaw, D., **Cooper, J. W.,** Karpinska, B., Quain, M. D., Makgopa, E. M., Kunert., K. J., Foyer, C. H. (2015). Redox markers for drought-induced nodule senescence, a process occurring after drought-induced senescence of the lowest leaves in soybean (Glycine max). Annals of botany,116(4). 497-510. DOI:10.1093/aob/mcv030

The candidate was responsible for the extraction of RNA and the generation of figures pertaining to the regulation of redox-related transcripts in drought exposed soybean crown root nodules.

Chapter 5:

Cooper, J. W., Dasgan, H. Y., Foyer, C. H. (2015). Understanding chilling tolerance in legumes. Aspects of Applied Biology, 124. 117-121.

The candidate was responsible for the generation of all data and figures within this publication.

Chapter 6:

Cooper, J. W., Wilson, M., Derk, M., Smit, S., Kunert, K. J., Cullis, C., Foyer, C. H. (2016). Application of short sequence reads provides improved genomic resources in faba bean (*Vicia* faba L.). Journal of Experimental Botany – submitted.

The candidate was responsible for the sequencing and assembly and interpretation and representation of all data.

Acknowledgments

Firstly I wish to thank my supervisor, Professor Christine Foyer, whose guidance and support have helped me to become a better scientist. I would also like to give a special thanks to Professor Karl Kunert, for helping to pioneer this project and for providing stimulating discussions over the past 4 years. Many thanks go to my industrial partner, Wherry and Sons Ltd, and to the BBSRC for funding this project. Thanks also to Peter Smith, whose foresight laid the foundation for this research.

I thank my Mother, Deirdre, and my Father, Graeme, for their love and support throughout my studies. They have always been available to provide advice on life, the universe and everything. I couldn't ask for better parents. I would also like to thank Adam Churchman, for his patience, understanding and unwavering support.

I thank Barbara Karpinska for helping me take my first steps in the lab. She taught me that with enough coffee and willpower you can master anything. I would also like to thank the other members of the Foyer lab, both past and present, for providing such a wonderfully diverse environment to work in. In particular I should mention my fellow PhD Students, Daniel Shaw and Ambra de Simone. My PhD journey would have been infinitely blander without them.

Special thanks go to Dr Mary O'Connell, Dr Sandra Smit and Martijn Derks for helping me to take my first fledgling steps into bioinformatics. Perhaps my biggest mention of gratitude goes to Dr Michael Wilson, who has been a friend, mentor and a general source of peace and knowledge. My understanding of bioinformatics has been due to his guidance and assistance. May the force be with you!

I thank my collaborators: Dr Jeremy Harbinson for his assistance in constructing the freezing chamber, Professor Christopher Cullis for his help with genomic sequencing, Dr Stefan van Wyk for his knowledge of legumes and Professor Yildiz Dasgan, who guided me through the subtleties of plant growth. I also thank Masters Student, Leila Beyouddh, who taught me how to be a better teacher and whose efforts have been so greatly appreciated.

Finally I wish to thank Grace Hoysted and the rest of the PhD group, as well as the Leeds University Union Sub-Aqua Club and my pub quiz group. Without them life would have been very boring indeed. Special thanks go to Jamie Bojko and Jack Goode for their limitless moral support.

Dedicated to my Nan, Doreen Cooper, who was never too old to be young.

Abstract

Legumes underpin the global food network, providing the majority of the world's dietary protein. However, global productivity of grain legumes is limited by environmental stresses, particularly chilling and freezing. For example, chilling temperatures (0-15 ºC) limit the production of soybean (*Glycine max*; a tropical legume), while extreme freezing temperatures (<0 ºC) limit use of temperate legumes such as faba bean (*Vicia faba* L). The following studies were performed to gain new insights into chilling and freezing tolerance in these two important legumes. Transgenic soybean lines, overexpressing the rice cysteine protease inhibitor, oryzacystatin I (OCI), showed decreased chilling-induced inhibition of photosynthesis compared to wild type (Wt). These lines also showed an increased abundance of transcripts encoding the strigolactone (SL) biosynthesis enzymes: carotenoid cleavage dioxygenases 7 and 8 (CCD7, CCD8). Pea (*rms3*, *rms4*, *rms5*) and *Arabidopsis thaliana* (*max2-1*, *max3-9*, *max4-1*) mutants, deficient in SL synthesis and signalling, showed enhanced sensitivity to dark-chilling. Differences in chilling and freezing sensitivity were also identified in 5 faba bean cultivars. Transcriptome profiling comparisons were performed on the most chilling sensitive (Wizard) and most chilling tolerant (Hiverna) cultivars to identify specific differences in gene expression, underpinning stress tolerance. Moreover, genome sequencing of the Wizard cultivar enabled the assembly and annotation of the mitochondrial and chloroplast genomes. Single nucleotide polymorphisms (SNP) were found in several organelle genes, when comparing read sequences to published references. Furthermore, based on published SNP orientated linkage maps, contiguous read sequences could be mapped to chromosomal loci, leading to the identification of 8 putative nuclear gene sequences and an increase in sequence length data at 147 loci. Together with these new genomic resources, the discovery that cysteine proteases, phytocystatins and SL are important in legume low temperature tolerance will enable the development of stress tolerance markers, for use in faba bean selective breeding programs.

.

Table of Contents

List of Abbreviations

°C – Degrees Celsius

Ca^{2+} - Calcium ion

CaM – Calmodulin

ROS – Reactive oxygen species

AFP – Antifreeze proteins

CBF – Cold binding factor

DREB – Dehydration responsive element binding factor

ERD – Early response to dehydration

COR – Cold responsive (genes)

GA – Gibberellic acid

BR – Brassinosteroids

CK – Cytokinin

ABA – Abscisic acid

ET – Ethylene

SA – Salicylic acid

JA – Jasmonic acid

SL – Strigolactone

LHC – Light harvesting complex

PET –Photosynthetic electron transport

MET – Mitochondrial electron transport

NADH – Nicotinamide adenine dinucleotide

NADPH – Nicotinamide adenine dinucleotide phosphate

ROS – reactive oxygen species

UV - Ultraviolet

CDPK – Calcium dependent protein kinase

CRT/DRE – C-repeat/dehydration responsive element

PQ – Plastoquinone

PC-Plastocyanin

ATP – Adenine triphosphate

FD – Ferrodoxin

FNR – Ferrodoxin-$NADP^{+}$ reductase

RuBisCO – Ribulose-1,5-bisphosphate carboxylase/oxygenase

OCI – Oryzacystatin I

CP – cysteine protease

NFR –Nodulation factor receptor

MATK – Maturase K

P_i – Inorganic phosphate

Da – Dalton

kDA – Kilodalton

PCD – Programmed cell death

RNA – Ribonucleic acid

DNA – Deoxyribonucleic acid

PolyA – Polyadenylated

C_T – Thermocycle number

MS – Murashige and Skoog

SL – Strigolactone

Wt - Wild type

CO_2 - Carbon Dioxide

Col-0 - Colombia-0

EMS - Ethyl methanesulphonate

CCD7 – Carotenoid cleavage dioxygenase 7

CCD8 – Carotenoid cleavage dioxygenase 8

µmol – Micromoles

µM - Micromolar

cm – Centimetre

m – Metre

s – Second

h – Hour

µl – Microliters

ml – Millilitres

l – Litres

g – Gram

g – Gravity (units of)

V – Volts

v/v – Volume/Volume

bp – Base pairs

List of tables

List of figures

Chapter 1

Chapter 2

Chapter 3

Chapter 4

Chapter 5

Chapter 6

Chapter 7

Chapter 8

“Look deep into nature, and then you will understand everything better.”

-Albert Einstein

1. Introduction

1.1. Low temperature stress

Plants are sessile organisms that are constantly subjected to changes in their environment. When a plants environment prevents it from fulfilling its genotypic potential, it is considered to be under stress (Osmond et al., 1987; Kranner et al., 2010). To survive stress, plants must alter their biological processes in accordance with environmental change (Qin et al., 2011). Their ability to alter both metabolism and biochemical makeup is dependent on their underlying genetic composition. Thus, stress acts as a major component for selection, with stress tolerance being the product of a plants evolutionary history (Wassink and Stolwijk, 1956).

Stresses can be classified as biotic or abiotic. Biotic stresses are biological factors which act to inhibit an organism's functionality, for example the activities of pathogens and herbivores (Atkinson and Urwin, 2012). Abiotic stresses include passive environmental factors such as extreme temperatures, poor water availability and nutrient deficiency (Mahajan and Tuteja, 2005). Stress exposure is the major limiting factor to agricultural productivity, with more than 50% of projected yield loss in crops being attributed to abiotic stress (Boyer, 1982; Wang et al., 2003). Moreover, abiotic stresses such as low temperature limit the agricultural distributions of key crop species, such as soybean (Van Heerden et al., 2003).

Low temperature is a collective term, incorporating two distinct but related stresses - chilling and freezing. Chilling temperatures fall in the range of 0 – 15 ºC, while freezing temperatures are below 0 ºC. While there is some commonality between the metabolic impact of chilling and freezing, their physiological impacts differ. However, both chilling and freezing can have extremely harmful effects on plant functions (Thomashow, 1999). Those plant species unable to withstand exposure to chilling are referred to as "chilling sensitive", while plants unable to withstand freezing temperatures are referred to as "freezing sensitive". The sensitivities of plants to low temperatures are broadly correlated with their agro-environmental distribution. For example, plants of temperate zone origin may exhibit chilling injury in the 0 – 4 ºC range and have varying degrees of freezing tolerance. However plants of tropical origin will exhibit signs of chilling induced injury at a much higher temperature range of 8 - 12 ºC, and have no inherent capacity to withstand freezing exposure (Lyons, 1973).

1.2. Low temperature stress: damage, perception and transduction

Several visual symptoms of chilling injury are exhibited by sensitive plant species. The most noticeable of these is the wilting of aerial organs, resulting from reduced water retention capacity. This is attributed both to cytoplasmic thickening in leaves and inhibited water uptake by the roots (Lukatkin, 2005). The appearance of leaf surface lesions is also characteristic of chilling sensitive plant species. Moreover, prolonged chilling exposure can cause accelerated ageing that is characterised by a loss of leaf colouration. Ultimately the prolonged exposure of sensitive plant species to chilling stress results in tissue necrosis or plant death (Figure 1.2-1; Lukatkin et al., 2012). However, the processes underpinning the initiation and regulation of programmed cell death are not yet fully understood (Van Durme and Nowack, 2016).

Freezing occurs in plants when they cannot avoid nucleation – the process whereby water molecules come together to form a stable ice nucleus. Ice crystal nucleation is unlikely to occur spontaneously, with the homogenous nucleation of pure water occurring only at extremely low temperatures (-38.5 C; Franks, 1985). However, homogenous nucleation is more likely to occur in moist climates (Pearce, 2001). The catalysed formation of ice crystals (heterogeneous nucleation) is facilitated by the production of nucleating agents, which comprise of various organic and inorganic molecules. These nucleating agents are either extrinsic to the plant, stimulating ice crystal formation on its surface, or they localise nucleation to the extracellular spaces. However, following the formation of extracellular ice, subsequent freezing exposure leads to intracellular ice formation (Figure 1.2-1). When ice is formed in the intracellular spaces the result is cell death (Pearce, 2001). This can be attributed to a number of causes, for example: large ice masses affecting tissue or organ structure, opportunistic pathogen infection through ice induced lesions, or ice-encasement resulting in secondary hypoxic stress (Pearce, 2001). Moreover the formation of extracellular ice can lead to cellular dehydration, attributed to the difference in water potential between liquid water and ice. Freeze-induced dehydration can cause plasma membrane phase-transition and additional mechanical stresses, leading to electrolyte leakage and a loss of cell compartmentation (Pearce, 2001; Yamazaki et al., 2009).

Every cellular compartment is affected by low temperature exposure. Moreover, membrane bilayers themselves are directly affected by chilling and freezing exposure. Indeed, temperature-dependent changes in bilayer structure are believed to be essential to the perception and transduction of temperature information (Murata and Los, 1997). Upon exposure to chilling membrane bilayers undergo a reduction in fluidity. Membrane fluidity is used to describe molecular motion within the bilayer, with reduced fluidity being attributed to the unsaturation of membrane lipids (Murata and Los, 1997). Loss of fluidity can result in a phenomenon known as leakage – the loss of essential

solutes from the plant cell, indicating a loss of the membranes semi-permeable nature. However, when membrane fluidity is reduced the altered physical state of the membrane may also regulate the conformation and activity of bound proteins, such as calcium ion channels (Los and Murata, 2004). This has been proposed to enable the transduction of temperature perception to the nucleus via calcium ion influx (Ca^{2+}). Thus the plasma membrane itself it thought to act as a "biological thermometer", playing an integral role in the plant temperature-sensing machinery (Los and Murata, 2004).

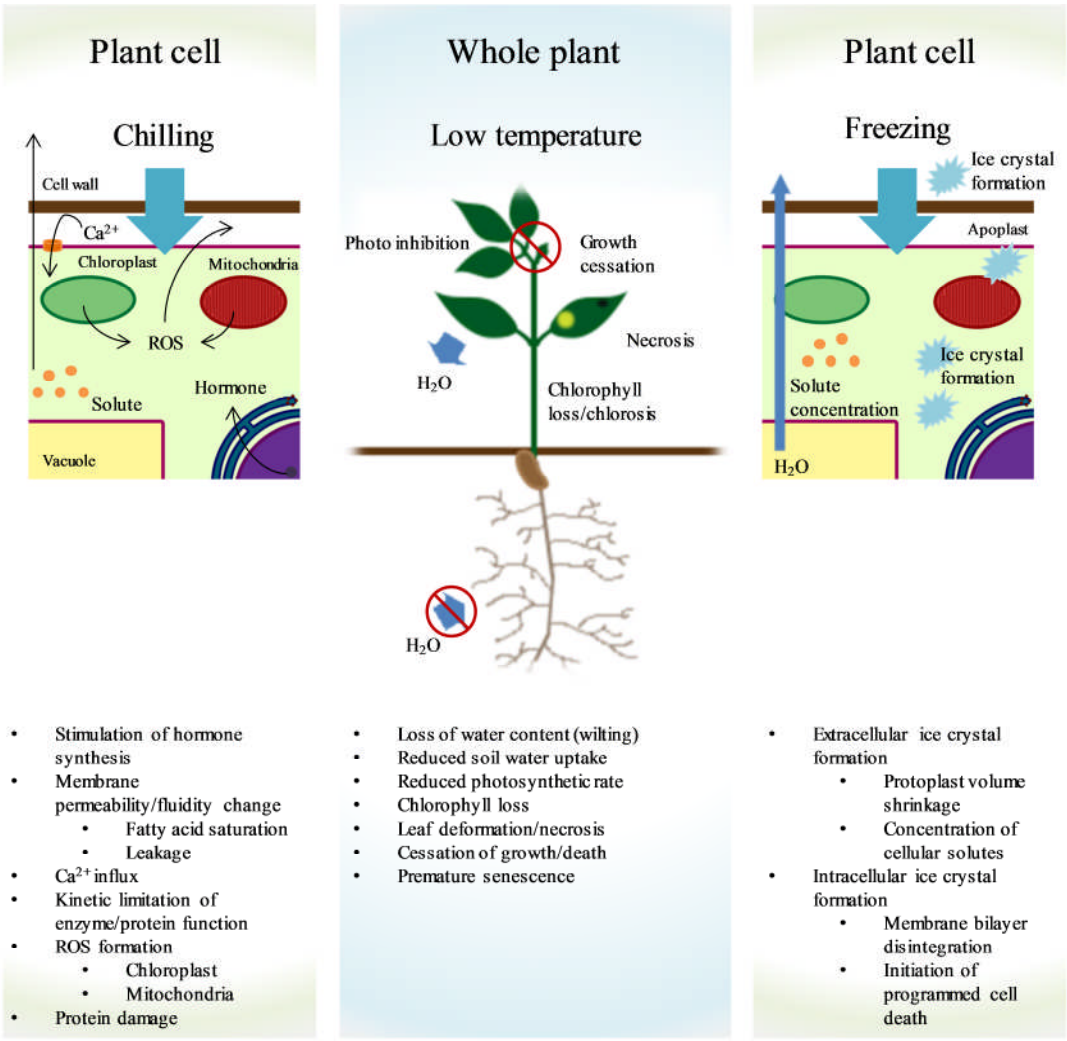

Figure 1.2-1: The impact of chilling and freezing stress on cellular function and plant physiology. Chilling stress induces the formation of reactive oxygen species (ROS) in cellular organelles, promotes stress hormone biosynthesis, alters membrane permeability, facilitates the influx of calcium ions (Ca^{2+}), kinetically limits cellular enzymes and proteins, and causes changes to protein conformation/induces protein damage. Freezing stress may either cause extracellular ice crystal formation, thereby creating a difference in water potential leading to cellular dehydration and increased solute concentration, or cause intracellular ice crystal formation leading to direct disintegration of membrane bilayers. Both chilling and freezing may lead to a loss of plant water content through reduced soil water uptake and/or increased transpiration, reduced photosynthesis, chlorophyll loss, leaf deformation and/or necrosis, cessation of growth, premature senescence or programmed cell death.

An increase in cytoplasmic Ca^{2+} is essential to the low temperature signalling cascade. While the mechanisms of Ca^{2+} influx are not fully understood, (Carpaneto et al., 2007), down-stream receptors have been classified. Increased Ca^{2+} concentration is detected by receptors such as calmodulin (CaM), calcineurin-B-like proteins and calcium dependent protein kinases (Yang et al., 2010). These in turn are upstream of the plant-stress response. The influx of Ca^{2+} from both apoplastic and intracellular storage spaces is facilitated by proteins encoding for numerous channels, pumps and transporters. The routes of entry for Ca^{2+} into the cytosolic space are numerous, and whilst many facilitating proteins have been putatively characterised on the molecular level, few channels have been physiologically characterised. However it has been found that some calcium transport proteins are responsive to the presence of reactive oxygen species (ROS; Hetherington and Brownlee, 2004). As such ROS signalling is another component of the low temperature signalling network.

The presence of ROS is central to the transduction of stress (Suzuki and Mittler, 2006). ROS are a natural by-product of oxygen metabolism, playing essential roles in cell signalling and homeostasis. However ROS are highly chemically active and perturbations to the reduction-oxidation balance of a cell (redox homeostasis) can lead to ROS accumulation and subsequently cell damage. This is known as oxidative stress. ROS are the result of partial reduction of atmospheric O_2, forming a superoxide radical ($O_2^{\cdot-}$), hydrogen peroxide (H_2O_2) or a hydroxyl radical ($HO^{\cdot}$). O_2 can also be excited to form singlet oxygen ($^1O_2$) where a valance electron moves to a high energy state via photonic energy transfer (Mittler, 2002). Singlet oxygen is the most chemically active form of reactive oxygen. In the absence of cellular redox control mechanisms ROS would uncontrollably oxidise all components of the cell, resulting in a range of destructive effects such as; disintegration of the lipid bilayer, RNA destabilisation and protein damage (Schmidt and Kunert, 1986). In plants, ROS are produced primarily at the photosynthetic electron transport chain (PET) with photosystems I and II being the major sites of production for O_2^1 and $O_2^{\cdot-}$. The mitochondrial electron transport chain (MET) also acts as a site for the generation of $O_2^{\cdot-}$ with the specific sites being complex I (NADH dehydrogenase), complex II (reverse electron flow) and the ubiquinone-cytochrome region of complex III (Gill and Tuteja, 2010). ROS are also formed at the plasma membrane through the activities of NADPH oxidase, the cell wall (via cell wall associated peroxidases), the apoplast (via cell wall associated oxalate oxidase) and in the peroxisome (xanthine oxidase; Hasanuzzaman et al., 2009). Despite their destructive potential, ROS primarily act as secondary messengers and regulate a range of cellular processes. Therefore the tight regulation of redox state is essential in ensuring that ROS function to correctly regulate, rather than inhibit plant cell function (Mittler et al., 2004).

Chilling sensitive plant species are unable to withstand prolonged exposure to low temperatures. However, tolerant species are able to activate suites of protective genes through the effective translation of perceived environmental change into cytosolic signals, generally via Ca^{2+} and ROS

dependent pathways. The process whereby a plant acquires tolerance to a given stress is known as acclimation, with acclimation to chilling and freezing temperatures (sometimes referred to as hardening) being dependent on an earlier period of exposure to chilling (Penfield, 2008). Tolerance to low temperatures is the result of three distinct cellular events; the initial perception of low temperature, the transduction of temperature sensing, and the induction of protective genes (Winfield et al., 2010). While gene induction is primarily attributed to Ca^{2+} and ROS, the non-specific nature of these signals makes the presence of specific parallel signals likely (Monroy et al., 1998; Mahajan and Tuteja, 2005).

1.3. Low temperature gene induction: acclimation and vernalization

Cold-response genes encode many proteins that act to protect the plant, either directly or through acting as transcription factors (Riechmann et al., 2000). Encoded proteins include: enzymes that are linked to cellular respiration and carbohydrate metabolism, lipid synthesis and stability, phenylpropanoid and antioxidant pathways, molecular chaperones, antifreeze proteins (AFP) and proteins linked to dehydration (Chinnusamy et al., 2003). These genes play an essential role in the plant acclimatory response to cold (Figure 1.3-1).

Numerous cold-response factors and genes have been identified in *Arabidopsis thaliana*, many of which are dependent on Ca^{2+} signal transduction via kinases (Knight et al., 1996). In *A. thaliana* the kinases responsible for Ca^{2+} signalling belong to the CDPK/SNF1-related kinase family, a unique family that couples calcium sensing with direct kinase binding (Sanders et al., 2002). These kinases may act directly, or feed into mitogen-activated protein kinase cascades (Sinha et al., 2011). Thomashow (1999) demonstrated that the *A. thaliana* CRT/DRE regulon is calcium responsive and enhances freezing tolerance, playing a central role in the acclimatory response. This transcription factor binds to the cold binding factor (CBF) drought responsive element binding factor (DREB) (Kasuga et al., 1999), responsible for the regulation of; cold responsive genes (*COR*), early response to dehydration (*ERD*) genes and presumably unidentified cold-regulated gene families (*XYZ*). Taken together these form the cold binding factor regulon (CBF) (Thomashow, 2001; Figure 1.3-1).

The genes responsible for low temperature acclimation are also involved in drought response, highlighting the often shared nature of stress responses (cross-talk). CBF induced genes act to protect plant function at low temperature, though the mechanisms of protection have not yet been fully elucidated. This is with the exception of the *COR15a* gene which is targeted to the chloroplastic stroma and is believed to prevent deleterious lipid phase shift upon freezing (Artus et al., 1996). There is also evidence to suggest that the activation of *CBF* genes leads to the sustained transcription

and subsequent translation of other *CBF* family members, notably in the case of *ERD10* and *CBF/DREB* (Kim and Nam, 2010). Additional factors have been identified that act to regulate *CBF/DREB*; these are the ICE1 transcription factor (Inducer of CBF Expression 1) and the sensitive to freezing mutants (*sfr*). Constitutive expression of ICE1 has been shown to enhance freezing tolerance in *A. thaliana* through interaction with the *CBF* regulon (Chinnusamy et al., 2003), whilst *sfr* mutants have shown an increase in freezing sensitivity. The genomic identities of the *sfr* mutants have not been resolved in full, though identified mutants have been shown to play various roles in sugar metabolism (Amid et al., 2012; Thorlby et al., 2004). Additionally it is thought that *SFR* genes may act to regulate *CBF/DREB* elements, or *COR/ERD* genes directly (Thomashow, 2001).

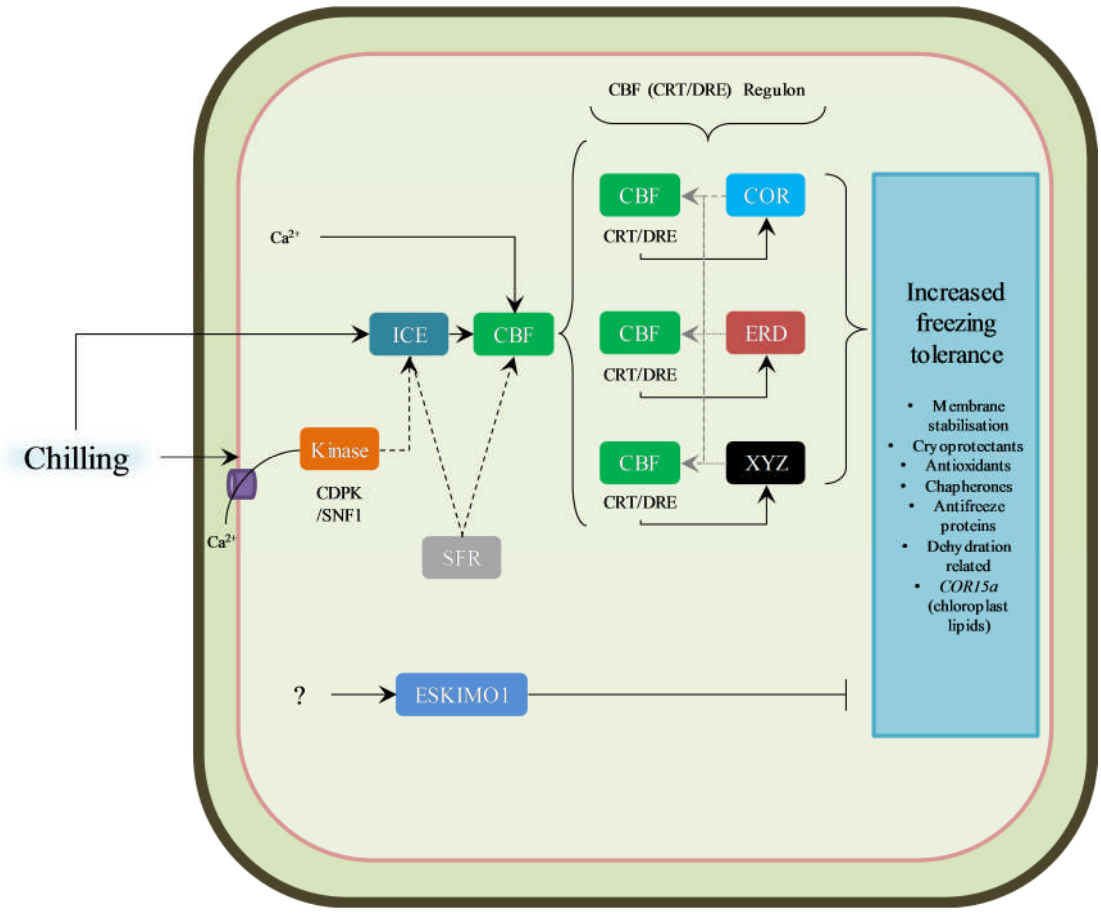

Figure 1.3-1: Schematic representation of the *Arabidopsis thaliana* cold acclimation pathway, derived from Thomashow, (2001) and Xin and Browse, (2000). Chilling exposure causes the rapid induction of CBF/DRE genes, including the Cold Responsive genes (COR), Early Response to Dehydration genes (ERD) and probably undiscovered genes (XYZ). The activation of COR, ERD and XYZ may cause a positive feedback, stimulating the continued expression of the CBF regulon (grey dashed arrows). The activation of the CBF regulon is likely to be downstream of a calcium activated kinase cascade, though calcium may activate the CBF regulon independently of kinases. Chilling temperatures are thought to activate the Inducer of Cold Expression (ICE) transcription factor, or its interacting partners. SFR mutants display increased sensitivity to low temperatures and are thought to act between CRT/DRE transcription and the induction of CBF genes. Mutants of the ESKIMO1 gene have shown increased chilling sensitivity, thus ESKIMO1 is thought to be a negative regulator of low temperature acclimation.

Taken together, the *CBF/DREB* regulatory elements would seem to act as master integrators of the acclimation response in *A. thaliana*. However Xin and Browse (1998) described a cold acclimation gene, *ESKIMO1*, that appears to act independently of the *CBF* regulon. In mutant lines of *ESKIMO1* the accumulation of proline and increase of dehydrin associated transcripts was observed, thus the gene is thought to act as a negative regulator of acclimation. In a proteomic analysis of acclimated cultivars of red clover (*Trifolium pratense* L.), acclimated plants were found to have an increased abundance of vegetative storage proteins (necessary for plant regrowth) and dehydrins –a group II late embryogenesis abundance protein family member that are required for the survival of dehydration, though their current mechanisms are unknown (Bertrand et al., 2016). The acclimatory response pathways found in *A. thaliana* appear to be conserved in other plant species, including tomato and wheat (Jaglo et al., 2001). *CBF/DREB* family genes are also found in soybean, though there is an apparent inability of soybean *CBF*s to regulate downstream gene expression (Yamasaki and Randall, 2016). The regulation of the genetic elements responsible for cold tolerance is multifactorial, with the roles of many identified elements yet to be characterised. Moreover, while some effort has been made to translate studies into soybean, there is still progress to be made in the understanding of the genetic basis of acclimation in legumes as a plant family. However, there is potential for the identification of novel genes and regulatory factors that have not been identified in the well-studied *A. thaliana* model (Calzadilla et al., 2016).

Broadly, plants will aim to regulate their growth and development to maximise reproductive success. This is dependent on perception of environmental conditions and retention of this information. For example many plants depend on a prolonged period of exposure to cold in order to transition from vegetative growth to flowering – a process known as vernalization (Sheldon et al., 2000). Vernalisation is a multifactorial process, reliant upon a plants ability to perceive both photoperiod and temperature in relation to developmental stage. Vernalization is a metabolically active process and as such freezing temperatures are ineffective for its initiation (Kim et al., 2009). The molecular basis of vernalization in *A. thaliana* (in which flowering is best characterised) is dependent on many genes. Flowering itself results from the induction of floral meristem identity genes, i.e. the MADS-box family of transcription factors which are conserved in the plant kingdom (Smaczniak et al., 2012). Upstream of the floral meristem identity genes are floral integrators – FD (a bZIP transcription factor), FT (FLOWERING LOCUS T) and SOC1 (SUPPRESSOR OF CONSTANS 1) (Abe et al., 2005; López-González et al., 2014). Floral integrator expression is regulated by flowering pathways, themselves responsive to environmental conditions (photoperiod/cold) or developmental cues such as gibberellic acid (GA). Whilst flowering is dependent on the coordination of all associated pathways, the FLC clade of genes (FLOWERING LOCUS C) has been identified as a major factor in development. FLC acts antagonistically to floral integrator genes, however it demonstrates a low temperature-dependent down regulation which is attributed to the initiation of the flowering response

(Sheldon et al., 2000). Studies of flowering in cereal grains have shown a high degree of conservation in the vernalization pathway, whilst legumes show some degree of evolutionary divergence.

Crop legumes are divided between two sister clades; the phaseoloid and the galegoid (Foyer et al., 2016). These clades represent temperately adapted long day plants (galegoid) and tropically adapted short day plants (phaseoloid). Whilst studies of vernalization in legumes are comparatively limited, two models have emerged for each lineage – pea (*Pisum sativum*), representing temperate legumes and soybean (*Glycine max*) representing tropical legumes (Weller and Ortega, 2015). Although the genes and gene families central to flowering time are largely conserved between legumes and *A. thaliana*, there are numerous examples of gene duplication and loss. For example legumes lack the *phyC* clade of photoreceptor genes, having only three phytochromes for the detection of day length (phyA, phyB and phyE (Hecht et al., 2007). With regards to the flowering locus gene family, *FT/TFL1*, both clades show gene family expansion, with the galegoid clade showing two distinctly divergent sequences from *A. thaliana*. Interestingly the *FLC* clade, shown to be critical in the *A. thaliana* flowering response, is apparently absent among galegoid legumes and soybean. These data indicate that within the legume family there are fundamental differences with regards to the initiation of flowering and the perception of light and temperature.

1.4. Cold associated hormone signalling

Stress induced changes in gene expression may participate in the generation and regulation of plant hormones (Mahajan et al., 2005). Moreover, hormones themselves can regulate gene expression through a complex interaction of molecular circuits. Cold adaptation requires transcriptional reprogramming and it is hypothesised that growth suppression allows for the reallocation of resources to tolerance development and maintenance (Eremina et al., 2016). Suppression of growth is induced by plant hormones – low molecular weight compounds that signal information from their site of synthesis to their site of action. Homeostasis is maintained through the biosynthesis, catabolism and transport of plant hormones, with sensitivity being determined by the presence and responsiveness of specific hormone receptors (Eremina et al., 2016). Hormone action in response to low temperature stress is influenced by cross-talk with signalling cascades, initiated as a result of other environmental stimuli and developmental phase transition cues (Penfield, 2008; Franklin, 2009). The role of hormones in the cold tolerance response is not well characterised and species-specific differences in hormonal roles are common. However general roles have been identified for the major classes of phytohormone (Eremina et al., 2016), which are discussed here.

Gibberellic acid (GA) is associated with cell elongation and division. It is synthesised from trans-gerenylgerenyl diphosphate in the methylerythritol phosphate pathway (MEP) (Hedden and Thomas, 2012). The regulation of GA is attributed to the activity of DELLA-domain proteins (Schwechheimer, 2012) which themselves are regulated by the 26S proteasome. There is evidence for CBF's repressing GA in response to cold. Moreover DELLA knockout mutants of *A. thaliana*, inhibited in their ability to degrade GA, were more sensitive to freezing exposure than controls (Achard et al., 2008).

Brassinosteroids (BR) are campesterol derived hormones with roles in cell division and expansion, xylem differentiation, seed germination, vegetative growth and apical dominance (Sasse, 2003). Their synthesis is dependent on the activities of cytochrome p540s. BRs interact closely with GA and act to promote growth, with BR and GA acting on each other's biosynthesis (Unterholzner et al., 2015; Stewart Lilley et al., 2013). However, there is no evidence of a BR-GA synergism in response to low temperature exposure. BR has been shown to be a positive regulator of the cold tolerance response with ectopic expression leading to enhanced tolerance in sensitive species (Xia et al., 2009; Jiang et al., 2013). Moreover, *DWARF4* and *CONSTITUTIVE PHOTOMORPHOGENESIS AND DWARFISM* (*CPD*) overexpression led to enhanced chilling tolerance in *A. thaliana* with an accumulation of the COR15a transcription factor and promoted *CBF* gene expression (Divi and Krishna, 2010; Kagale et al., 2007). However earlier studies of BR activity have shown a reduced cold tolerance or no change in tolerance in response to increased BR abundance. Thus further verification of BRs roles is needed (Eremina et al., 2016).

Auxin is a well characterised, tryptophan-derived phytohormone (Mashiguchi et al., 2011). However, the roles of auxin in cold stress remain to be elucidated. Auxin regulated genes are affected by cold exposure in both *A. thaliana* and rice, with the application of auxin analogues leading to an increase in cryoprotective metabolites in brassicas (Hannah et al., 2005; Jain and Khurana, 2009; Gaveliene et al., 2013). Bioactive auxin (indole acetic acid, IAA) has been correlated with enhanced low temperature tolerance (Du et al., 2013). Moreover, low temperature exposure has been shown to block auxin cycling through impairment of PIN2 and PIN3, inhibiting root gravitropic responses in *A. thaliana* (Shibasaki et al., 2009).

Cytokinins (CK) are adenine derivatives with aromatic or isoprenoid side chains. They control directional growth, such as gravitropism and are known to interact with auxin (Mok and Mok, 2001). The most abundant plant cytokinins are isopentyladenine and zeatin (Sakakibara, 2006), the external application of which has been shown to enhance *A. thaliana* freezing tolerance (Jeon et al., 2010). However CKs have also been shown to be down regulated in response to cold, thus providing evidence for cold tolerance models where CKs are both positive and negative regulators (Maruyama et al., 2014).

Abscisic acid (ABA) is an isoprenoid hormone that plays a central role in seed dormancy, abscission and abiotic stress signalling (Nakashima et al., 2014). Accumulation of ABA is correlated with increased freezing tolerance. Recent evidence has emerged showing that MYB96, an ABA transcription factor, is cold-induced and controls CBF induction (Lee and Seo, 2015). Further evidence suggests a role for MYB96 in HEPTAHELICAL PROTEIN (HHP) activity. HHP in turn interacts with ICE1, ICE2 and CAMTA. Thus MYB96 would interact with all CBF family members, possibly acting as a central regulator for low temperature tolerance (Lee and Seo, 2015; Chen et al., 2010), though further evidence for this is needed.

Ethylene (ET) is a gaseous hormone synthesised from methionine. The role of ET in the cold response is not yet clear, with evidence supporting its conference of both sensitivity and tolerance (Tian et al., 2011; Zhang et al., 2009). However current models suggest that is it a negative regulator of tolerance (Eremina et al., 2016). Decreases in ET are attributed to decreased biosynthesis (Catala et al., 2014), though cold responsive abundance is species specific (Ciardi et al., 1997; Kosová et al., 2012; Guo et al., 2014). In *Medicago truncatula* ET application reduced freezing tolerance, whereas biosynthesis inhibition promoted tolerance (Shi et al., 2012; Zhao et al., 2014). Whilst the role of ET is currently unclear current evidence suggests that it restricts plant growth in response to low temperature exposure.

Salicylic acid (SA) is a phenolic compound associated with low-temperature induced growth retardation. SA is causative of the hypersensitive response (HR) and leads to the formation of necrotic lesions (Rivas-San Vicente and Plasencia, 2011). A chorismate derived phytohormone (Chen et al., 2009), cold has been shown to induce SA content in plant species (Dong et al., 2014; Kim et al., 2013; Huang et al., 2010). However the mechanisms of cold-induced SA biosynthesis are unknown. Low SA levels in plants treated with L-α-aminooxy-β-phenylpropinoic acid (AOPP) had suppressed expression of CBFs and COR47 in low temperature treatment of cucumber. Low SA correlated with reduced photosynthetic activity and increased membrane damage (Dong et al., 2014). However SA has apparent species-specific effects, with no evidence of SA influencing photosynthetic efficiency in *A. thaliana* (Scott et al., 2004).

Jasmonic acid (JA) is an oxylipin involved in biotic and abiotic stress responses. Cold exposure increases JA levels in plant species such as rice and *A. thaliana*. This increase is associated with an increase in JA biosynthetic genes and a repression of genes linked to JA catabolism. JA is synthesised from linolenic acid and is activated by isoleucine conjugation, enabling binding to an F-box receptor – COI1 (CORONATINE INSENSITIVE 1). COI1 initiates JA signalling by ubiquitinating and stimulating proteasome dependent degradation of JASMONATE ZIM DOMAIN (JAZ) proteins,

which repress expression of JA responsive genes. In *A. thaliana*, JA application enhanced induction of CBFs and CBF regulated genes, promoting freezing tolerance (Hu et al., 2013). Moreover, JA compromised plants were more sensitive to freezing. JA mediated growth suppression occurs through DELLA protein stabilisation, therefore cold induced JA accumulation may contribute to plant growth suppression through GA crosstalk (Kosová et al., 2012; Schwechheimer, 2012).

The roles of phytohormones in low temperature-tolerance responses are diverse, varying in a species dependent manner. However, while the general roles of the major phytohormone classes have been explored in the literature, the influence of each of these hormones on cold-stress adaptation is likely to be species specific.

1.5. Mechanisms of protection from low temperature stress

As poikilothermic organisms the temperature of plants is at equilibrium with their environment. However there are exceptions whereby plants may raise the temperature of specific systems above ambient. For example the sacred lotus (*Nelumbo nucifera*) may raise its floral temperature through the alternative oxidase pathway (Watling et al., 2006). Optionally plants may lower organ temperature through transpirational cooling, as seen in *Arabidopsis thaliana* leaves when grown at high temperature (Crawford et al., 2012). Generally, plants are dependent upon environmental cues such as temperature and day length for developmental transition. The perception of environment is also essential for stress tolerance, where the detection of stressful environmental conditions (biotic or abiotic) is crucial for the initiation of defensive pathways. The plant-temperature response can be divided into three separate events; temperature perception, signal transduction and response induction (Ruelland and Zachowski, 2010).

Following the transduction of low-temperature and the induction of cold-responsive genes and hormones, plant cells adjust their chemical composition to protect against the negative effects of low temperatures (Sanghera et al., 2011). The dominant constraints placed on plants by chilling are: reduced water uptake, lower enzymatic rate and decreased membrane stability. As such cold-induced genes act to protect water status through the production of soluble osmolytes which prevent the osmotic movement of water from within the cell (Warren, 1998). Reduced enzyme activity places inherent restrictions on growth rate through decreased photosynthetic efficiency (Kingston-Smith et al., 1997; Du et al., 1999; Figure 1.5-1). Moreover the speed at which toxic cellular elements, such as ROS, can be processed is decreased (Lee and Lee, 2000). To mitigate the accumulation of ROS, plants may increase the abundance of enzymatic and non-enzymatic antioxidant components such as: superoxide dismutases, specific peroxidases, ascorbate and glutathione reductases (Lee and Lee,

2000). This is essential at the PET and MET where uncontrolled ROS production, particularly of singlet oxygen at the PET, can result in reduced efficiency or destruction of cell machinery (Jaleel et al., 2009). However it is essential to note that ROS production is integral to cellular function, acting either in signalling or in the regulation of enzymes like RuBisCO (Figure 1.5-1; Moreno et al., 2008). As such increased antioxidant production is not required for the elimination of ROS, but for the fine balancing of redox state (Baxter et al., 2014).

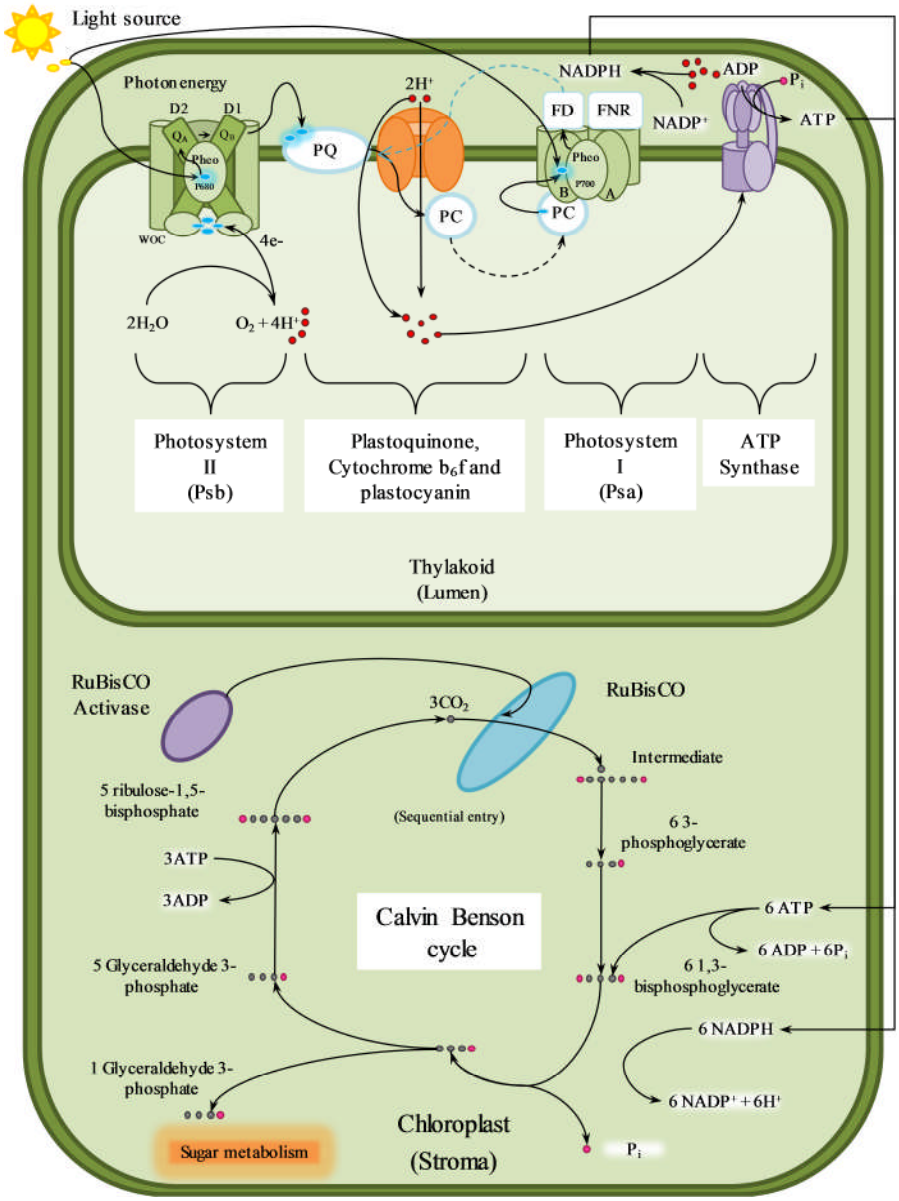

Figure 1.5-1: Schematic representation of a chloroplast, showing the reactions underpinning C3 photosynthesis. The light dependent reactions of the thylakoid are shown, detailing the excitation of electrons at PSII by photons and the subsequent transfer of high energy electrons to cytochrome b6f and PSI, ultimately driving the synthesis of ATP and NADPH. The light independent reactions of the chloroplast stroma are also shown (Calvin Benson cycle), detailing the enzymatic reactions required for the fixation of atmospheric CO2 into the sugar precursor – glyceraldehyde 3-phosphate.

There is some overlap between chilling and freezing protection, with genes acting to confer tolerance to chilling also conferring tolerance to the effects of freezing. For example the osmolytes that increase cellular water potential will also increase the freezing temperature of the cell (Warren, 1998). These soluble factors may also act as nucleation points, directing ice crystal formation to the extracellular spaces of the plant cell or presenting on the outer surface of the plant. The process whereby cytoplasm thickens and the osmotic potential of plant cells is increased is referred to as vitrification (the acquisition of a "liquid glass" state). Vitrification is thought to be responsible for the extreme low temperature tolerance demonstrated by tree species, such as poplar (Pearce, 2001).

1.6. Stress induced protein turnover

The growth and development of plants occurs as a result of the balance between protein synthesis and degradation. Protein degradation is essential in processes such as germination, cell biogenesis, senescence and programmed cell death (Palma et al., 2002), and is carried out by proteolytic enzymes called proteases. These can act at the terminus of a polypeptide chain (exopeptidases) or within a chain (endopeptidases; González-Rábade et al., 2011). Proteolytic enzymes in plants are divided into four classes: serine proteases, aspartic proteases, metallo-proteases and cysteine proteases (van der Hoorn, 2008). In addition to their roles in development, proteases are essential to plant stress tolerance. Their abundance and activity is central to both the degradation of aberrant proteins and the subsequent provision of amino acids for protein synthesis (Vierstra, 1996). Moreover, the redox state of cellular compartments has been shown to regulate both proteases and protein kinases. For example, redox controlled thylakoid protein kinases allow the exposure of dephosphorylated photosynthetic Light Harvesting Complex II (LHCII) proteins to acclimative proteolysis (Yang et al., 2001).

Cysteine proteases (CPs) are redox responsive proteases, possessing a redox-active thiol group on the cysteine residue of their active site. As such their activity is highly responsive to their redox environment (Wang et al., 2012). CPs are essential to plant development and stress related protein turnover (Toyooka et al., 2000). They are induced in response to biotic stress factors such as fungal infiltration, but their abundance also increases in response to biotic stresses such as wounding, drought and low temperature (Harrak et al., 2001). There are currently thought to be 140 cysteine proteases in plants, belonging to 15 families and 5 clans, with each having a distinct structure (van der Hoorn, 2008).

Together with biochemical environment, the activity of cysteine proteases is regulated by the presence or absence of dedicated inhibitors called cystatins (Benchabane et al., 2010). Cystatins constitute a large super-family of proteins, ranging in size from 5->25 kDa (Figure 1.6-1). Analysis of

the structural biology of the first characterised cystatin, chicken egg white cystatin, and the first characterised plant cystatin, oryzacystatin I (OCI), has shown their functional biology to be highly similar, with both proteins containing multiple sites for the inhibition of protease activity (Kiggundu, 2008; Benchabane et al., 2010). OCI was originally derived from the seeds of rice (*Oryza sativa* L.) in the work of Abe et al., (1987). It acts to inhibit the activity of the papain-like cysteine proteases – the most numerous family of cysteine proteases (Arai et al., 1991).

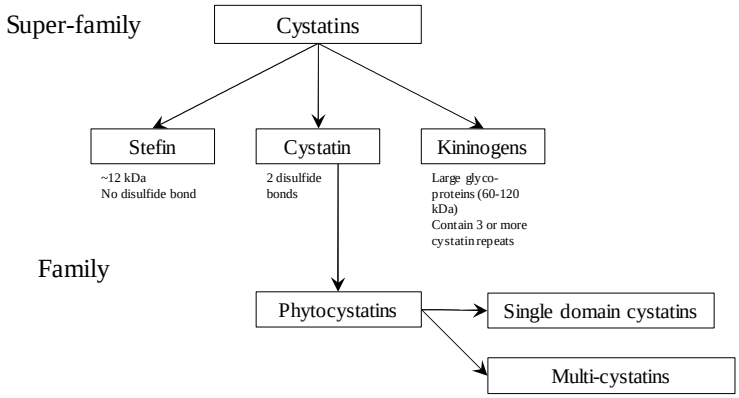

Figure 1.6-1: General classification of the cystatin super-family. Phytocystatins are grouped as members of the cystatin family containing single and multiple domain cysteines. Adapted from Kiggundu, (2008).

The three-dimensional structure of OCI shows the main body to consist of an α-helix and a five-stranded antiparallel β-sheet (Nagata et al., 2000). The inhibitory action of OCI is dependent on the action of a primary cystatin loop structure that directly inhibits the active site of papain and papain-like proteases (Figure 1.6-2).

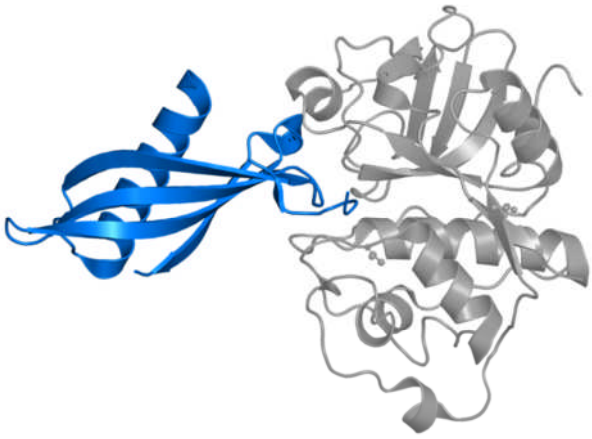

Figure 1.6-2: The complex structure of tarocystatin (*Colocasia esculenta*) and papain, showing the inhibition of the papain active site (grey) by the conserved cystatin loop structure (blue). Derived from Chu et al., (2011).

Protease inhibitors regulate many metabolic functions, and can suppress programmed cell death (PCD) triggered by oxidative stress (Levine et al., 1999). Like their cysteine proteinase targets, cystatins are also regulated by developmental and environmental cues (Belenghi et al., 2003). Moreover, their expression has been shown to enhance tolerance to a range of biotic and abiotic stresses. For example cystatins were shown to be differentially regulated in maize plants in response to cold stress and drought (Massonneau et al., 2005). Additionally the constitutive expression of cysteine protease inhibitors in *A. thaliana* has been shown to confer protection against oxidative stresses, salt stress, drought and cold stress (Tan et al., 2014; Zhang et al., 2008). As such, phytocystatins have been highlighted as having the potential to improve agronomic traits in crop species, with a particular focus on legumes (Kunert et al., 2015).

1.7. Legumes

Grain legumes (also known as pulses, including: pea, bean, chickpea, and lentil) are important sources of dietary protein for much of the world's population. They are rich in amino acids, containing high amounts of leucine, lysine, aspartic acid, glutamic acid and arginine (Boye et al., 2010). Moreover they offer a complimentary nutritional profile to cereal crops and are a mineral rich food source. Their dietary inclusion has been shown to have positive health effects, such as a reduction in cholesterol, cardiovascular disease and a reduced incidence of all-cause mortality (Trinidad et al., 2010; Nothlings et al., 2008; Chang et al., 2012). Moreover, legumes are key components of sustainable agriculture and their use in crop rotation leads to a reduction in agricultural CO_2 emissions and a decrease in nitrogen fertiliser application (Lassaletta et al., 2014; Barton et al., 2014).

Legumes are botanically characterised by their dehiscence pod structure, unusual flower morphology and capacity for nitrogen fixation. Interestingly, the nitrogen fixing capacity of legumes is not a ubiquitous trait, with approximately 88% of described legumes showing this ability (Graham and Vance, 2003). However, the capacity of legumes for nitrogen fixation is central to their agricultural and economic importance. Nitrogen fixation is achieved through symbiotic interactions with organisms in the soil microbiome, consisting of bacterial species belonging to the α-protobacteria and the order Rhizobiales (collectively called rhizobia), and arbuscular mycorrhizal fungi (Spaink, 2000). Whilst most land plants develop some form of beneficial interaction with soil microorganisms, leading to enhanced water and nutrient supply (in particular phosphate, Parniske, 2008), legumes are able to access atmospheric nitrogen fixed in the forms of ammonia (NH_3), nitrate (NO_3^-) or ureides (Atkins, 1987). This is due to a symbiosis occurring in nodules - specially developed organs located in the roots of plant. Nodulation is a phenomenon that is thought to have arisen on 4 separate

occasions within the legume family (Sprent and James, 2007). Nodules can be either determinate or indeterminate in form (Figure 1.7-1).

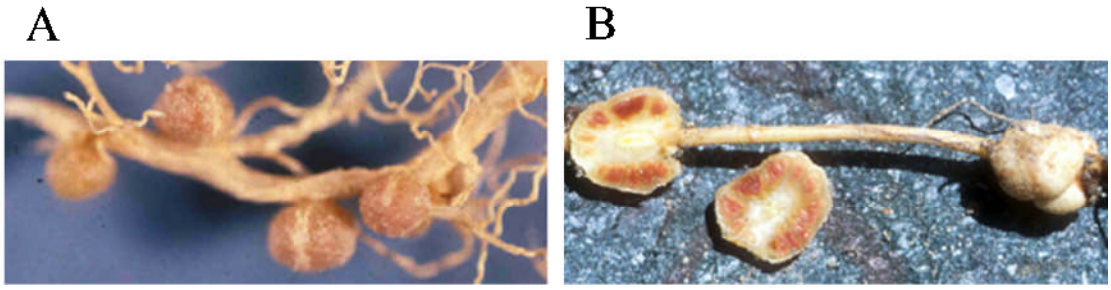

Figure 1.7-1: A) Determinate form nodules (demodioid) B) Indeterminate form nodules (lupinoid). Figure adapted from Sprent et al., (2013).

The fixation of atmospheric nitrogen into ureides is characteristic of tropical legumes belonging to the milletoid clade, which form determinate root nodules (Figure 1.7-1). The integration of atmospheric nitrogen into NH_3/NH_4^+ and its integration into amino acids is characteristic of the galegoid clade of legumes, which form indeterminate nodules (Atkins, 1987; Sprent and James, 2007).

Nodule formation is divided into three stages; pre-infection, nodule initiation and differentiation (Figure 1.7-2). Formation is regulated by two parallel processes; the organogenic formation of the nodule at the lateral root and the infection of the nodule by bacteria. In the first stage legume roots release flavonoids in response to low nitrogen conditions (Figure 1.7-2). Strigolactone (SL) are also postulated to play a role in nodulation, though their precise function has not been resolved (Steinkellner et al., 2007). Flavonoids act as chemoattractants for bacteria which in turn release nodulation factors (NF). The perception of NFs by nodulation factor receptors (NFR) at the plasma membrane initiates signalling cascades that result in the modified development of lateral root hairs (Desbrosses and Stougaard, 2011).

Root hairs will curl around isolated bacteria, which then multiply to form colonies. Infection threads will extend from the colony to the cortex of the primary root, providing a route for further rhizobial proliferation within the root cortex (Figure 1.7-2). Through sustained bacterial division and root cell differentiation, a nodule is formed. Mature nodules are able to fix nitrogen which is supplied to the plant in return for plant-fixed carbon (Ferguson et al., 2010). Rhizobia fix atmospheric nitrogen through nitrogenase enzymes, resulting in the formation of ammonium (NH_4^-) (Garg and Geetanjali, 2007). Ammonium is subsequently transported to the chloroplast where it is converted to the amino acid, glutamate, through the glutamate cycle (Rhodes et al., 1980).

1

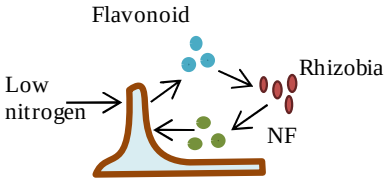

Root hairs form under low nitrogen conditions and flavonoids are secreted. Rhizobia release nodulation factors in response.

2

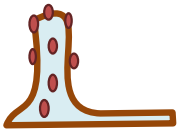

Rhizobia migrate towards the newly formed root hair and attach to its surface. Nodulation factors are detected by NF receptors, inducing nodule formation.

3

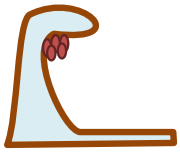

Root hair architecture changes, curling around the rhizobia to form a protective layer.

4

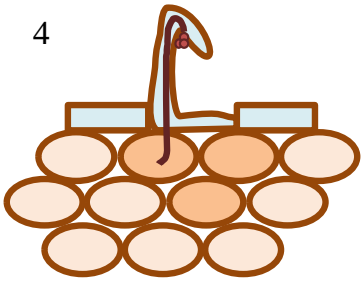

Cortical cells begin to divide and an infection thread is formed, progressing from the rhizobia to the outer cortex.

5

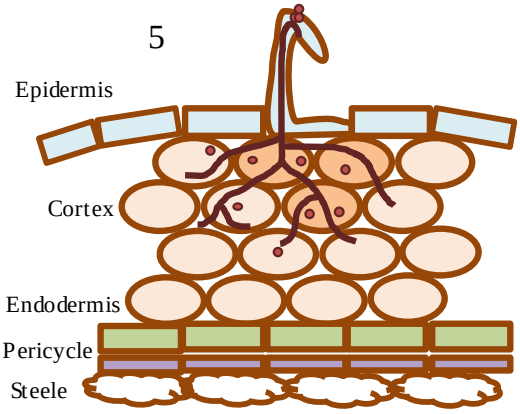

Infection threads progress towards nodule primordium and rhizobia differentiate. Root cells begin differentiation to form nodule.

6

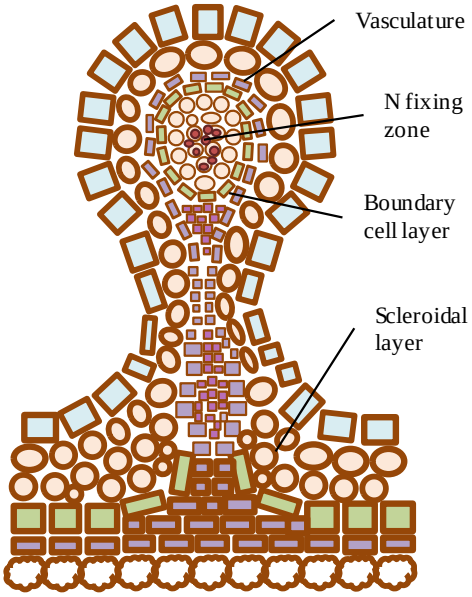

Continued rhizobial invasion and root cell differentiation lead to the formation of the nodule. The mature nodule consists of a rhizobial core surrounded by a later of boundary cells, fed by a vasculature connected to the plant body.

Fixed nitrogen is then transported to the plant where it is fixed into biologically accessible glutamate.

Figure 1.7-2: A simplified representation of determinate nodule formation; 1, initial flavonoid and nodulation factor signalling; 2, rhizobial adherence to a newly formed root hair; 3, root hair bending and deformation to accommodate the rhizobial colony; 4, the growth of an infection thread into the root cortex; 5, the start of root cell differentiation and the propagation of rhizobia in the cortex; 6, the fully mature root nodule with differentiated root cells and the formed nitrogen fixing zone. Figure adapted from Ferguson et al., 2010.

Despite the proven benefits of legume utilisation, yield increases have not kept pace with those of cereal crops. Global increases in legume production are a result of increased land usage, rather than a direct increase in crop productivity (Siddique et al., 2012; Foyer et al., 2016). Pulse crops are members of a diverse family of plants, the ecological and nutritional characteristics of which are well matched to the varied challenges of climate change, calorific provision and nutritional demand. However in order to sufficiently address these challenges a greater level of research must be conducted into legume biology, with a specific focus on the enhancement of legume survival and productivity under stress conditions (Foyer et al., 2016). Low temperatures in particular place a significant constraint on global legume yields and those legumes of significant dietary importance must be studied further.

1.8. Legume responses to low temperature exposure

While the general mechanisms of low-temperature tolerance have been characterised in the plant kingdom, extensive research has not been conducted on the factors underpinning low temperature tolerance in legumes. However, cereal crops have received some dedicated interest (Winfield et al., 2010). Research has highlighted the importance of cell membrane composition changes in enhancing low temperature tolerance (Vigh et al., 1985). Additionally redox state, protease activity and the abundance of specific transcription factors are integral to the low temperature tolerance response. While these mechanisms are likely conserved between cold tolerant plant species, diverse and unique strategies have evolved across all kingdoms for the management of exposure to cold (Huston et al., 2000) and species-specific strategies are likely to exist within the plant kingdom. Recent evidence has emerged showing that cold tolerance may be enhanced through favourable interactions between plants and the soil microbiome (Subramanian et al., 2016). This finding is particularly interesting when considered in the context of legumes, which are characterised by their intimate links with the soil microbiome.

Low temperature is a phenomenon that impacts agricultural productivity on every continent. In the United States an estimated 25% of the reduction in crop productivity was attributed to low temperatures (Boyer, 1982). Exposure to cold is also a limiting factor in the agricultural distribution of legume crops in Australia (Maqbool et al., 2010) and Africa. Africa in particular has warm day temperatures, but can encounter chilling and freezing temperatures during the night – a problem that is exacerbated by high elevation. Indeed elevation is a key limiting factor in the productivity of soybean crops grown in Africa (Van Heerden et al., 2003). Moreover in Europe severe cold weather events limit overwintering legumes such as faba bean (*Vicia faba*) and chickpea (*Cicer arietinum;* Link et al., 2010; Hekneby et al., 2006; Singh et al., 1993). As such, the development of low

temperature tolerant legume crops is of critical importance for the protection of food security (Herzog, 1987; Link et al., 2010).

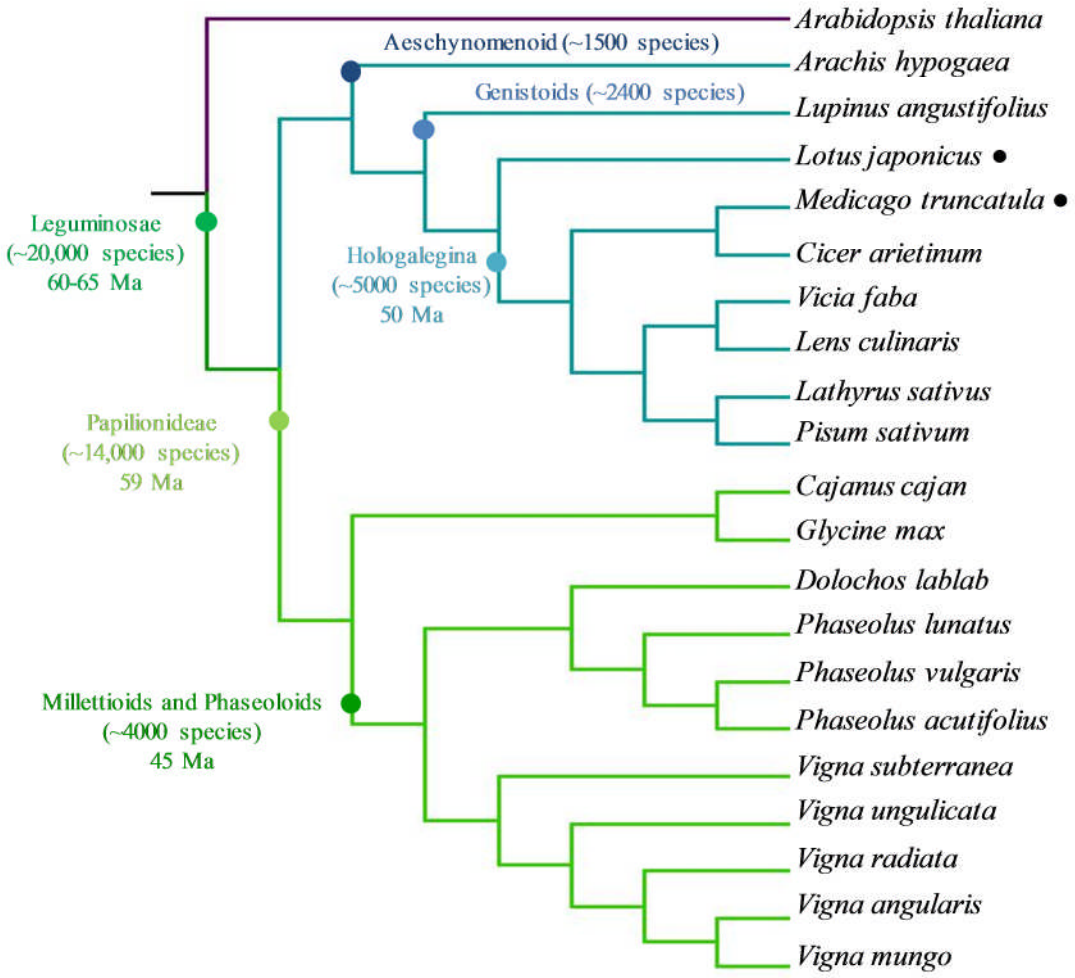

Figure 1.8-1: A molecular phylogeny of the legume family based on the protein sequence similarity of maturase K (MATK). Tree is rooted from the *Arabidopsis thaliana* MATK sequence and shows the major legume species used for food and feed. Coloured circles show evolutionary clades. *Lotus japonicus* and *Medicago truncatula*, denoted by ●, have been included as model legumes. Figure adapted from (Foyer et al., 2016).

Yield reduction is the dominant consequence of stress exposure. Plants are vulnerable to cold stress at all stages of development, with susceptibility being particularly high during seedling establishment and seed formation. However, plants employ numerous strategies for the survival of low temperature stress. Indeed temperature adaptation is a defining characteristic of the hologalegina clade of the legume family, which has adapted to temperate climates and is considered to be chilling tolerant (Figure 1.8-1). Conversely, the phaseoloid clade is adapted to tropical climates and considered chilling sensitive.

While the genetic and biochemical factors underpinning low temperature tolerance have been extensively characterised in *A. thaliana* and cereals (Thomashow, 2001; Winfield et al., 2010), limited research has been conducted on the mechanisms of low temperature tolerance in legumes. Biotechnology has provided some insight into the genetic factors contributing to stress tolerance; however focus has been placed on abiotic stresses. Moreover, the resolution of causative genetic factors tends only to extend to the level of genomic loci. As such progress needs to be made in the elucidation of single gene location and function (Dita et al., 2006). However, some understanding of the mechanisms through which plants protect against abiotic stress exposure has been gained through transgenic studies. For example the activity of cysteine proteases, as determined by the transgenic expression of a rice cysteine protease inhibitor, has been shown to enhance tolerance to drought and low nitrogen in soybean (Quain et al., 2014, 2015). These transgenic lines also displayed enhanced shoot branching, leading to the proposal of a model whereby the expression of cystatins influenced the production of the phytohormone strigolactone (SL). Additionally, transgenic lines of tobacco overexpressing the rice cysteine protease inhibitor, oryzacystatin I, were shown to have enhanced tolerance to chilling stress (Van der Vyver et al., 2003b). As such cysteine proteases present a promising target for the enhancement of tolerance to a range of abiotic stresses, including low temperature (Kunert et al., 2015). However, the legume family is diverse and gene based tools must be developed to further understand its under-represented taxa (Young et al., 2003).

1.9. Genetic resources for grain legumes

The enhancement of stress tolerance depends upon understanding an organism's genetic makeup. Through characterising the genes and networks underpinning tolerance, tools can be developed to enhance agronomically favourable traits (Mickelbart et al., 2015). The enhancement of abiotic stress tolerance is particularly important within the legume family (Foyer et al., 2016). Legumes comprise the majority of the world's dietary protein, either as direct components of human diets, or through their use a feed and forage crops. Soybean (*Glycine max*) is the world's most abundant protein crop, occupying an estimated 6% of the world arable land. However, it is primarily grown for the production of oil and protein meal (Hartman et al., 2011). The primary dietary legumes for humans are pea (*Pisum sativum*), chickpea (*Cicer arietinum*), broad bean (*Vicia faba*), pigeon pea (*Cajanus cajan*), cowpea (*Vigna unguiculata*) and lentil (*Lens* sp.), (Graham and Vance, 2003).

Soybean maintains one of the best characterised genomes among the grain legumes (Schmutz et al., 2010; Goodstein et al., 2012). Its genome size is 1.085 Gb, with a haploid chromosome number of n=40 arranged in pairs (Foyer et al., 2016). However, the genomic resources available for other legumes are comparatively limited with 13 legume genome sequences available at varying levels of

annotation (Dash et al., 2015). Of these 13 genomes, 9 accessions belong to grain legumes across 7 species (Table 1).

Table 1: Legume species for which genome databases are available.

Legume species	Agricultural use	Reference
Arachis duranensis (wild peanut)	Grain	(Bertioli et al., 2016)
Arachis ipaensis (wild peanut)	Grain	(Bertioli et al., 2016)
Cajanus cajan (piegeon pea)	Grain	(Varshney et al., 2011)
Cicer arietinum (chickpea, kabuli cv)	Grain	(Varshney et al., 2013)
Cicer arietinum (chickpea, desi cv)	Grain	(Parween et al., 2015)
Glycine max (soybean)	Oil/Forage/Meal	(Schmutz et al., 2010)
Lotus japonicus (bird's-foot trefoil)	Forage	(Sato et al., 2008)
Lupinus angustifolius (narrow-leafed lupin)	Grain	(Yang et al., 2013)
Medicago truncatula (barrel medic)	Forage	(Young et al., 2011)
Phaseolus vulgaris (common bean)	Grain	(Schmutz et al., 2014)
Trifolium pratense (red clover)	Forage	(De Vega et al., 2015)
Vigna angularis (adzuki bean)	Grain	(Kang et al., 2015)
Vigna radiata (mungbean)	Grain	(Kang et al., 2014)

While genome sequences are available for chickpea and piegeon pea, resources are lacking for pea and faba bean. This is not surprising as both pea and faba bean share the genomic trait of being large and highly repetitive (Macas et al., 2007; Ellwood et al., 2008). Until recently genomes with a large size and repetitive nature were difficult to characterise using next generation sequencing tools (Treangen and Salzberg, 2012). However, the development of long read sequencing platforms, and the potential for read augmentation with optical mapping technologies (Dong et al., 2012), means that these genomes may be unlocked in the near future.

While the pea and faba bean genomes are currently not characterised, gene based resources are available. In particular, linkage studies have been conducted in both species to elucidate the loci underpinning low temperature tolerance (Klein et al., 2014; Maqbool et al., 2010). However, concerted efforts must be made to further understand low temperature tolerance in these important cool season legume species.

1.10. Hypothesis and objectives

The hypothesis on which the following studies were based is that low temperature tolerance is influenced by phytocystatin expression and the strigolactone pathway.

These studies were conducted on chilling sensitive soybean, and the chilling tolerant species: pea, *A. thaliana* and faba bean.

The specific objectives of this thesis were:

- To characterise the effects of OCI expression on dark-chilling tolerance in soybean.
- To characterise the effects of the strigolactone pathway on the dark-chilling tolerance of pea and *A. thaliana*.
- To physiologically and genetically characterise low temperature tolerance in faba bean and provide genetic information for tolerance marker development.

"Measure what is measurable, and make measurable what is not so."

Attributed to Galileo Galilei

2. Materials and Methods

2.1. Plant material and growth conditions

2.1.1. Vicia faba

2.1.1.1. Growth on vermiculite under control conditions

Vicia faba cultivars Buzz, Clipper, Hiverna, Sultan and Wizard, were obtained from Wherry and Sons Ltd (The Old School, High Street, Rippingale, Lincolnshire, PE10 0SR). 50 dry seeds were sown per cultivar, per tray (38x24cm tray) in a mixture of 50% Sinclair Standard P35 perlite, 50% Sinclair V3 medium vermiculite (Albion Works, Ropery Road, Gainsborough, DN21 2QB). Water was added to saturation (1L per tray) and the seedlings were allowed to germinate for 7 days in a controlled environment chamber at 25 ºC day/20 ºC night temperatures and a 12 h photoperiod, with an irradiance of 200-250 $\mu mol.m^2.s^{-1}$. On day 7 seedlings that had developed 2 leaves (developmental stage 004) were transferred to 8x8cm pots containing vermiculite and watered once with 50 ml of modified full strength Hoagland's solution, shown in Table 2 (Hoagland and Arnon, 1950). They were then grown for a further 9 days, with 50 ml full strength Hoagland fertilisation every 2 days. Saturation of vermiculite was ensured throughout plant growth. Plants were harvested 14-23 days after sowing.

2.1.1.2. Growth on vermiculite under dark chilling conditions

Vicia faba cultivars Buzz, Clipper, Hiverna, Sultan and Wizard were grown as above. However after seedling selection plants were grown for a further 3 days until the first leaf had unfolded (stage 006, Figure 5.1-1). Following this seedlings either remained under control conditions for 9 consecutive nights or were moved to a cold room for their night cycle, being returned to control conditions for their day cycle (12h day/night 25 ºC/4 ºC ± 1 ºC). To ensure dark conditions were maintained for the night cycle, each tray was covered with a foil lid.

2.1.1.3. Growth on compost – acclimation and freezing

100 dry seeds of the above mentioned cultivars were sown in trays (38x24 cm) containing compost (Petersfield potting supreme, Petersfield Growing Mediums, 45 Cambridge Road, Cosby, Leicester, LE9 1SJ). Each tray was watered with 1 l of tap water and placed in a controlled environment chamber under optimal conditions; 25 ºC day/20 ºC night temperatures, 12 hour photoperiod, irradiance of 200-250 µmol.m^2.s^{-1}. Plants were allowed to grow for 7 days before seedlings having reached emergence (stage 004, Figure 5.1-1) were transferred to individual 6x6 cm pots. Plants were allowed to grow for a further 7 days until their first leaf had unfolded (stage 006, Figure 5.1-1).

At this stage 24 plants of each genotype were either; maintained under control conditions for 10 consecutive nights; subjected to chilling temperatures during their night cycle for 10 consecutive nights (25 ºC day/4 ºC ± 1 ºC night, 12 hour photoperiod, irradiance of 200-250 µmol.m^2.s^{-1}). 10 nights was described by Herzog (1989) as being the minimum necessary period of chilling exposure to induce acclimation in *V. faba*. On the 10th night of dark chilling plants were moved to a freezing chamber 0-4 hours prior to the end of their night cycle. Here they were exposed to freezing temperature stresses of - 5 ºC for 30 minutes. Experimental design detailed in Figure 2.1.1.3-1.

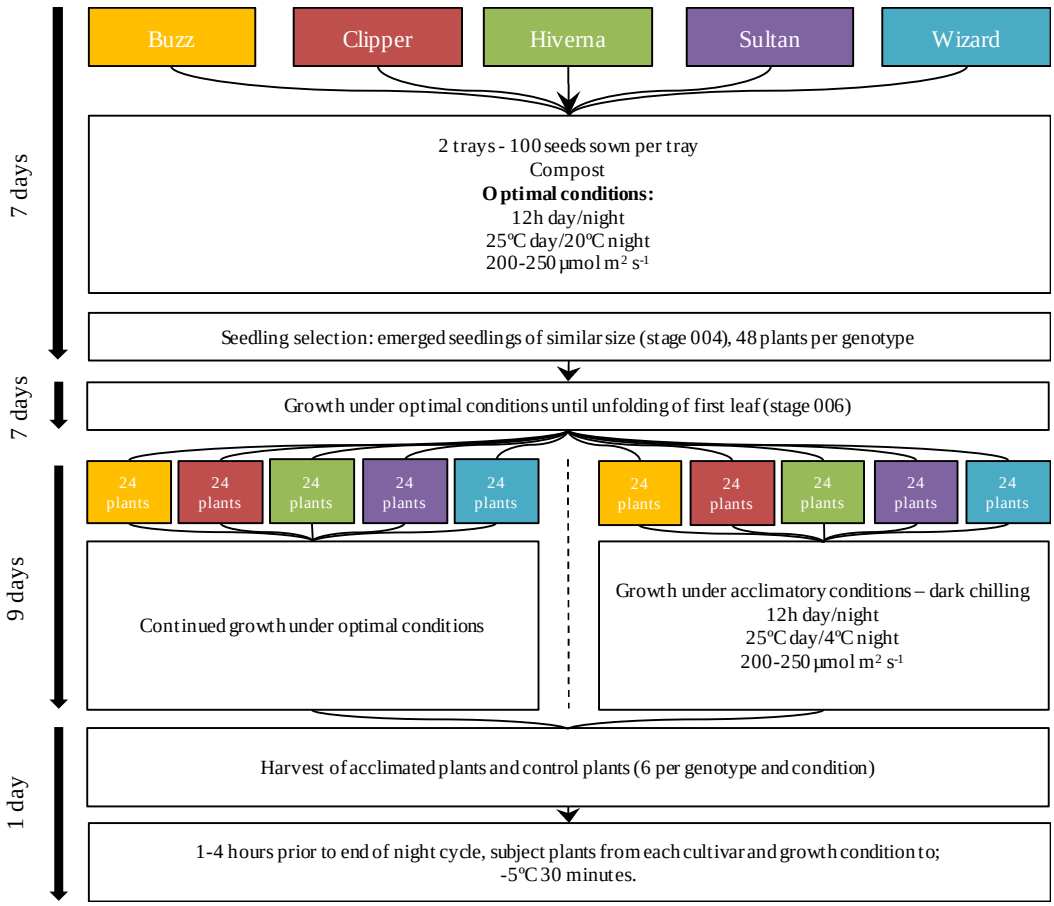

Figure 2.1.1.3-1: Experimental design for *Vicia faba* dark chilling and dark freezing experiments.

Table 2: Composition of modified Hoaglands plant media; Nitrogen replete and Nitrogen deficient (brought to pH 6 using HCl).

Nitrogen replete	**MW**	**Stock molarity (mM)**	**Per litre Hoagland (ml/L)**	**Final molarity (µM)**
Macronutrients				
$Ca(NO_3).4H_2O$	236.15	999.37	2.5	2.5
$MgSO_4.7H_2O$	246.5	1030.42	5	5.15
NH_4NO_3	80.04	999.5	1	1.00
KH_2PO_4	136.09	999.34	3	3.00
Fe-EDTA	367.05	34.46	1	0.034
Micronutrients				
H_3BO_3	61.83	46.26	2	0.093
$MnCl_2.4H_2O$	197.9	9.15	2	0.018
$ZnSO_4.7H_2O$	287.55	0.77	2	0.002
$CuSO_4.5H_2O$	249.69	0.32	2	0.001
$Na_2MoO_4.2H_2O$	241.95	0.5	2	0.001
Nitrogen deficient	**MW**	**Stock molarity (mM)**	**Per litre Hoagland (ml/L)**	**Final molarity (µM)**
Macronutrients				
K_2SO_4	172.259	500	6	3.00
$MgSO_4.7H_2O$	246.5	1000	5	5.00
$Ca_3(PO4)_2$	310.1767	49.97	20	1.00
Fe-EDTA	367.05	34.46	1.5	0.052
Micronutrients				
H_3BO_3	61.83	46.26	2	0.093
$MnCl_2.4H_2O$	197.9	9.15	2	0.018
$ZnSO_4.7H_2O$	287.55	0.77	2	0.002
$CuSO_4.5H_2O$	249.69	0.32	2	0.001
$Na_2MoO_4.2H_2O$	241.95	0.5	2	0.001

2.1.2. Glycine max

2.1.2.1. Growth on vermiculite

2.1.2.1.1. Nodulation and drought exposure

In experiments performed by Dr Belen Marquez-Garcia, University of Leeds (UK), seeds of *Glycine max* (Williams 82 variety) were obtained from Iowa State University (Plant Transformation Facility, Iowa State University, G405 Agronomy Hall, Ames, Iowa 50011-1010, United States of America). Seeds were inoculated with 0.5 grams per seed of a cell powder of *Bradyrhizobium japonicum* strain WB74-1 (Soygro bio-fertilized Limited, South Africa) and placed in 3x3 cm pots (one seed per pot) filled with vermiculite (Sinclair V3 medium vermiculite (Albion Works, Ropery Road, Gainsborough, DN21 2QB). Seedlings were watered twice per week with nitrogen free Hoagland's nutrient solution (Table 2) and demineralised water was added on the remaining days to keep optimum conditions. Plants were kept in a glass house with 16 h day length and 30/25 °C day/night temperature, with a light intensity of 1000 μmol $m^{-2}.s^{-1}$. The drought treatment was started at the age of five weeks, when the plants presented a developmental stage of the fifth trifoliate leaves. A total of 30 plants were divided into two groups: control and drought. Control plants received nutrients and water normally for 3 weeks, while drought exposed plants were deprived of both for 3 weeks.

2.1.2.1.2. Nodulation and chilling exposure

Soybean wild type (*Glycine max* cultivar Williams 82) and 3 independent transformed transgenic lines expressing the rice cysteine protease inhibitor, oryzacystatin I (SOC-1, SOC-2 and SOC-3), were obtained from Iowa State University (Plant Transformation Facility, Iowa State University, G405 Agronomy Hall, Ames, Iowa 50011-1010, United States of America). Seeds were grown on 100% vermiculite in 3x3 cm pots for 7 days under glasshouse conditions of 25 ºC day/20 ºC night temperatures, 16 h photoperiod. 20 seedlings of the same developmental stage were then selected for further growth and were transplanted to 4l pots containing 100% vermiculite and inoculated with with 0.5 grams per seed of a cell powder of *Bradyrhizobium japonicum* strain WB74-1 (Soygro bio-fertilized Limited, South Africa). Seedlings were maintained under glasshouse conditions for 3 weeks and watered on alternate days with 1 l of distilled water or 1 l of nitrogen free Hoaglands media (Table 2). Following this half the plants of each genotype were either maintained under glasshouse conditions or were subjected to 7 consecutive nights of dark chilling with night temperatures of 4 ºC

±1 ºC. This work was performed with the assistance of Dr Stefan van Wyk (University of Pretoria, SA).

2.1.2.1.3. Nodule development

The growth of soybean for developmental analysis was conducted by Dr Stefan van Wyk and associates at the University of Pretoria, South Africa. Soybean (*Glycine max*) cultivar Prima 2000 was obtained from Pannar Seed, South Africa. Each pot was inoculated with 0.5 g of SoyGro inoculum (SoyGro Bio-Fertilizer Limited, RSA), containing *Bradyrhizobium japonicum* of the strain WB74-1, prior to planting in fine vermiculite (Mandoval PC, RSA). Plants were grown under controlled conditions in a greenhouse, 13h photoperiod at an average light intensity of 1600 $\mu mol.m^{-2}.s^{-1}$, with 3 h of supplementary light from metal-halide lamps and using a day/night temperature of 25 ℃/17 ℃ and 60% relative humidity. Distilled water was used for plant watering and twice a week watered with a nitrogen-poor nutrient solution. Crown nodules were harvested from a minimum of three plants at developmental time points, 4, 8 and 14 weeks and were then flash frozen in liquid nitrogen.

2.1.2.1.4. Chilling exposure in young plants

Soybean wild type (*Glycine max* cultivar Williams 82) and 3 independent transformed transgenic line expressing the rice cysteine protease inhibitor, oryzacystatin I (SOC-1, SOC-2 and SOC-3), were obtained from Iowa State University (Plant Transformation Facility, Iowa State University, G405 Agronomy Hall, Ames, Iowa 50011-1010, United States of America). Seeds were grown on 100% vermiculite in 3x3cm pots for 7 days under optimal conditions of 25 ºC Day/20 ºC night temperatures, 12 h photoperiod and an irradiance of 200-250 $\mu mol.m^{-2}.s^{-1}$. Seedlings were then transferred to individual 10x10cm pots containing vermiculite and supplied with full strength Hoagland's medium, and grown for a further 7 days. 14 days after sowing seedlings were selected on the basis developmental stage (2 fully formed trifoliates). Plants from each the wild type and the transgenic lines were then either maintained under optimal conditions or were subjected to 9 consecutive nights of dark chilling (25 ºC Day/4 ºC night temperatures, 12 h photoperiod and an irradiance of 250-300 $\mu mol.m^{-2}.s^{-1}$). This work was conducted in collaboration with Professor H. Yildiz Dasgan.

2.1.2.2. Growth on compost

2.1.2.2.1. Developmental analysis

Soybean wild type (*Glycine max* cultivar Williams 82) and 3 independent transformed transgenic lines expressing the rice cysteine protease inhibitor, oryzacystatin I were sown in 10x10cm pots containing compost (Petersfield potting supreme, Petersfield Growing Mediums, 45 Cambridge Road, Cosby, Leicester, LE9 1SJ). Plants were allowed to grow for 4 weeks before being transferred to 4l pots, with a final transfer to 10l pots 6 weeks after sowing. Plants were maintained under glasshouse conditions with 16 h day length and 30/25 °C day/night temperature and an average light intensity of 1500 µmol $m^{-2}.s^{-1}$. 3 plants were harvested from each genotype at 2 weeks, 4 weeks, 6 weeks and 8 weeks.

2.1.2.2.2. Chilling exposure in young plants

Soybean wild type (*Glycine max* cultivar Williams 82) and 3 independent transformed transgenic line expressing the rice cysteine protease inhibitor, oryzacystatin I (SOC-1, SOC-2 and SOC-3), were obtained from Iowa State University (Plant Transformation Facility, Iowa State University, G405 Agronomy Hall, Ames, Iowa 50011-1010, United States of America). Seeds were sown on 100% vermiculite in 28x24cm trays and watered to saturation with tap water before being moved to a controlled environment chamber. Seeds were allowed to germinate for 7 days under control conditions of 25 ºC Day/20 ºC night temperatures, 12 h photoperiod and an irradiance of 200-250 µmol m^{-2} s^{-1}. Seedlings were selected on the basis developmental similarity before being transferred to individual 10x10 cm pots. 14 days after sowing Plants from each the wild type and the transgenic lines were then either maintained under optimal conditions or were subjected to 9 consecutive nights of dark chilling (25 ºC Day/4 ºC night temperatures, 12 h photoperiod and an irradiance of 250-300 µmol m^{-2} s^{-1}).

2.1.3. Pisum sativum

2.1.3.2. Growth on compost and chilling exposure

Pisum sativum genotypes; L107, BL298, K164, K487 and K564 were obtained from the laboratory of Professor Christine Bevridge (University of Queensland, Australia). Cultivars were either wild type

(L107, Torsdag cultivar) or had been subjected to EMS mutation and were deficient in strigolactone biosynthesis and perception (BL298, *rms5-3*; K164, *rms4-1*; K487, *rms3-1*). Seeds were first placed on paper towel lined petri dishes saturated with distilled water and allowed to germinate for 5 days under control conditions (12h day length, 25/20 °C day/night temperature and a light intensity of 250-300 $\mu mol.m^{-2}.s^{-1}$). Given the sensitivity of peas to hypoxic conditions, ventilation was allowed by leaving the petri dish lids partially open. Following germination, seedlings of similar developmental stages (plumule apparent) were transferred to individual 10x10 cm pots containing compost (Petersfield potting supreme, Petersfield Growing Mediums, 45 Cambridge Road, Cosby, Leicester, LE9 1SJ) and maintained under control conditions. Following 2 weeks of growth under control conditions, half of the plants from each genotype were either maintained under these conditions for 7 days, or were exposed to 7 consecutive nights of dark chilling at 4 ºC.

2.1.4. Arabidopsis thaliana

2.1.4.2. Growth on compost and chilling exposure

Arabidopsis thaliana ecotype Colombia-0 (col-0/Wt) and mutagenic lines *max2-1*, *max3-9* and *max4-1* seeds were obtained from Dr Belen Marquez-Garcia, University of Leeds (UK). All mutagenic lines were a product of EMS treatment and were deficient in either strigolactone biosynthesis or signalling proteins. Seeds were sown, 4 per pot, in 6x6 cm pots containing compost (Petersfield potting supreme, Petersfield Growing Mediums, 45 Cambridge Road, Cosby, Leicester, LE9 1SJ) before being placed into a tray (38x24cm). Each tray was watered with 1L of tap water and placed in a controlled environment chamber under optimal conditions; 25 ºC day/20 ºC night temperatures, 12 hour photoperiod, irradiance of 200-250 $\mu mol.m^{2}.s^{-1}$. Plants were allowed to grow for 7 days before seedlings were transferred to either; individual 6x6cm pots and allowed to grow for a further 7 days or individual 50 ml Falcon tubes containing compost and having been watered to saturation. In both cases plants were grown for a further 2 weeks before being either; maintained under control conditions or subjected to 7 consecutive nights of dark chilling at 4 ºC.

2.1.4.3. Growth on ½ MS media and chilling exposure

Wild type, *max 2-1*, *max 3-9* and *max 4-1* seeds were surface sterilised using chlorine gas. Microfuge tubes containing approximately 200 seeds were placed into a sealed Nalgene® desiccator with a beaker containing 300 ml of bleach to which 4 ml of concentrated hydrochloric acid was added for

the evolution of chlorine gas. Seeds were sterilised for a period of 3 hours, sealed and stored at room temperature. Sterilised seeds were sown on 12x12cm square, ventilated petri dishes containing ½ Murashige and Skoog (MS) base medium. Per litre of distilled water; 10g agar-agar, 10 g sucrose, 2.2 g MS, 0.1 g myo-inisitol (Fisher scientific, Bishop Meadow Rd, Loughborough, Leicestershire LE11 5RG, UK), 0.5g MES (4-Morpholineethanesulfonic acid monohydrate, Alfa Aesar, Shore Rd, Port of Heysham Industrial Park, Heysham LA3 2XY, UK) was added. Media pH was brought to 5.7 using potassium hydroxide, following which media was autoclaved for 20 minutes at 121 °C. Media was allowed to cool to 50 °C before being supplemented with the synthetic strigolactone, GR24. 1 mg of GR24 (Prof. Dr. Binne Zwanenburg, Utrecht University, NL) was dissolved in 330 µl of 100% acetone and 100 µl was added per litre of ½ MS media, to a final concentration of 2 µM GR24. Non-supplemented control media had 100 µl of 100 % acetone added. Following supplementation media was poured onto plates under a UV sterile laminar flow hood. Surface sterilised seeds of each genotype were suspended in sterile water and were sown onto ½ MS plates using a p200 pipette. Plates were sealed with Parafilm® and placed in a 4 °C cold room to imbibe for 72 hours. Imbibed seed plates were then transferred to a controlled environment chamber (12h day length, 25/20°C day/night temperature and a light intensity of 250-300 $\mu mol.m^{-2}.s^{-1}$). Seeds were allowed to germinate for 4 days before being either; subjected to 7 consecutive nights of dark chilling (4 °C) or maintained under control conditions. This work was conducted in collaboration with Masters Student Leila Beyyoudh.

2.2. Physiological measurements

2.2.1. Nodule harvest and measurement

The entire plant was excised from its vermiculite growth media and the root system was gently washed in distilled water to eliminate vermiculite particulate. The total number of nodules per plant was counted and crown root nodules were harvested from soybean roots using a scalpel. The diameter of harvested nodules was measured using ImageJ (Rasband, 2015).

2.2.2. Shoot and root measurement

The number of leaves and stems per plant was counted. The shoot was then cut from the root using a scalpel and the fresh weight was measured on a balance (Ohaus PA413, Ohaus Europe GmbH, Heuwinkelstrasse 3, CH-8606 Nänikon, CH). Tissue was placed in pre-weighed aluminium foil and dried at ~80 °C for 3 days for dry weight measurement. For plants grown on vermiculite the plant was excised from the media and the roots were thoroughly washed in distilled water, with care being taken to preserve lateral roots. The root system was cut from the plant and dried with tissue before being measured for fresh weight. Dry weight was determined by removing the root system to pre weighed aluminium foil and drying for 3 days at ~ 80 °C before weighing.

2.3. Arabidopsis rosette measurements

The rosette area of *A. thaliana* plants was measured by photographing plants with a Nikon D5100 DSLR digital camera. Each photo contained a reference scale and ImageJ (Rasband, 2015) was used to calculate whole rosette area.

2.3.1. Photosynthetic parameters: gas, fluorescence and pigments

Photosynthetic gas exchange measurements were made using a LI-6400XT portable photosynthesis system (LI-COR Biotechnology UK Ltd, St. John's Innovation Centre, Cowley Road, Cambridge, CB4 0WS, UK). Photosynthetic carbon assimilation, stomatal conductance and intracellular CO_2 concentration were measured using infra-red gas analysis. The LI-6400XT delivered a light intensity of 800 µmol.m^{-2}.s^{-1} and a CO_2 level of 400 µmol mol^{-1}. When measuring faba bean, soybean and pea,

the oldest leaf of each plant was inserted into a 3x2 cm 6400-02B LED gas exchange chamber. When measuring Arabidopsis the whole plant was placed in a 6400-17L lighted whole plant Arabidopsis chamber. Plants were allowed to photosynthetically stabilise for 15 minutes prior to data recording. The protocol followed was essentially that of Soares et al. (2008).

Chlorophyll fluorescence (Fv/Fm) was determined by fluorepen measurement of dark adapted leaves (Photon Systems Instruments, Drasov 470, 664 24 Drasov, Czech Republic). Leaf pigment content was determined via the method of Lichtenthaler, (1987) with weighed leaf samples being ground in liquid N_2 and having their pigment extracted via centrifugation with 95% ethanol at 10,000 *g*. Pigment content (µg/ml) was calculated as follows; calculate the pigment concentrations (µg/mL):
Chlor a = 13.36A664 – 5.19649, Chlor b = 27.43A649 – 8.12A664, Ca+b = 5.24A664 + 22.24A649
Carotene = (1000A470 – 2.13Ca – 97.64Cb)/209.

2.4. Construction of dark freezing chamber

To conduct experiments into low temperature tolerance an environment chamber capable of freezing temperatures was constructed. This was performed in collaboration with Dr Jeremy Harbinson (University of Wageningen, Netherlands) who designed and constructed the temperature control module, and Mr Tarsem Hunjan (University of Leeds, United Kingdom) who assisted in the assembly of the freezing chamber. The dark freezing chamber was operated by running a commercial freezer, capable of achieving temperatures of -20 °C, to its maximum capacity. The freezer, having attained its minimum possible temperature, could then have its internal temperature raised through the application of heat. Through frequent applications of small levels of heat, a stable internal temperature could be maintained. Monitoring of the chambers internal temperature and calculation of the level of heat application was carried out by a temperature control module (Figure 2.4.1-1). The module was able to self-calibrate and monitor the rate and extent of temperature change relative to the amount of energy delivered to the heating cable.

2.4.1. Temperature control module

The temperature control module (Figure 2.4.1-1) was constructed using the materials listed in Table 3. Construction was conducted at the University of Wageningen (NL) by Dr Jeremy Harbinson. Testing of the module and its implementation in a controlled environment system was carried out at the University of Leeds.

Table 3: Materials needed for construction of temperature control module.

Part	Manufacturer	Item number	Quantity
Plastic-aluminium case	Multicomp	1526705	1
3-pin fused power inlet switch	Multicomp	1516059	1
3 pin power outlet	Schruter	9657029	2
Type K thermocouple socket	Labfacility	7086386	1
Green rocker switch, illuminating	Multicomp	1454388	2
Fuse holders	Littelfuse	9516395	2
Solid state relay	Crydom	1200213	1
RS232 D connector	ITT cannon	1760329	1
CAL3300200 temperature controller	West control solutions	-	1

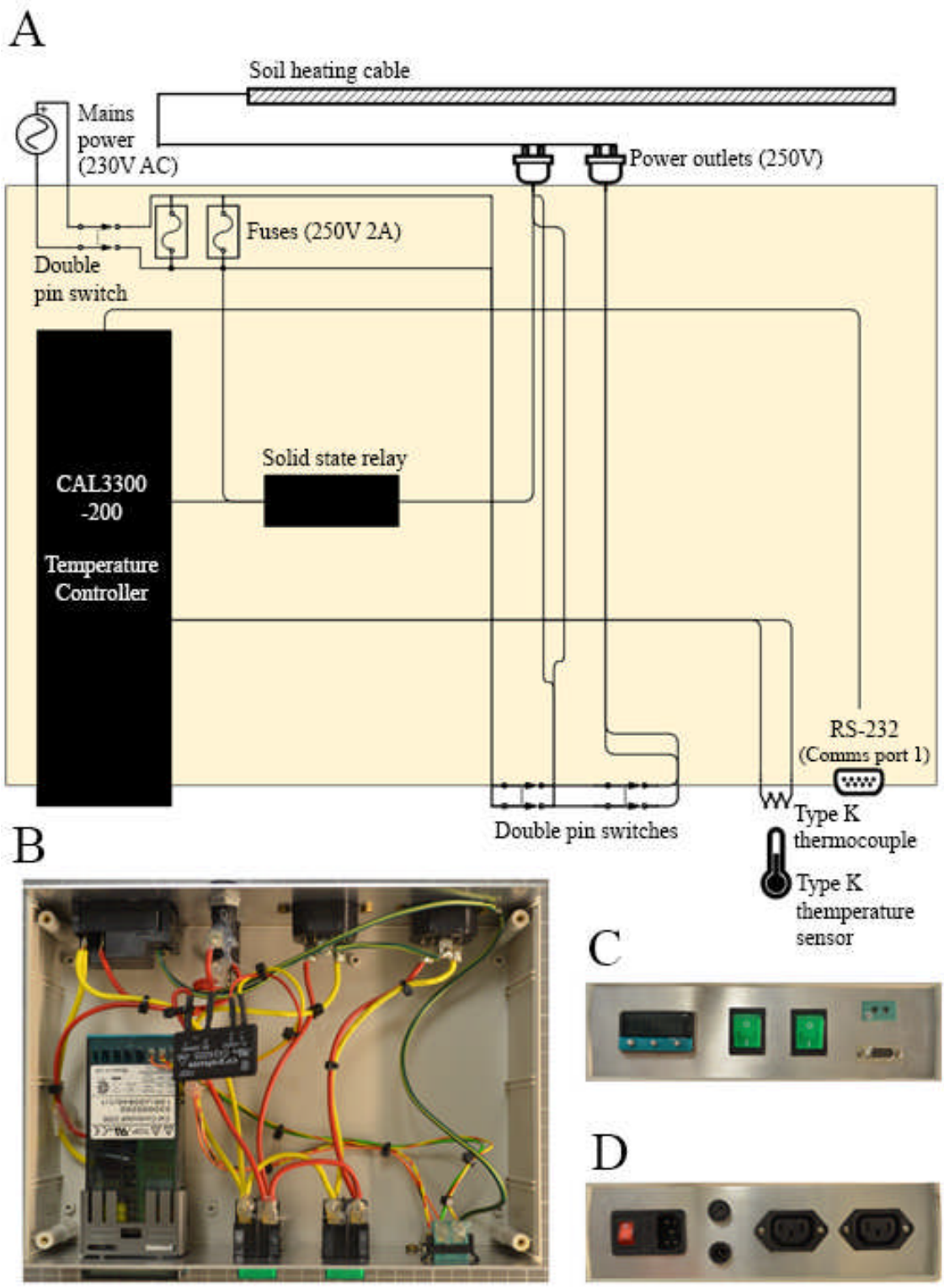

Figure 2.4.1-1: A) Schematic diagram of dark freezing chamber temperature control module, showing mains power being fed to a CAL3300200 temperature controller and 2 double pin power switches, connected to 250 V power outlets via 250 V 2 A fuses. The CAL3300200 is also connected to a type K thermocouple and an RS232 communication port. B) Photograph of the assembled temperature control unit C) Control unit front D) Control unit rear.

2.4.2. The dark freezing chamber.

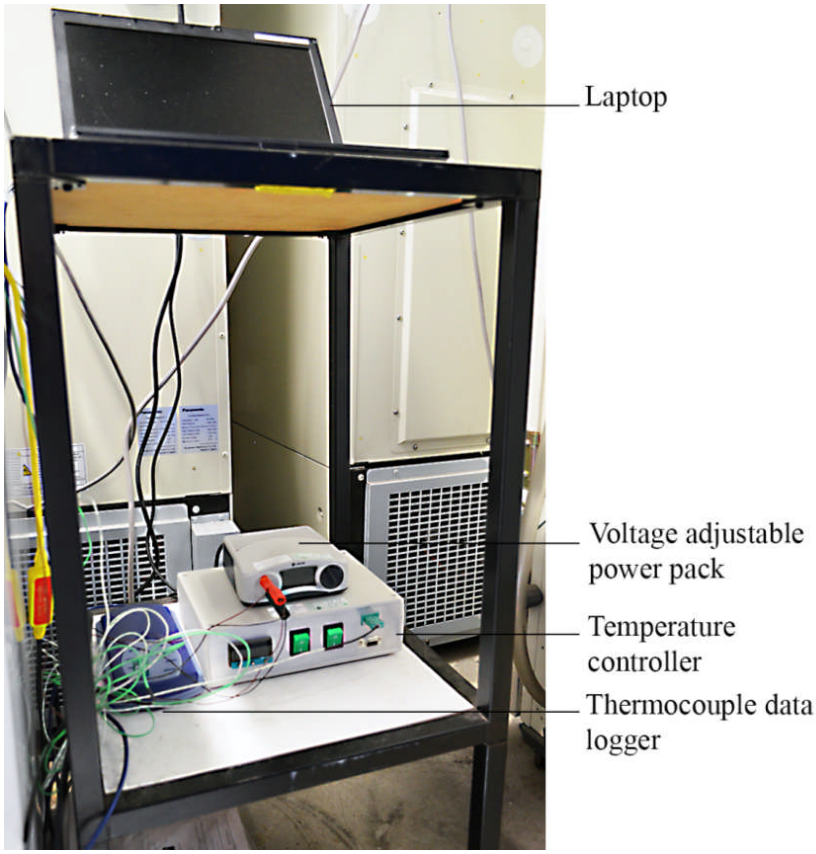

Figure 2.4.2-1: Control and power units for the dark freezing chamber showing; a laptop attached to a thermocouple data logger as a confirmatory temperature sensing system; a voltage adjustable power pack attached to 12 V fans for air circulation; a temperature controller to accurately maintain chamber temperature by delivering heat through a soil heating cable.

A commercial household freezer (Candy Chest Freezer, CHZE 6089, Pentrebach, Merthyr Tydfil, Mid Glamorgan, CF48 4TU, UK) was fitted with an aluminium scaffold on which soil heating cable was hung. Computer fans (San Ace 92L fans, Farnell Electronics, Maybrook Industrial Estate, Castleton Rd, Leeds LS12 2EN, UK) were attached to the scaffolding to circulate air in the chamber and maintain a constant temperature (Figure 2.4.2-2). Fans were powered by a voltage adjustable power pack. Type K temperature sensors was mounted near the fans, with the data being fed to both a thermocouple data logger (TC-08 thermocouple data logger, Picotech Ltd, James House, Colmworth Business Park, St Neots, Cambridgeshire, PE19 8YP, UK) and the temperature control module. The thermocouple data logger was USB linked to a laptop where chamber temperature could be monitored and recorded in real time.

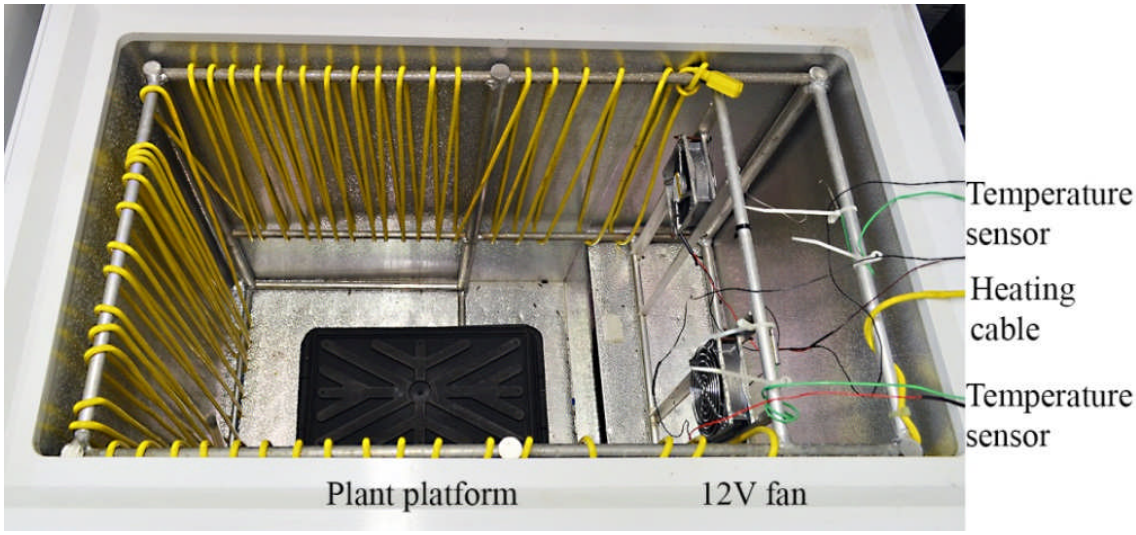

Figure 2.4.2-2: Dark freezing chamber internal configuration showing; temperature sensors (green wire), soil heating cables (yellow wire) and 12 V fans with power feeds (red and brown wires).

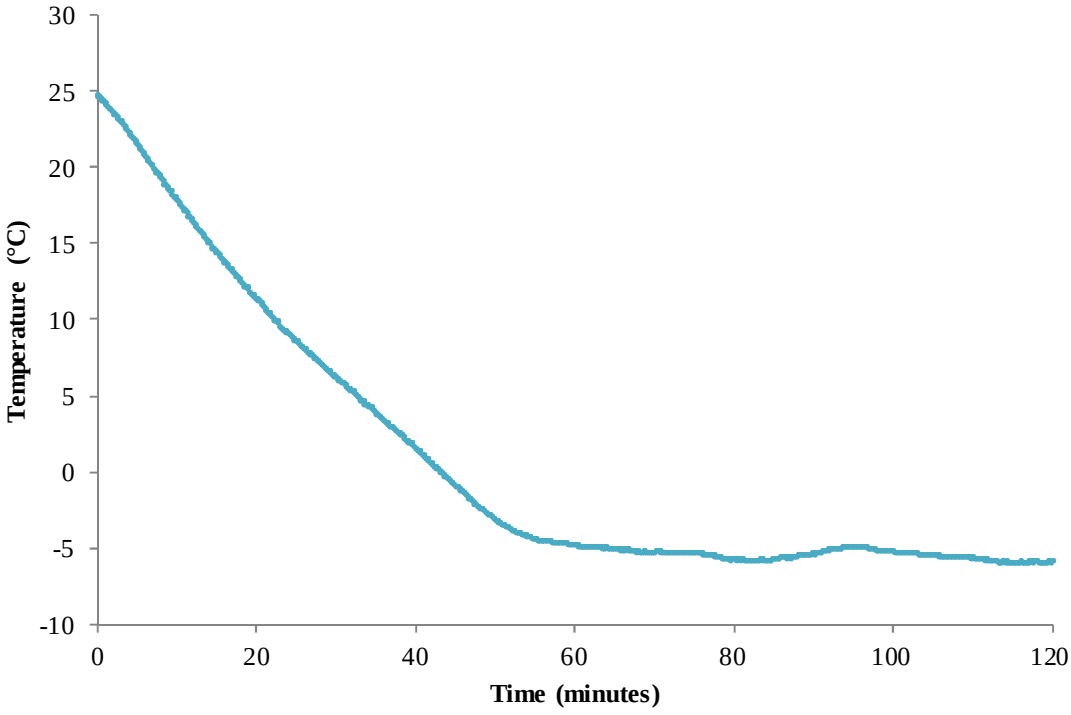

Figure 2.4.2-3: The time taken for internal chamber temperature to reach target value.

On power up it took 1 hour for the chamber to reach its target temperature. This temperature was maintained with an accuracy of ± 0.5 °C.

2.5. Nucleic acid extraction

2.5.1. DNA extraction from *Vicia faba* embryonic axis

DNA extraction was performed using the Qiagen DNeasy plant mini kit (Qiagen Ltd, Skelton House, Lloyd Street North, Manchester, M15 6SH, UK) employing a modified protocol. 10 seeds of *Vicia faba* (Wizard cv) were incubated in distilled water for 72 hours. Embryonic axes were extracted and ground in liquid N_2 in a pestle and mortar. 800 µl of buffer AP1 was added to the mortar and allowed to thaw, followed by the addition of 8µl of RNAse. Lysate was added to a 1.5 ml microfuge tube. The mortar was rinsed with an additional 400 µl of AP1 which was also added to the microfuge tube. Tube was incubated at 65 °C for 10 minutes. Into a separate 1.5 mL microfuge tube 800 µl of lysate was transferred and 260 µl of buffer P3 was added (3:1 v/v P3:AP1). This was incubated on ice for 5 minutes and spun at 20,000 *g* for 5 minutes. Supernatant was divided equally into 2 shredder columns and spun for 2 minutes at 20,000 *g*. This process was repeated until all supernatant had been spun through the shredder column with each flow through being collected into a separate 2 ml microfuge tube. Volumes of each tube were measured and 1.5 volumes of buffer AW1 were added to each. From each subsample 650 µl was added to a DNeasy spin colum and spun at 6000*g* for 1 minute. This was repeated for any remaining sample. Spin columns were placed into new collection tubes, washed with 500 µl of buffer AW2 by spinning at 6000 *g* for 1 minute and further washed with an additional 500 µl of AW2 by spinning at 20,000 *g* for 2 minutes. Column membrane was dried by spinning at 20,000 *g* for 2 minutes. Columns were placed into new collection tubes and 50 µl of distilled, nuclease free water was added directly to the membrane. Column was left at room temperature for 5 minutes, following which it was spun at 6000 *g* for 1 minute to elute the column bound DNA. This step was repeated to produce a second column elution. The two elutes were then combined. Quality and abundance was confirmed by agarose gel electrophoresis, running 10 µl of sample on a 1% gel at 80 V for 1 hour.

2.5.2. DNA extraction from leaf tissue

DNA was extracted from leaf tissue using a Qiagen DNeasy plant kit, as per manufacturer protocol (Qiagen Ltd, Skelton House, Lloyd Street North, Manchester M15 6SH, UK). A minimum of 80 mg and a maximum of 100 mg of plant tissue was used per extraction.

2.5.3. RNA extraction from plant tissue

RNA was extracted from plant material (leaf, stem or root) using the Sigma-Aldrich Spectrum Plant Total RNA kit, as per manufacturer protocol (Sigma Aldrich, Homefield Road, Haverhill CB9 8QP, UK). A minimum of 80 mg and a maximum of 100 mg of plant tissue was used per extraction.

2.6. Genomic and transcriptomic sequencing and bioinformatics

2.6.1. Genomic sequencing

Genome sequencing was performed at the University of Leeds Next Generation Sequencing Facility (Institute of Molecular Medicine, St James' University Hospital, Beckett Street, Leeds, West Yorkshire, LS9 7TF). Using an Illumina HiSeq2500 platform (Illumina, 2014). A single paired-end library was produced from DNA extracted from *V. faba* root embryonic axes. Library was run on two flow cell lanes (Figure 2.6.2-1).

2.6.2. Transcriptome sequencing

Transcriptome sequencing was performed at the University of Leeds Next Generation Sequencing Facility (Institute of Molecular Medicine, St James' University Hospital, Beckett Street, Leeds, West Yorkshire, LS9 7TF). Using an Illumina HiSeq2500 platform (Illumina, 2014), 24 paired-end libraries were produced and run on a single flow cell with 2x12 samples being loaded across 4 lanes. Sequencing employed polyA RNA.

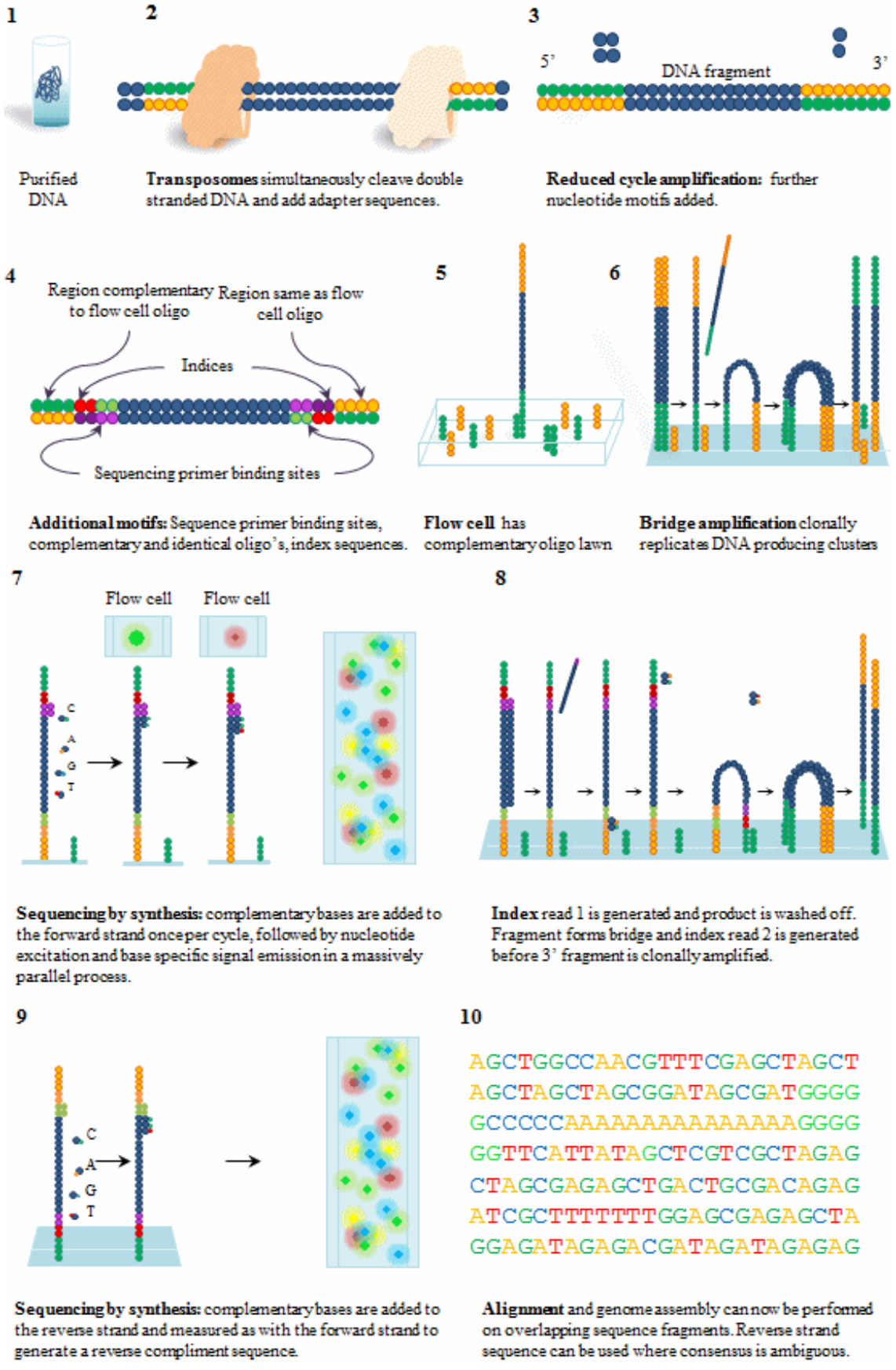

Figure 2.6.2-1: DNA sequencing on an Illumina HiSeq2500 paired end platform. 1-4 show DNA cleavage and adapter sequence addition. 5-7 show sequencing by synthesis of the forward DNA strand. 8-10 show the sequencing by synthesis of the reverse strand and the resulting sequence data.

2.7. Bioinformatics

2.7.1. *De novo* genome assembly

FastQC analysis (Andrews, 2010) was performed on raw sequenced reads and TrimGalore! (Andrews, 2015)was used to remove adapter sequences and all bases below a moving window average Phred quality score of 30. ABySS (Simpson et al., 2009) was used for *de novo* paired end sequence assembly, with kmer sizes of 32 and 64.

2.7.2. Contig database for BLAST

The NCBI BLAST toolkit was used to create a BLAST+ nucleotide database of ABySS assembled *Vicia faba* genomic contigs.

2.7.3. Linkage enhanced genome contigs

Linkage marker sequences were obtained from the cool season grain legume database (Humann et al., 2016) on the basis of work conducted by Webb et al., (2016). Linkage markers were BLASTED against the contig BLAST+ database. Homologous reads were selected, where length and identity were >90%. Successful BLAST hits could be putatively mapped to *V. faba* chromosomes, whereby genomic DNA scaffolds were searched against the *Medicago truncatula* DNA database (Phytozome) and gene orthologues were identified.

2.7.4. Organellar genome comparisons

Chloroplast and mitochondrial reference sequences for *Vicia faba* and several related species, together with publicly available DNA-seq reads, were downloaded from NCBI. Bowtie2 (Langmead and Salzberg, 2012) was used to align the DNA-seq reads and relevant reference genome for chloroplast, and mitochondria where available. Samtools mpileup (Li, 2011) was used to identify single nucleotide variants (SNV). A core set of chloroplast and mitochondrial genes was assembled by BLAST between pairs of species, where one or more genes were present in annotated reference sequences from all species. SNVs in DNA-seq reads were visualised using IGV (Thorvaldsdóttir et

al., 2013). Further comparisons were made of between-species variance, with homology being assessed within a 10 bp window. A multi-species homology map was constructed for each core gene of the chloroplast and mitochondria with map visualisation being performed in Microsoft Office Excel.

2.7.5. Transcriptomic dataset analysis

Raw transcriptome reads were quality trimmed using the Tim Galore! bioinformatics program, using FastQC to identify primer and adapter sequences, to a quality score (phred) of 30 (Andrews, 2015). To eliminate the possibility of contaminants sequences were scanned against a 106 Gb contaminant database (Wood and Salzberg, 2014). The Salmon program (Patro et al., 2015)was used to quantity the RNA Seq against the Cool Season Food Legume database (Humann et al., 2016). The quantified RNA Seq data was imported into R/Bioconductor (R Core Team, 2015; Huber et al., 2015) using tximport (Soneson et al., 2015) and counts were normalised using EdgeR (Robinson et al., 2010). Differential expression was calculated using LIMMA (Ritchie et al., 2015) Gene ontology was determined using FATIGO (Al-Shahrour et al., 2004). Principle component analysis was conducted and visualised in R (R Core Team, 2015) using pcaMethods (Stacklies et al., 2007) and ggplot2 (Wickham, 2009).

2.8. qPCR and PCR

Polymerase chain reaction (PCR) was carried out using BioMix Red reaction mix (Bioline reagents limited, Unit 16 The Edge Business Centre, Humber Road, London, NW2 6EW). 5 µl of DNA was added to 10 µl of BioMix red and 5 µl of PCR primer (Table 4). Reaction volume was brought to 20 µl using distilled water. PCR was run on a thermocycle program of 5:00 minute denaturation at 95ºC, a further denaturation for 1:00 minute at 95 °C, elongation at appropriate temperature for 0:30 minutes with 44 repetitions of 1:00 minute denaturation and 0:30 minute of elongation. PCR products were run on a 1% Agarose gel in 1% TAE buffer against a 1 kb+ gene rule (3 Fountain Drive, Inchinnan Business Park, Paisley PA4 9RF, UK) to determine product size and identity.

Quantitative real time polymerase chain reaction (qPCR) was performed using a Quiagen QuantiTect SYBR Green PCR Kit and a BIO RAD CFX96 Real Time System with C1000 Thermal Cycler (www.bio-rad.com). Samples were pipetted on to clear, low skirted 96 well plates (StarLabs, www.starlab.co.uk). Each well contained; cDNA 4µl (10 ng/µl), SYBR Green 10 µl, Forward and reverse primers 1.8 µl (5mM), Distilled water (DNAse free) 4.2 µl. The BIORAD qPCR system was

programmed to run a 2 step melting curve using the following program: Initial denaturation at 95 °C for 5:00 minutes; a further denaturation step at 95 °C for 1:00 minute; an elongation step at appropriate temperature for 0:30 seconds; 44 repeats of 1:00 minute denaturation and 0:30 second elongation; melting curve analysis from 55 °C to 95 ºC in 0.5 °C increments for 0:05 seconds. qPCR data was processed using the Livak method ($2^{-\Delta\Delta Ct}$) (Schmittgen and Livak, 2008). Calculated as:

[(C_T gene of interest – C_T internal control) sample A – (C_T gene of interest – C_T internal control) sample B)]

Table 4: qPCR primers for use with *G. max*

Accession	ID	Forward sequence	Reverse sequence	Function
Glyma02g08180	GR1	TCCGCCACTTTCTGTAGTTG	GTGAAAACCAACAGATCGCC	Glutathione reductase (Mt)
Glyma02g16010	GR2	CCTCAAGCTATCACGAAGTCAG	TTTCACACCAACAGACTCCAG	Glutathione reductase (Chlor)
Glyma06g44050	GRX2	CGATTGCTATTGGGTCTTGGG	AAACCGCTGGAAATTGCATC	Glutaredoxin
Glyma08g22430	GRX3	ACTTGGTTCACTCGAATGGC	CCATTTAAGGGTCTGCTGAGAG	Glutaredoxin
Glyma09g07040	GRX4	TCTCCAATCTTCAGCTTCAGC	CTTCTACAGTACGGGCAATAGG	Glutaredoxin
Glyma20g3844	GST	TGAATCCTGAAGGGAAGGTG	TATCTTTGATCCCACGGAGG	Glutathione S transferase
Glyma06g41610	TX1	CAGTGGATAAAATTGTGGGTGC	GGCAACTGTTCAATGTGTTCG	Thioredoxin
Glyma03g40280	CSD1	ATTCCTCTCACTGGACCAAAC	GATACCACAAGCTACTCTGCC	Cu-Zn superoxide dismutase
Glyma16g27020	CSD2	AGTGACAGGGTTGTCCAAG	GAGGACCTGGGGTAGAGGAG	Cu-Zn superoxide dismutase
Glyma04g39930	MSD	CGATCTGGATTACGACTATGGC	AGTTGGTGATGTAAGTCTGGTG	Fe-Mn superoxide dismutase (Mt)
Glyma10g07820	MDAR1	TTGATCATTCTCGCAAATCG	TCGTTTACCAAAATCCGTCC	Monodehydroascorbate reductase
Glyma17g04210	DLD	CTAACTCTTGAACCGGCTGC	TCGTTTACCAAAATCCGTCC	Dihydrolipoyl dehydrogenase
Glyma08g04370	ALDH	AATTAGTCTCAGTCCCCAACG	AGAGCTTGGTGAACTTGATCG	Aldehyde dehydrogenase
Glyma11g16370	CCD7	CACCAAACCCCTCCCTCTAT	CCTTCCACGGTGCTTAGAGT	Carotenoid cleavage dehydrogenase
CCD8	CCD8	CTTGTTCCTGACATGCCTCA	CTAGTCCATGCAACGTGGT	Carotenoid cleavage dehydrogenase
Glyma16g10700	40S	GCCAGCCTGCTAACACTAAG	AAGAGTCTGAGTACGCACAAG	40S ribosomal subunit
Glyma18g52780	Actin	TGTTCCCTGGTATTGCTGAC	AAGGTGCTAAGAGATGCCAAG	Actin
Glyma02g44460	Elf 1-β	GTGGTACGATGCTGTCTCTC	CCACTGAATCTTACCCCTTGAG	Ribosomal elongation factor
TC224926	CYP2	CGGGACCAGTGTGCTTCTTCA	CCCCTCCACAAAGGCTCG	Cyclophilin 2 – Protein folding
N/A	OCI	ATGTCGAGCGACGGAGGG	TTGCACTGGCTACGACAGGC	Oryzacystatin I

“The fact that we live at the bottom of a deep gravity well, on the surface of a gas covered planet going around a nuclear fireball 90 million miles away and think this to be normal is obviously some indication of how skewed our perspective tends to be.”

-Douglas Adams, The Salmon of Doubt: Hitchhiking the Galaxy One Last Time

3. The characterisation of OCI expressing soybean under drought and chilling

3.1. Introduction

The growth and productivity of soybean plants is limited by environmental stresses such as low temperatures and drought (Kunert et al., 2016),which can inhibit both leaf and nodule functions. For example, both stresses alter the nodule oxygen diffusion barrier, particularly by effects on respiratory activity (Van Heerden et al., 2008). Nitrogen fixation in the nodules depends on the absence of oxygen. Nodule respiration is therefore supported by oxygen transfer via leghaemoglobin (Goldberg et al., 1987). When nodules are exposed to stress the delicate oxygen balance of the system is perturbed leading to inhibition of symbiotic nitrogen fixation, increasing the likelihood of reactive oxygen species production. However, the nodules have a robust antioxidant system comprised of; metallo-protein superoxide dismutases, catalases, ascorbate and glutathione, all serving to protect against enhanced oxidation (Naya et al., 2007).

Soybean (*G. max*) is inherently sensitive to chilling with temperature-dependent limitations on growth, development and yield being apparent below 15 ºC (Gass et al., 1996). Soybeans are particularly sensitive to lower temperatures during flowering with a single night of dark-chilling (8 °C minimum), being sufficient to inhibit pod formation (Hume and Jackson, 1981). In addition, soybean photosynthesis is highly sensitive to inhibition by dark-chilling, a trait that is linked to loss of photosynthetic enzyme activity (Van Heerden et al., 2003) and effects on photosystem II efficiency (Krüger et al., 2014). Moreover, the sensitivity of photosynthesis to dark-chilling in nodulated soybeans is strongly contributed to by chilling-induced inhibition of symbiosis (Van Heerden et al., 2008). Despite the importance of soybean in world agriculture, relatively little information is available in the literature about the mechanisms that cause or contribute to chilling sensitivity. Indeed, the most studied aspect of chilling tolerance in soybean have focused on stress exposure during seed germination (Cheng et al., 2010), and yield reduction as a product of chilling exposure during flowering (Gass et al., 1996). However, enhanced tolerance to chilling is an important trait at every stage of plant development, with photosynthetic efficiency being inherently linked to crop yield (Richards, 2000; Zhu et al., 2010). Thus the maintenance of photosynthesis in soybean that are exposed to chilling temperatures is a desirable trait, though limited research has been conducted in this area (Van Heerden et al., 2004b).

Both drought and dark-chilling lead to extensive loss of chlorophyll from the leaves, suggesting that the chilled soybean leaves enter premature senescence (Van Heerden et al., 2003, 2008; Kunert et al.,

2016). Senescence occurs as genetically-programmed stage of leaf development but it can also be induced at earlier developmental stages by environmental exposure to stresses. Senescence is reversible until the final stages, where accumulation of salicylic acid induces programmed cell death (PCD) (Van Doorn and Woltering, 2004; Zhang et al., 2013). The onset of PCD and senescence is marked by changes in protein content and composition, particularly a shift from protein metabolism to catabolism. Cysteine proteases are particularly important enzymes catalysing protein degradation during senescence, but their precise functions in stress-induced senescence are not well understood (Beers et al., 2000; Bhalerao et al., 2003; Guo, 2013). Whilst many cysteine proteases are localised in the vacuole and cytosol, they are also observed in senescence-associated vesicles (SAV, also known as senescence associated vacuoles). In leaves, these vesicles have a lower pH than the primary cell vacuole and are believed to transport chloroplast proteins to the central vacuole for degradation during senescence (Otegui et al., 2005; Carrión et al., 2014; Martínez et al., 2008). RuBisCO is the most abundant plant protein, with functions both in photosynthesis and in nitrogen storage, prior to nitrogen remobilization to the developing seed during senescence. The pathway of RuBisCO degradation remains uncertain but evidence shows that the protein may be degraded both inside and outside of the chloroplast (Irving and Robinson, 2006). Whilst metallo-proteases and aspartic proteases participate in chloroplast protein turnover (Nair and Ramaswamy, 2004; Kato et al., 2004), cysteine proteases have also been implicated in chloroplast protein degradation (Prins et al., 2008).

The activity of cysteine proteases in plant cells is predominantly modulated through the presence of specific inhibitors called cystatins. The best characterised plant cystatin is oryzacystatin I (OCI), derived from rice (*Oryza sativa*) (Masoud et al., 1993). Transgenic tobacco lines that constitutively express OCI under the control of the cauliflower mosaic virus 35S promoter have a slower growth phenotype and show enhanced tolerance to chilling temperatures (Van der Vyver et al., 2003b). Moreover, the leaves of OCI expressing tobacco plants show increased accumulation of RuBisCo compared to Wt controls, (Prins et al., 2008). Additionally ectopic cystatin expression blocks stress-induced PCD in soybean (Solomon et al., 1999).

To explore the role of cysteine proteases and their inhibitors in the regulation of stress responses, independent transgenic soybean lines expressing OCI (SOC1, SOC-2 and SOC-3) were produced and characterised in terms plant growth and sensitivity to drought (Quain et al., 2014) and low nitrogen-induced senescence (Quain et al., 2015). The following studies were designed to characterise transgenic soybean lines ectopically expressing OCI, focussing particularly on responses to dark-chilling. In addition, experiments were performed to identify senescence-associated redox transcripts in soybean nodules and to compare how these transcripts were changed in response to drought. For these studies, Wt plants and plants of the three independent transgenic soybean lines expressing OCI (SOC1, SOC-2 and SOC-3) were grown to maturity in the absence of stress to compare the effects of

OCI expression on the shoot phenotype. Subsequently, the effects of dark-chilling on nodule, root and shoot parameters were assessed in the Wt and transgenic lines. Finally, the effects of drought stress on gene expression in the nodule were determined. Together, these measurements provide a brief overview of the effects of OCI expression on soybean phenotype in the absence and presence of stress.

3.2. Results

3.2.1. Effect of OCI expression on shoot morphology

Wild type (Wt) soybeans and three independent transformed lines of soybean expressing OCI (SOC-1, SOC2, SOC-3; Appendix I) were sown in soil and grown to maturity (Figure 3.2.1 1). The shoots of the transgenic lines were visibly different from the Wt after 12 weeks growth under glasshouse conditions, having a more "bushy" phenotype than the Wt (Figure 3.2.1 1 A). Moreover, the OCI expressing lines had significantly more shoot branches (Figure 3.2.1 1 B).

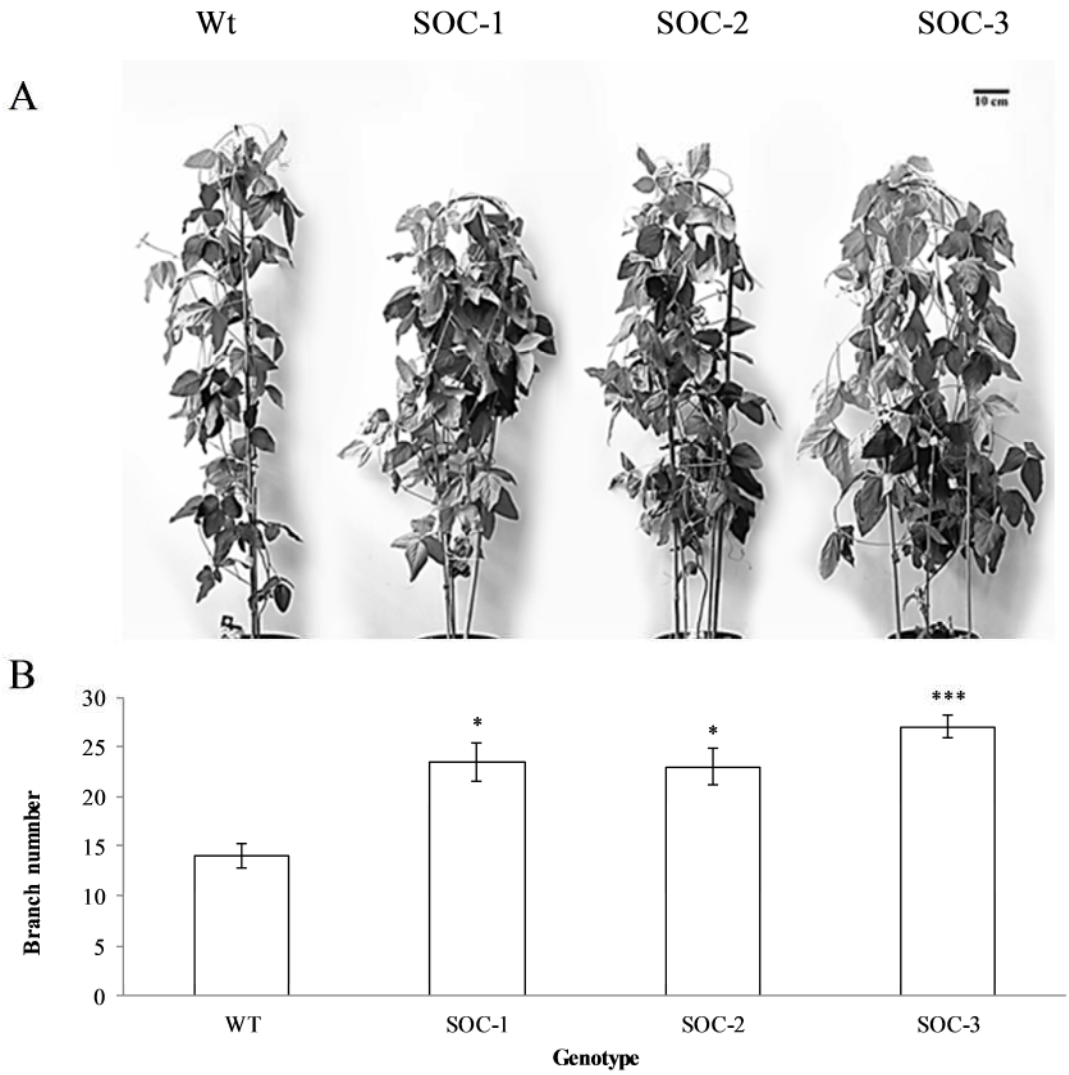

Figure 3.2.1-1: Shoot phenotype (A) and branch number (B) in 12 week old soybean wild type (Wt) and OCI expressing lines (SOC-1, SOC-2, SOC-3). Means ± SE (n=12). Students *t*-test between Wt and OCI lines indicated by asterisks (* = P<0.05, ** = P<0.01, *** = P<0.001).

3.2.2. The effect of OCI expression on root nodules and their responses to chilling

For these experiments, the Wt and OCI (SOC-1, SOC-2 and SOC-3) expressing lines (Quain et al., 2015) were inoculated with *Bradyrhizobium japonicum* and grown on vermiculite with nitrogen-free Hoagland's solution for 3 weeks. Half of the plants were grown under these conditions for a further 7 days (Control conditions) and half were exposed to 7 consecutive nights of dark-chilling (4 °C; Chilled). After the 7th night of dark-chilling the root systems were removed from vermiculite and gently washed with distilled water. A visual inspection of the root systems (Figure 3.2.2-1) revealed that in the absence of stress root architecture was more extensive in the Wt and SOC-3 plants than the other two lines (Figure 3.2.2-1, Control). Surprisingly, the root systems of the plants that had been exposed to 7 nights of dark-chilling (Figure 3.2.2-1, Chilled) were visibly more extensive than the roots of unstressed controls (Figure 3.2.2-1, Control).

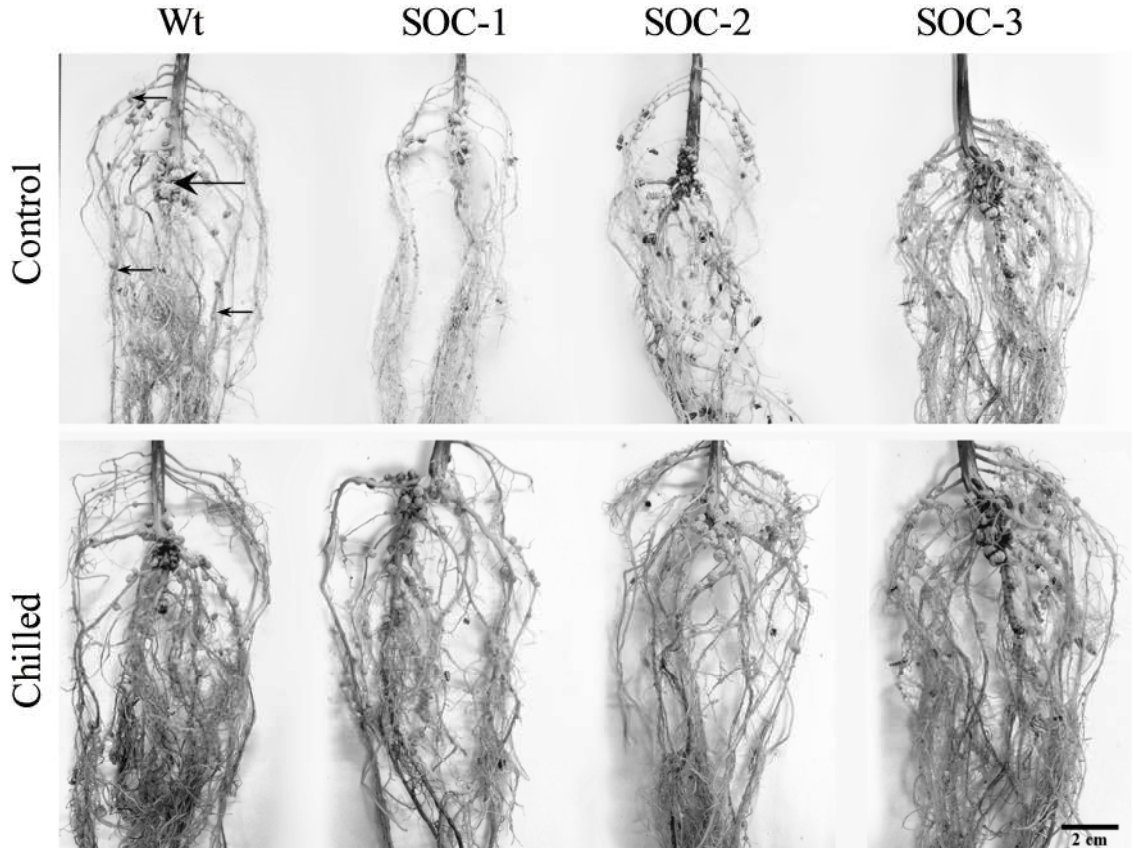

Figure 3.2.2-1: Root phenotypes of 4 week old soybean; Wt and OCI lines (SOC-1, SOC-2 and SOC-3). Plants were inoculated with *Bradyrhizobium japonicum* on vermiculite media and grown in glasshouse for 3 weeks before exposure to either 7 consecutive nights of dark-chilling or maintenance under glasshouse conditions. Large and small black arrows on Wt control indicate crown root nodules and lateral root nodules respectively. Scale bar represents 2 cm.

Root biomass was determined as the fresh weight of whole root system at 4 weeks under control conditions (Figure 3.2.2-2). The Wt, SOC-2 and SOC-3 plants had significantly greater root biomass than the SOC-1 line (Figure 3.2.2-2) in the absence of stress. Root biomass was similar between the Wt, SOC-2 and SOC-3 lines following 7 consecutive nights of dark chilling, with root biomass in these lines being significantly greater than SOC-1 (Figure 3.2.2-2). However, 7 consecutive nights of dark chilling did not cause a significant decrease in the root biomass of SOC-1 when compared to SOC-1 plants grown under control conditions. However, a significant decrease in fresh root biomass was observed in all other lines (Figure 3.2.2-2).

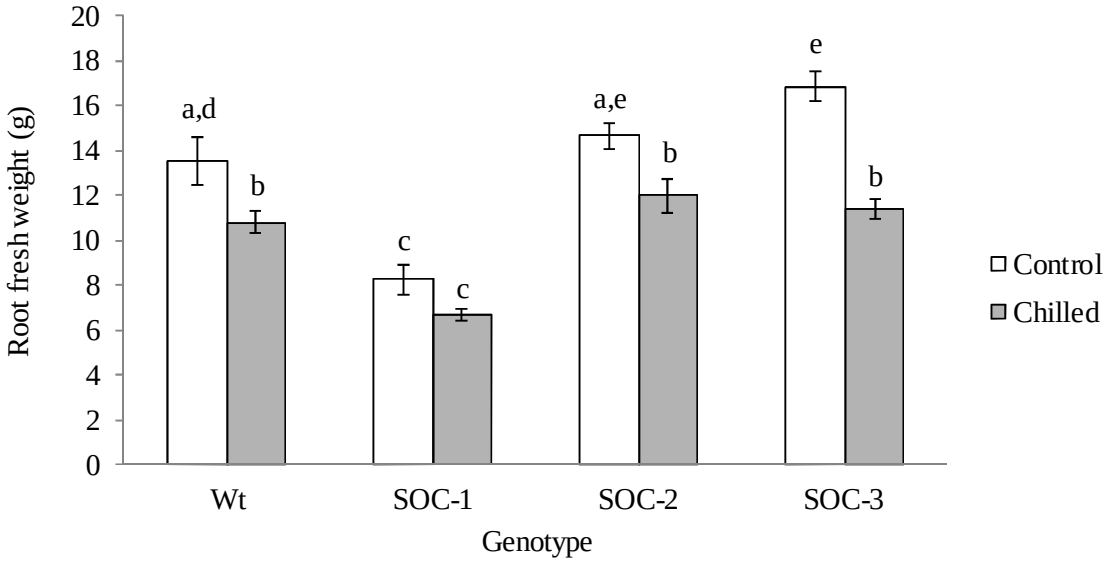

Figure 3.2.2-2: Root fresh weight of 4 week old soybean, wild type; (Wt) and three independent transformed lines expressing OCI; SOC-1, SOC-2, SOC-3. Plants were inoculated with *Bradyrhizobium japonicum* in vermiculite media and grown in glasshouse for 3 weeks before exposure to either 7 consecutive nights of dark-chilling or maintenance under glasshouse conditions. Data are mean values ± SE (n = 8). Open bars show control plants, grey bars show dark-chilled plants. Significance was determined by Students *t*-test. Where letters are shared there is no significant difference.

Nodule parameters were measured by excising the crown root nodules and the lateral root nodules from the root system. A visual inspection of the crown root nodules (Figure 3.2.2-3) revealed that nodules were larger in the Wt than the OCI expressing lines, under both control conditions and after plants that had been exposed to 7 consecutive nights of dark-chilling. Most notably the nodules of SOC-1 line were the smallest, both under control conditions and after exposure to dark-chilling (Figure 3.2.2-3).

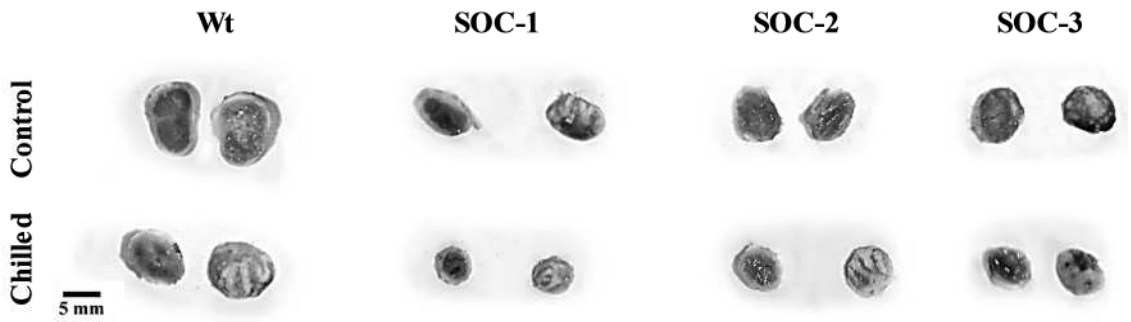

Figure 3.2.2-3: Crown root nodules of 4 week old soybean wild type; (Wt) and three independent transformed lines expressing OCI (SOC-1, SOC-2 and SOC-3). Plants were inoculated with *Bradyrhizobium japonicum* in vermiculite media and grown in glasshouse for 3 weeks before exposure to either 7 consecutive nights of dark-chilling or maintenance under glasshouse conditions. Scale bar represents 5mm.

Although the nodules of all three transgenic lines appeared to be smaller than the Wt, only the SOC-1 and SOC-3 nodules had a significantly smaller diameter than the Wt, in the absence of chilling stress (Figure 3.2.2-4). The diameter of the Wt, SOC-1 and SOC-2 nodules was not significantly decreased after 7 consecutive nights of dark-chilling (Figure 3.2.2-4). However, the diameter of SOC-1 nodules was significantly smaller as a result of exposure to chilling stress. Although the SOC-2 and SOC-3 lines tended towards a smaller nodule diameter following dark-chilling, values were not significantly different from those measured in the absence of stress (Figure 3.2.2-4).

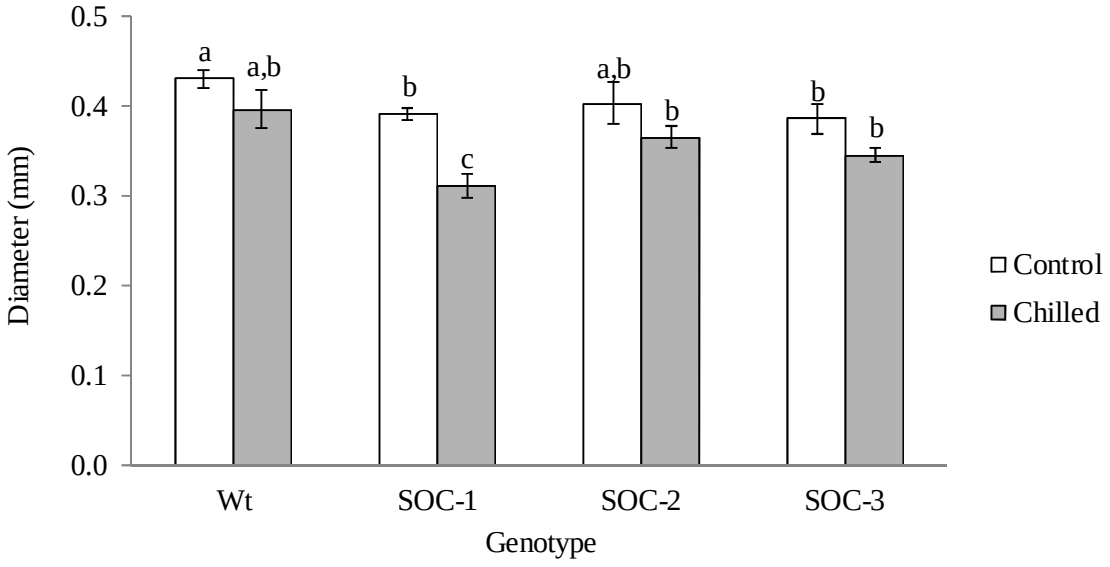

Figure 3.2.2-4: Nodule diameter of 4 week old soybean, displaying wild type; (Wt) and three independent transformed lines expressing OCI; SOC-1, SOC-2 and SOC-3. Plants were inoculated with *Bradyrhizobium japonicum* in vermiculite media and grown in glasshouse for 3 weeks before exposure to either 7 consecutive nights of dark-chilling or maintenance under glasshouse conditions. Data are mean values ± SE (n = 8). Open bars show control plants, grey bars show dark-chilled plants. Significance was determined by Students *t-test*. Where letters are shared no significant difference is present.

The number of nodules per plant was determined by counting both crown and lateral root nodules. In the absence of stress all three transgenic lines had significantly greater nodule numbers than the Wt (Figure 3.2.2-5). The roots of the Wt plants that had been exposed to 7 consecutive nights of dark-chilling has significantly more nodules than those that had been maintained at higher night temperatures (Figure 3.2.2-5). In contrast, nodule numbers per plant tended to be lower in the root systems all the transgenic lines after exposure to chilling stress than in plants maintained without chilling (Figure 3.2.2-5). However, nodule numbers were only significantly decreased after dark-chilling in the SOC-2 roots (Figure 3.2.2-5).

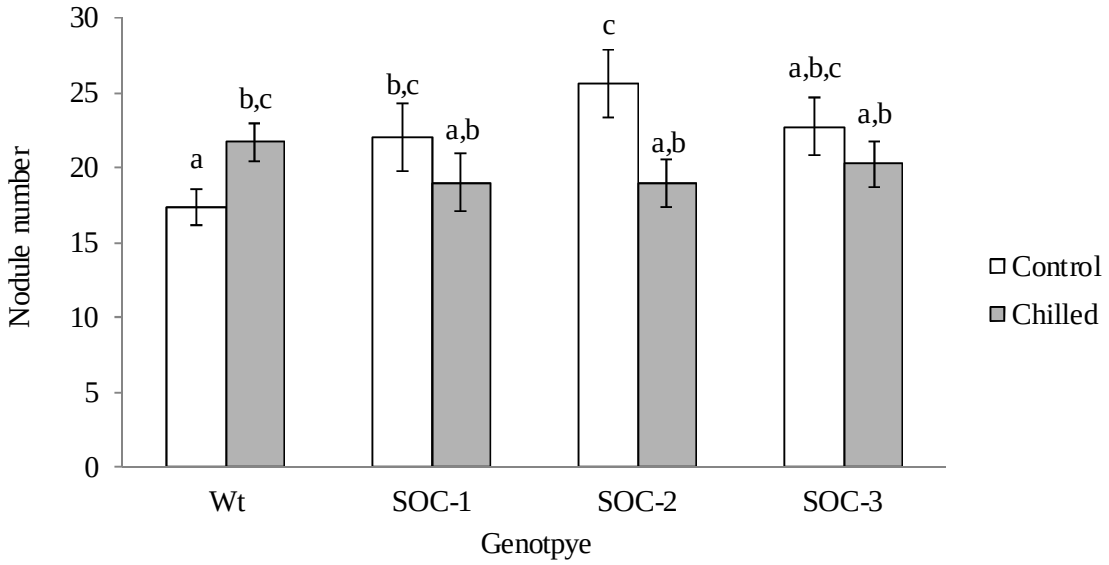

Figure 3.2.2-5: Number of crown and lateral root nodules of 4 week old soybean plants, displaying wild type; (Wt) and three independent transformed lines expressing the rice cysteine protease inhibitor oryzacystatin I (OCI); SOC-1, SOC-2 and SOC-3. Plants were inoculated with *Bradyrhizobium japonicum* in vermiculite media and grown in glasshouse for 3 weeks before exposure to either 7 consecutive nights of dark-chilling or maintenance under glasshouse conditions. Open bars show control plants, grey bars show dark-chilled plants. Data are mean values ± SE (n = 8). Significance was determined by Students *t*-test. Where letters are shared no significant difference is present.

3.2.3. 3 nights dark-chilling: photosynthetic parameters

In the following experiments, soybean plants were grown without nodulation for 2 weeks on vermiculite media with full strength Hoagland's solution. Half of the plants were then grown under these conditions for a further 3 days (Control conditions) and half were exposed to up to 3 consecutive nights of dark-chilling (4 °C; Chilled).

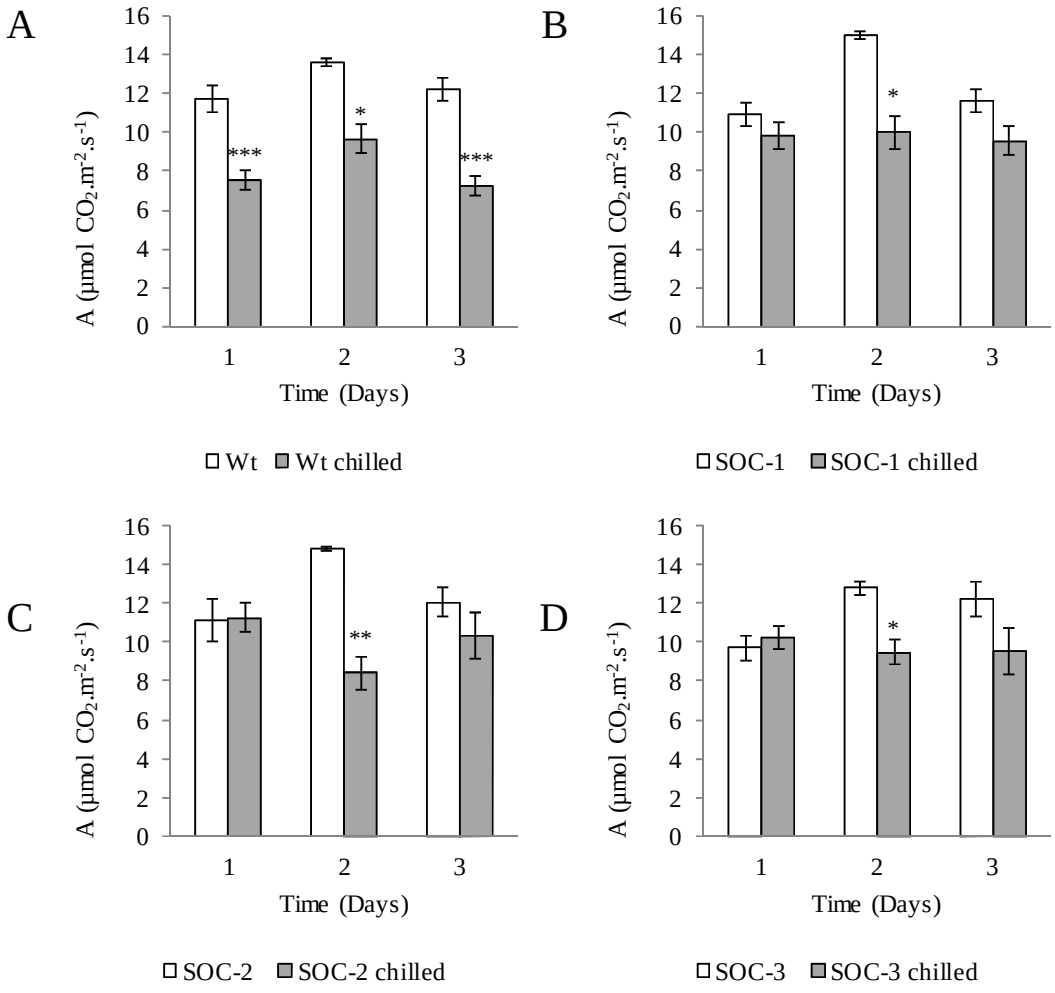

Figure 3.2.3-1: Carbon assimilation rates of soybean after 1, 2 and 3 consecutive nights of dark-chilling or maintenance under control conditions. Panels show; A) Wild type soybean; three independent transformed lines expressing OCI; B) SOC-1 C) SOC-2 and D) SOC-3. Significant difference between control grown and chilled plants has been determined using Students *t*-test, indicated by asterisks (* = P<0.05, ** = P<0.01, *** = P<0.001). Data are mean values ± SE (n = 12). Open bars show control plants, grey bars show dark-chilled plants.

Under control conditions photosynthetic rates were similar in all lines. However, Wt photosynthesis was significantly decreased after 1 night of dark-chilling (Figure 3.2.3-1 A). The rates of

photosynthesis were decreased to similar levels compared to unchilled controls after 2 and 3 consecutive nights of dark-chilling (Figure 3.2.3-1 A). In contrast to the Wt, exposure to 1 night of dark-chilling had no effect on the photosynthetic rate of any transgenic line. This was also the case after 3 consecutive nights of dark-chilling. Even though there was a trend towards lower photosynthesis in the chilled plants, this was not significant, however there was a significant decrease in photosynthesis in all lines after 2 consecutive nights of chilling (Figure 3.2.3-1 B, C, D).

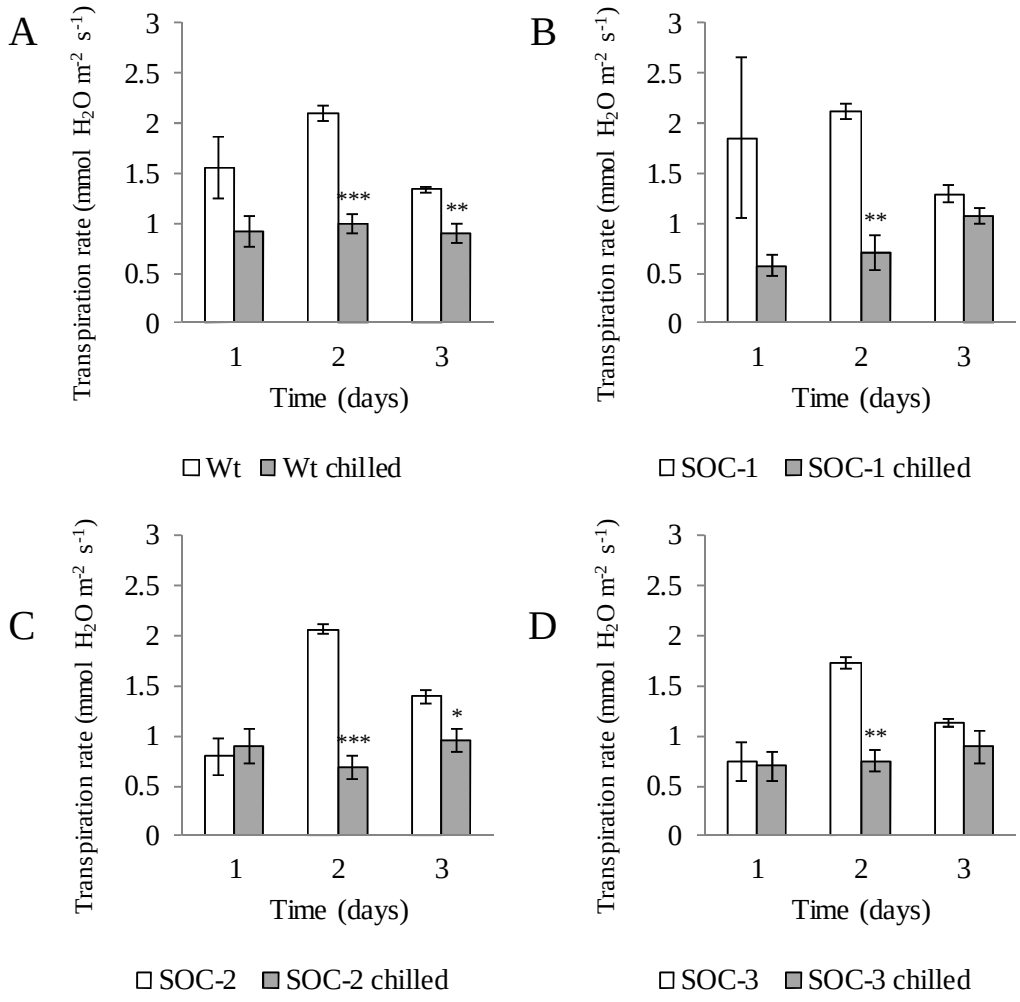

Figure 3.2.3-2: Transpiration rates of soybean after 1, 2 and 3 consecutive nights of dark-chilling or maintenance under control conditions. Panels show; A) Wild type soybean; three independent transformed lines expressing OCI; B) SOC-1 C) SOC-2 and D) SOC-3. Significant difference between control grown and chilled plants has been determined using Students *t*-test, indicated by asterisks (* = P<0.05, ** = P<0.01, *** = P<0.001). Data are mean values ± SE (n = 12). Open bars show control plants, grey bars show dark-chilled plants.

The rate of transpiration was decreased in the Wt and SOC-2 in response to 3 nights of dark-chilling (Figure 3.2.3-2 A, C). However, 3 consecutive nights of dark-chilling did not cause a significant decrease in the rate of transpiration for the SOC-1 and SOC-3 lines (Figure 3.2.3-2 B, D).

3.2.4. 3 nights dark-chilling: biomass accumulation

Shoot and root dry biomass was determined in soybean plants that had been grown for 2-weeks under control conditions and then grown for a further 3 days under these conditions or subjected to 3 consecutive nights of dark-chilling. Under control conditions the shoots of the Wt plants had significantly greater dry weight than the transgenic lines (Figure 3.2.4-1). Dark-chilling had little effect on the dry biomass of the shoots in any of the lines; although the SOC-1 and SOC-3 shoots had a significantly greater mass after exposure to dark-chilling for 3 nights than the plants maintained under control conditions (Figure 3.2.4-1).

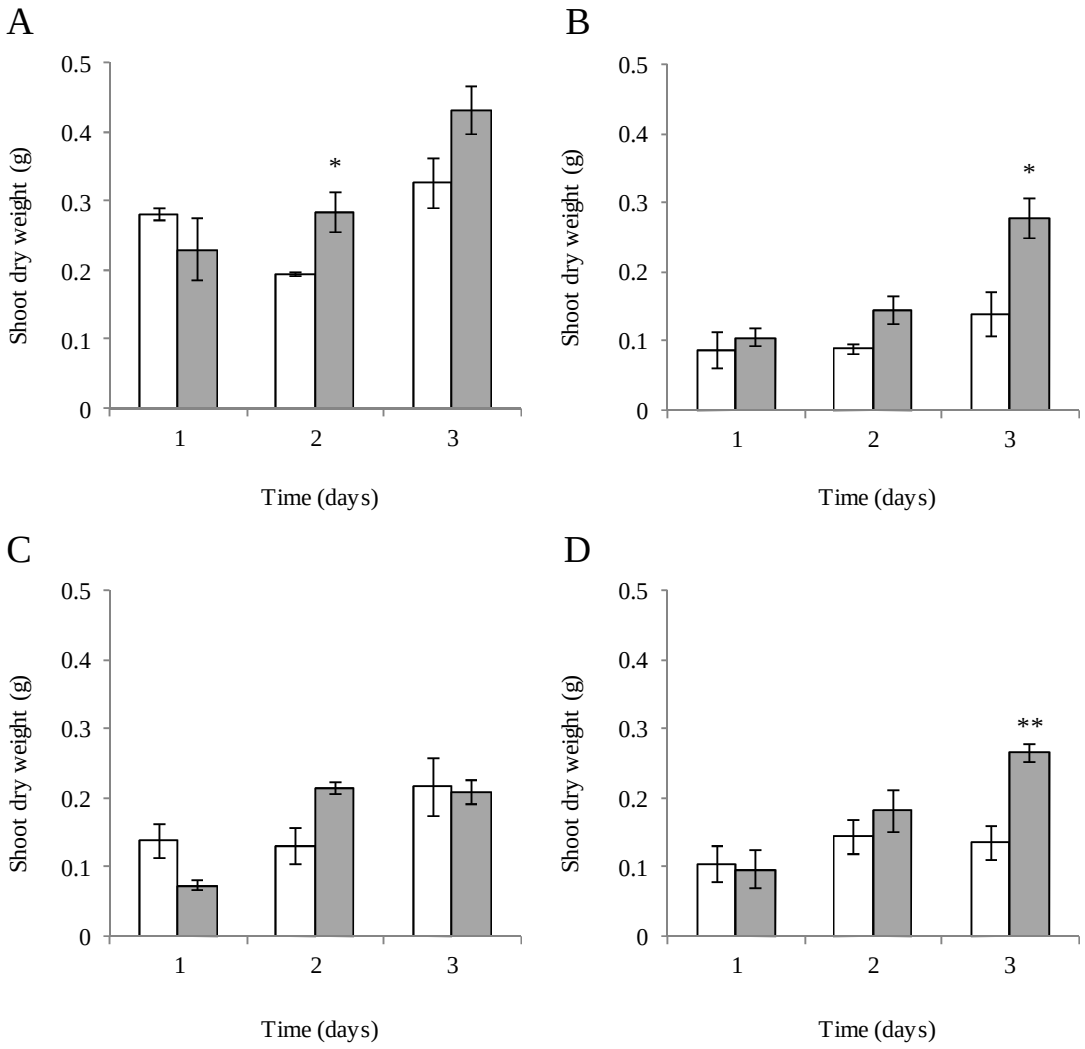

Figure 3.2.4-1: Shoot dry weight of soybean after 1, 2 and 3 consecutive nights of dark-chilling or maintenance under control conditions. Panels show; A) Wild type soybean; three independent transformed lines expressing OCI; B) SOC-1 C) SOC-2 and D) SOC-3. Significant difference between control grown and chilled plants has been determined using Students *t*-test, indicated by asterisks (* = P<0.05, ** = P<0.01, *** = P<0.001). Data are mean values ± SE (n = 12). Open bars show control plants, grey bars show dark-chilled plants.

Like the shoots, the roots of the Wt plants had significantly greater dry weight than the transgenic lines in the absence of stress (Figure 3.2.4-2). Dark-chilling did not inhibit dry biomass accumulation in the roots in any of the lines. The Wt roots had a significantly greater biomass after 2 or 3 nights of dark-chilling compared to the plants maintained under control conditions (Figure 3.2.4-2). This trend was also observed in the roots of the transgenic lines but in this case values were not always significant.

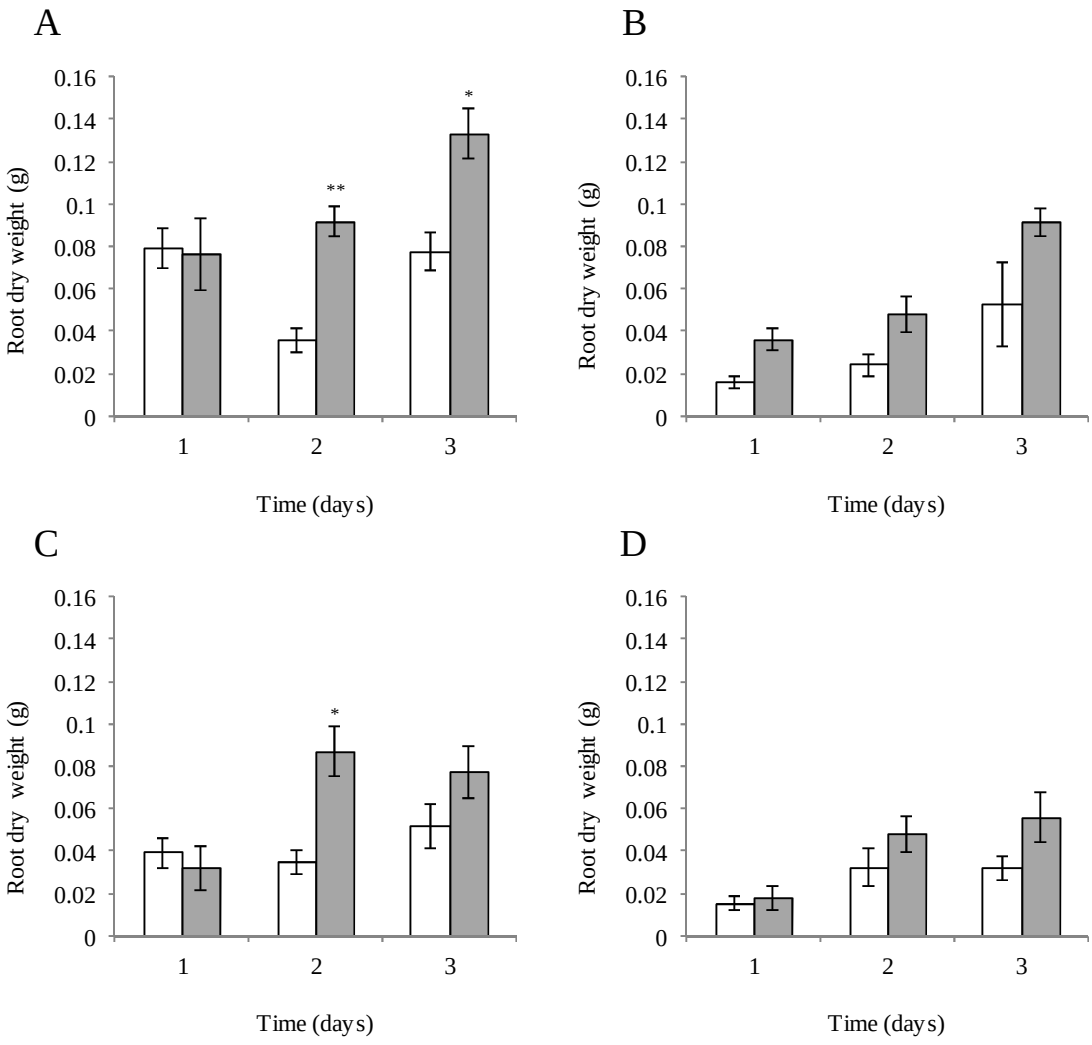

Figure 3.2.4-2: : Root dry weight of soybean after 1, 2 and 3 consecutive nights of dark-chilling or maintenance under control conditions. Panels show; A) Wild type soybean; three independent transformed lines expressing OCI; B) SOC-1 C) SOC-2 and D) SOC-3. Significant difference between control grown and chilled plants has been determined using Students *t*-test, indicated by asterisks (* = P<0.05, ** = P<0.01, *** = P<0.001). Data are mean values ± SE (n = 12). Open bars show control plants, grey bars show dark-chilled plants.

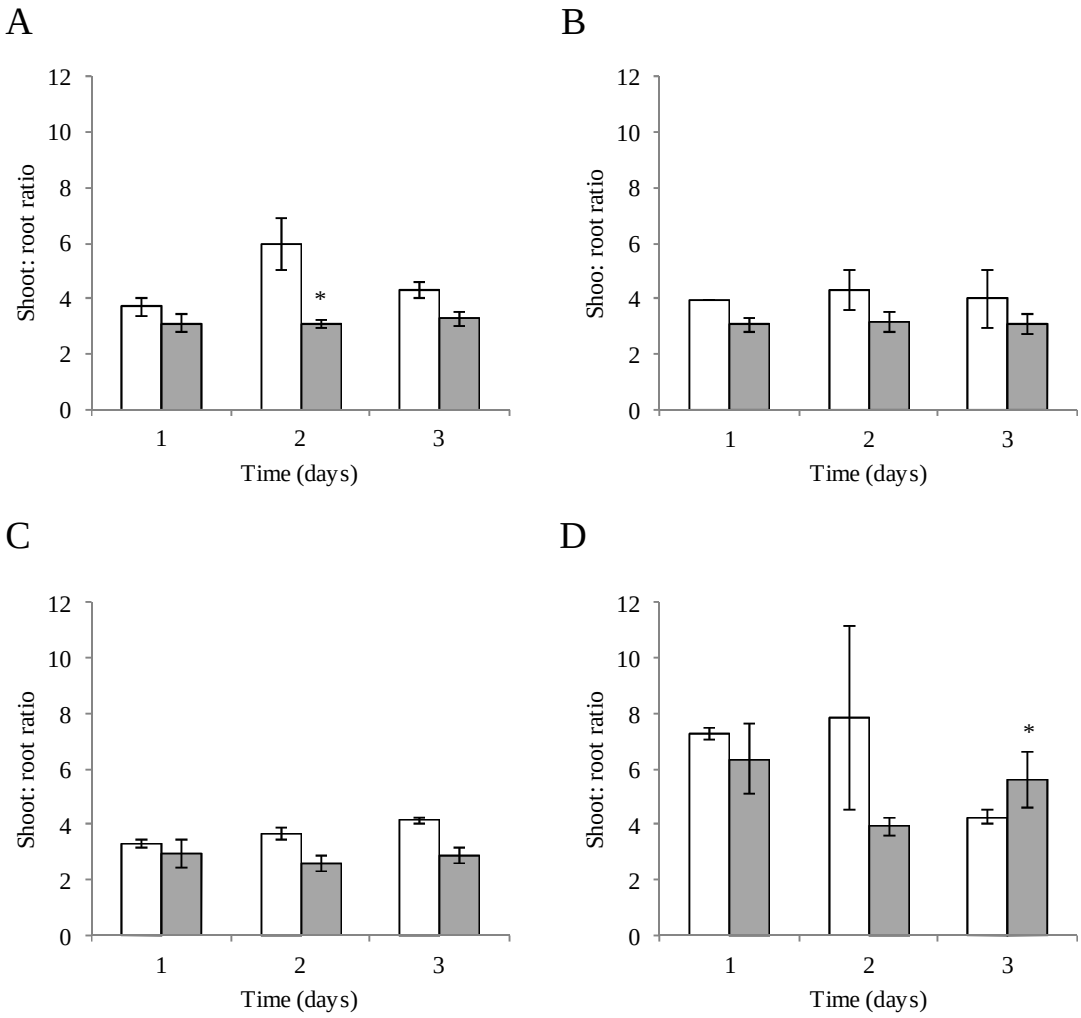

Figure 3.2.4-3: Shoot: Root ratio of soybean after 1, 2 and 3 consecutive nights of dark-chilling or maintenance under control conditions. Panels show; A) Wild type soybean; three independent transformed lines expressing OCI; B) SOC-1 C) SOC-2 and D) SOC-3. Significant difference between control grown and chilled plants has been determined using Students *t*-test, indicated by asterisks (* = P<0.05, ** = P<0.01, *** = P<0.001). Data are mean values ± SE (n = 12). Open bars show control plants, grey bars show dark-chilled plants.

The biomass partitioning between shoots and roots was not generally altered by OCI expression. However, the SOC-3 line has twice the shoot/root ratios of the other lines (Figure 3.2.4-3). In general, shoot: root ratios were not significantly affected by dark-chilling (Figure 3.2.4-3).

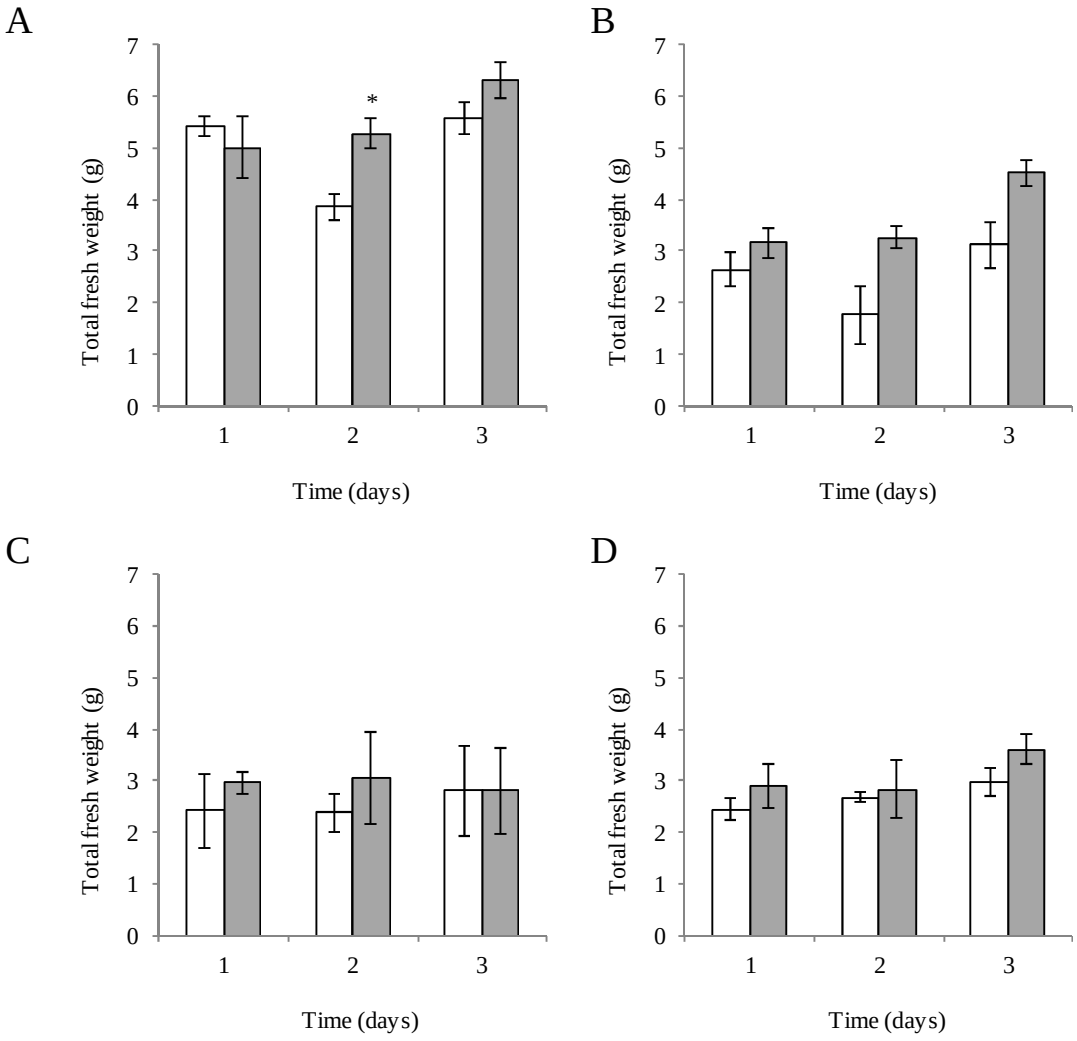

Figure 3.2.4-4: Total fresh weight of soybean after 1, 2 and 3 consecutive nights of dark-chilling or maintenance under control conditions. Panels show; A) Wild type soybean; three independent transformed lines expressing OCI; B) SOC-1 C) SOC-2 and D) SOC-3. Significant difference between control grown and chilled plants has been determined using Students *t*-test, indicated by asterisks (* = P<0.05, ** = P<0.01, *** = P<0.001). Data are mean values ± SE (n = 12). Open bars show control plants, grey bars show dark-chilled plants.

Whole plant biomass measured as fresh weight was only about half in the OCI-expressing lines than the Wt (Figure 3.2.4-4). Dark-chilling had little effect on whole plant fresh weight (Figure 3.2.4-4).

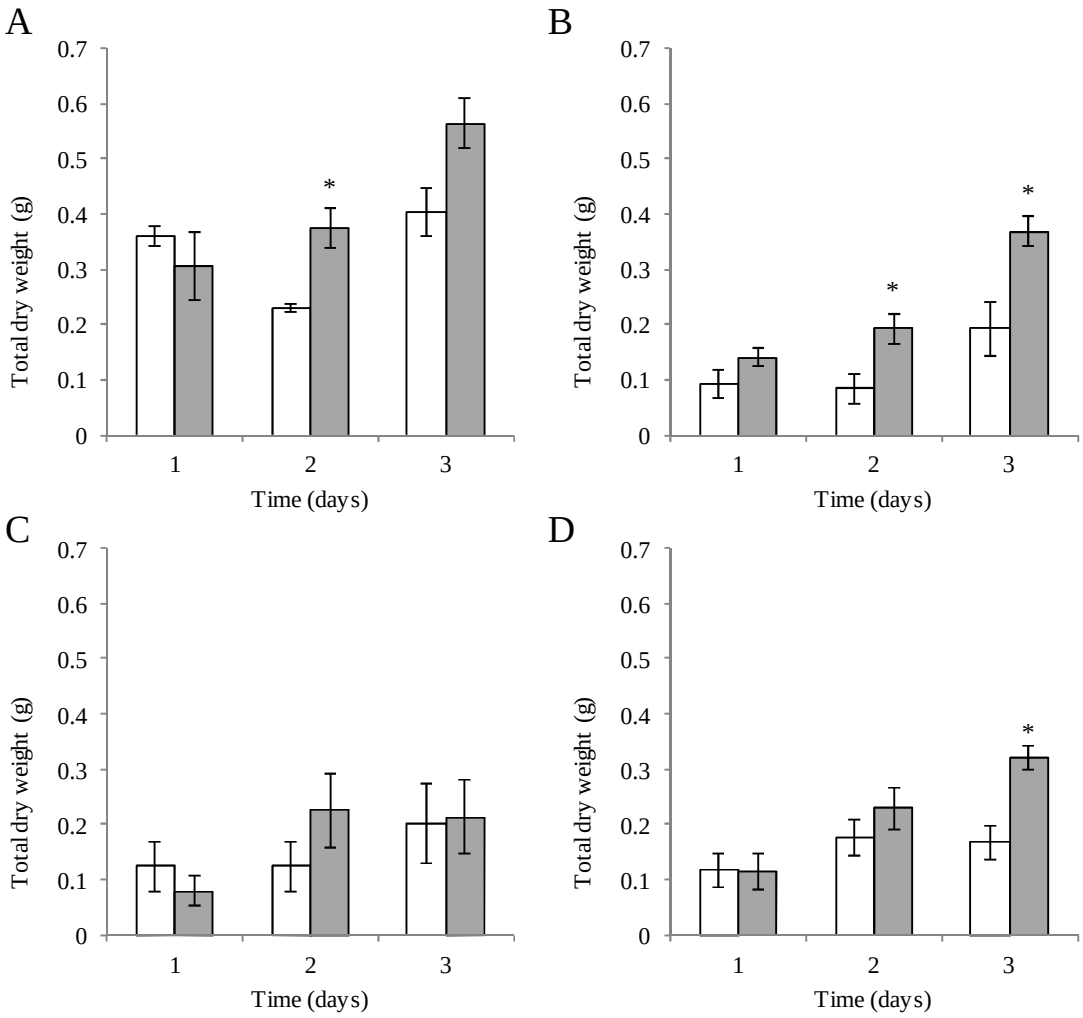

Figure 3.2.4-5: Total dry weight of soybean after 1, 2 and 3 consecutive nights of dark-chilling or maintenance under control conditions. Panels show; A) Wild type soybean; three independent transformed lines expressing OCI; B) SOC-1 C) SOC-2 and D) SOC-3. Significant difference between control grown and chilled plants has been determined using Students *t-test*, indicated by asterisks (* = P<0.05, ** = P<0.01, *** = P<0.001). Data are mean values ± SE (n = 12). Open bars show control plants, grey bars show dark-chilled plants.

Whole plant biomass measured as dry weight was only about half in the OCI-expressing lines than the Wt (Figure 3.2.4-5). Dark-chilling had little effect on whole plant dry weight (Figure 3.2.4-5).

Whole plant fresh/dry weight ratios were about double in the OCI-expressing lines than the Wt (Figure 3.2.4-6). Dark-chilling tended to decrease FW/DW (Figure 3.2.4-6) but this effect was independent of genotype.

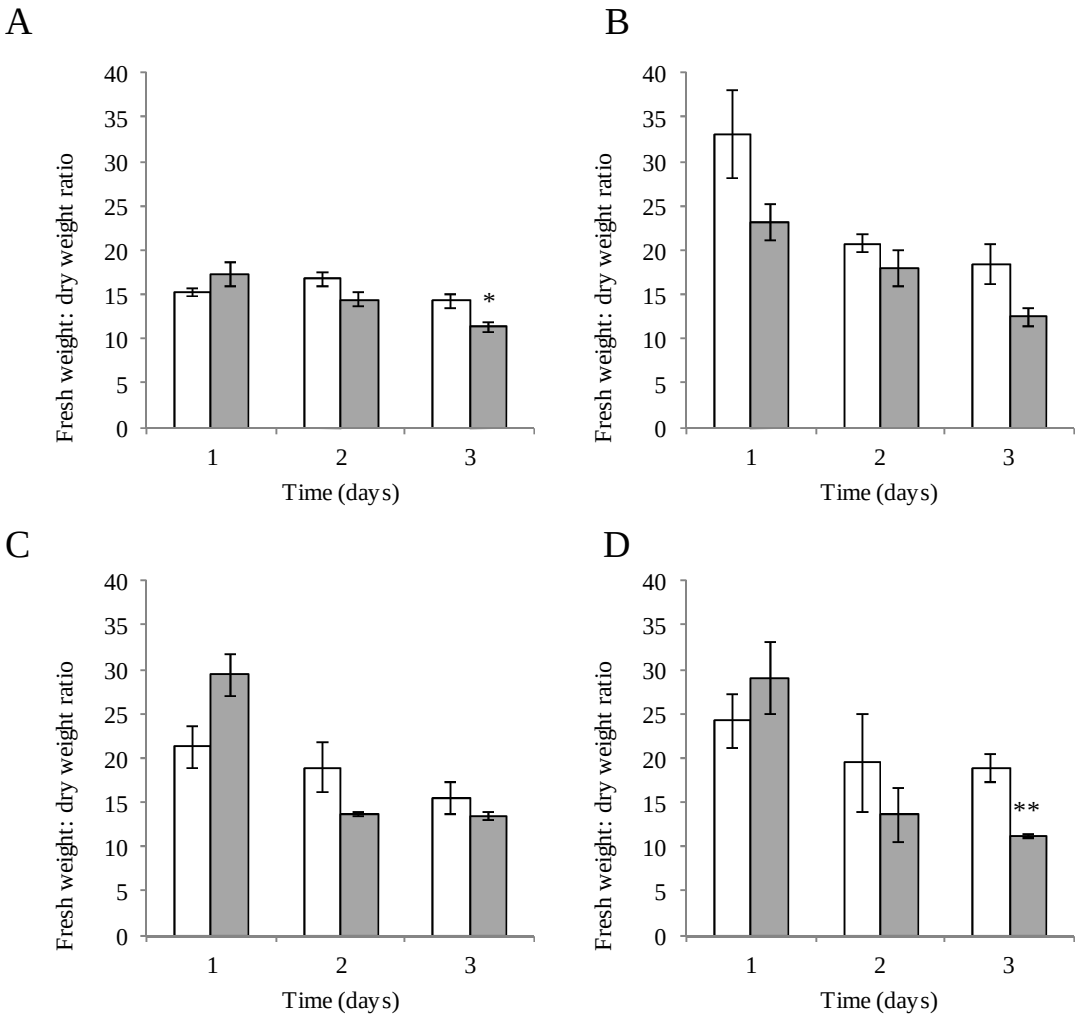

Figure 3.2.4-6: Fresh weight: dry weight ratio (FW/DW) of soybean after 1, 2 and 3 consecutive nights of dark-chilling or maintenance under control conditions. Panels show; A) Wild type soybean; three independent transformed lines expressing OCI; B) SOC-1 C) SOC-2 and D) SOC-3. Significant difference between control grown and chilled plants has been determined using Students *t-test*, indicated by asterisks (* = $P<0.05$, ** = $P<0.01$, *** = $P<0.001$). Data are mean values ± SE (n = 12). Open bars show control plants, grey bars show dark-chilled plants.

3.2.5. 9 nights dark-chilling: phenotype

While 3 consecutive nights of dark-chilling resulted in a decrease in photosynthesis, no inhibition of biomass accumulation was observed. The chilling treatment was therefore extended from 3 to 9 nights. Plants were therefore grown for14 days under control conditions followed by either maintenance under control conditions or exposure to 9 consecutive nights of dark-chilling. A visual inspection of the soybean shoots grown under this regime of control conditions showed that the Wt, SOC-1 and SOC-2 plants had a similar size and had the same number of leaves (Figure 3.2.5-1 Control). However SOC-3 shoots remained visibly smaller than the other lines.

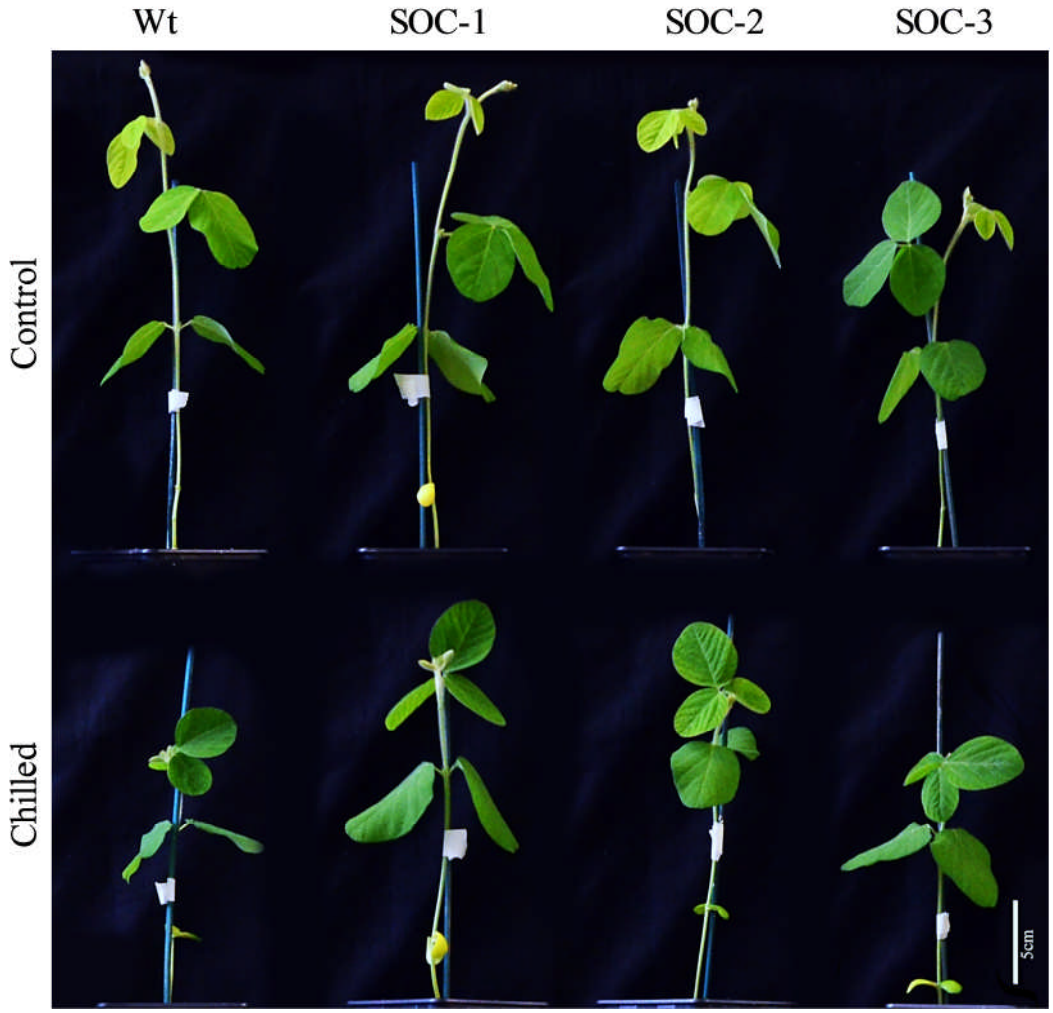

Figure 3.2.5-1: A comparison of the shoot phenotypes of soybean, displaying wild type; Wt (*Glycine max* 'Williams 82') and three independent transformed lines expressing the rice cysteine protease inhibitor oryzacystatin I (OCI); SOC-1, SOC-2 and SOC-3. Plants were grown for 2 weeks on nutrient supplemented vermiculite under control conditions before exposure to either 9 consecutive nights of dark-chilling (4ºC ±1ºC) or maintenance under control conditions.

Nine consecutive nights of dark-chilling led to a decrease in the stem height, together with the presence of fewer leaves in all of the lines (Figure 3.2.5-1 Chilled). The control plants had developed a second trifoliate leaf but this was absent from the plants exposed to dark-chilling. Wt plants were visibly smaller after the dark-chilling treatment, and showed the greatest chilling-induced reduction in height. Moreover, 2 of the OCI expressing lines (SOC-1 and SOC-2), showed a greater shoot height after chilling compared to the Wt (Figure 3.2.5-1).

3.2.6. 9 nights dark-chilling: photosynthesis

In the absence of stress, photosynthetic carbon assimilation was the similar in all the lines (Figure 3.2.6-1 Control). Photosynthesis was significantly decreased in all the lines after 9 consecutive nights of exposure to dark-chilling. However, SOC-1, SOC-2 and SOC-3 leaves displayed significantly higher rates of carbon assimilation compared to Wt after chilling treatment (Figure 3.2.6-1 Chilled).

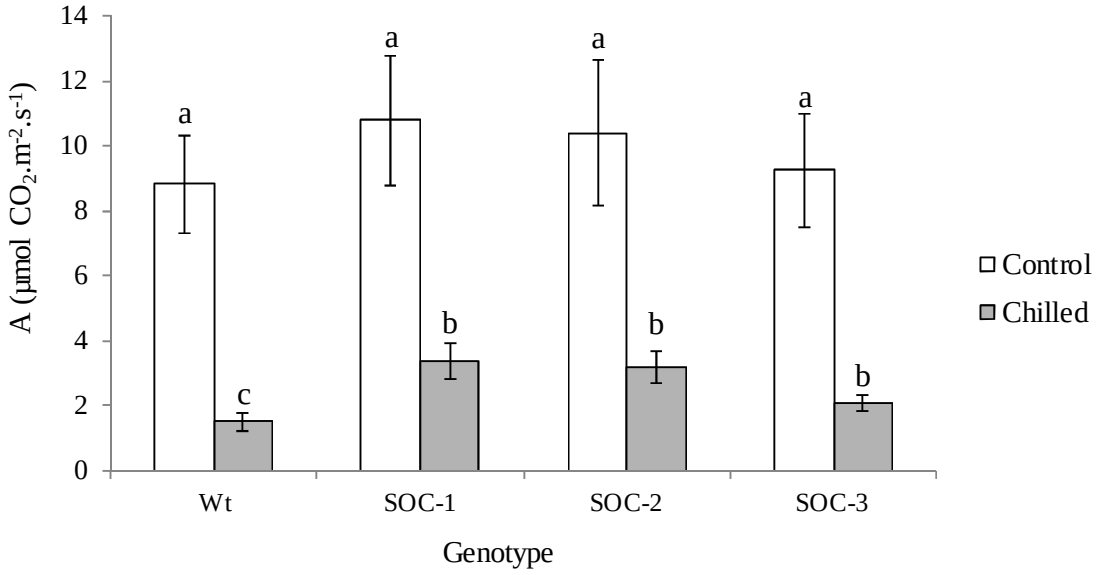

Figure 3.2.6-1 A comparison of the photosynthetic rates of soybean wild type (Wt) and three independent transformed lines expressing oryzacystatin I (OCI); SOC-1, SOC-2 and SOC-3. Data are the mean values of photosynthesis ± SE (n = 12). Significance is shown by *t-test* (P=<0.05). Where letters are shared there is no significant difference.

Exposure to 9 consecutive nights of dark-chilling significantly decreased transpiration rates in the Wt leaves. In comparison, the chilled leaves of the SOC-1, SOC-2 and SOC-3 lines either displayed comparable rates of transpiration to the leaves maintained under control conditions, or in the case of SOC-2, the leaves showed a higher rate after chilling exposure (Figure 3.2.6-2).

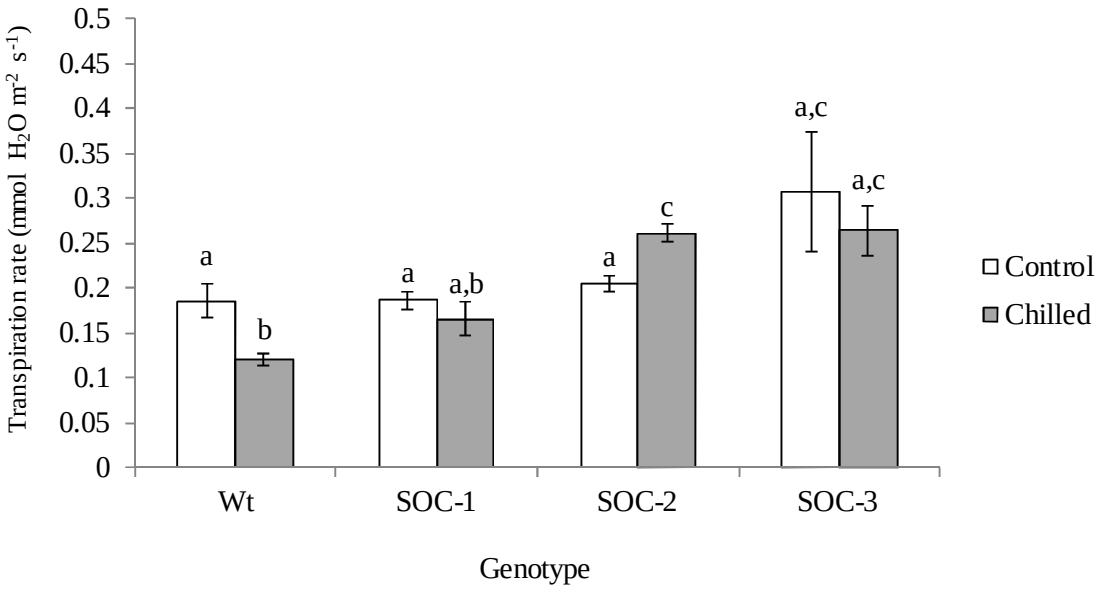

Figure 3.2.6-2: A comparison of the transpiration rates of soybean, wild type (Wt) and three independent transformed lines expressing oryzacystatin I (OCI); SOC-1, SOC-2 and SOC-3. Data are the mean values of photosynthesis ± SE (n = 12). Significance is shown by *t-test* (P=<0.05). Where letters are shared there is no significant difference.

3.2.7. 9 nights dark-chilling: biomass accumulation

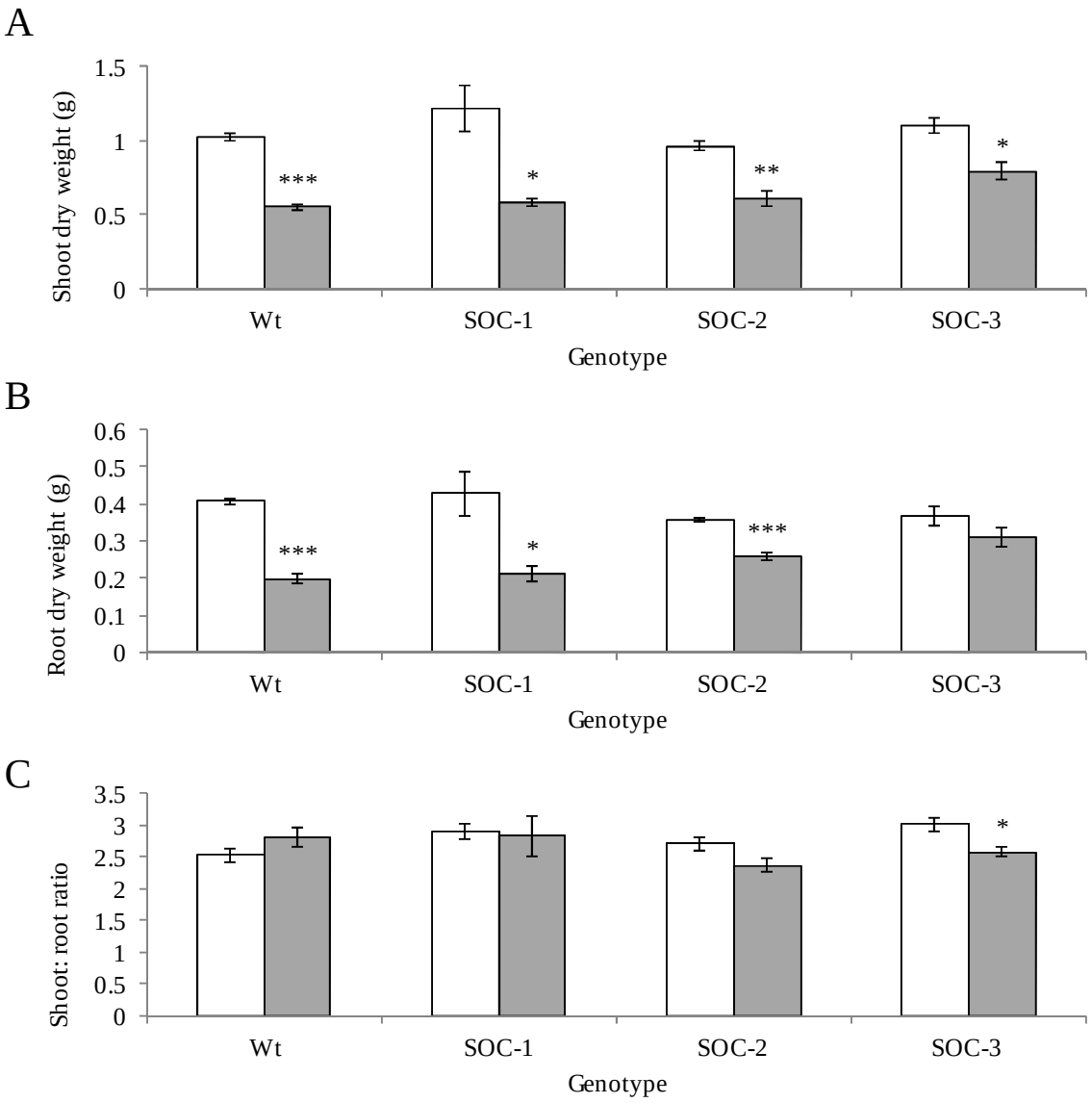

Figure 3.2.7-1: A) shoot dry biomass B) root dry biomass C) shoot: root ratio of soybean wild type (Wt) and three independent transformed lines expressing OCI; SOC-1, SOC-2 and SOC-3. Plants were grown in a controlled environment chamber for 2 weeks before exposure to either 9 consecutive nights of dark-chilling or maintenance under control conditions. Data are mean values ± SE (n = 12). Values that are significantly different between control plants and chilled plants have been determined using Student's *t*-test, indicated by asterisks (* = <0.05, ** = <0.01, *** = <0.001).

In the absence of the chilling treatment, the accumulation of dry weight in shoots (Figure 3.2.7-1 A) and roots (Figure 3.2.7-1 B) was similar in all the lines at the 23 day growth stage. The shoot: root ratios were the same in all the lines that were maintained under control conditions (Figure 3.2.7-1 C). The dry weight of the shoot was decreased in all the lines after 9 consecutive nights of exposure to dark-chilling (Figure 3.2.7-1 A). Similarly the Wt, SOC-1 and SOC-2 lines showed a chilling-induced

decrease in root dry weight after chilling (Figure 3.2.7-1 B). However, the SOC-3 plants showed no significant reduction in root dry weight after chilling treatment (Figure 3.2.7-1 C). The shoot: root ratios were not altered by chilling. Under dark-chilling conditions, there were no apparent differences in the Wt, SOC-1 and SOC-2 lines in terms of shoot: root ratio. However there was an observable difference in the shoot: root ratio of SOC-3 after dark-chilling exposure (Figure 3.2.7-1 C).

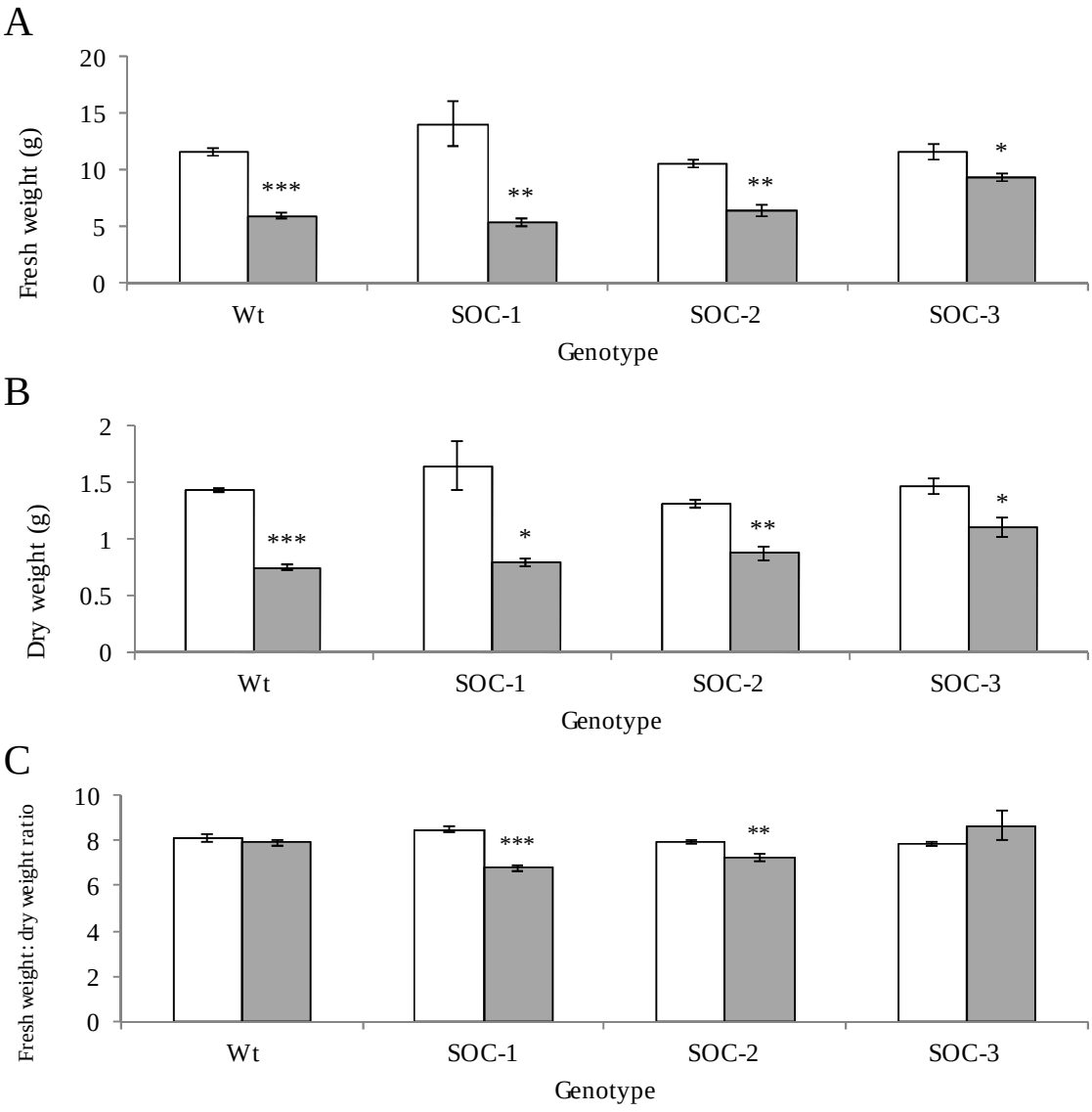

Figure 3.2.7-2: A) fresh weight; B) dry weight; C) fresh weight: dry weight ratio (FW/DW); of soybean wild type (Wt) and three independent transformed lines expressing OCI; SOC-1, SOC-2 and SOC-3. Plants were grown in a controlled environment chamber for 2 weeks before exposure to either 9 consecutive nights of dark-chilling or maintenance under control conditions. Data are mean values ± SE (n=12). Values that are significantly different between control plants and chilled plants have been determined using Students *t*-test, indicated by asterisks (* = P<0.05, ** = P<0.01, *** = P<0.001).

In the absence of dark-chilling treatment the fresh weight of all genotypes was comparable (Figure 3.2.7-2 A). However, a significant decrease in their total fresh biomass was observed in all genotypes after exposure to 9 consecutive nights of dark-chilling (Figure 3.2.7-2 A). Similarly, the total dry weight was the same in all lines after 23 days of growth under control conditions. Dark-chilling caused a significant reduction in dry biomass accumulation in all genotypes (Figure 3.2.7-2 B). The FW/DW was comparable in all lines that had been maintained under control conditions. However, while dark-chilling exposure caused a decrease in the FW/DW ratio in the SOC-1 and SOC-2 lines, chilling treatment had no apparent effect on this parameter for the Wt and SOC-3 lines (Figure 3.2.7-2 C).

3.2.8. Dark-chilling's effect on the levels of *CCD7* and *CCD8* transcripts

The following studies were designed to characterise the effect of both OCI expression and dark-chilling on the abundance of transcripts encoding the strigolactone biosynthesis enzymes, carotenoid cleavage dioxygenase (CCD)7 and (CCD)8. As an initial step the differential abundance of these transcripts between tissues was measured in Wt plants that had been maintained under control conditions for 15 days. The levels of *CCD7* (Figure 3.2.8-1A) and *CCD8* (Figure 3.2.8-1B) transcripts were lowest in stems and leaves, being more than 10 fold lower in these tissues than in roots.

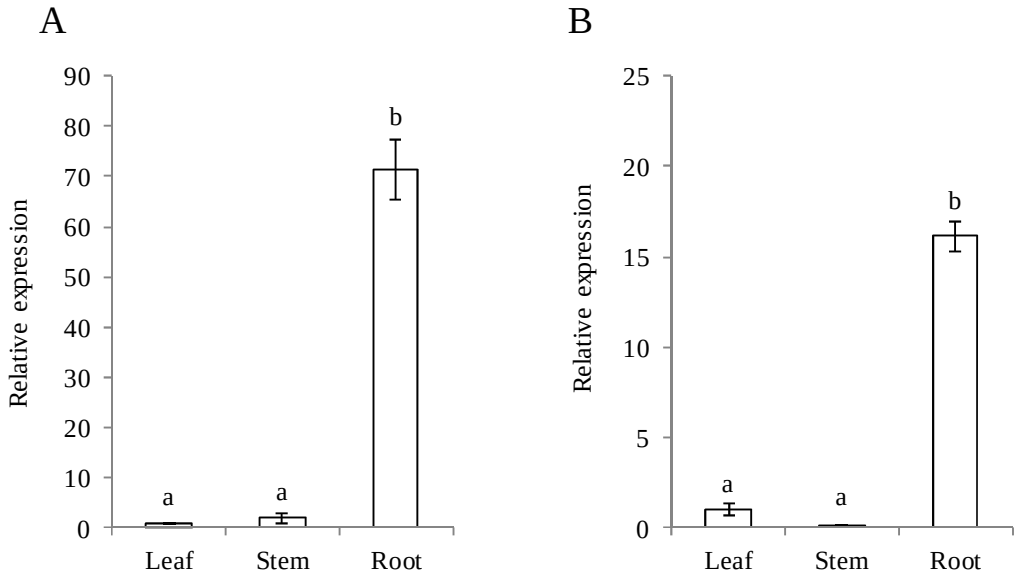

Figure 3.2.8-1: The relative levels of *CCD7* and *CCD8* transcripts in soybean leaf, stem and root tissues. Data are expressed relative to *ELONGATION FACTOR 1-β.* Fold expression changes are relative to expression in leaves; A) *CCD7* transcript levels; B) CCD8 transcript levels. Data are means ± SE (n=9). Significance is shown by Students *t-test* (P=<0.05).

Further qPCR was performed on Wt and the OCI expressing lines after 3 consecutive nights of dark-chilling (Figure 3.2.8-2). In the absence of chilling, the level of *CCD7* transcripts was lower in Wt leaves than in the OCI expressing lines (Figure 3.2.8-2 A). Exposure to dark-chilling did not have a significant effect on the abundance of *CCD7* transcripts in the leaves of any line, with the exception of SOC-2 which showed the highest levels of *CCD7* transcripts under chilling stress (Figure 3.2.8-2 A). Levels of *CCD7* expression in stem were lower in the Wt than the OCI expressing lines (Figure 3.2.8-2 B). Chilling had no significant effect on the levels of *CCD7* transcripts in the stems of any genotype, with the exception of SOC-2, which showed the highest levels of stem *CCD7* transcripts of all lines (Figure 3.2.8-2 C). The levels of *CCD7* transcripts were lower in SOC-1 roots than the Wt.

However, under dark-chilling conditions SOC-1 roots had the highest level of transcripts of all lines (Figure 3.2.8-2 C).

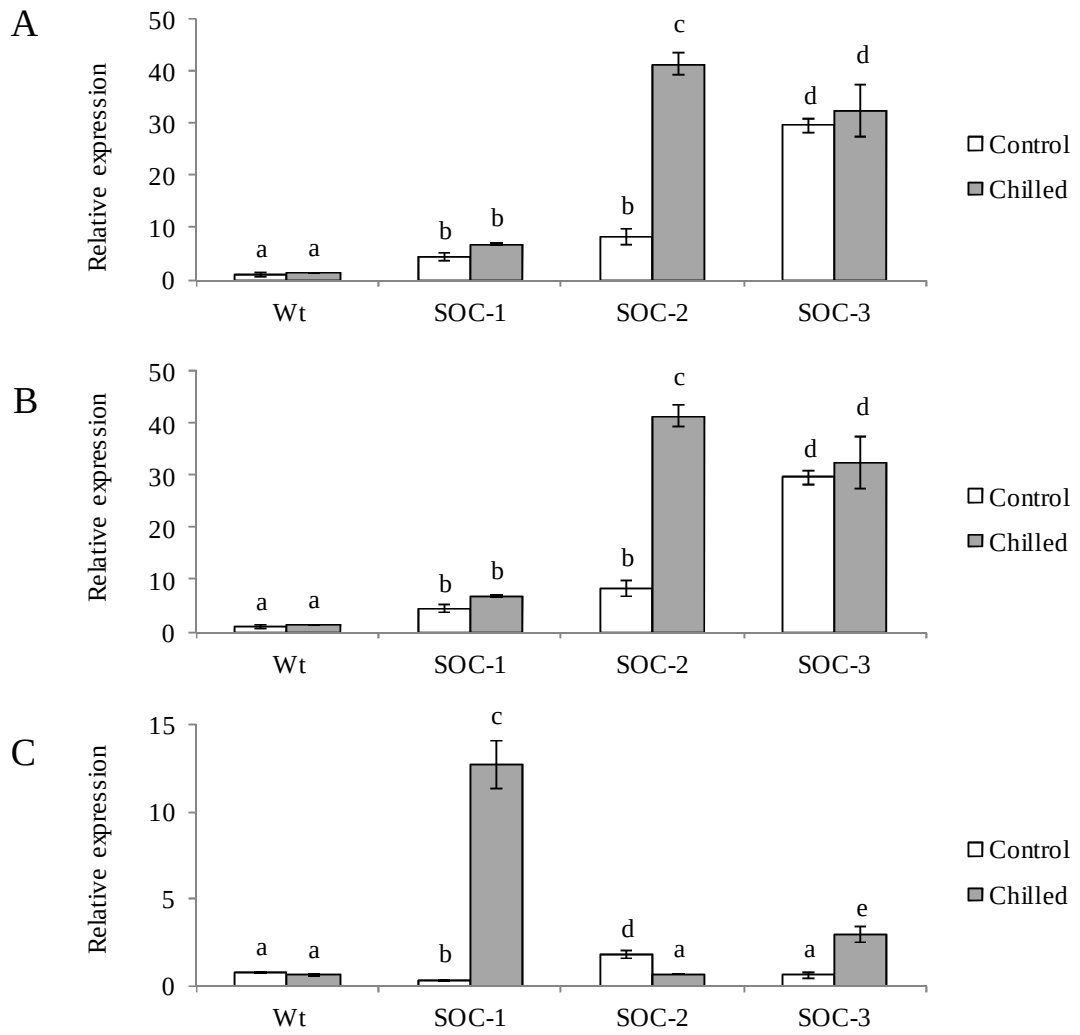

Figure 3.2.8-2: The relative levels of *CCD7* transcript in soybean leaves (A), stems (B) and roots (C). Plants were harvested after 14 days of growth under control conditions and an additional 3 days of either; maintenance under control conditions or exposure to 3 consecutive nights of dark-chilling. Data show expression levels normalised to the housekeeping gene elongation factor 1-β with fold expression change relative to expression in leaf tissue. Data are means ± SE (n=9). Open bars show control group, grey bars show dark-chilled group. Significance is shown by Students *t*-test (P=<0.05). Where letters are shared no significant difference is present.

Levels of *CCD8* transcripts were higher in the leaves of all OCI expressing lines than in the Wt (Figure 3.2.8-3). Dark-chilling had no significant effect on leaf *CCD8* transcripts, with the exception of SOC-2 which showed significantly higher levels of *CCD8* transcripts than controls and dark-chilled plants of all other lines (Figure 3.2.8-3 A). The levels of *CCD8* transcripts were similar in stem tissue from Wt, SOC-2 and SOC-3 plants under control conditions (Figure 3.2.8-3 B). However, SOC-1 stems showed significantly lower levels of *CCD8* transcripts than the other lines under control

conditions. Dark-chilling had no significant effect on *CCD8* transcripts in the stems of any line. Similarly, root tissue displayed no OCI or chilling dependent difference in CCD8 expression (Figure 3.2.8-3 C).

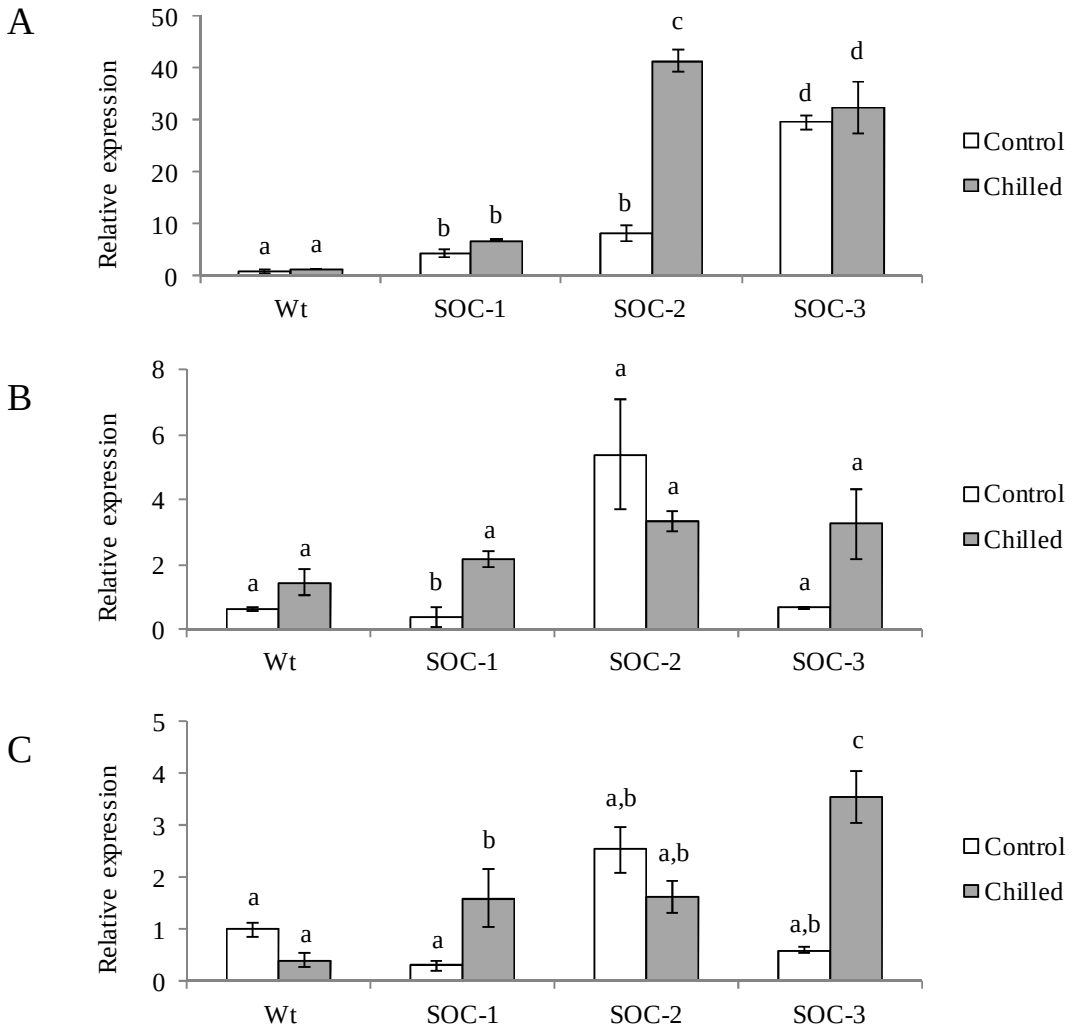

Figure 3.2.8-3 The relative levels of *CCD8* transcript in soybean leaves (A), stems (B) and roots (C). Plants were harvested after 14 days of growth under control conditions and an additional 3 days of either; maintenance under control conditions or exposure to 3 consecutive nights of dark-chilling. Data show expression levels normalised to the housekeeping gene elongation factor 1-β with fold expression change relative to expression in leaf tissue. Data are means ± SE (n=9). Open bars show control group, grey bars show dark-chilled group. Significance is shown by Students *t*-test (P=<0.05). Where letters are shared no significant difference is present.

3.2.9. Transcript changes in the nodules of soybean plants exposed to drought

A further series of experiments were performed to determine whether exposure to drought resulted in changes in the levels of redox-associated transcripts in the nodules of soybean plants exposed to drought (for which many signalling pathways are shared with chilling). The drought studies were performed by Dr Belen Marquez Garcia, who grew nodulated soybean under well-watered glasshouse conditions for 2 weeks. Thereafter, plants were either maintained under control conditions or deprived of water for up to 21 days. Nodules were harvested and RNA was extracted from the nodules of well-watered (control) plants and the drought-exposed plants. The levels of selected redox-associated transcripts (superoxide dismutase (*CSD* and *MSD*), glutathione-related (*GR*. *GRX*, *GST*), monodehydroascorbate reductase (*MDAR*), Dihydrolipoyl dehydrogenase (*DLD*) and aldehyde dehydrogenase (*ALDH*)), that had been identified previously in a soybean nodule transcriptome, and shown to be expressed in the developmental senescence of soybean nodules by Professor Karl Kunert (University of Pretoria, South Africa), were measured by quantitative real time PCR (qPCR).

A previous transcriptome comparison of the profiles of crown nodules harvested from 4 and 14 week-old plants had showed that copper-zinc superoxide dismutase 1 (*CSD1*) mRNAs were increased at the later stage of development (Figure 3.2.9-1) but copper-zinc superoxide dismutase 2 (*CSD2*) mRNAS were similar at both growth stages. The levels of magnesium/iron superoxide dismutases (*MSD*) mRNAs decreased at 14 weeks compared to the earlier developmental stages (Figure 3.2.9-1). qPCR analysis of these transcripts in soybean nodules from well-watered plants compared to those deprived of water for 21 days. The levels of *CSD1* transcripts were significantly lower under drought compared to well-watered conditions (Figure 3.2.9-2). In contrast the abundance of *CSD2* transcripts was increased in the nodules subjected to drought (Figure 3.2.9-2). Drought had no significant effect on the *MSD* transcript levels (Figure 3.2.9-2).

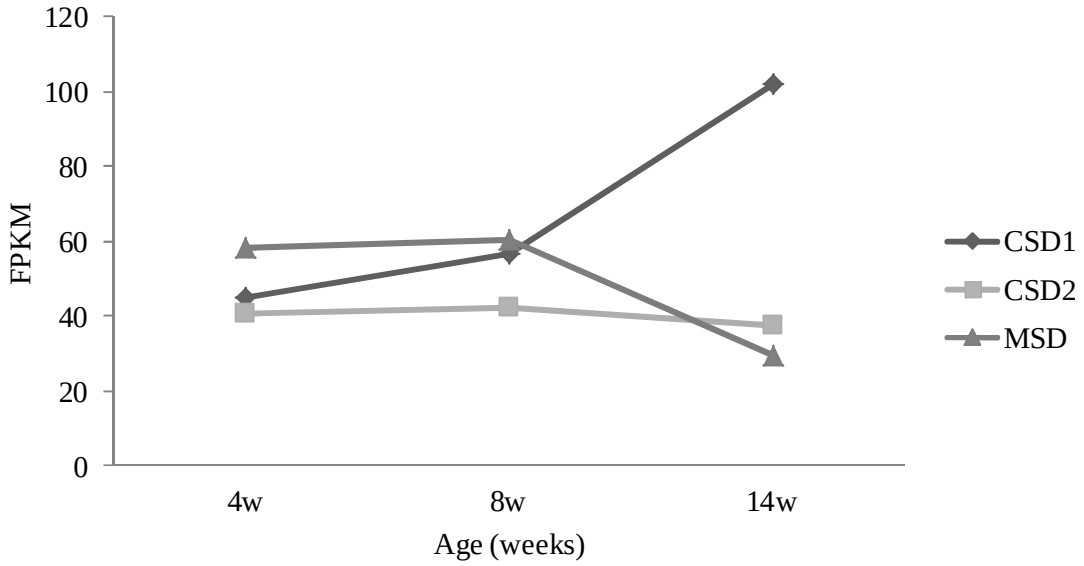

Figure 3.2.9-1 The abundance of manganese or iron superoxide dismutase (*MSD*), copper-zinc superoxide dismutase (*CSD*)1 and *CSD*2 transcript read fragments in soybean crown root nodules harvested from plants at 4, 8 and 14 weeks of development. Data show the fragments per Kilobase of transcript per million mapped reads (FPKM). Transcriptome sequencing was performed by Professor Karl Kunert (University of Pretoria, South Africa).

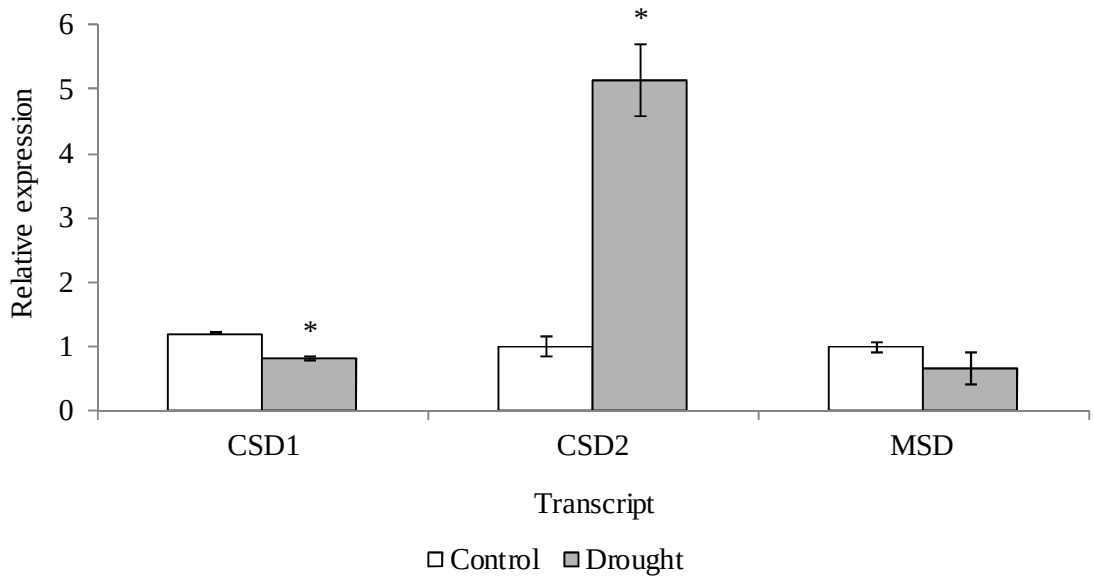

Figure 3.2.9-2 The abundance of manganese/iron superoxide dismutase 1 (*MSD*), copper-zinc superoxide dismutase (*CSD*)1 and *CSD2* transcripts in soybean crown root nodules from 5 week old plants, that had either been subjected to drought 21 days (open bars) or maintained under well-watered conditions (grey bars). Data are the mean ± SE (n = 3). Values that are significantly different between control plants and drought exposed plants have been determined using Students *t*-test, indicated by asterisks (* = P<0.05).

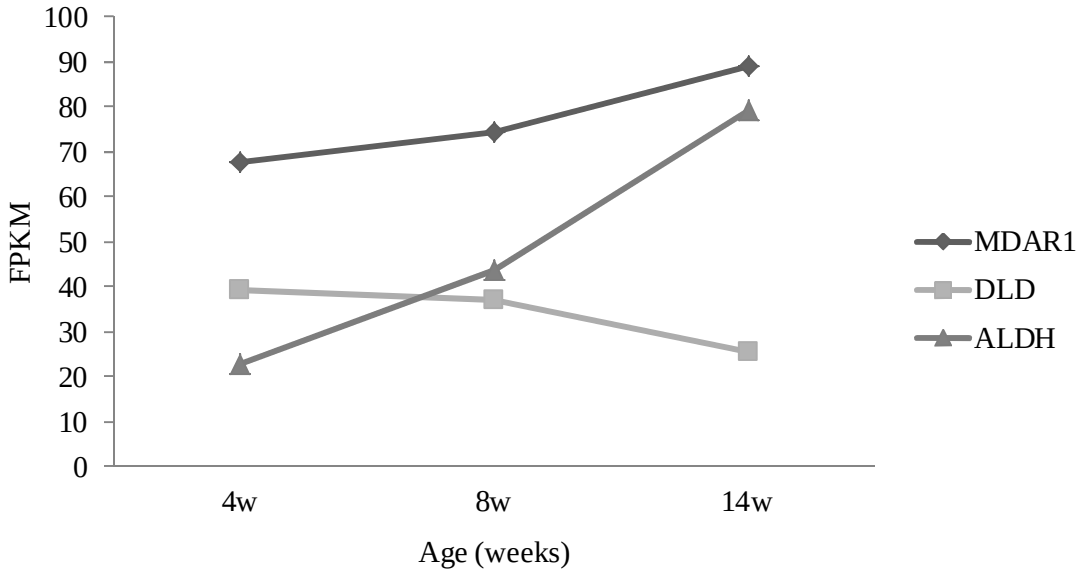

Figure 3.2.9-3:The abundance of monodehydroascorbate reductase 1 (*MDAR1*), dihydrolipoyl dehydrogenase (*DLD*) and aldehyde dehydrogenase (*ALDH*) transcript read fragments in soybean crown root nodules harvested from plants at 4, 8 and 14 weeks of development. Data show the fragments per Kilobase of transcript per million mapped reads (FPKM). Transcriptome sequencing was performed by Professor Karl Kunert (University of Pretoria, South Africa).

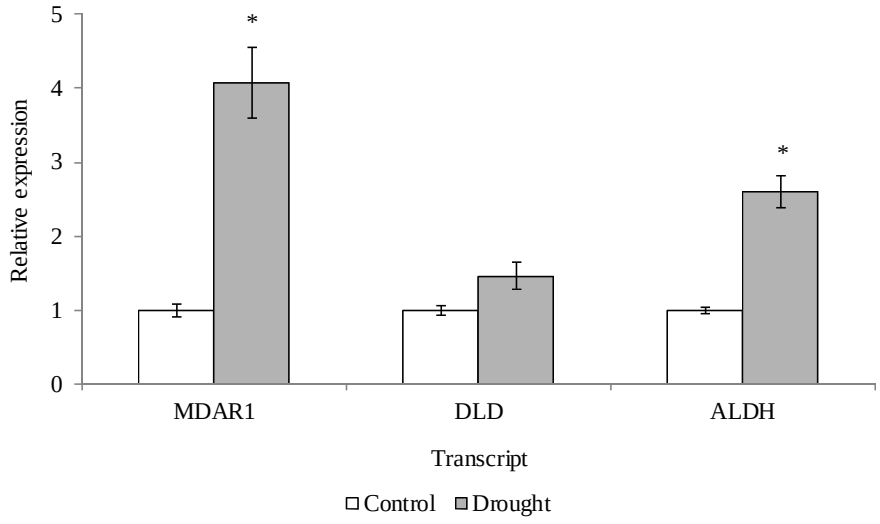

Figure 3.2.9-4: The relative abundance of monodehydroascorbate reductase 1 (*MDAR1*), dihydrolipoyl dehydrogenase (*DLD*) and aldehyde dehydrogenase (*ALDH*) transcripts in soybean crown root nodules from 5 week old plants, that had either been subjected to drought 21 days (open bars) or maintained under well-watered conditions (grey bars). Data are the mean ± SE (n = 3). Values that are significantly different between control plants and drought exposed plants have been determined using Students *t*-test, indicated by asterisks (* = $P<0.05$).

Transcriptional profiling showed differential expression of monodehydroascorbate reductase (*MDAR1*), dihydrolipoyl dehydrogenase (*DLD*) and aldehyde dehydrogenase (*ALDH*) between 4 and 14 weeks. Both *MDAR1* and *ALDH* showed an increased abundance between 4-14 weeks, whilst *DLD* showed a decreased abundance (Figure 3.2.9-3). When these transcripts were measured by qPCR in nodules that had been grown under 21 days of drought, or maintained under well-watered conditions *MDAR1* and *ALDH* showed increased expression under drought conditions. However the abundance of *DLD* was not significantly affected by drought exposure (Figure 3.2.9-4).

Transcriptomic data showed glutathione reductases (*GR1*, *GR2*), glutaredoxins (*GRX*) and glutathione S-transferases (*GST*) to be differentially regulated with age. During senescence there was an apparent decrease in *GRX2*, *GRX3*, *GRX4*, *GR1* and *GST*. *GR2* was the only transcript that demonstrated an increase in abundance throughout nodule aging (Figure 3.2.9-5). When these transcripts were measured by qPCR there was a demonstrably different trend in regulation under drought (Figure 3.2.9-6). *GR1* showed up regulation under drought conditions, whilst *GR2* remained stable. *GRX2* showed no significant expression change in response to drought; however *GRX3* and *GRX4* showed significant up regulation. *GST* also showed an increase in abundance under drought conditions (Figure 3.2.9-6).

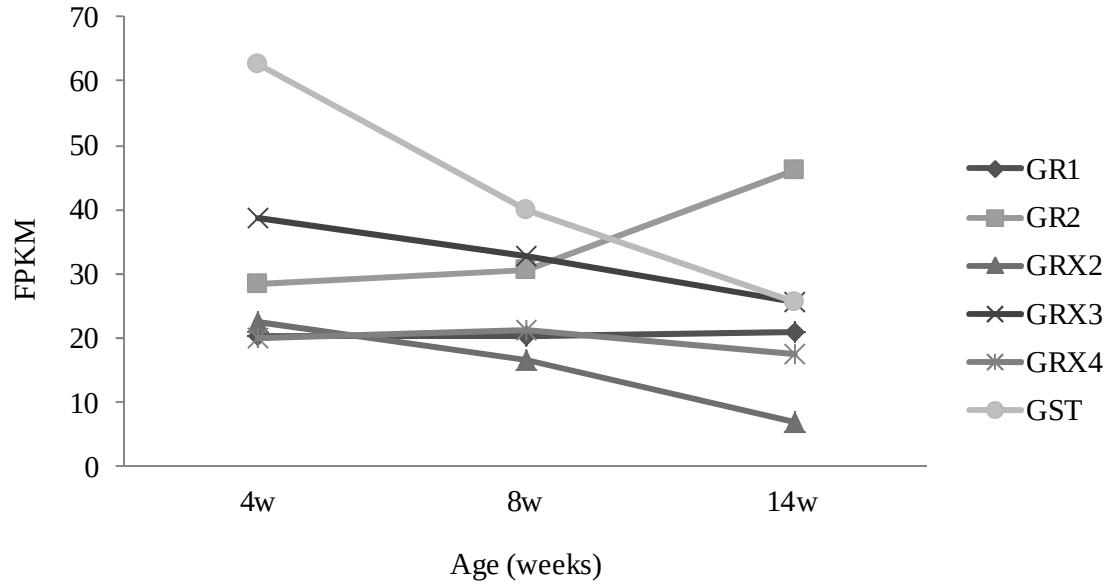

Figure 3.2.9-5: The abundance of glutathione reductase 1 (*GR1*), glutathione reductase 2 (*GR2*), glutaredoxin 2 (*GRX2*), glutaredoxin 3 (*GRX3*), glutaredoxin 4 (*GRX4*) and glutathione s-transferase (*GST*) transcript read fragments in soybean crown root nodules harvested from plants at 4, 8 and 14 weeks of development. Data show the fragments per Kilobase of transcript per million mapped reads (FPKM). Transcriptome sequencing was performed by Professor Karl Kunert (University of Pretoria, South Africa).

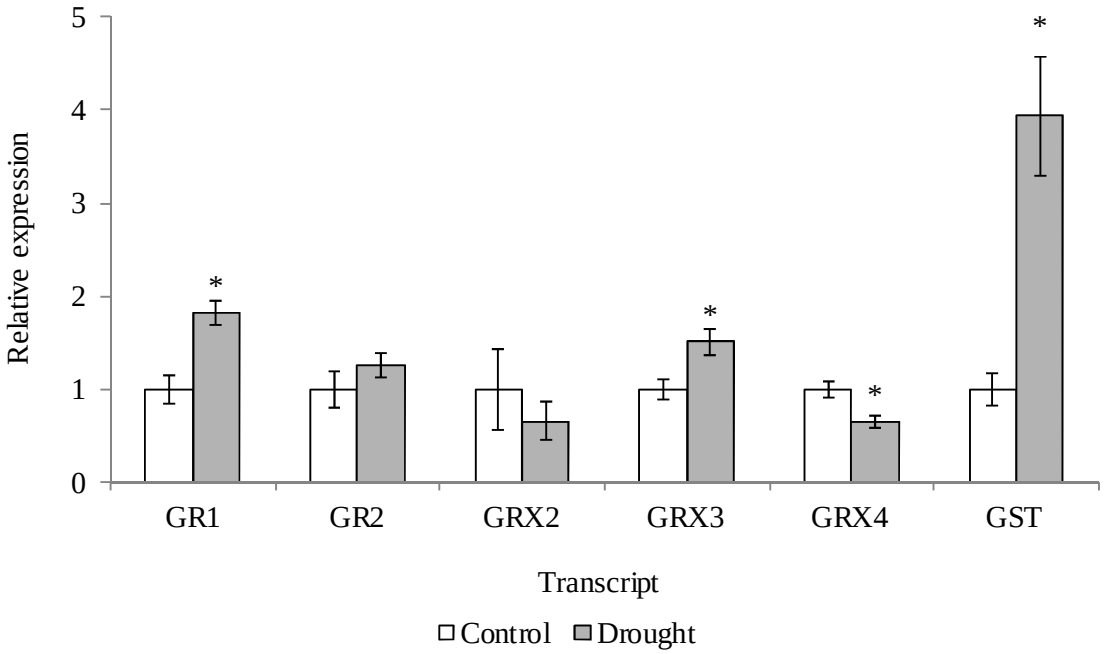

Figure 3.2.9-6 The relative abundance of glutathione reductase 1 (*GR1*), glutathione reductase 2 (*GR2*), glutaredoxin 2 (*GRX2*), glutaredoxin 3 (*GRX3*), glutaredoxin 4 (*GRX4*) and glutathione S-transferase (*GST*) in soybean crown root nodules from 5 week old plants, that had either been subjected to drought 21 days (open bars) or maintained under well-watered conditions (grey bars). Data are the mean ± SE (n = 3). Values that are significantly different between control plants and drought exposed plants have been determined using Students *t*-test, indicated by asterisks (* = P<0.05).

3.3. Discussion

The studies described in this chapter were performed to assess the effect of OCI expression on soybean growth, together with leaf (photosynthesis, transcript levels) and nodule characteristics (size, transcript levels) in the presence and absence of stress. These studies were conducted on three independent OCI transformed lines; SOC-1, SOC-2 and SOC-3, that had been characterised previously (Quain et al., 2015, 2014). As shown previously, the shoots of soybean plants expressing OCI were more branched and had a "bushy" phenotype compared to the Wt, when grown under control conditions. Transgenic tobacco plants overexpressing OCI had previously been shown to have a slow growth phenotype at the early stages of development (Prins et al., 2008). This was also seen in the soybean seedlings for up to 2 weeks after germination. Thereafter, the biomass accumulation in roots and shoots was similar in the soybean plants overexpressing OCI to the Wt. While the roots of transgenic soybean plants overexpressing OCI had similar fresh and dry weights, OCI expression had a marked effect on the nodulated roots. The OCI lines had greater nodule numbers compared to Wt under control conditions. However, the nodules tended to be smaller on the OCI lines than the Wt. Taken together, these observations show that inhibition of plant cysteine proteases by OCI had a significant effect on growth and development and this extends as far as nodule development. While the mechanisms that underpin these observations are unknown, previous studies have linked the developmental changes to effects on phytohormones, particularly strigolactones (Foo and Davies, 2011). The data presented here show that *CCD7* and *CCD8* transcripts are more highly expressed in roots than in stems or leaves and are concordant with previous findings (Al-Babili and Bouwmeester, 2015). Moreover, these transcripts were more highly expressed in the OCI lines than the Wt. It is therefore possible that OCI-mediated effects on strigolactone signalling alter the nodule parameters measured here. Addition of the artificial strigolactone GR24 has previously been shown to influence nodule numbers in a concentration-dependent manner; high levels of GR24 causing a decrease in nodule number and low concentrations increasing the number of nodules formed (De Cuyper et al., 2015).

The data presented here show that the abundance of *CCD7* and *CCD8* transcripts was very low in leaves of the Wt. However, *CCD7* and *CCD8* transcripts were higher in the leaves of the OCI-expressing lines than the Wt. This finding is in contrast to that reported by Quain et al., (2014), who found that *CCD7* and *CCD8* transcripts were lower in the leaves of the OCI-expressing lines than Wt. This discrepancy is hard to explain and merits further investigation, particularly because branching properties are determined by the interplay between several phytohormones and not just strigolactone alone. The higher levels of *CCD7* and *CCD8* transcripts observed in the OCI-expressing lines is not consistent with the enhanced branching measured in the transgenic plants, as discussed previously

(Quain et al., 2014). However Drummond et al., (2011) noted that strigolactone transcript abundance differs with age. The increased abundance of the *CCD7* and *CCD8* transcripts described in these studies may help to explain the enhanced chilling stress tolerance, discussed below.

The data presented here confirm that soybean plants are sensitive to inhibition by dark-chilling, as shown previously (Van Heerden et al., 2003; Strauss et al., 2007; Krüger et al., 2014). However, taken together, the data show that the OCI expressing lines are less sensitive to dark chilling than the Wt. Whilst significant differences were apparent in the relative sensitivities of Wt and OCI expressing soybean after 3 consecutive nights of dark-chilling, longer exposures to stress showed that the OCI expressing lines were more resistant to the stress in terms of maintenance of photosynthesis rates and growth. For example, data obtained from plants exposed to 9 consecutive nights of dark-chilling treatment showed that the OCI expressing lines had better growth and higher rates of photosynthesis compared to Wt. Although all lines had reduced photosynthesis compared to unchilled controls, all of the OCI expressing lines had higher carbon assimilation rates after the chilling treatment than the Wt, These findings are consistent with those reported by Van der Vyver et al., (2003), who found that OCI expressing tobacco lines were better able to maintain photosynthesis after chilling treatment.

Despite a chilling-induced reduction in the total fresh biomass and total dry weight in all lines, the fresh weight: dry weight ratios were significantly reduced only in the SOC-1 and SOC-2 lines. This indicates that the SOC-1 and SOC-2 lines lost more water under dark-chilling conditions than the SOC-3 and Wt lines. This finding might be attributed to differences in the transpiration rates between the lines after chilling stress. All three OCI expressing lines tended to have higher transpiration rates after chilling compared to the Wt. The SOC-2 and SOC-3 lines maintained significantly higher transpiration rates after 9 nights of chilling compared to the SOC-1 and Wt lines.

Taken together, the data on chilling-mediated inhibition of carbon assimilation and its alleviation in the OCI expressing lines presented in this chapter provides further evidence that cysteine proteases play a role in the regulation of photosynthesis under stress conditions (Prins et al., 2008). Previous evidence has suggested that RuBisCO protein turnover is altered in plants overexpressing OCI (Prins et al., 2008).

The enhanced photosynthesis rates observed in the OCI lines under dark-chilling might also be related to the higher levels of *CCD7* and *CCD8* transcripts observed in the stems and leaves of OCI expressers under these conditions. Some mutants that are defective in strigolactone signalling show delayed leaf senescence and maintain leaf chlorophyll even under stress, an effect that might be related to changes in nutrient availability (Yamada and Umehara, 2015). In addition *Arabidopsis*

thaliana strigolactone-deficient mutants show increased sensitivity to drought and osmotic stress (NaCl) conditions (van Ha et al., 2014). As the abundance of strigolactone encoding transcripts was increased in OCI expressing lines, these data form the basis for a model where strigolactone may confer tolerance to abiotic stresses. Strigolactone signalling has also been linked to ROS signalling and redox responses (Pandey et al., 2016). Redox signalling is essential in plant defence to environmental stresses, such as chilling and drought. While relatively few parameters related to redox processes have been measured in these studies, the nodule senescence transcriptome revealed a number of redox-related transcripts, which were examined in terms of responsiveness to drought. A qPCR analysis of soybean nodules that had been exposed to 21 days of drought showed that the expression of several superoxide dismutases (SODs) including *CSD1* was regulated by this stress. The nodule antioxidant system has previously been shown to be important in protection against stress (Tausz et al., 2004), but the specific roles of genes identified here in nodule functions has not been characterised in detail.

CSD1 transcripts had higher abundance in senescent nodules than mature nodules, suggesting that this transcript functions in the nodule senescence process. While *CSD2* mRNAs were similar in mature and senescing nodules, the level of these transcripts was increased in nodules exposed to drought. In contrast, *CSD1* transcripts were decreased in drought-induced senescence. These data show that *CSD1* and *CSD2* are differentially regulated in response to developmental and stress-induced senescence in a way that might be important for H_2O_2 removal (Bowler et al., 1992). Similarly, the expression of other SODs and *DLD* appear to be differentially regulated by developmental senescence, but not by drought. While the roles of *DLD* have not been extensively studied in plants the protein is likely to be mitochondrially targeted. *Saccharomyces cerevisiae* mutants deficient in *DLD* synthesis showed decreased production of ROS (Tahara et al., 2007). In contrast, the levels of *MDAR1* and *ALDH* transcripts were increased during both developmental senescence and drought.

Glutathione reductases (GR) are encoded by the *GR1* and *GR2* genes. *GR1* transcripts, which encode the cytosolic form of GR, were decreased during developmental senescence but increased in nodules of plants exposed to drought. Like *CSD1* and *CSD2, GR1* expression therefore appears to be differentially regulated in response to developmental and stress-induced senescence. *GR2* transcripts, which encode plastid and mitochondrial forms, were increased during developmental senescence but were unaffected by drought exposure. Similarly *GRX3* was increased under drought-induced senescence whereas *GRX4* was down regulated. Taken together, the data a show that the patterns of accumulation of redox-related transcripts differ under drought-induced and developmental senescence, suggesting that these processes are different in terms of gene expression and programming.

“One thing my pea plants taught me: always do science with things you can make into a soup.”

-Gregor Mendel

4. A role for strigolactone pathways on chilling tolerance in pea and Arabidopsis

4.1. Introduction

Strigolactones (SL), which were first identified as a component of root exudates in cotton (*Gossypium sp;* Cook et al., 1972), were initially shown to break seed dormancy and stimulate the growth of parasitic plants. These carotenoid-derived plant metabolites are not only released into the rhizosphere but they have also been shown to possess phytohormone activity in different plants, where they play a significant role in plant development. Molecular genetic approaches to investigate the regulation of bud growth led to the identification of SL as an auxiliary branching regulator. Branching has historically been attributed to the hormones auxin and cytokinin. Thus the identification of SL as a third regulator added an additional layer of control to this model (Dun et al., 2009). The garden pea (*Pisum sativum*) has the most extensively described range of non-pleiotropic increased branching mutants and has become a model in branching study (Johnson et al., 2006). Five branching mutant backgrounds in pea, termed *ramosus* (rms), are currently available comprising over 30 distinct lines. The five *rms* branching loci are; *rms1-rms5*. Each locus is directly or putatively attributed to a protein involved in the synthesis or the signalling of SL (Johnson et al., 2006). In addition to inhibiting shoot branching, SL also control root architecture. SLs also act as exogenous signals leading to the establishment of symbiotic interactions with arbuscular mycorrhizal fungi (Lopez-Obando et al., 2015).

The synthesis of SL involves the sequential cleavage of β-carotene (Figure 4.1-1), in a pathway that is conserved across the plant kingdom. Together with pea, *A. thaliana* presents a second species for which well characterised branching mutants are available (Bennett et al., 2006). These are termed the *more axillary branching* (*max*) mutants. Each identified stage of SL synthesis and signalling, together with known mutants, is described in Figure 4.1-1. The carotenoid cleavage dioxygenase (CCD) 7 and CCD8 enzymes, together with a cytochrome p450, have been definitively attributed to the *RMS5/MAX3*, *RMS1/MAX4* and *MAX1* loci respectively. However, the proteins coded at the *RMS2* and *RMS3* loci remain to be elucidated, though the *RMS2* locus has been tentatively linked to SL feedback signalling via interactions with the PsBRC1 transcription factor (Braun et al., 2012). Evidence has also identified *RMS4/MAX2* as an F-box signalling protein (Arite et al., 2009).

Considerable progress has been made recently in our understanding of the SL signalling pathway DWARF14 (D14) and KARRIKIN INSENSITIVE 2 (KAI2) are two closely related alpha/beta-hydrolases that have been shown to perceive specific enantiomers of the synthetic SL analogue, GR24. Both receptor proteins interact with MAX2. This F-box protein family interacts with the

SKP1-CULLIN-F-BOX PROTEIN (SCF) complex. Different associations of the SL receptor proteins with MAX2 are suggested to give rise to the ubiquitination and subsequent 26S proteasomal degradation of specific members of the SMAX-Like (SMXL) family in Arabidopsis. The D14/MAX2/SMXL6,7,8 signalling complexes have been shown to be involved in the signalling of natural SL controlling processes such as shoot branching. Moreover, the KAI2/MAX2/SMAX1 signalling complex is involved in the perception of smoke-derived karrikins, and probably other molecules that control seed germination and hypocotyl growth.

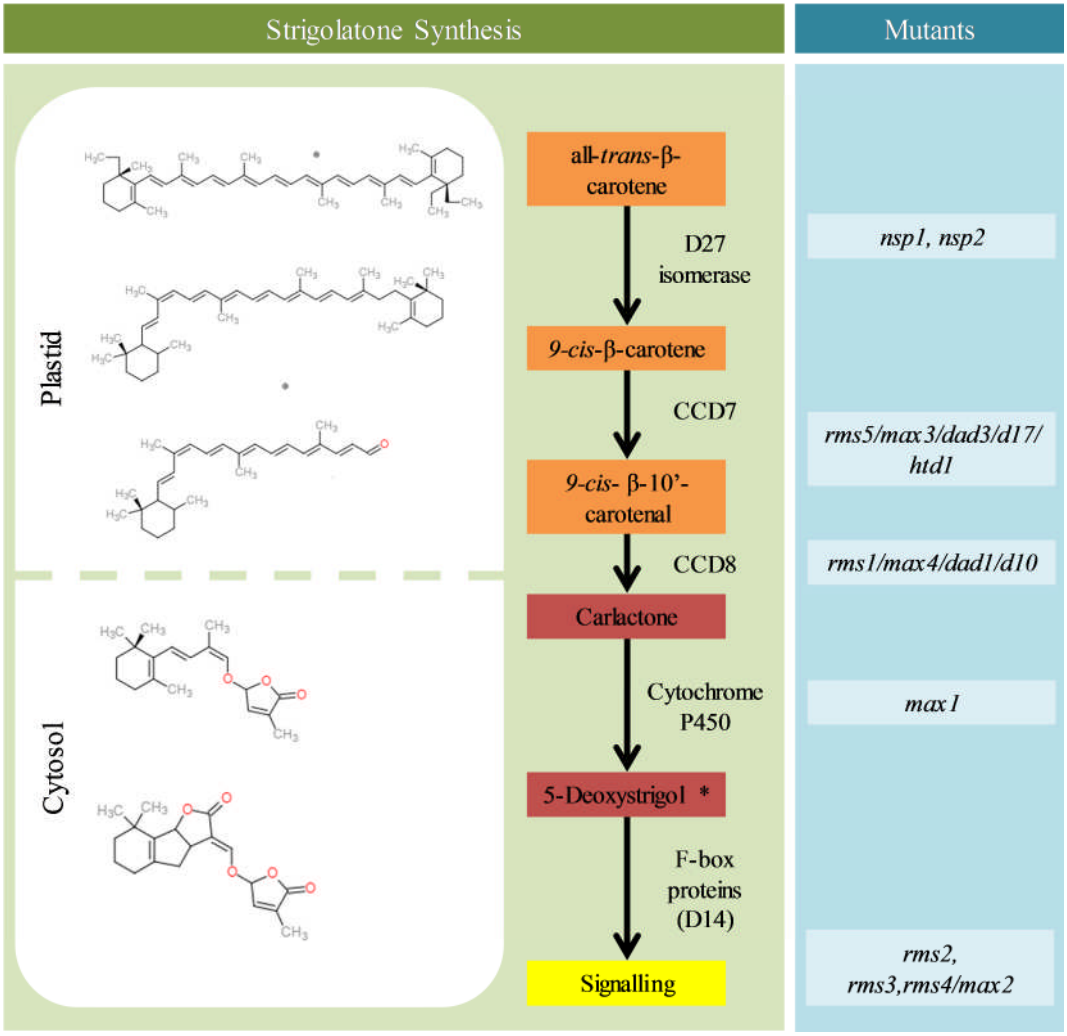

Figure 4.1-1: Model for the synthesis of strigolactone, showing the sequential cleavage of all-trans-β-carotene to carlactone by carotenoid cleavage dioxygenases 7 and 8 (CCD7, CCD8). Carlactone is exported from the plastid where it is converted to the strigolactone precursor 5-deoxystrigol. The mutant identities for each step in strigolactone synthesis and signalling are listed in the blue box (right). The mutants *nsp* were identified in *Medicago truncatula*, *rms* mutants were identified in *Pisum sativum*, *max* mutants were identified in *Arabidopsis thaliana*, *dad* mutants were identified in *Petunia hybrid*, the d10 mutant was identified in *Oryza sativa* and the htd1 mutant was identified in *Zea mays*. Figure was composed using information from Lopez-Obando et al., (2015) and Braun et al., (2012).

In addition to functions in branching regulation, studies on the *A. thaliana* mutants called *ore9*, which is analogous to *max2*, showed that SL have a role in senescence (Woo et al., 2001). Moreover, the *max2*, *max3* and *max4* lines of *A. thaliana* have shown increased sensitivity to both drought and salt stresses. As such the role of SL appears to extend beyond branching regulation, acting in both development and stress tolerance responses. However, the role of SL in temperature stress tolerance has not yet been characterised (Pandey et al., 2016). The results presented in chapter 3 provide evidence that OCI expression in soybean led to an increase in the abundance of the transcripts encoding the CCD7 and CCD8 dioxygenases, and conferred tolerance to dark chilling, as determined by measurements of photosynthesis and growth. Mutants defective in SL synthesis and signalling are not yet available in soybean. The following experiments were therefore performed in *A. thaliana* and pea, where such mutants are available, in order to investigate whether SL plays a role in chilling tolerance. Unlike soybean, *A. thaliana* and pea are chilling tolerant. If the tolerance to chilling in these species is dependent on SL then it might be predicted that sensitivity to dark chilling will be increased when SL synthesis and signalling are impaired.

4.2. Results

The following studies were preformed to characterise the functions of SL synthesis and signalling in plant low temperature tolerance. Studies were performed in a legume, pea (*P. sativum*) and *A. thaliana*, which are both chilling tolerant species. EMS mutants of pea deficient in SL synthesis or signalling that had previously been characterised by Beveridge et al., (2009) were used in these studies, together with EMS mutants of *A. thaliana* deficient in SL signalling and synthesis (Bennett et al., 2006). The mutant lines utilised in the following studies, together with their functions, are described in Table 5.

Table 5: : EMS mutants, their associated proteins and function in pea and *A. thaliana*

Function	Coded protein	Pea	*A. thaliana*
-	-	L107 (Wt)	Col-0 (Wt)
Synthesis	CCD7	rms5 (BL298)	max3
Synthesis	CCD8	-	max4
Signalling	F-box	rms4 (K164)	max2
Signalling (probable)	unknown	rms3 (K487)	-

4.2.1. The effect of dark chilling stress on pea mutants that are defective in strigolactone synthesis or signalling

As a first step in these investigations a visual inspection of pea Wt and SL pathway mutants was conducted (Figure 4.2.1-1). Under control conditions (Figure 4.2.1-1, Control) the Wt was shown to have a taller, less branched phenotype than the SL mutants. Of these, the SL synthesis mutant BL298 was shorter than the Wt with more extensive shoot branching. The SL signalling mutant K164 was visibly shorter than the Wt and SL synthesis line BL298, but showed similar enhanced branching compared to the Wt. Under control conditions both the SL signalling mutant K164 and the putative SL signalling mutant K487 had shorter stems compared to the other two genotypes but had a similar degree of axillary branching (Figure 4.2.1-1, control). Under dark chilling conditions the SL synthesis mutant BL298 had a similar height to the Wt, but with greater branch formation. Following chilling, the SL signalling mutant K164 and the putative SL signalling mutant K487 had shorter stems than the other 2 genotypes but they retained the enhanced branching phenotype (Figure 4.2.1-1, chilled).

These mutants were visibly smaller than the other two genotypes after exposure to 7 consecutive nights of dark-chilling (Figure 4.2.1-1).

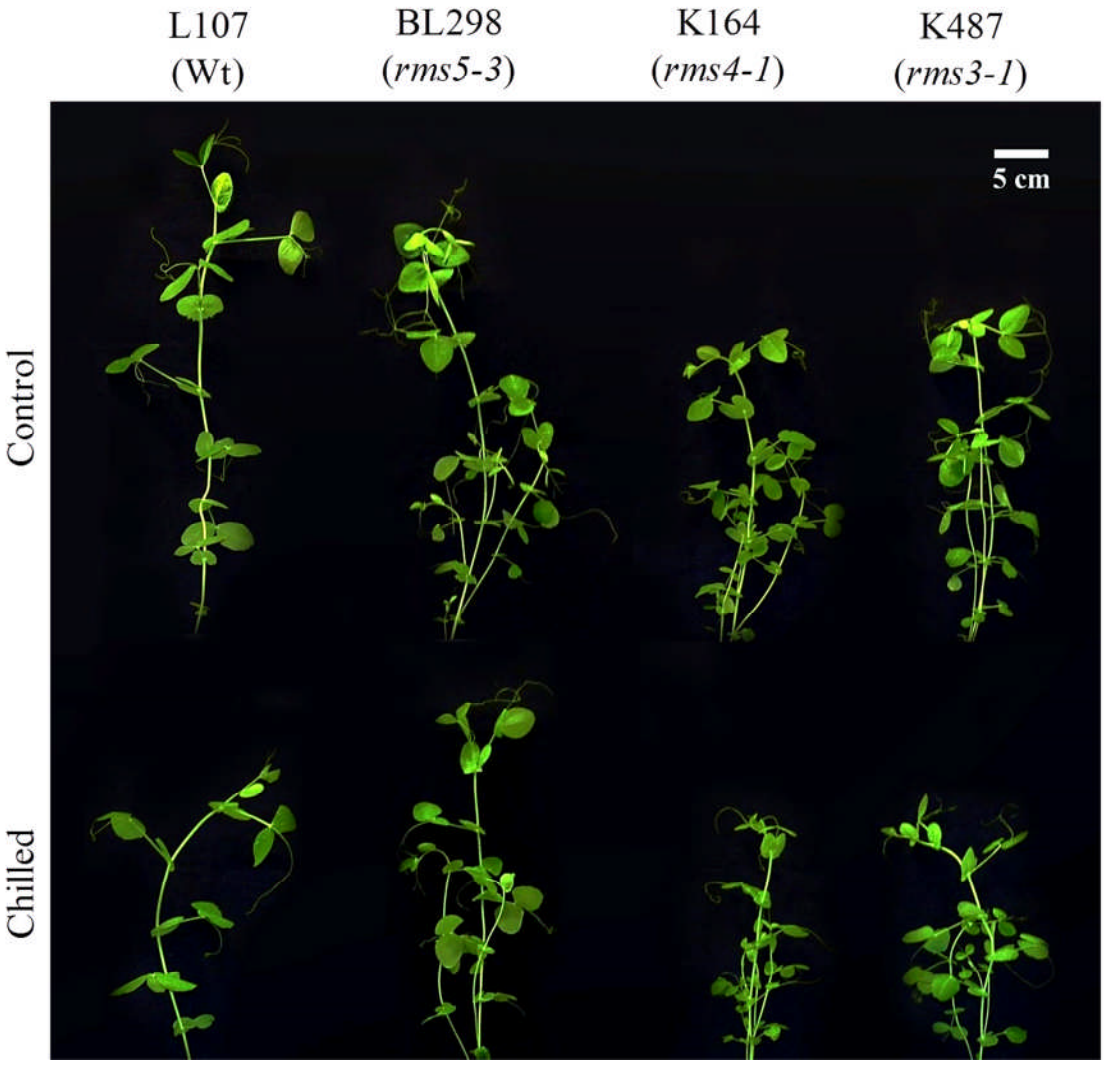

Figure 4.2.1-1: Shoot phenotypes of pea wild type; (L107; Wt) and three SL mutant lines deficient in either strigolactone synthesis or signalling proteins; BL298 (*rms5-3;* SL synthesis mutant); K164 (*rms4-1*; SL signalling); K487 (*rms3-1*; SL signalling). Plants were grown for either 3 weeks on compost under control conditions (Control) or for 2 weeks under control conditions followed by 7 consecutive nights of dark chilling (4ºC ±1ºC; Chilled). Scale bar shows 5cm.

Exposure to dark chilling did not significantly change the number of shoot branches within each genotype. However, branch number varied between genotypes under control and dark chilled conditions (Figure 4.2.1-2).

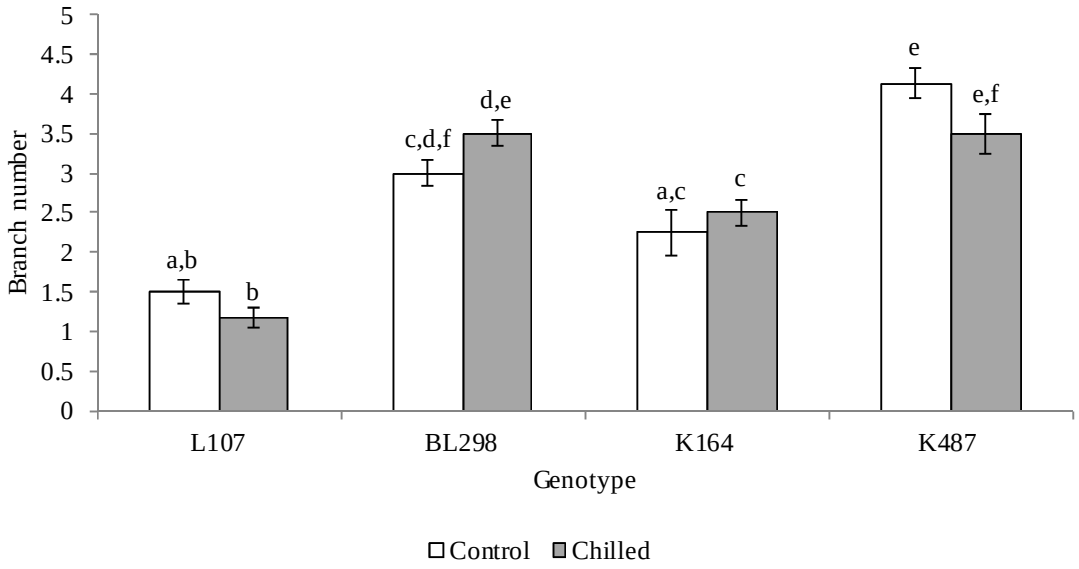

Figure 4.2.1-2: Number of branches in pea wild type; (L107; Wt) and three SL mutant lines deficient in either strigolactone synthesis or signalling proteins; BL298 (*rms5-3;* SL synthesis mutant); K164 (*rms4-1*; SL signalling); K487 (*rms3-1*; SL signalling). Plants were grown for either 3 weeks on compost under control conditions (Control) or for 2 weeks under control conditions followed by 7 consecutive nights of dark chilling (4 ºC ±1 ºC; Chilled). Data show average values ± SE. Open bars are control values, grey bars are chilled values. Significance is shown by Students *t*-test at P=<0.05 (n=12).

Exposure to dark-chilling led to an increase in the total number of leaves in each genotype (Figure 4.2.1-3). Under control conditions the Wt had a similar number of leaves to the SL signalling mutant K164. However both of these genotypes had fewer leaves than the other two genotypes under control or dark-chilled conditions. After 7 consecutive nights of dark-chilling or maintenance under control conditions both the SL synthesis mutant BL298 and the putative SL signalling mutant K487 had a comparable number of leaves. Although the SL signalling mutant K164 had more leaves after dark chilling than under control conditions, the number of leaves present on chilled K164 plants was still lower than that of the SL synthesis mutant BL298 and of the putative SL signalling mutant K487 lines under control conditions (Figure 4.2.1-3).

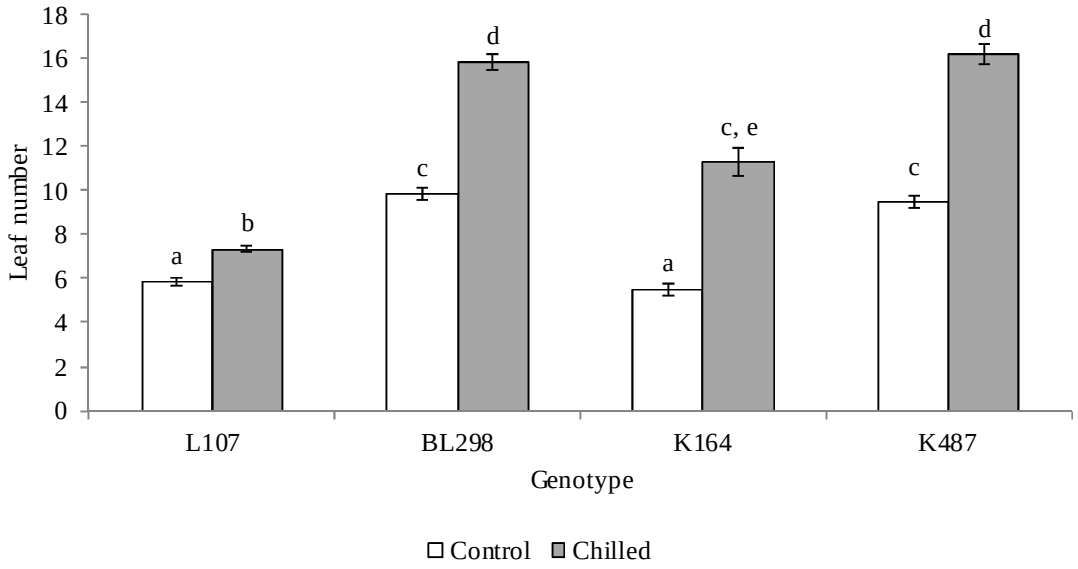

Figure 4.2.1-3: Number of leaves in pea wild type; (L107; Wt) and three SL mutant lines deficient in either strigolactone synthesis or signalling proteins; BL298 (*rms5-3;* SL synthesis mutant); K164 (*rms4-1*; SL signalling); K487 (*rms3-1*; SL signalling). Plants were grown for either 3 weeks on compost under control conditions (Control) or for 2 weeks under control conditions followed by 7 consecutive nights of dark chilling (4 ºC ±1 ºC; Chilled). Data show average values ± SE. Open bars are control values, grey bars are chilled values. Significance is shown by Students *t*-test at P=<0.05 (n=12).

Under control conditions the L107, BL298 and K487 shoots had comparable fresh biomasses; however K164 displayed a significantly lower fresh biomass than the other genotypes (Figure 4.2.1-4 Control). Similarly L107, BL298 and K487 had a comparable fresh shoot biomass under dark chilling conditions, and K164 had the lowest shoot biomass under these conditions (Figure 4.2.1-4 Chilled). All genotypes were reduced in terms of fresh shoot biomass as a result of exposure to 7 consecutive nights of dark-chilling; however K164 had the lowest fresh shoot biomass of all genotypes under dark-chilling conditions (Figure 4.2.1-4).

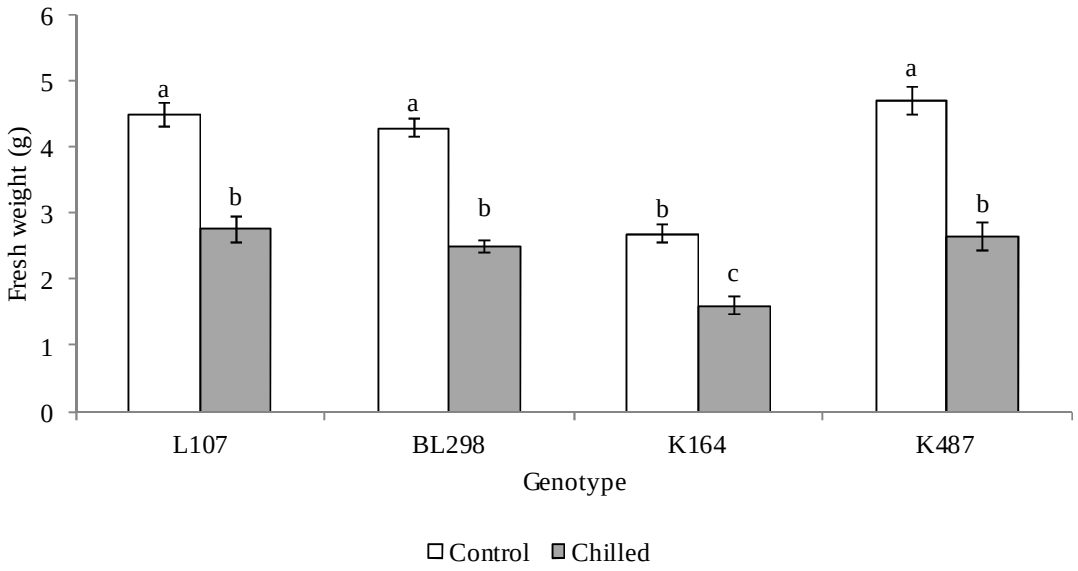

Figure 4.2.1-4: Fresh shoot biomass of pea wild type; (L107; Wt) and three SL mutant lines deficient in either strigolactone synthesis or signalling proteins; BL298 (*rms5-3;* SL synthesis mutant); K164 (*rms4-1*; SL signalling); K487 (*rms3-1*; SL signalling). Plants were grown for either 3 weeks on compost under control conditions (Control) or for 2 weeks under control conditions followed by 7 consecutive nights of dark chilling (4 ºC ±1 ºC; Chilled).). Data show average values ± SE. Open bars are control values, grey bars are chilled values. Significance is shown by Students *t*-test at P=<0.05 (n=12).

Under control conditions L107, BL298 and K487 showed similar dry shoot weights, however K164 showed a significantly lower dry shoot weight than the other genotypes when grown under control conditions (Figure 4.2.1-5). After exposure to 7 consecutive nights of dark-chilling, L107 had the highest dry shoot biomass of all genotypes. K487 had a higher dry shoot biomass than BL298 and K164 after exposure to dark chilling, with dark-chilled BL298 and K164 plants having statistically comparable dry biomasses. Interestingly whilst BL298 and K487 showed significant reductions in dry shoot biomass after exposure to dark-chilling, K164 was not significantly affected by chilling exposure.

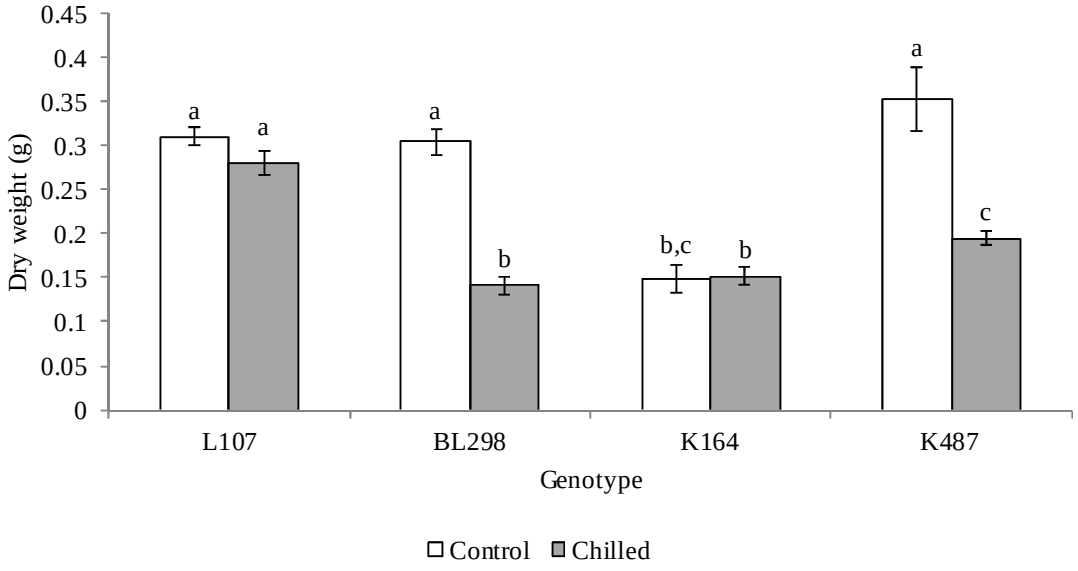

Figure 4.2.1-5: Dry shoot biomass of pea wild type; (L107; Wt) and three SL mutant lines deficient in either strigolactone synthesis or signalling proteins; BL298 (*rms5-3;* SL synthesis mutant); K164 (*rms4-1*; SL signalling); K487 (*rms3-1*; SL signalling). Plants were grown for either 3 weeks on compost under control conditions (Control) or for 2 weeks under control conditions followed by 7 consecutive nights of dark chilling (4ºC ±1ºC; Chilled).). Data show average values ± SE. Open bars are control values, grey bars are chilled values. Significance is shown by Students *t*-test at P=<0.05 (n=12).

.

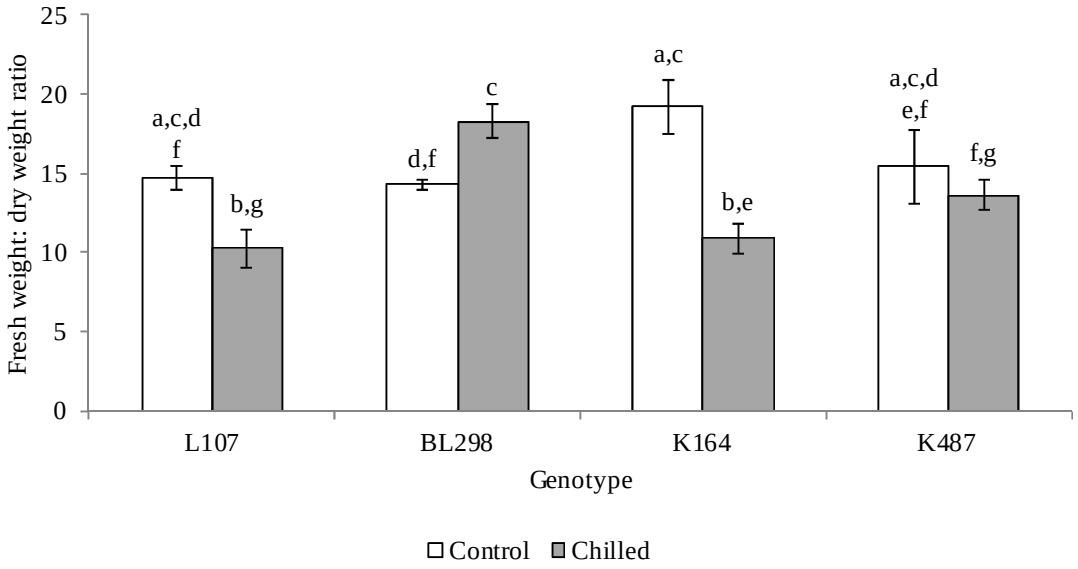

Figure 4.2.1-6: Fresh weight: dry weight ratios (FW/DW) of pea wild type; (L107; Wt) and three SL mutant lines deficient in either strigolactone synthesis or signalling proteins; BL298 (*rms5-3;* SL synthesis mutant); K164 (*rms4-1*; SL signalling); K487 (*rms3-1*; SL signalling). Plants were grown for either 3 weeks on compost under control conditions (Control) or for 2 weeks under control conditions followed by 7 consecutive nights of dark chilling (4 ºC ±1 ºC; Chilled).). Data show average values ± SE. Open bars are control values, grey bars are chilled values. Significance is shown by Students *t*-test at P=<0.05 (n=12).

The fresh weight to dry weight ratios (FW/DW) were measured under control and dark-chilling conditions. FW/DW was similar in the L107, BL298 and K487 lines but BL298 had a lower FW/DW than K164 under control conditions (Figure 4.2.1-6 Control). There were significant differences in FW/DW between genotypes after 7-consecutive nights of exposure to dark-chilling (Figure 4.2.1-6). L107 and K164 had a comparably low FW/DW when compared to K487 and BL298. BL298 had the highest FW/DW after dark-chilling (Figure 4.2.1-6 Chilled). Both L107 and K164 had a significantly lower FW/DW after chilling, whilst BL298 had a significantly higher ratio. The FW/DW of K487 was not significantly affected by dark-chilling (Figure 4.2.1-6).

To further investigate the effect of dark-chilling on growth and metabolism, photosynthetic parameters were measured in all genotypes. All genotypes had similar photosynthetic carbon assimilation rates under control conditions (Figure 4.2.1-7 Control). The leaves of Wt (L107) plants that had been exposed to dark-chilling had similar rates of photosynthesis whether they were grown under control or dark chilling conditions (Figure 4.2.1-7). Moreover, the L107 leaves had significantly higher rates of carbon assimilation than those of the other genotypes (BL298, K164 and K487) dark chilling conditions. There was a significant chilling-dependent inhibition of carbon assimilation in the BL298, K164 and K487 leaves after exposure to 7 consecutive nights of dark-chilling (Figure 4.2.1-7).

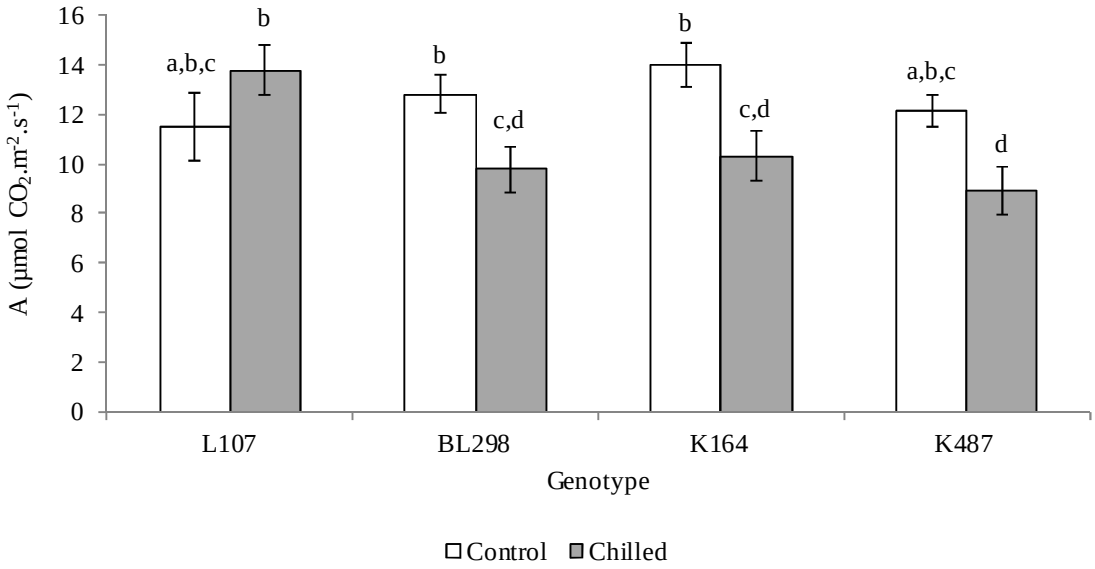

Figure 4.2.1-7: Photosynthetic carbon assimilation rates (µmol $CO_2.m^{-2}.s^{-1}$) of pea wild type; (L107; Wt) and three SL mutant lines deficient in either strigolactone synthesis or signalling proteins; BL298 (*rms5-3;* SL synthesis mutant); K164 (*rms4-1*; SL signalling); K487 (*rms3-1*; SL signalling). Plants were grown for either 3 weeks on compost under control conditions (Control) or for 2 weeks under control conditions followed by 7 consecutive nights of dark chilling (4 ºC ±1 ºC; Chilled). Measurements were taken at an atmospheric CO_2 concentration of 400 µmol at 20 ºC and a light concentration of 800 µmol.m.$^{-2}.s^{-1}$.). Data show average values ± SE. Open bars are control values, grey bars are chilled values. Significance is shown by Students *t*-test at P=<0.05 (n=12).

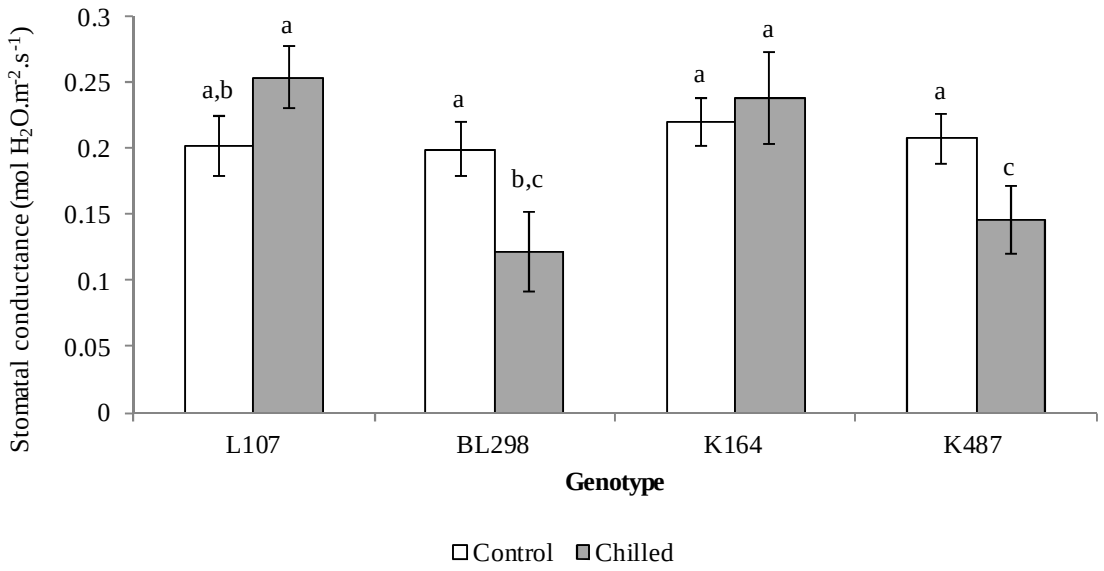

Figure 4.2.1-8: Stomatal conductance (mmol $H_2O.m^{-2}.s^{-1}$) of pea wild type; (L107; Wt) and three SL mutant lines deficient in either strigolactone synthesis or signalling proteins; BL298 (*rms5-3;* SL synthesis mutant); K164 (*rms4-1*; SL signalling); K487 (*rms3-1*; SL signalling). Plants were grown for either 3 weeks on compost under control conditions (Control) or for 2 weeks under control conditions followed by 7 consecutive nights of dark chilling (4 ºC ±1 ºC; Chilled). Measurements were taken at an atmospheric CO_2 concentration of 400 µmol at 20 ºC and a light concentration of 800 µmol.$m^{-2}.s^{-1}$.). Data show average values ± SE. Open bars are control values, grey bars are chilled values. Significance is shown by Students *t*-test at P=<0.05 (n=12).

All genotypes had similar stomatal conductance rates under control conditions. The L107 and K164 leaves showed similar stomatal conductance under dark-chilling as in control conditions (Figure 4.2.1-8). However, the BL298 and K487 leaves had significantly lower rates of stomatal conductance after dark-chilling (Figure 4.2.1-8). BL298 and K487 had the lowest rates of stomatal conductance following dark-chilling (Figure 4.2.1-8).

The leaves of K487 plants had a significantly lower intracellular CO_2 concentrations ($C_{i\ )}$ than the other genotypes under control conditions. Ci values were comparable in the L107, BL298 and K164 leaves in the absence of stress. Dark chilling had no significant effect on C_i in any of the genotypes although the SL synthesis mutant BL298 leaves tended to have lower Ci values under dark-chilled conditions (Figure 4.2.1-9).

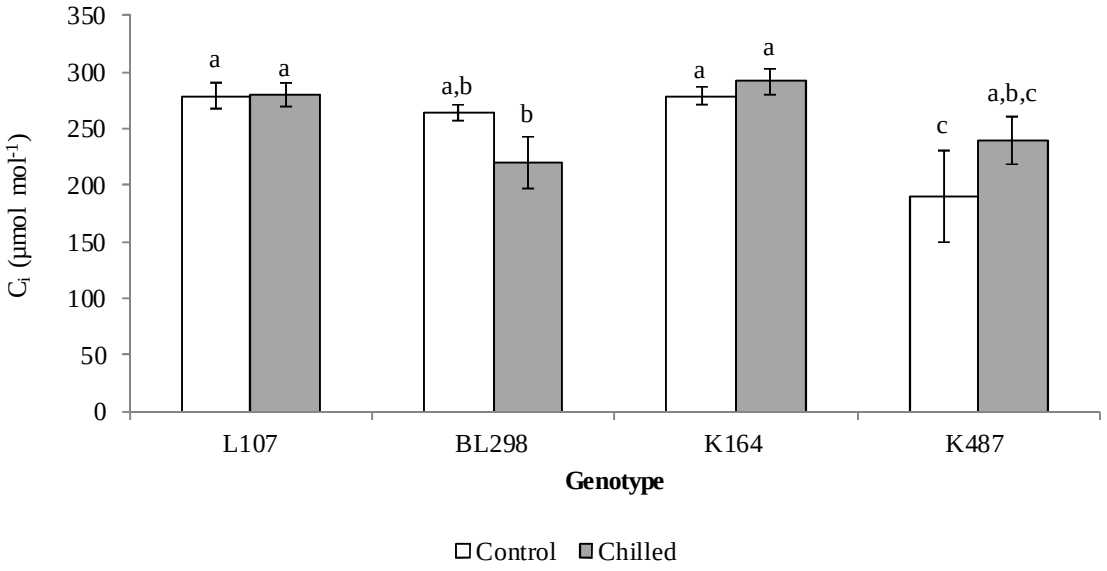

Figure 4.2.1-9: Intracellular CO_2 concentrations (µmol CO_2 mol^{-1}) of pea wild type; (L107; Wt) and three SL mutant lines deficient in either strigolactone synthesis or signalling proteins; BL298 (*rms5-3;* SL synthesis mutant); K164 (*rms4-1*; SL signalling); K487 (*rms3-1*; SL signalling). Plants were grown for either 3 weeks on compost under control conditions (Control) or for 2 weeks under control conditions followed by 7 consecutive nights of dark chilling (4 ºC ±1 ºC; Chilled). Measurements were taken at an atmospheric CO_2 concentration of 400µmol at 20ºC and a light concentration of 800 µmol.m^{-2}.s^{-1}.). Data show average values ± SE. Open bars are control values, grey bars are chilled values. Significance is shown by Students *t*-test at P=<0.05 (n=12).

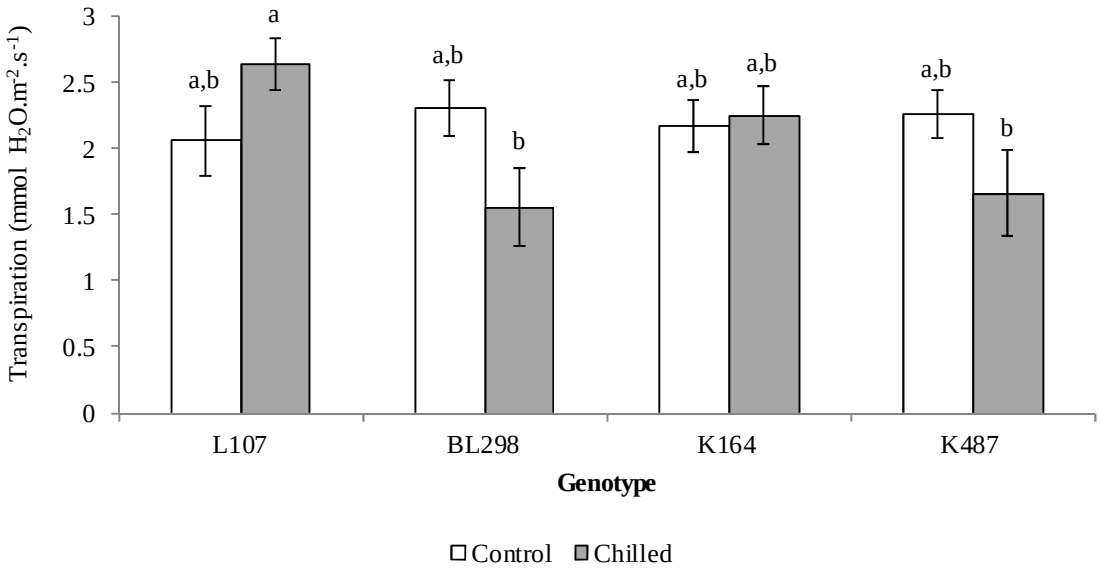

Figure 4.2.1-10: Transpiration rates (mmol $H_2O.m^2.s^{-1}$) of pea wild type; (L107; Wt) and three SL mutant lines deficient in either strigolactone synthesis or signalling proteins; BL298 (*rms5-3;* SL synthesis mutant); K164 (*rms4-1*; SL signalling); K487 (*rms3-1*; SL signalling). Plants were grown for either 3 weeks on compost under control conditions (Control) or for 2 weeks under control conditions followed by 7 consecutive nights of dark chilling (4ºC ±1ºC; Chilled). Measurements were taken at an atmospheric CO_2 concentration of 400µmol at 20ºC and a light concentration of 800µmol.$m^{-2}.s^{-1}$.). Data show average values ± SE. Open bars are control values, grey bars are chilled values. Significance is shown by Students *t*-test at P=<0.05 (n=12).

Transpiration rates were similar in each genotype under control and dark-chilling conditions. However, L107 leaves had higher transpiration rates after 7 consecutive nights of dark-chilling than the leaves of the BL298 and K487 genotypes (Figure 4.2.1-10).

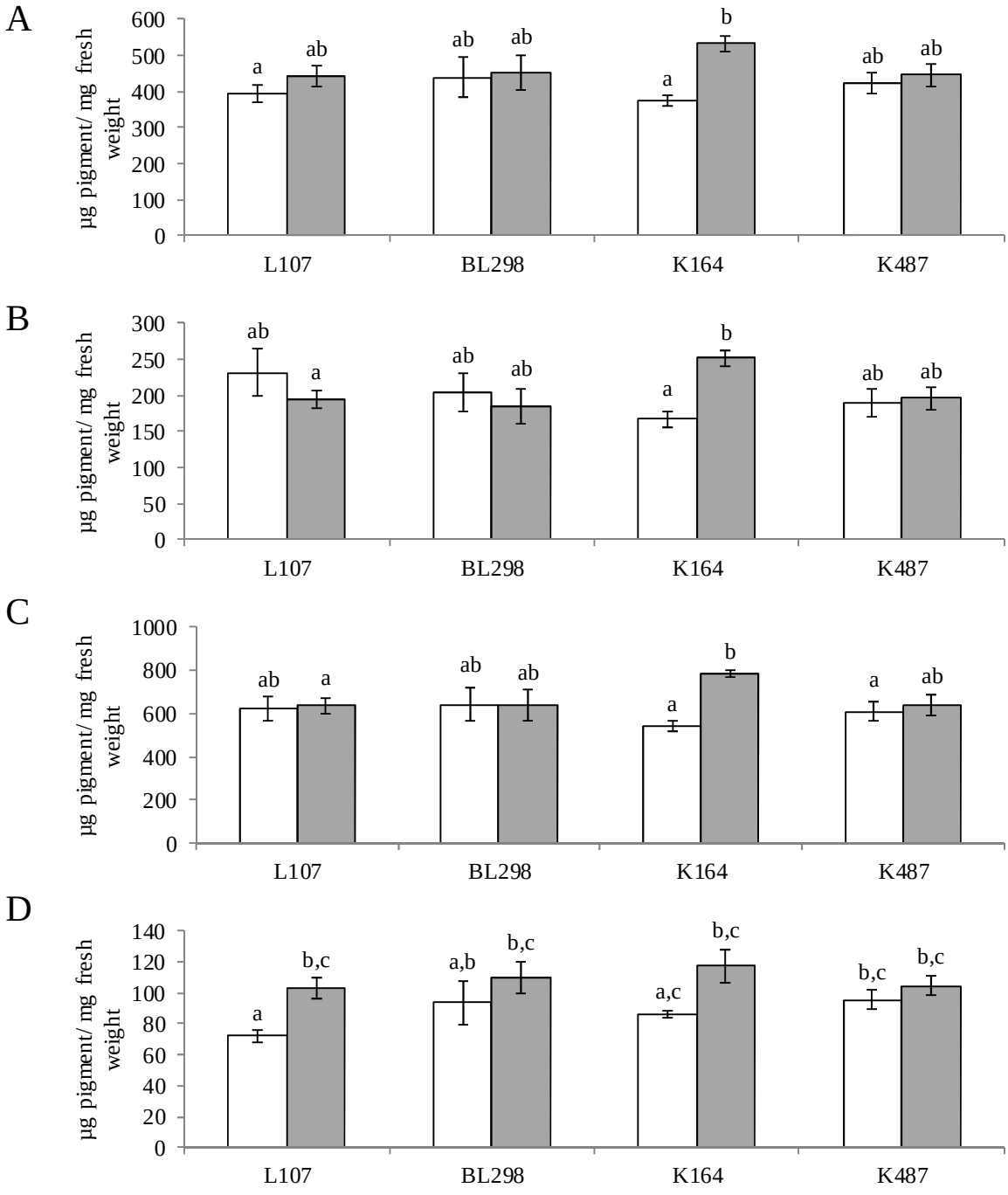

Figure 4.2.1-11: A comparison of the A) chlorophyll a B) chlorophyll b C) chlorophyll a+b D) carotenoid composition of pea leaves; wild type; (L107; Wt) and three SL mutant lines deficient in either strigolactone synthesis or signalling proteins; BL298 (*rms5-3;* SL synthesis mutant); K164 (*rms4-1*; SL signalling); K487 (*rms3-1*; SL signalling). Plants were grown for either 3 weeks on compost under control conditions (Control) or for 2 weeks under control conditions followed by 7 consecutive nights of dark chilling (4 ºC ±1 ºC; Chilled). Data show average values ± SE. Open bars are control values, grey bars are chilled values. Significance is shown by Students *t*-test at P=<0.05 (n=12).

No statistically significant differences in photosynthetic pigments were observed between genotypes under control conditions (Figure 4.2.1-11). Similarly when grown under dark chilling conditions all genotypes had comparable levels of chlorophyll a (Figure 4.2.1-11, A). However, the K164 leaves

that had been subjected to dark chilling had more chlorophyll a than the Wt L107 under control conditions (Figure 4.2.1-11, A). The K164 leaves also had significantly more chlorophyll b after dark chilling than under control conditions (Figure 4.2.1-11, B). The total chlorophyll (a plus b; Figure 4.2.1-11, C) content was similar in all genotypes under control conditions. However, K164 leaves had significantly more chlorophyll than under control conditions (Figure 4.2.1-11 ,C). The leaves of all genotypes had similar carotenoid levels under control conditions (Figure 4.2.1-11, D). However, the leaves subjected to dark-chilling tended to have higher carotenoid levels than those of plants grown under control conditions. The Wt leaves had significantly higher carotenoid contents under dark-chilling than under control conditions.

4.2.2. The effect of dark-chilling and GR24 on the growth of wild type and strigolactone-deficient *A. thaliana* mutants grown on plates

The following studies were conducted to characterise the effect of SL pathway mutations (*max2-1* (signalling), *max3-9* (synthesis) and *max4-1* (synthesis)) on dark-chilling tolerance in *A. thaliana*. Moreover, GR24 (2 μM) was applied to the growth media of both Wt (Col-0) and SL mutant lines to determine whether this artificial SL would reverse any effects observed in the SL-synthesis lines. Hence, in these studies seedlings were grown for 7 days on plates containing ½ MS media (with or without GR24) under unstressed (control) conditions. They were then either maintained under control conditions for a further 11 days or subjected to 11 consecutive nights of dark-chilling, similar to the growth regime used in the experiments with pea and soybean. The visual phenotype of all lines was first characterised as shown in (Figure 4.2.2-1).

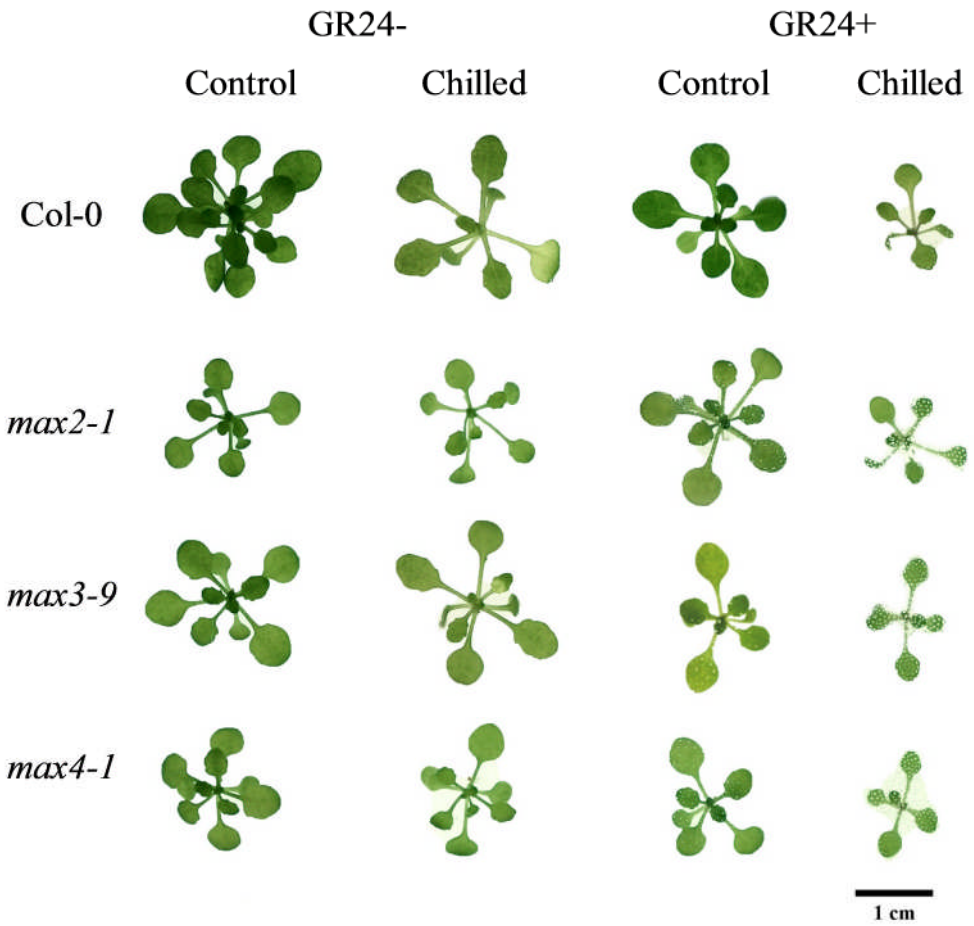

Figure 4.2.2-1: Shoot phenotypes of *Arabidopsis thaliana* Wt plants (Col-0) and three mutant lines deficient in strigolactone signalling (*max2-1*) or strigolactone synthesis (*max3-9, max4-1*). Plants were grown either in the absence of stress (control conditions) in the presence or absence of the artificial strigolactone, GR24, or under dark-chilling conditions in the presence or absence of GR24. Scale bar shows 1cm.

A visual inspection showed that Col-0, grown under control conditions in the absence of GR24 had the largest rosette. Under the same conditions all of *max2-1*, *max3-9* and *max4-1* showed a smaller rosette size than Col-0, with *max2-1* presenting the smallest phenotype (Figure 4.2.2-1, GR24- control). Under dark-chilling conditions, in the absence of GR24, all genotypes showed a decrease in rosette area, the chilled plants having visually smaller rosettes than those grown under control conditions (Figure 4.2.2-1, GR24- chilled). The Col-0 rosettes were visibly smaller when treated with GR24 under control growth temperatures. In contrast, the *max2-1* rosettes were visibly larger in the presence of GR24 and a smaller phenotype was shown by *max3-9* and *max4-1* (Figure 4.2.2-1, GR24+ control). When grown in the presence of GR24 under dark-chilling conditions, all genotypes displayed a smaller rosette. There were no apparent visual differences between genotypes under dark-chilling conditions in the presence of GR24 (Figure 4.2.2-1, GR24+ chilled).

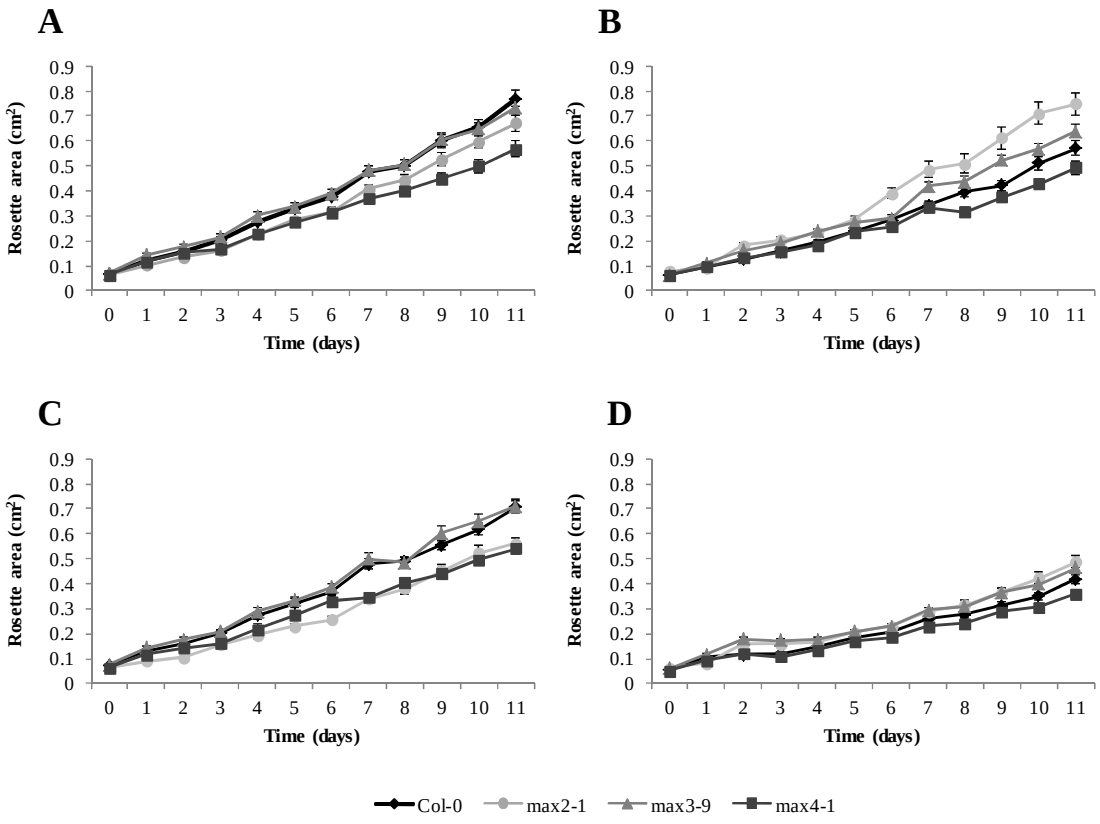

Figure 4.2.2-2: The rosette diameter of *Arabidopsis thaliana* wild type (Col-0) and three mutant lines deficient in either strigolactone signalling *max2-1* or strigolactone synthesis (*max3-9*; *max4-1)*. Plants were grown for 7 days under control temperatures, either in the presence or absence of GR24. Time 0 indicates the point when 11 consecutive nights of dark chilling were imposed; A) Control temperature in the absence of GR24; B) Control temperature in the presence of GR24; C) Dark-chilling in the absence of GR24; D) Dark chilling in the presence of GR24. Bars represent the SE of the mean. Each data point represents an n>=90.

To further investigate the effects of dark-chilling exposure on plant growth, rosette area was measured at daily intervals for all genotypes from the point where the dark chilling stress was

imposed (Figure 4.2.2-2). For simplicity, only the final time-point growth measurements are reported in detail here to illustrate how dark-chilling and GR24 regulate shoot growth (Figure 4.2.2-3).

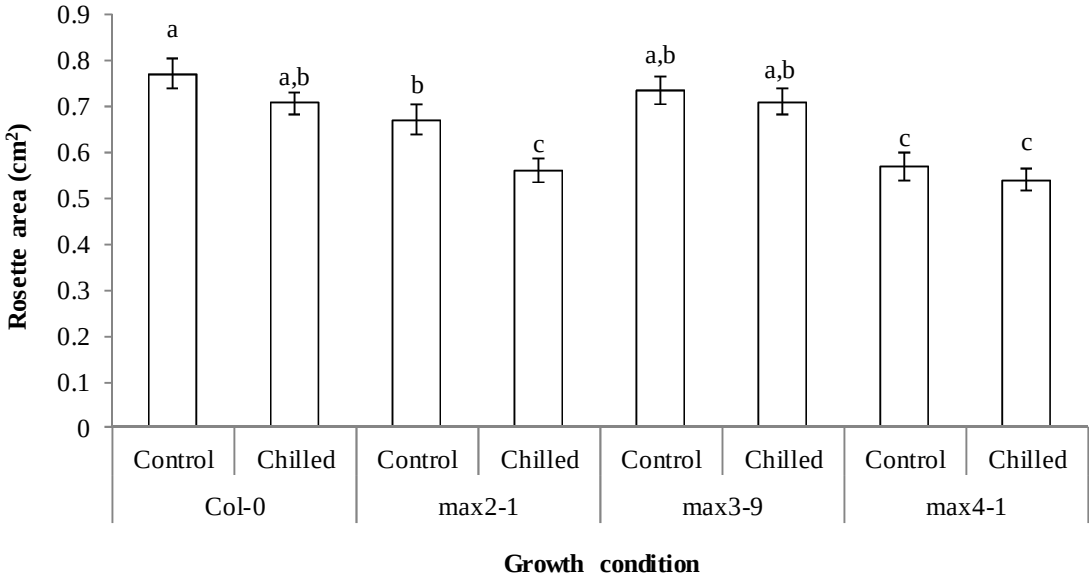

Figure 4.2.2-3: A comparison of the rosette diameters of 4 *Arabidopsis thaliana* genotypes, showing Col-0 (Wt), the strigolactone signalling mutant max2-1 and the strigolactone synthesis mutants; max3-9, max4-1. Data shown are for plants at 18 days of age, consisting of 7 days growth under control conditions followed by 11 days of maintenance under control conditions, or exposure to 11 consecutive nights of dark-chilling. Bars represent the SE of the mean (n>=90). Statistical significance is shown by *t*-test at P=<0.05.

The max *4-1* mutants were significantly smaller than the Col-0, *max3-9* and max *2-1* plants in the absence of chilling stress. As predicted, 11 consecutive nights of dark-chilling had little effect on rosette diameter in the *A. thaliana* wild type (Col-0: Figure 4.2.2-3). Similarly, rosette diameter was unaffected by dark chilling in the *max3-9* and *max4-1* mutants. However, the *max2-1* plants displayed a significant reduction in rosette area following stress exposure (Figure 4.2.2-3) with a similar rosette area to the *max4-1* following chilling.

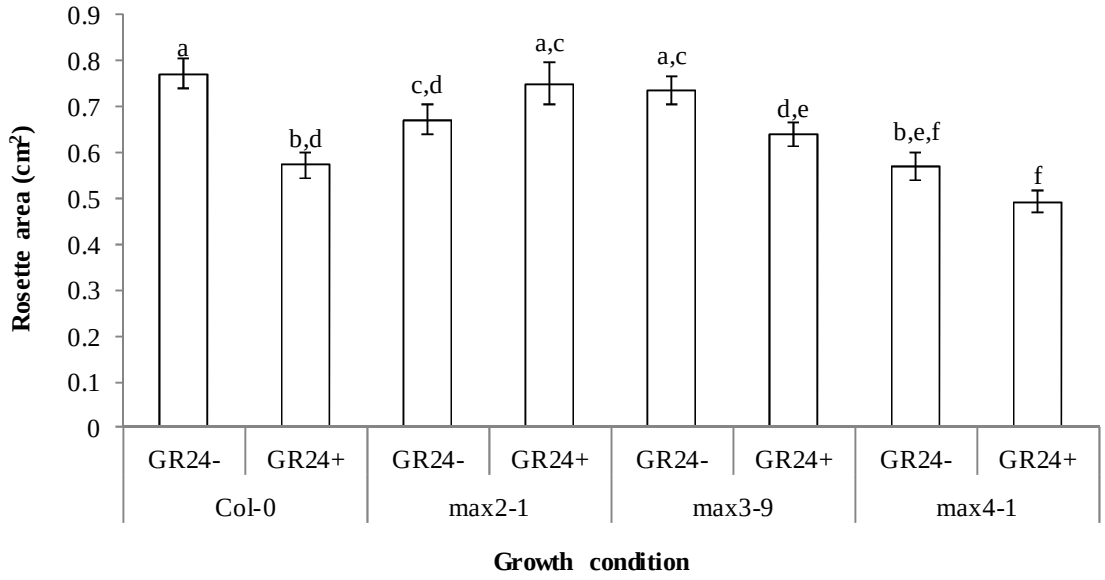

Figure 4.2.2-4: A comparison of the rosette diameters of 4 *Arabidopsis thaliana* genotypes, showing Col-0 (Wt), the strigolactone signalling mutant *max2-1* and the strigolactone synthesis mutants; *max3-9*, *max4-1*. Data shown are for plants at 18 days of age, consisting of 7 days growth under control conditions followed by 11 days of maintenance under control conditions, or exposure to 11 consecutive nights of dark-chilling. Plants were grown either in the presence (GR24+) or absence (GR24-) of 2 µmol GR24. Bars represent the SE of the mean (n>=90). Statistical significance is shown by *t*-test at P=<0.05.

When grown under control conditions, the application of GR24 had a significant inhibitory effect on the growth of Col-0 (Figure 4.2.2-4) but not on the *max2-1* mutants. However, rosette area was decreased as a result of GR24 application in the *max3-9* and *max4-1* mutants (Figure 4.2.2-4). The rosette area was similar in the *max3-9* and *max2-1* plants to Col-0 in the presence of GR24 (Figure 4.2.2-4).

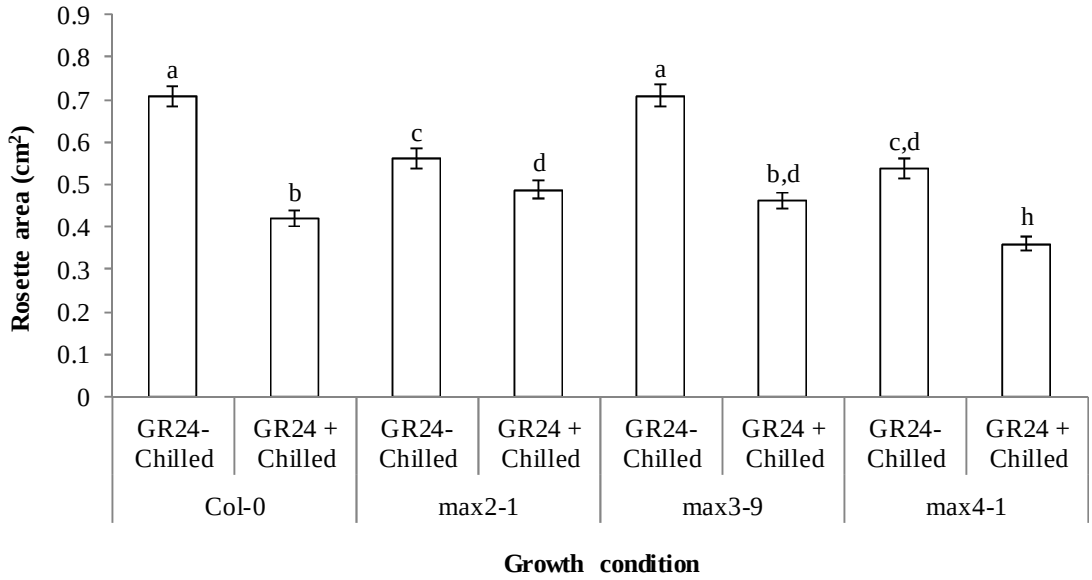

Figure 4.2.2-5: A comparison of the rosette diameters of 4 *Arabidopsis thaliana* genotypes, showing Col-0 (Wt), the strigolactone signalling mutant *max2-1* and the strigolactone synthesis mutants; *max3-9*, *max4-1*. Data shown are for plants grown on ½ MS media, either in the absence or presence of 2µM GR24. Plants were grown to 18 days, consisting of 7 days growth under control conditions followed by 11 consecutive nights of dark-chilling. Bars represent the SE of the mean (n>=90). Statistical significance is shown by *t*-test at P=<0.05.

Under dark-chilling conditions Col-0 and *max3-9* had a similar rosette area, but the rosette areas were significantly lower in *max2-1* and *max4-1* plants (Figure 4.2.2-5 GR24-). GR24 caused a significant decrease in rosette area in all genotypes that had been exposed to 11 consecutive nights of dark-chilling (Figure 4.2.2-5). Under dark-chilling conditions in the presence of GR24 (GR24+), *max2-1* had the greatest rosette area, being comparable to both *max3-9* in the absence of GR24 (Figure 4.2.2-5 GR24+).

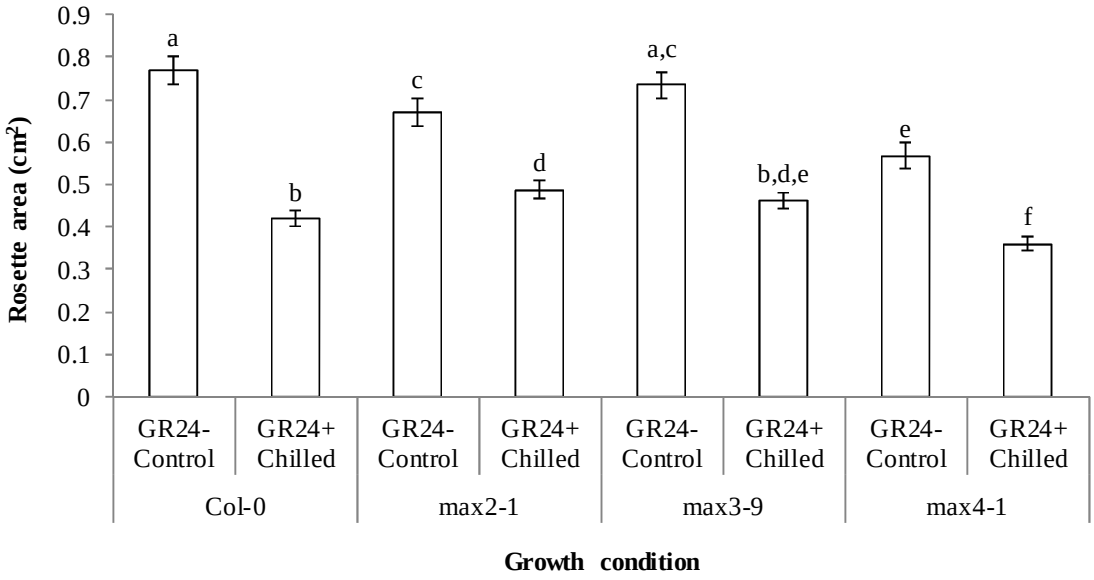

Figure 4.2.2-6: Rosette diameters of 4 *Arabidopsis thaliana* genotypes, showing Col-0 (Wt), the strigolactone signalling mutant *max2-1* and the strigolactone synthesis mutants; *max3-9*, *max4-1*. Data shown are for plants grown on ½ MS media, either in the absence of GR24 grown under control conditions, or presence of 2µM GR24 grown under 11 consecutive nights of dark-chilling. Plants were grown to 18 days, consisting of 7 days growth under control conditions followed by 11 consecutive nights of dark-chilling. Bars represent the SE of the mean (n>=90). Statistical significance is shown by T-test at P=<0.05.

Col-0 plants grown in the presence of 2µM GR24 under dark-chilling conditions were significantly smaller (by about 50%) than those grown without GR24 in the absence of stress (Figure 4.2.2-6). In contrast, the inhibitory effect of GR24 was smaller (up to 25%) in the mutant lines (Figure 4.2.2-6).

4.2.3. The effect of dark-chilling on strigolactone deficient mutants and the wild type plants grown on soil

The *A. thaliana* mutants were also grown together with the wild type on soil. In these experiments, plants were grown for 3 weeks under optimal temperatures and then exposed to either 7 consecutive nights of dark-chilling or maintained under control conditions.

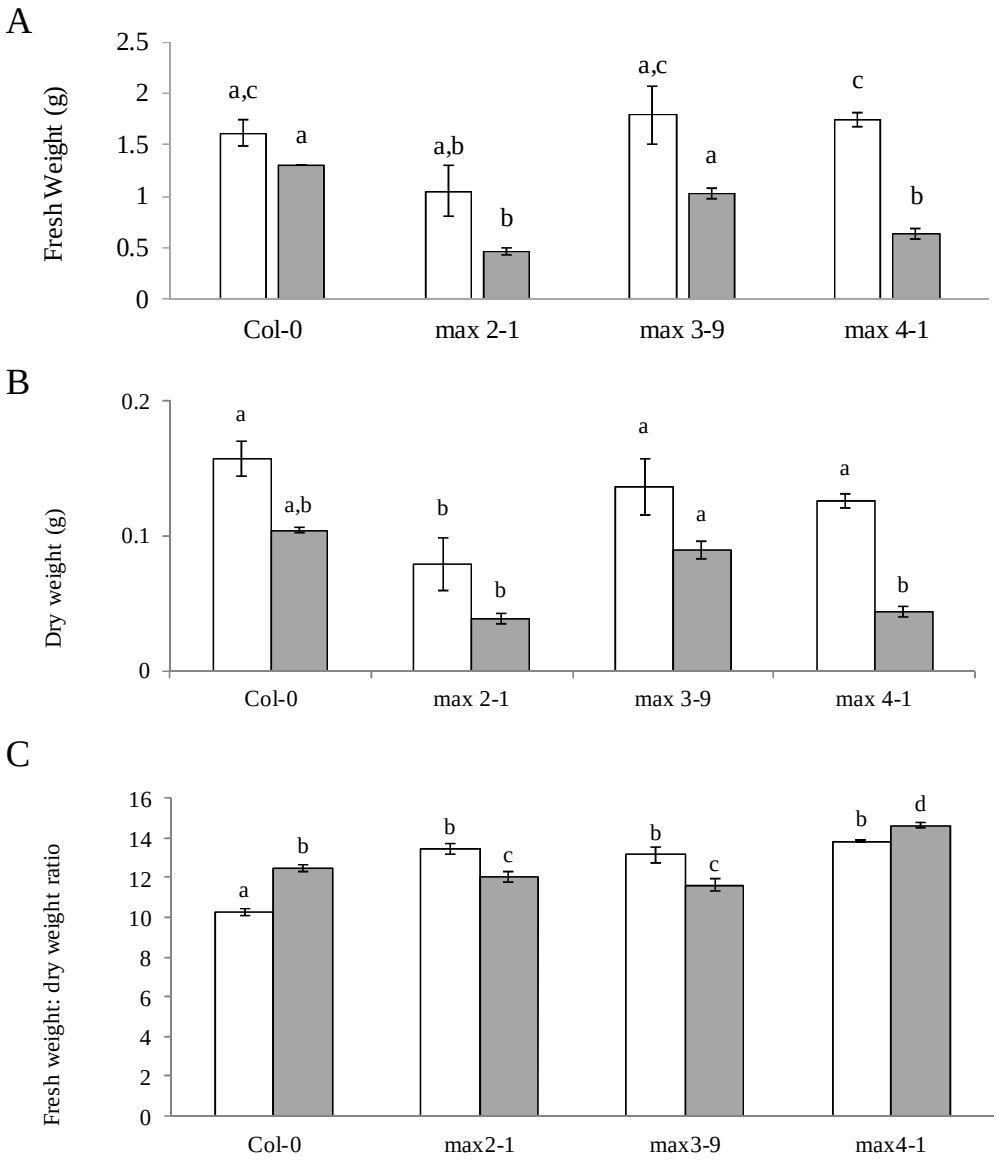

Figure 4.2.3-1: A) Fresh weight; B) Dry weight; C) Fresh weight: dry weight ratio; of Col-0 (Wt), the strigolactone signalling mutant *max2-1* and the strigolactone synthesis mutants; *max3-9*, *max4-1*. Plants were grown for 28 days, consisting of 21 days growth under control conditions followed by 7 consecutive nights of dark-chilling. Data are average values ± SE (n=12). Open bars show control values, grey bars show dark-chilled values. Statistical significance is shown by *t*-test at P=<0.05.

When grown on soil under control conditions all genotypes had a similar fresh shoot biomass than *max2-1* (Figure 4.2.3-1 A). After exposure to 7 consecutive nights of dark-chilling there was no significant reduction in fresh weight in Col-0. In contrast, the fresh weight of all the mutant genotypes was significantly decreased by the stress (Figure 4.2.3-1 A). Exposure to dark-chilling caused a significant reduction in dry biomass in all the lines (Figure 4.2.3-1 B). Under control conditions the fresh weight: dry weight ratios were higher in all mutant lines than Col-0 (Figure 4.2.3-1 C). However, exposure to dark-chilling caused a significant increase in the fresh weight: dry weight ratios in the Col-0 and *max4-1* lines. In contrast, the fresh weight: dry weight ratios were reduced by dark-chilling for *max2-1* and *max3-9* (Figure 4.2.3-1 C).

As a further step in these investigations the effect of dark-chilling on photosynthetic parameters was measured.

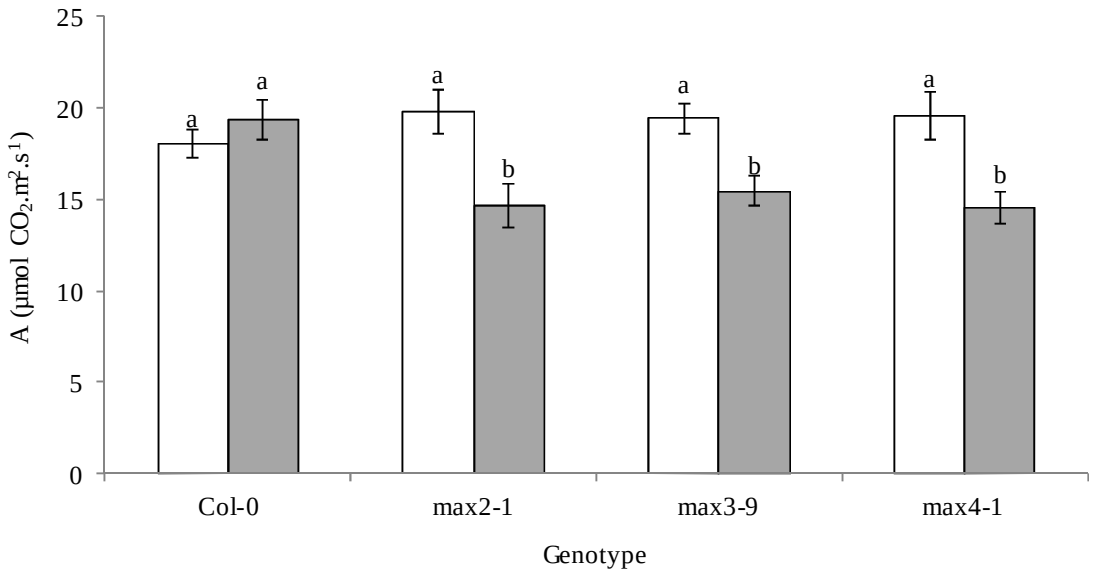

Figure 4.2.3-2: Carbon assimilation rates of Col-0 (Wt), the strigolactone signalling mutant *max2-1* and the strigolactone synthesis mutants; *max3-9*, *max4-1*. Plants were grown for 28 days, consisting of 21 days growth under control conditions followed by 7 consecutive nights of dark-chilling. Data are average values ± SE (n=12). Open bars show control values, grey bars show dark-chilled values. Statistical significance is shown by *t*-test at P=<0.05.

Under control conditions, photosynthetic carbon assimilation was comparable in all lines. However, while exposure to 7 consecutive nights of dark-chilling had not effect on photosynthesis in Col-0, the stress caused a significant decrease in photosynthesis in all lines deficient in SL pathway proteins (Figure 4.2.3-2).

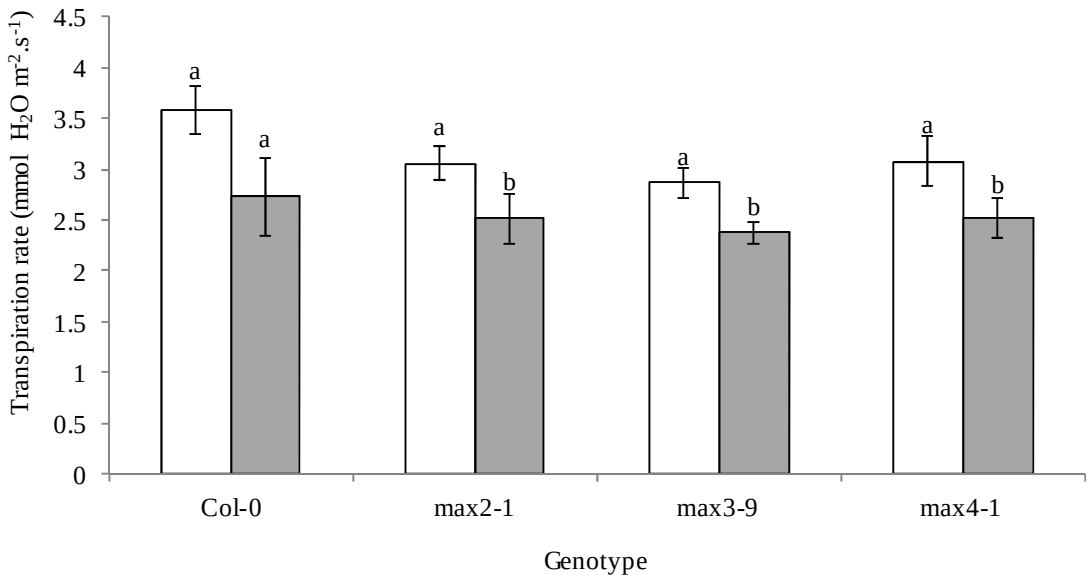

Figure 4.2.3-3: Transpiration rates of Col-0 (Wt), the strigolactone signalling mutant *max2-1* and the strigolactone synthesis mutants; *max3-9*, *max4-1*. Plants were grown for 28 days, consisting of 21 days growth under control conditions followed by 7 consecutive nights of dark-chilling. Data are average values ± SE (n=12). Open bars show control values, grey bars show dark-chilled values. Statistical significance is shown by *t*-test at P=<0.05.

Under control conditions the transpiration rate of all lines was comparable. Exposure to 7 consecutive nights of dark-chilling caused a reduction in transpiration in all lines (Figure 4.2.3-3).

4.3. Discussion

These studies described in this chapter sought to determine the role of strigolactone (SL) in the low temperature tolerance of pea and *A. thaliana*. Taken together, the data presented here show that SL synthesis and signalling are required for low temperature tolerance in both species. While photosynthesis was unaffected by 7 nights of dark chilling in the Wt peas, a chilling-induced inhibition of photosynthesis was observed in the mutants defective in either SL synthesis (BL298) or signalling (K164 and K487). Similarly, photosynthesis was unaffected by dark chilling in Wt *A. thaliana*. However, photosynthesis was susceptible to inhibition by dark chilling in mutant lines defective in SL synthesis (*max3-9* and *max4-1*) or signalling (*max2-1*) when plants were grown on soil. While chilling had no effect on leaf C_i in any of the pea lines, chilling had an inhibitory effect on stomatal conductance and transpiration in the SL synthesis (BL298) and signalling (K487) lines. These findings suggest that SL has an effect on chilling sensitivity that is linked its effects on stomatal density and functions. However, chilling had a similar negative impact on all the *A. thaliana* genotypes. This observation is surprising given that the *A. thaliana max* mutants have increased stomatal densities relative to Wt (Ha et al., 2014). The *max* mutants exhibited increased leaf water loss during dehydration (Ha et al., 2014) but this did not appear to occur following dark chilling, the *max* mutants showing a variable response in terms of leaf fresh weight/dry weight ratios.

The *max* mutants have also been shown to exhibit slower ABA-induced stomatal closure. Moreover, the *max2* mutants accumulated less ABA than Wt plants (Yao and Finlayson, 2015). ABA has a central role in the tolerance of *A. thaliana* plants to chilling and freezing (Jarillo et al., 1993; Shi et al., 2014), it is possible that the absence of SL pathways alters chilling sensitivity through its effects on ABA. However, SL are positive regulators of ABA synthesis and ABA-regulated gene expression was shown to be enhanced in *max2* mutants (Bu et al., 2014). Thus, it is unlikely that SL influence dark chilling sensitivity through its effects on ABA, because chilling sensitivity is enhanced in the mutants defective in SL pathways. However, as in the case of chilling, the *max2* mutant seedlings were also hypersensitive to osmotic stress, SL may play a role in the control of plant responses to these stresses through the regulation of ABA-independent pathways, as described by Shinozaki et al., (2003).

In contrast to the hypothesis that SL exert a positive control on plant chilling stress tolerance, the addition of the artificial SL, GR24, enhanced chilling sensitivity in all *A. thaliana* genotypes when the plants were grown on plates. This apparent contradictory result may be explained either by the concentration of GR24 used, which might not be optimal for induction of chilling responses, or that other factors in the growth media such as sucrose also had an impact on chilling sensitivity that

counteracts the effects of loss of SL functions. However, GR24 has an effect on chilling sensitivity even in the *max2-1* mutants suggesting that the negative effect of GR24 on chilling sensitivity is not dependent on SL-signalling pathways. In a similar manner. the length of the primary roots of the *A. thaliana* Wt and *max* mutants has been shown to be negatively regulated by increasing concentrations of GR24 (Ruyter-Spira et al., 2011). Moreover, phytopathogenic fungi have been shown to have a decreased colony area with increased concentrations of GR24 in their growth media (Dor et al., 2011).

While the enhanced sensitivity of the SL-deficient pea and *A. thaliana* mutants is not always translated into effects on biomass accumulation, a decrease in dry biomass was found to accompany an enhanced sensitivity of photosynthesis to dark chilling in both species. In cases where this relationship was not observed, the apparent anomaly might be explained by slower growth and biomass accumulation rates. Taken together, the data presented here show that lack of SL functions increase sensitivity to dark-chilling exposure in pea and *A. thaliana* plants grown in soil. Further work is required to determine the mechanisms by which SL influences chilling tolerance, especially through crosstalk with other hormones that control stress tolerance.

"The two most powerful warriors are patience and time"

-Leo Tolstoy

5. Characterising the low-temperature tolerance of 5 *Vicia faba* cultivars

5.1. Introduction

Faba bean (*Vicia faba* L) is one of the three most important cool season food legumes globally (O'Sullivan and Angra, 2016; FAOSTAT, 2016). There are two seasonal groupings of faba bean: winter and spring. While the protein content of spring types is marginally higher than winter types (Bond and Toynbee-clarke, 1968), winter types have a greater yield and better tolerance to low temperatures (Inci and Toker, 2011). Within the winter and spring types there are a multitude of different cultivars, each bred for a specific agronomic trait (Knott et al., 1994).

The genus *Vicia* comprises of approximately 166 members (Enneking, 1994), with *V. faba* containing 4 distinct agricultural varieties; major, minor, equina and paucijuga. However, the phylogenetic placement of *V. faba* is contentious and the evolutionary history of the Leguminosae remains an active field of study (Wojciechowski et al., 2004). Moreover, the evolutionary history of *V. faba* itself is unresolved. It has a high level of intraspecies diversity; as well as being divided into 4 varieties, each variety can be further subdivided into spring and winter cultivars (Knott et al., 1994). Historic landraces of *V. faba* are thought to be extinct, however anthropological research has suggested its history to be closely tied to early crop domestication practices, extending back approximately 10,000 years (Duc et al., 2010).

Traces of the *Vicia* genus have been found at stone, bronze and iron age sites, particularly in the near east and Mediterranean basin. It is thought that the centre of origin for the *Vicia* genus is in the fertile crescent, in northern Iraq (Cubero, 1974). From its proposed centre of origin in the Near East, *V. faba* has prevailed as a crop of agricultural interest in Europe. Whilst the breeding history remains somewhat obscure, a possible route of entry for a winter variety faba bean into the United Kingdom has been proposed (Bond and Crofton, 1999). Two winter types, named "Russian" and "Little Winter", were introduced into the United Kingdom in 1825 (though their sources are unknown). The 'Russian' type in particular was recommended for growth in Scotland, indicating that it had been bred for cold tolerance traits. However it should be noted that no record exists as to whether these cultivars were introduced into the current *V. faba* breeding germplasm pool.

The obscure evolutionary and breeding history of *V. faba* makes the phylogenetic resolution of the crop challenging. However, the modern day prevalence of faba bean in North America, South America, Europe, Asia, India and Australia, highlight the adaptability of faba bean to a range of different agro-environmental conditions (de la Vega et al., 2012). The utilisation of modern genomic

sequencing tools could allow for the rapid identification of thee causative genetic factors, underpinning the range of environmental conditions to which faba bean cultivars have adapted.

Despite the inherent tolerance of winter faba bean cultivars to chilling and freezing, they are currently limited in their agro-environmental distribution by sensitivity to low temperatures extremes. For example, in Germany and eastern regions of Europe no faba bean is currently grown. This is because of the harsh winter temperatures in these regions (Link et al., 2010). Therefore, the improvement of low temperature tolerance in faba bean, especially in northern and central European countries which are subject to winter temperatures below -6 °C, is critically important (Herzog, 1987).

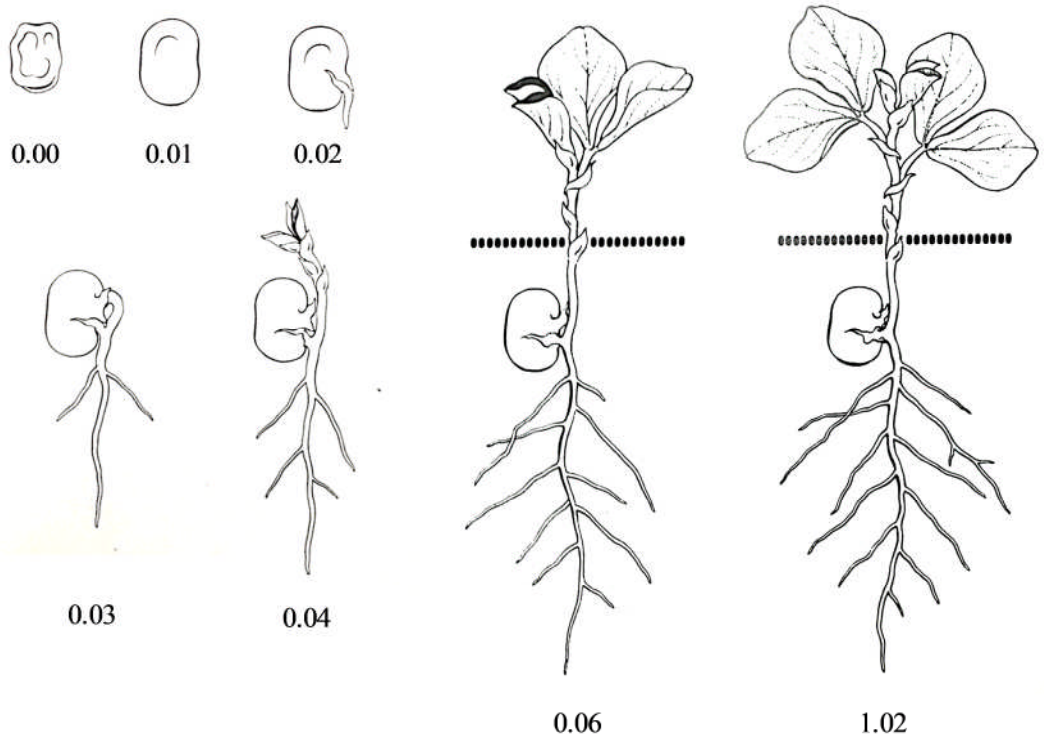

Figure 5.1-1: Stages of faba bean germination and growth; Dry seed 0.00; imbibed seed 0.001; radicle apparent 0.02; plumule and radicle apparent 0.03; emergence 0.04; first leaf unfolded 0.06; second node stage 1.02. Figure adapted from Knott et al., (1994).

To mitigate the adverse impact of low temperature stress, an understanding of the processes underpinning tolerance and sensitivity is needed. The tolerance of winter faba bean cultivars to low temperatures is dependent on the ability of plants to acclimate. Herzog, (1989) stated that the minimum necessary acclimation period for faba bean survival of freezing is 10 days. Acclimation is a complex biological process in which the chemical composition and genetic regulation of a cell will

change, resulting in enhanced tolerance to low temperature stress (Xin and Browse, 2000). While research has been conducted to identify the factors underpinning successful acclimation in faba bean, this has focused primarily on leaf fatty-acid content (Arbaoui and Link, 2008). In general, trait improvement of faba bean has employed traditional quantitative trait loci mapping (QTL) approaches. While such approaches have been useful in the development of stress tolerance, there are inherent limitations, such as the poor sampling of allelic variation; low resolution and lack of segregation (Long et al., 2013; Sallam and Martsch, 2015). Moreover QTL mapping does not give a clear idea of which physiological, cellular and genetic processes underpin desirable traits. Potential phenotypic traits have been suggested as freezing tolerance markers, such as flower colour (Inci and Toker, 2011). However, such markers are imprecise. Therefore, in order to accelerate faba bean breeding programs molecular and metabolic markers should be identified for use in marker assisted selection programs (O'Sullivan and Angra, 2016).

Faba bean is generally sown in the UK in October/November, with optimal sowing ensuring the establishment of the 1-2 node stage for over-wintering (Figure 5.1-1). While most commercial winter cultivars of faba bean are hardy to chilling and freezing temperatures, exceptionally severe winter freezing can cause the total destruction of the vegetative mass (Knott et al., 1994). A better understanding of the factors underpinning stress tolerance in young plants is needed. The results shown in chapters 3 and 4 have identified photosynthetic carbon assimilation as a metabolic marker of chilling stress tolerance. The following studies were undertaken to characterise the relative tolerances of 5 faba bean cultivars to chilling and freezing stress, using photosynthesis and growth as stress markers. These studies were performed with a view to identifying cultivars differing in low temperature tolerance, for use in further investigations.

5.2. Results

The following studies were performed to characterise the chilling and freezing sensitivities of 5 cultivars of *V. faba*: Buzz, Clipper, Hiverna, Sultan and Wizard. To investigate chilling sensitivity plants were grown under control conditions for 14 days, followed by maintenance under control conditions for a further 7 days (control) or exposure to 7 consecutive nights of dark-chilling (chilled). To investigate freezing tolerance plants were grown for 14 days under control conditions, followed by subjection to an acclimatory period of 10 consecutive nights of dark-chilling (acclimated) or maintenance under control conditions (control). For both control and acclimated plants, the 10th night of growth culminated in exposure to 30 minutes of freezing at -5 ºC in the final hour of the plants dark cycle (dark-freezing). Following the application of freezing treatment plants were maintained under control conditions for 24 hours before phenotypic measurements were made.

5.2.1. The effect of dark chilling stress on the growth of five faba bean cultivars

Under control conditions the fresh weights of Buzz, Clipper, Hiverna and Wizard were comparable. However, Sultan had a significantly lower total fresh weight than the other lines (Figure 5.2.1-1 A). After exposure to 7 consecutive nights of dark chilling, the total fresh biomass of Wizard and Hiverna was comparable, however Wizard had a significantly higher fresh biomass than all other lines under dark-chilling conditions (Figure 5.2.1-1 A). The Buzz and Clipper cultivars showed a significant reduction in total fresh biomass after dark-chilling exposure, however Hiverna, Sultan and Wizard did not show a reduced fresh weight as a result of dark-chilling (Figure 5.2.1-1 A). Total dry weight was comparable between Buzz and Clipper under control conditions, however Buzz had the highest total dry weight of any cultivar under these conditions (Figure 5.2.1-1 B). Under dark-chilled conditions Buzz, Clipper and Sultan performed comparably in terms of total dry biomass, with Hiverna and Wizard having a significantly higher dry biomass than the other cultivars (Figure 5.2.1-1 B). Dark-chilling caused a significant reduction in total dry biomass in Buzz and Clipper, however the total dry biomass of Hiverna, Sultan and Wizard was not affected by this treatment (Figure 5.2.1-1 B). The FW/DW ratio was highest in Hiverna under control conditions, with Buzz and Clipper performing similarly to Sultan and Wizard, but with Buzz having a significantly lower FW/DW ratio than Clipper (Figure 5.2.1-1 B). Under dark-chilling conditions Clipper, Hiverna and Wizard had a comparable FW/DW ratio with Buzz and Sultan showing comparably lower FW/DW ratios (Figure 5.2.1-1 C). Exposure to dark-chilling caused significantly higher FW/DW ratios in all lines compared to controls (Figure 5.2.1-1 C).

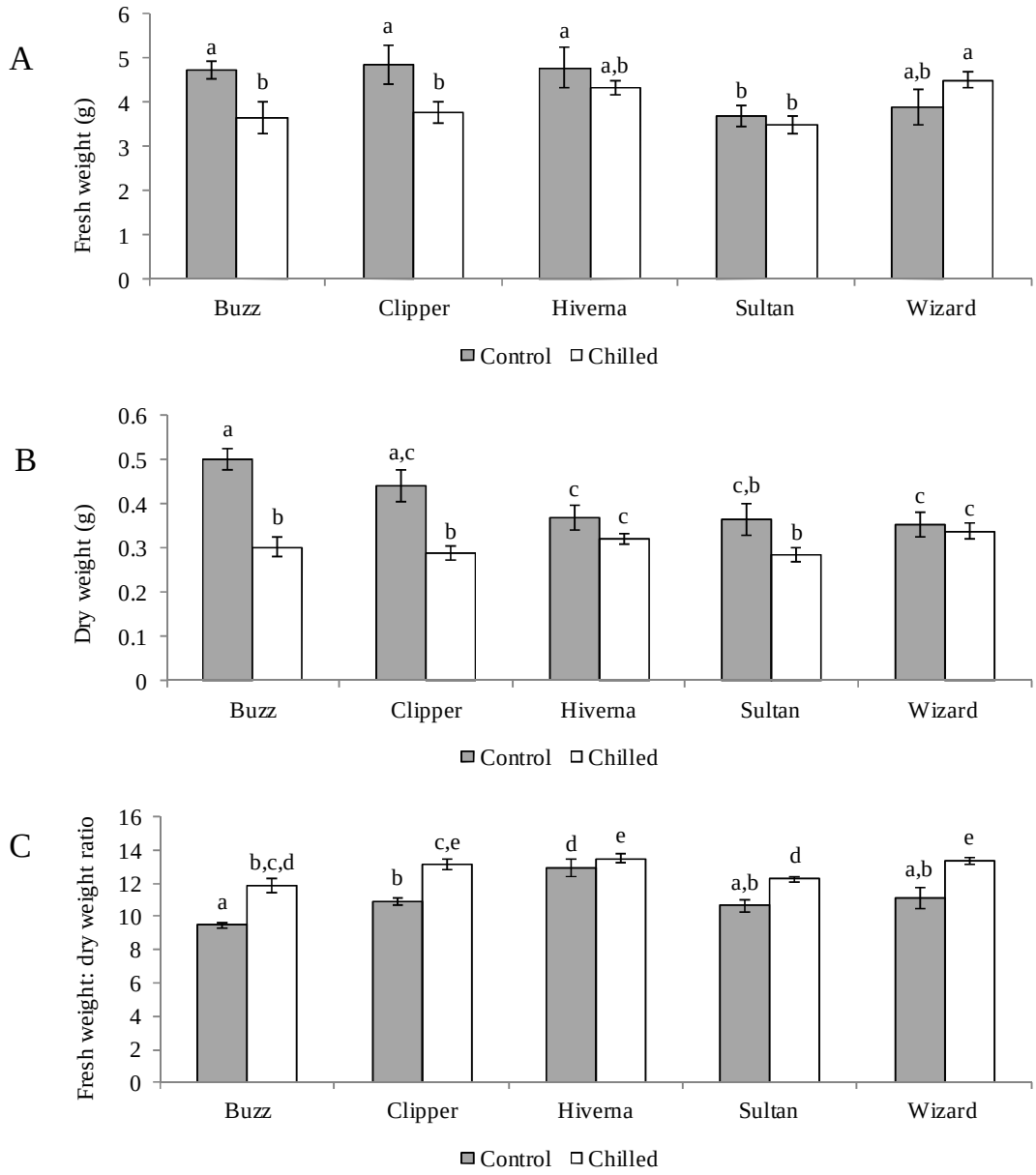

Figure 5.2.1-1: A) Total fresh weight of 5 *V. faba* cultivars grown under control conditions or subjected to dark-chilling treatment; B) Total dry weight of 5 *V. faba* cultivars grown under control conditions or subjected to dark-chilling treatment; C) Fresh weight: dry weight ratio of 5 *V. faba* cultivars grown under control conditions or subjected to dark-chilling treatment. The cultivars Buzz, Clipper, Hiverna, Sultan and Wizard were grown on compost for 21 days, either under control conditions or for 2 weeks under control conditions followed by 7 consecutive nights of exposure to temperatures of 4 °C. Grey bars show plants grown under control conditions and open bars show plants grown under acclamatory conditions ± SE (n = 16). Significance is shown by Student's *t*-test.

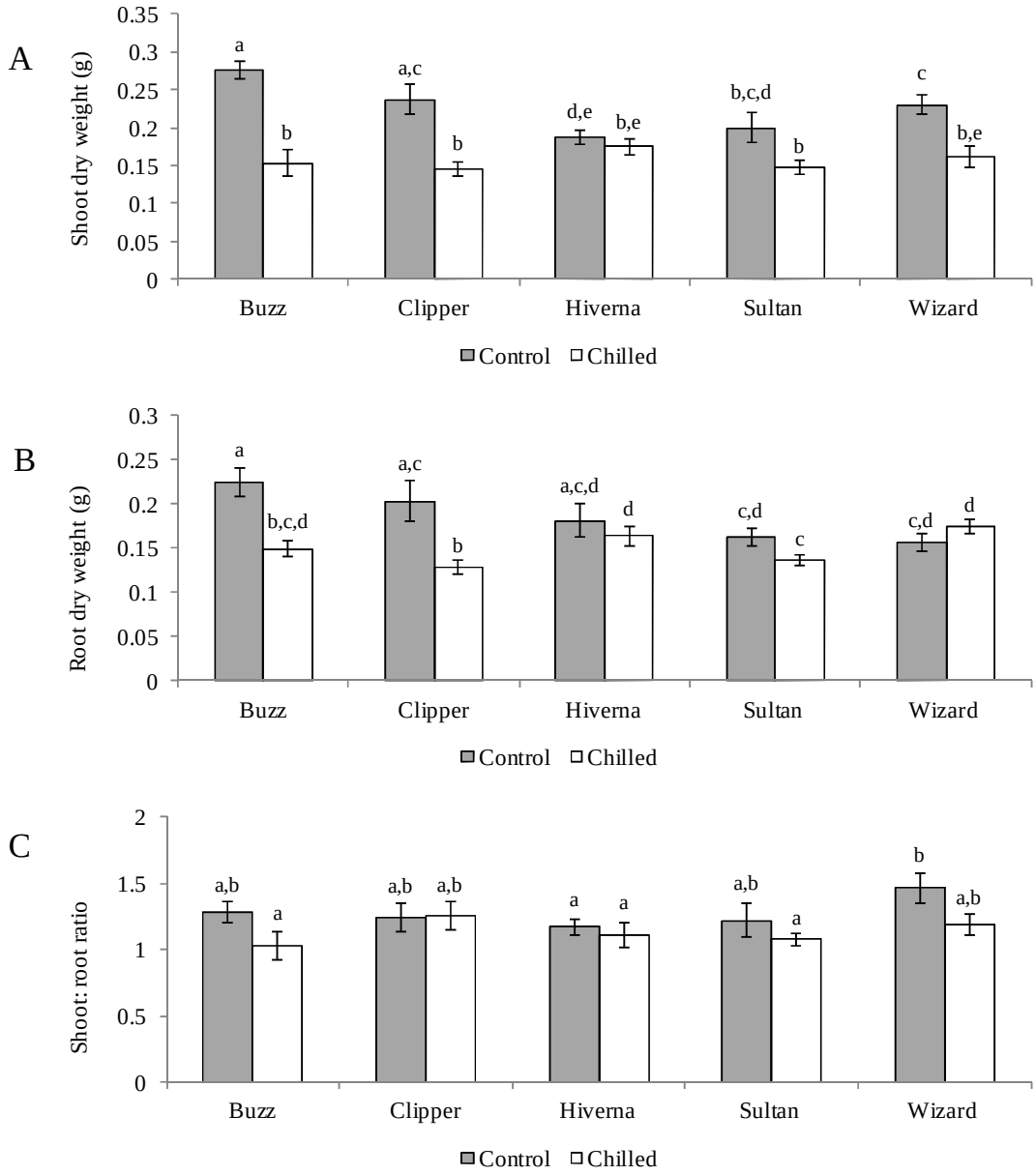

Figure 5.2.1-2: A) Shoot dry weight of 5 *V. faba* cultivars grown under control conditions or subjected to dark-chilling treatment; B) Root dry weight of 5 *V. faba* cultivars grown under control conditions or subjected to dark-chilling treatment; C) Shoot: root ratio of 5 *V. faba* cultivars grown under control conditions or subjected to dark-chilling treatment. The cultivars Buzz, Clipper, Hiverna, Sultan and Wizard were grown on compost for 21 days, either under control conditions or for 2 weeks under control conditions followed by 7 consecutive nights of exposure to temperatures of 4 °C. Grey bars show plants grown under control conditions and open bars show plants grown under acclamatory conditions ± SE (n = 16). Significance is shown by Student's *t*-test.

Under control conditions the dry weight of the shoot was highest in the Buzz and Clipper cultivars, with Clipper showing a comparable shoot dry biomass to Wizard. Hiverna and Sultan had a comparable shoot dry biomass under control conditions (Figure 5.2.1-2 A). After exposure to 7 consecutive nights of dark-chilling all cultivars performed similarly in terms of the shoot dry biomass (Figure 5.2.1-2 A). Comparing lines grown under control conditions to those subjected to dark-chilling treatment, significant reductions were seen in the shoot dry biomasses of Buzz, Clipper and

Wizard. However, Hiverna and Sultan were not significantly affected by this treatment (Figure 5.2.1-2 A). Under control conditions the root dry biomass was comparable between Buzz, Clipper and Hiverna with Sultan and Wizard having comparably lower values (Figure 5.2.1-2 B). After exposure to 7 consecutive nights of dark-chilling Buzz, Hiverna and Wizard displayed comparably high root dry biomass values. Buzz also showed a statistically similar root dry biomass to Clipper and Sultan, however Sultan had the lowest root dry biomass of all cultivars after 7 consecutive nights of dark chilling (Figure 5.2.1-2 B). Exposure to dark-chilling stress caused a decrease in root dry biomass for the Buzz and Clipper cultivars, however Hiverna, Sultan and Wizard all performed similarly to controls under dark-chilling conditions (Figure 5.2.1-2 B). Under control conditions the shoot to root ratio was comparable between all cultivars, with the exception of Wizard which showed a higher shoot: root ratio than Hiverna (Figure 5.2.1-2 C). Under dark-chilling conditions all cultivars performed similarly and there was no significant change in shoot: root ratio when comparing dark-chilled plants to those grown under control conditions (Figure 5.2.1-2 C).

5.2.2. The effect of acclimation on faba bean photosynthesis and freezing tolerance

Following exposure to 9 consecutive nights of dark-chilling (the minimum period necessary for low temperature acclimation) the photosynthetic parameters of the 5 *V. faba* cultivars were measured.

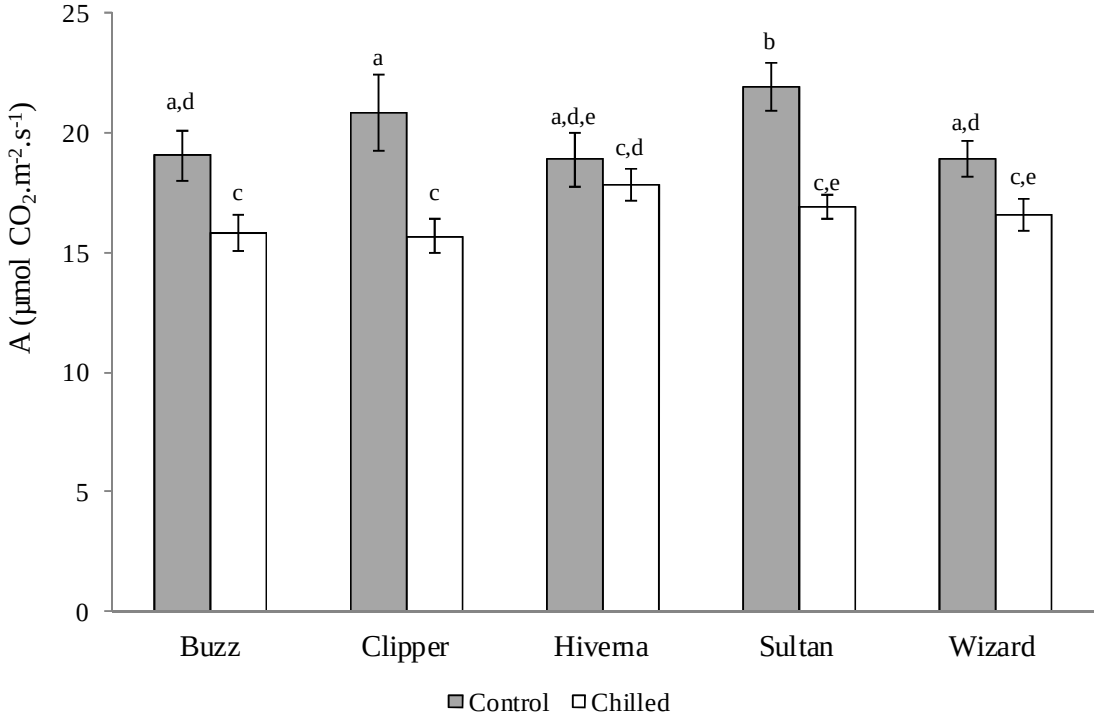

Figure 5.2.2-1: Photosynthetic carbon assimilation of 5 *V. faba* cultivars: Buzz, Clipper, Hiverna, Sultan and Wizard. Plants were grown on compost for 21 days, either under control conditions or for 2 weeks under control conditions followed by 9 consecutive nights of dark-chilling. Grey bars show plants grown under control conditions and open bars show plants grown under dark-chilling conditions ± SE (n=16). Measurements were taken at an atmospheric CO_2 of 400 µmol and a light intensity of 800 µmol.m^2.s^{-1}. Significance is shown by *t*-test.

Under control conditions Sultan displayed the highest rate of photosynthetic carbon assimilation, while carbon assimilation rate was comparable between the Buzz, Clipper, Hiverna and Wizard cultivars (Figure 5.2.2-1). After exposure to dark-chilling the rates of carbon assimilation were comparable between all cultivars. However when comparing assimilation values between plants grown under control conditions and plants exposed to 9 consecutive nights of dark-chilling, cultivar specific differences can be seen. The rate of carbon assimilation was not significantly decreased in the Hiverna cultivar, however all other cultivars showed a decreased carbon assimilation rate following dark-chilling (Figure 5.2.2-1).

Under control conditions the stomatal conductance rates of all cultivars was comparable. Under dark-chilling conditions the rate of conductance was also similar between cultivars. However, the rate of stomatal conductance appeared to be higher in all cultivars under dark-chilling conditions. This increase in conductance was significantly higher in the Buzz and Clipper cultivars (Figure 5.2.2-2).

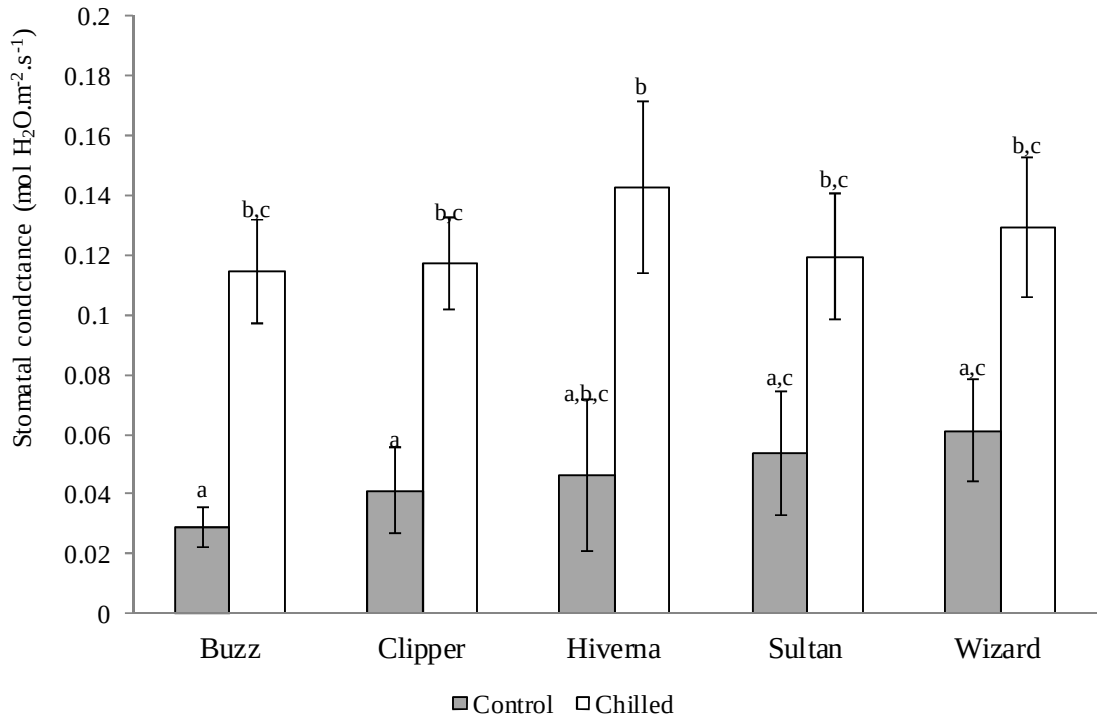

Figure 5.2.2-2: Stomatal conductance of 5 *Vicia faba* cultivars: Buzz, Clipper, Hiverna, Sultan and Wizard. Plants were grown on compost for 21 days, either under control conditions or for 2 weeks under control conditions followed by 9 consecutive nights of dark-chilling. Grey bars show plants grown under control conditions and open bars show plants grown under dark-chilling conditions ± SE (n=16). Measurements were taken at an atmospheric CO_2 of 400 µmol and a light intensity of 800 µmol.m^2.s^{-1}. Significance is shown by *t*-test.

The intracellular CO_2 concentration was comparable between all cultivars under both control and dark-chilled conditions. When comparing plants grown under control conditions to those grown under dark-chilling conditions, Buzz, Hiverna, Sultan and Wizard showed higher intracellular CO_2 concentrations. While the intracellular CO_2 concentration was not significantly higher in the Clipper cultivar, these data did trend toward a higher intracellular CO_2 concentration following dark-chilling (Figure 5.2.2-3).

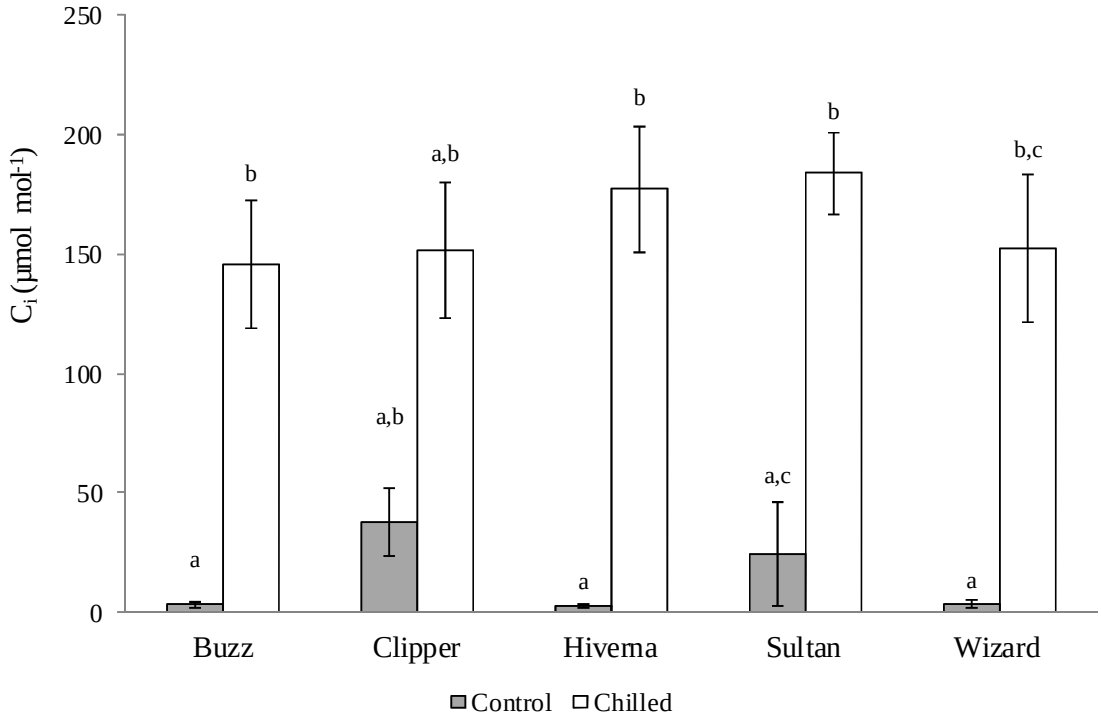

Figure 5.2.2-3: Intracellular CO_2 concentration of 5 *Vicia faba* cultivars: Buzz, Clipper, Hiverna, Sultan and Wizard. Plants were grown on compost for 21 days, either under control conditions or for 2 weeks under control conditions followed by 9 consecutive nights of dark-chilling. Grey bars show plants grown under control conditions and open bars show plants grown under dark-chilling conditions ± SE (n=16). Measurements were taken at an atmospheric CO_2 of 400 µmol and a light intensity of 800 µmol.m^2.s^{-1}. Significance is shown by *t*-test.

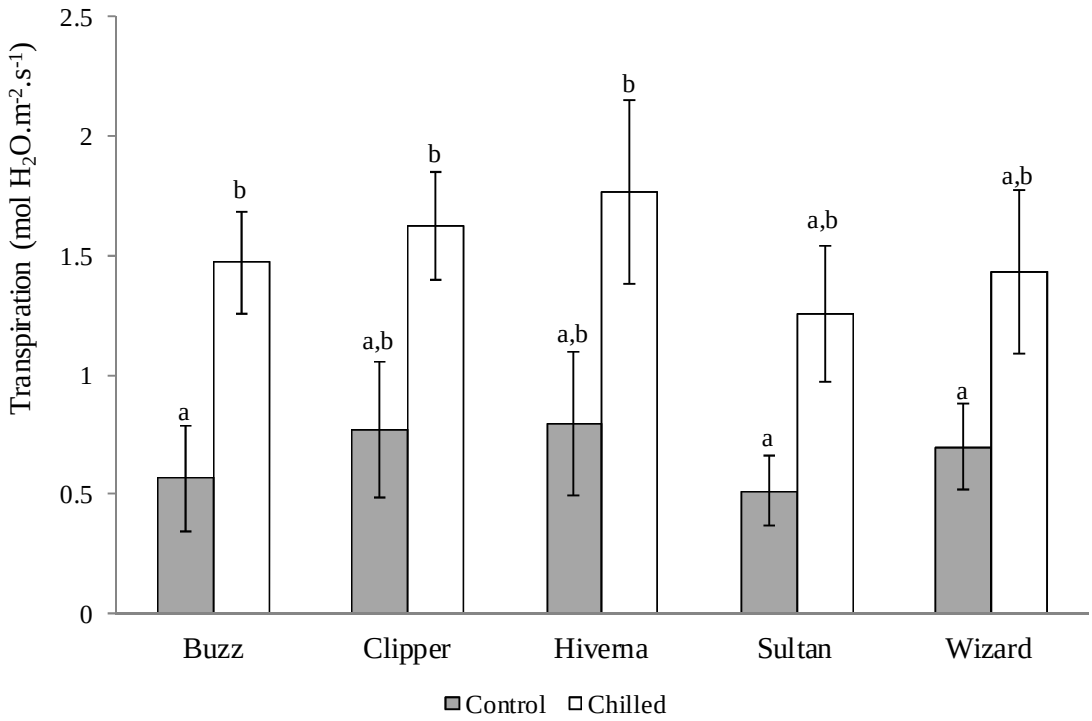

Figure 5.2.2-4: Transpiration rates of 5 *Vicia faba* cultivars: Buzz, Clipper, Hiverna, Sultan and Wizard. Plants were grown on compost for 21 days, either under control conditions or for 2 weeks under control conditions followed by 9 consecutive nights of dark-chilling. Grey bars show plants grown under control conditions and open bars show plants grown under dark-chilling conditions ± SE (n=16). Measurements were taken at an atmospheric CO_2 of 400 µmol and a light intensity of 800 µmol.m^2.s^{-1}. Significance is shown by *t*-test.

Under control conditions the rate of transpiration was comparable between all cultivars. Following 9 consecutive nights of dark-chilling, the rates of transpiration were similar between all cultivars. Transpiration rates were significantly higher in the Buzz cultivars following dark-chilling, however all dark-chilled cultivars trended toward higher rates of transpiration when compared to controls (Figure 5.2.2-4).

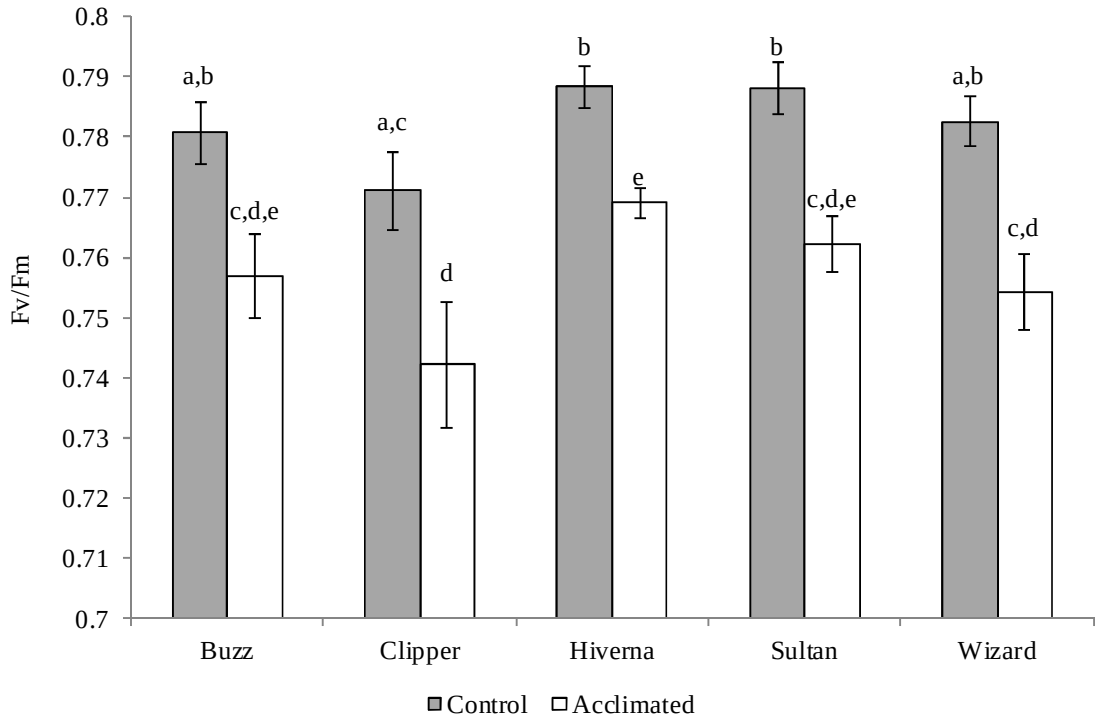

Figure 5.2.2-5: Chlorophyll fluorescence (F_v/F_m) of 5 *Vicia faba* cultivars: Buzz, Clipper, Hiverna, Sultan and Wizard. Plants were grown on compost for 21 days, either under control conditions or for 2 weeks under control conditions followed by 9 consecutive nights of dark-chilling. Grey bars show plants grown under control conditions and open bars show plants grown under dark-chilling conditions ± SE (n=16). Significance is shown by t-test.

Under control conditions chlorophyll fluorescence values (F_v/F_m) were highest in the Hiverna and Sultan cultivars, with these values being comparable to those of Wizard and Buzz when grown under control conditions. Clipper showed a comparable F_v/F_m to Buzz and Wizard under control conditions (Figure 5.2.2-5). Following 9 consecutive nights of dark-chilling the F_v/F_m values were comparable between all cultivars, however Hiverna showed a significantly higher F_v/F_m than Clipper and Wizard following chilling treatment. Comparing plants grown under control conditions to those grown under the acclimatory conditions of 9 consecutive nights of dark-chilling, chlorophyll fluorescence was significantly reduced in all cultivars (Figure 5.2.2-5).

A visual comparison of plants grown under control conditions for 23 days showed the Buzz cultivar to be larger than the other cultivars. Clipper, Hiverna and Wizard grew to a similar size, while Sultan appeared shortest in stature (Figure 5.2.2-7 Control prior to freezing). When grown under chilling acclimation conditions for 9 consecutive nights, all cultivars were similar in height, with the exception of the Sultan cultivar which was smaller (Figure 5.2.2-6 Chilling acclimated prior to freezing). Comparing plants grown under control conditions to plants grown under chilling acclimation conditions, prior to freezing, shows all lines to have a reduced size following chilling. However, the extent of this reduction is greatest in the Buzz cultivar (Figure 5.2.2-6). Plants grown under control conditions and then subjected to a 30 minute dark-freezing period all appeared to suffer extensive freezing induced damage. However, the Hiverna cultivar was able to maintain its youngest leaves (Figure 5.2.2-6).

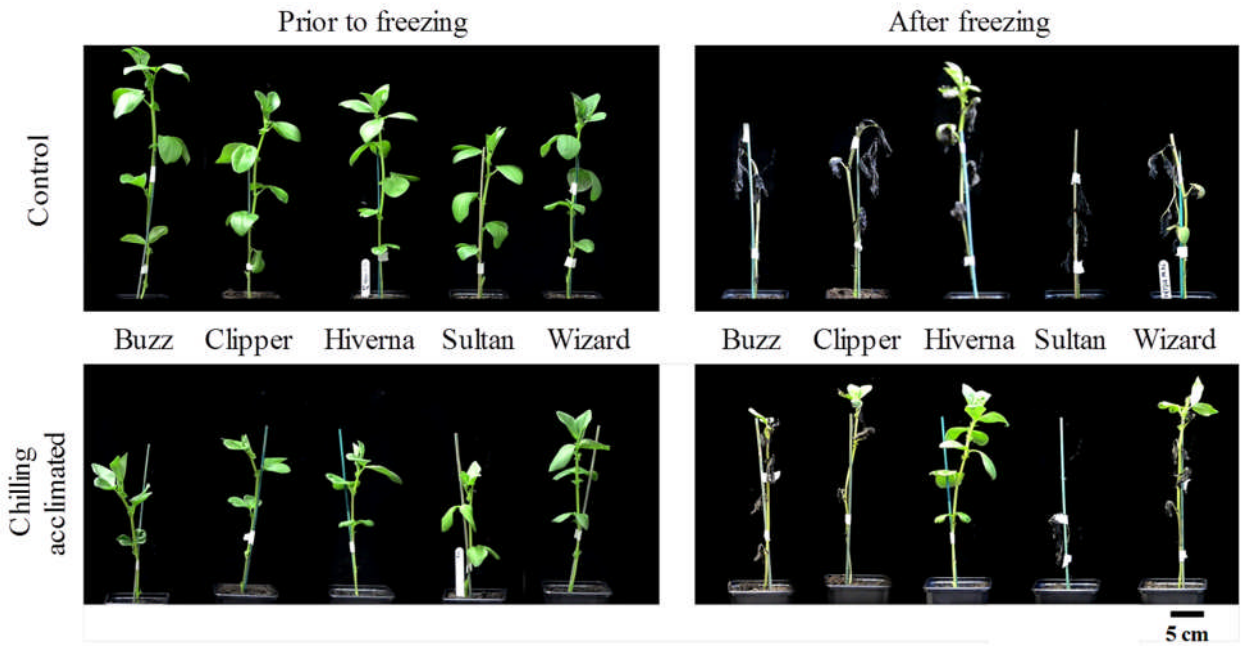

Figure 5.2.2-6: Shoot phenotypes of 5 *Vicia faba* cultivars: Buzz, Clipper, Hiverna, Sultan and Wizard. Plants were grown on compost for either 24 days under control conditions (Control prior to Freezing) or for 2 weeks under control conditions followed by 10 consecutive nights of acclimatory chilling (4ºC ±1ºC; Chilling acclimated prior to freezing). Following growth under either control or acclimatory conditions, plants were exposed to a 30 minute dark-freezing period of -5ºC. Scale bar shows 5cm.

When grown under acclimatory conditions and subjected to a 30 minute freezing period, the extensive damage was seen in all cultivars, with the exception of Hiverna which showed no signs of freezing induced injury (Figure 5.2.2-6 Chilling acclimated after freezing). When comparing plants that had been grown under acclimatory conditions to plants maintained under control conditions, the

Sultan cultivar showed no difference in low temperature tolerance. The Buzz cultivar showed a slight increase in freezing tolerance following acclimation when compared to control, with stem and youngest leaves better maintaining green colouration. The Clipper and Wizard cultivars showed an increase in their capacity to maintain vegetative tissues, however this was only visible in the stem and the youngest leaves. The Hiverna cultivar was the least affected by freezing exposure, both after maintenance under control conditions and growth under acclimatory conditions (Figure 5.2.2-6).

Measurement of the shoot fresh weight of plants that had been maintained under control conditions prior to freezing showed that the Clipper and Sultan cultivars had the lowest fresh weights. Following freezing the fresh shoot weights of all cultivars was comparable (Figure 5.2.2-7 A). However, while freezing exposure caused a reduction in the shoot fresh weights of Buzz, Clipper, Hiverna and Wizard; Sultan showed no significant change in weight following freezing (Figure 5.2.2-7 A). In plants grown under acclimatory conditions, prior to freezing the shoot fresh weight was comparable between all lines. Following freezing exposure the shoot fresh weight of acclimated plants was lowest in Sultan and Wizard, with fresh weight being comparable between Buzz and Clipper and highest in Hiverna (Figure 5.2.2-7 B). Comparing the fresh weight values of acclimated plants before and after freezing showed a significant decrease in values for Buzz, Sultan and Wizard. However there was no significant decrease in fresh weight for Clipper and Hiverna following freezing (Figure 5.2.2-7 B). When comparing the decrease in fresh weight between plants maintained under control conditions, all cultivars retained approximately 70% of their fresh weight following freezing (Figure 5.2.2-7 C). Plants that had been grown under 10 nights of acclimatory chilling, followed by 30 minutes of dark-freezing, also retained 70% of their fresh weight, with the exception of the Hiverna cultivar which maintained approximately 85% of its fresh weight following freezing (Figure 5.2.2-7 C). Following acclimation the Hiverna cultivar showed the highest maintenance of fresh weight of any cultivar.

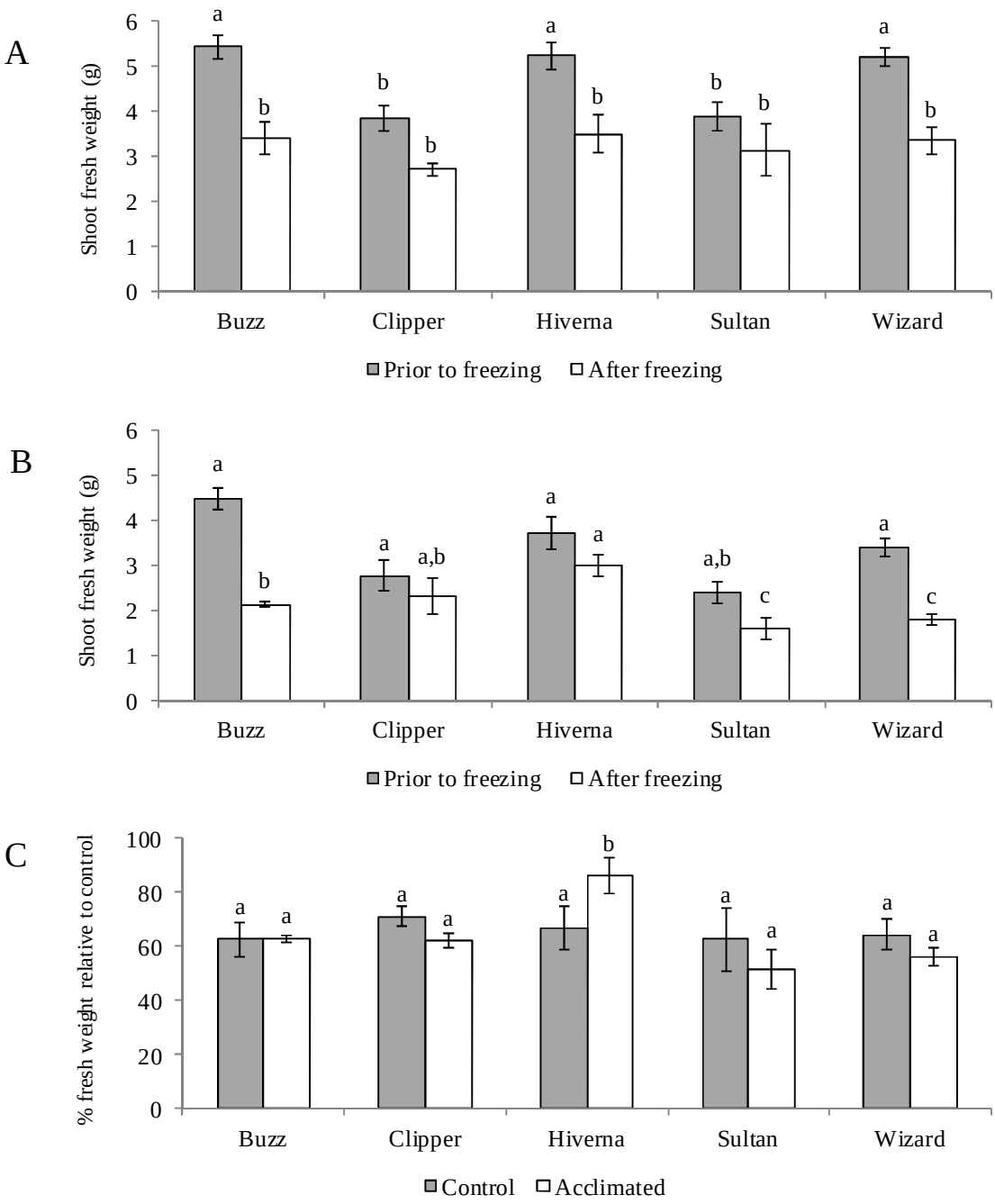

Figure 5.2.2-7: A) Shoot fresh weight of 5 *Vicia faba* cultivars grown under control conditions, before and after 30 minutes of exposure to -5 ºC; B) Shoot fresh weight of 5 *Vicia faba* cultivars grown under acclimatory conditions, before and after 30 minutes of exposure to -5 ºC; C) Percentage reduction in shoot fresh weight of 5 *Vicia faba* cultivars, grown under either control or acclimatory conditions and subjected to 30 minutes of freezing at -5 ºC. The cultivars Buzz, Clipper, Hiverna, Sultan and Wizard were grown on compost for 24 days, either under control conditions or for 2 weeks under control conditions followed by 10 consecutive nights of acclimatory chilling. Following growth under control or acclimatory conditions, plants were exposed to a 30 minute dark-freezing period of -5ºC and allowed to recover under control conditions for 24 hours. Grey bars show plants grown under control conditions and open bars show plants grown under acclimatory conditions ± SE (n=12). Significance is shown by *t*-test.

5.3. Discussion

The studies undertaken in this chapter sought to characterise the effect of chilling and freezing on the growth and photosynthesis of 5 *V. faba* cultivars. Taken together the data presented here show that cultivars differ in their response to both chilling and freezing exposure.

In terms of plant growth, following 7 consecutive nights of dark-chilling only the Buzz and Clipper cultivars saw a reduction in fresh weight. The Hiverna and Wizard cultivars were able to maintain comparable dry biomass to controls following dark-chilling treatment. The Hiverna cultivar showed the highest FW/DW ratio under control conditions, with FW/DW ratio being comparably high between the Hiverna and Wizard cultivars following dark-chilling. There was no effect of dark-chilling on the shoot: root biomass partitioning in any cultivar. Exposure to 9 consecutive nights of dark-chilling caused significant decreases in the photosynthetic carbon assimilation of all cultivars except Hiverna. However, the level of photosynthesis was comparable between all cultivars following dark-chilling, indicating that Hiverna may have a lower basal rate of photosynthesis. The lower stomatal conductance seen under control conditions is difficult to explain, as stomatal conductance would be expected to be lower following exposure to chilling stress. Similarly the lower levels of intracellular CO_2 concentration and transpiration following dark-chilling stress were unexpected. Dark-chilling caused a reduction in the F_v/F_m of all lines, indicating that chilling exposure causes a reduction in the efficiency of the photosystems. This finding is concordant with studies of other plant species exposed to chilling-stress, which show that low temperature exposure causes a reduction in chlorophyll fluorescence (Hakam et al., 2000; Van Heerden et al., 2004a; Strauss et al., 2006). Although dark-chilling caused a decrease in the F_v/F_m value of Hiverna, chilled Hiverna plants had a higher fluorescence value than other chilled cultivars. This suggests that the light harvesting machinery of Hiverna is better protected from chilling stress than the other cultivars. Given that chilling stress was applied during the night, when no light was present, damage to the photosystems is perhaps unusual. However, these findings are similar to studies conducted on soybean where dark chilling was found to have an inhibitory effect on photosynthetic electron transport, with tolerance to chilling being linked to leaf nitrate content (Van Heerden et al., 2004a).

The cultivars responded differently to both 10 consecutive nights of acclimatory chilling and exposure to freezing, both with and without acclimation. The most freezing tolerant cultivar was Hiverna, showing minimal freezing-induced damage and fresh biomass loss. To better understand the basis for these differences in stress tolerance, a deeper understanding of the genetic composition and breeding history of *V. faba* is needed.

Taken together the results presented in this chapter show that the Hiverna cultivar of *V. faba* is tolerant to both dark-chilling and dark-freezing stress. Of the other cultivars examined, levels of low-temperature stress tolerance were comparable. However, to identify the factors underpinning low-temperature tolerance, better genetic resources for faba bean are needed.

“Every component of the organism is as much of an organism as every other part.”

-Barbara McClintock

6. DNA sequencing and genomic assembly in *Vicia faba*

6.1. Introduction

Despite its importance in world agriculture, the development of gene based resources in legumes such as *Vicia faba* has not kept pace with cereal crops. However *V. faba* has a rich history of scientific utility, due in part to its large diploid genome (n=6) which made it an ideal tool for cytogenetic studies in the 1960s and 1990s (O'Sullivan and Angra, 2016). Since the pioneering work of Adela Erith (Erith, 1930), who characterised several important Mendelian inheritance characteristics for the faba bean crop, research in the field of *V. faba* genetics has seen only intermittent periods of interest.

Classical genetic analyses of *V. faba* initially focused on the cytogenetic characterisation of stress-induced chromosomal breaks. Links between these studies and modern molecular genetics were made by Sjodin, (1970, 1971), who identified asynaptic mutants, from which a series of trisomic lines were developed and analysed. Subsequently, genetic markers were assigned to physical chromosomes (Patto et al., 1999) and genes controlling rhizobial symbiosis and cotyledon pigmentation respectively were identified (Duc and Picard, 1986; Duc et al., 1999). The Mendelian inheritance of a seed dormancy gene was established through use of segregating Recombinant Inbred Lines (RIL; (Ramsay, 1997)). While few inbred populations have survived from these early studies, parental germplasm resources are still available (O'Sullivan and Angra, 2016). However, the characterisation of desirable oligogenic traits is dependent on high resolution molecular genetic profiling. Thus, the use of classical genetic approaches alone is no longer sufficient to identify the genes associated with quantitative trait loci (QTLs) for important traits (O'Sullivan and Angra, 2016).

The first molecular marker map for *V. faba* was produced by Torres et al., (1993) who used a combination of 66 isozymes and RAPD markers to identify 11 distinct linkage groups. The combined use of RILs with molecular markers (Restriction Fragment Length Polymorphism (RFLP), Amplified Fragment Length Polymorphism (AFLP), Random Amplification of Polymorphic DNA (RAPD), Simple Sequence Repeat (SSR or Microsatellite), Single Nucleotide Polymorphism (SNP)) has dominated the landscape of *V. faba* genetics over the last 20 years, allowing the identification of QTLs and the production of high resolution linkage maps (Torres et al., 2010). Moreover, these high resolution linkage-based sequences have been used, in part, to produce syntenic maps. For example, Webb et al., (2016) were able to identify and map 687 SNP markers in *V. faba*. These SNP markers were each assigned to individual orthologues in *Medicago truncatula*, with each marker belonging to a linkage group, analogous to one of the six *V. faba* chromosomes. This allowed putative alignment

of *M. truncatula* sequences to corresponding *V. faba* chromosomes. While extremely useful in the context of classical breeding, these maps are inherently limited with regard to the production of a genomic reference sequence, which will provide the gateway to the next meaningful step in faba bean breeding.

Very little *V. faba* sequence data is currently available in public data bases, which is surprising given the increasingly synergistic relationships between different forms of genomic data. Recent years have witnessed the generation of a number of mRNA-based data sets for *V. faba*. These range from the acquisition of EST data (Ray and Georges, 2010) to the generation of transcriptomic data sets. In studies designed to underpin SSR discovery, Kaur et al., (2012) performed 454 sequencing on cDNA extracted from multiple *V. faba* tissues. Over 50,000 single reads were produced in this way, ranging in length from 100->400bp. Subsequent studies have utilised Illumina sequencing of inbred lines to generate transcriptome information (Arun-Chinnappa and McCurdy, 2015; Zhang et al., 2015). To date, there are nine publically available transcriptomic datasets available for *V. faba*, as discussed by O'Sullivan and Angra, (2016). While this wealth of transcriptomic data has been produced, minimal genome sequencing data is available for *V. faba*. The only public data set of genomic *V. faba* DNA sequence was reported by Yang et al., (2012), who performed 454 sequencing on the pooled genomic DNA of 247 accessions in order to identify SSR markers. Therefore, while this approach to sequencing the faba bean genome is current, a much more intensive sequencing program is required.

The lack of genomic sequence data for *V. faba* is due to the intrinsic difficulties of assembling and annotating the huge (~13Gb) genome. However, the organelle genomes of *V. faba* have been successfully sequenced. Negruk (2013) annotated the mitochondrial genome of *V. faba* (Broad Windsor cv) by utilisation of plasmid/fosmid libraries. This mitochondrial genome characterisation revealed a low degree of homology to other sequenced mitochondrial genomes, but interestingly there was a 45% homology to the *M. truncatula* nuclear genome. Moreover the *V. faba* mitochondrial genome was shown to have extensive repetitive content. The chloroplast genome of *V. faba* was sequenced as part of a wider study on the inverted-repeat-lacking clade of legumes (Sabir et al., (2014). Crucially, while sequence data are available from these studies, no information was provided on the cultivars used. However, this study provided evidence for gene transfer from the chloroplast to the nucleus during legume evolution.

The following studies were performed to provide background information that would facilitate a more rapid identification of the genes and processes involved in chilling and freezing tolerance in *V. faba*. One of the *V. faba* cultivars (Wizard cv) that was identified as being chilling sensitive in the studies reported in Chapter 5 was used to sequence the *V. faba* genome, using the Illumina HiSeq 2500 platform.

6.2. Results

6.2.1. Genomic imaging and read assembly

For the visual characterisation of the faba bean chromosomes, seeds of *V. faba* cultivar Wizard, were imbibed for 3 days until germination i.e. the radicle had protruded from the seed coat. Germinated seeds were stored at 4 °C for a 24h period to allow cold-induced metaphase synchronisation. The root apex was then excised, fixed and stained (Figure 6.2.1-1).

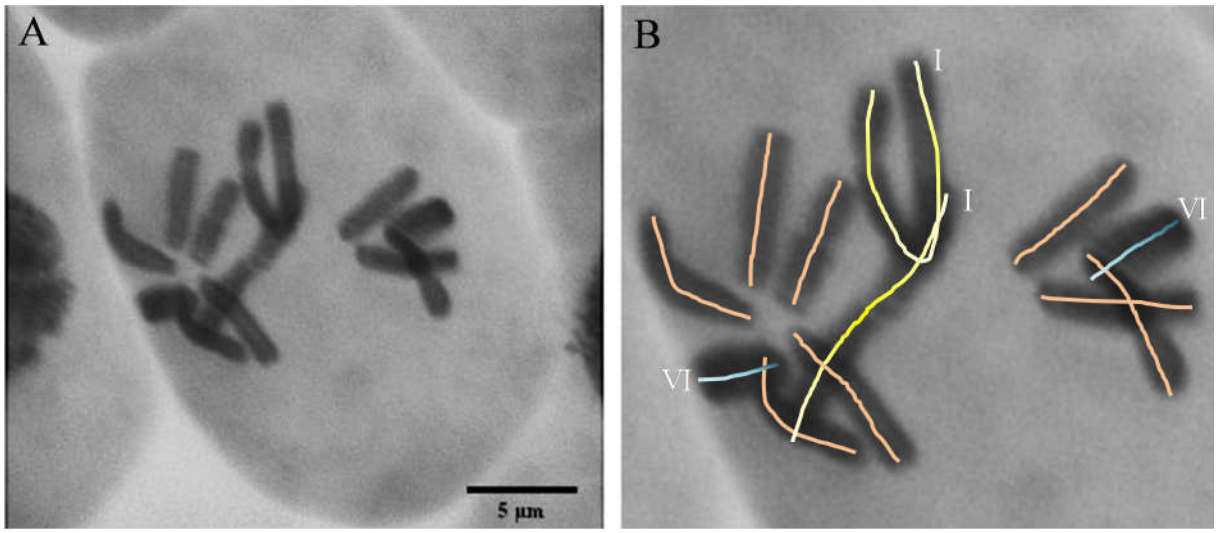

Figure 6.2.1-1: A) Light microscope image of *Vicia faba* chromosomes in metaphase, shown by Feulgen staining of DNA against a FastGreen cytoplasm stain. Scale bars shows 5 µm. B) Identification of individual chromosomes, showing chromosome I in yellow and chromosome VI in blue.

Cytogenetic analysis showed the *V. faba* chromosome number to be 2n=12 (Figure 6.2.1-1 A). The largest chromosome pair (I) and the smallest chromosome pair (VI) were identified, as shown in Figure 6.2.1-1 B. Chromosome I appeared to be considerably larger than the other chromosomes.

Following the visual characterisation of the *V. faba* chromosomes, next generation sequencing was performed on DNA extracted from developing embryos that had been excised from the imbibed seeds. DNA was sequenced on an Illumina HiSeq 2500 platform using 100 bp paired end reads of a single library across 2 lanes. Following quality trimming, raw reads were aligned to both chloroplast and mitochondrial reference sequences (Table 6).

Table 6: Quality-trimmed genomic read data for DNA extracted from *Vicia faba* (Wizard cv) detailing read number and coverage.

	Number of paired reads	**Reads accounted for (%)**	**Coverage**
Total number of reads	812,092,660	100.00	6x
Number of reads aligned to chloroplast reference	7,712,928	0.95	3466x
Number of reads aligned to mitochondria reference	8,657,582	1.07	650x
Number of reads aligned to faba bean transcriptome database	104,668,765	12.89	30x
Number of unaligned reads	691,053,385	85.10	<6x

12.89% of reads mapped to the CDS of *V. faba* with a coverage of 30 x. A small percentage (0.95%) of the reads aligned to the chloroplast reference genome with a coverage of 3466 x (Sabir et al., 2014). Similarly 1.07% of reads aligned to the mitochondrial reference genome with a coverage of 650 x (Negruk, 2013). However, 85.1% of reads could not be aligned to either the organellar genomes or the *V. faba* reference transcriptome (Table 6, Humann et al., (2016)).

Of the reads that could not be aligned, only 10.07% were identified in a repetitive element database (Bao et al., 2015). The Gypsy class of LTR retrotransposons formed the majority of the repetitive elements, accounting for 3.61% of the total reads. The VicSatellite, LTR (uncharacterised) and Copia class LTR elements comprised 2.49%, 2.09% and 0.99% of the genome respectively (Table 7).

Table 7: Quality-trimmed genomic read data aligned against repeat element databases, showing repetitive element identities, the number of paired reads mapped to these repetitive sequences and the total number of reads accounted for as a percentage.

Repetitive element	Number of paired reads	Total reads accounted for (%)
LTR/Gypsy	29,358,977	3.615225
VicSatellite	20,274,464	2.496570
LTR (uncharacterised)	16,974,274	2.090189
LTR/Copia	8,090,787	0.996289
rRNA	1,986,302	0.244591
Ogre	1,708,252	0.210352
Other/Simple	1,199,173	0.147665
Uncharacterised	1,054,668	0.129870
MobileElement	411,832	0.050712
DNA/En-Spm	332,062	0.040890
Retroelement	92,278	0.011363
Non LTR	53,835	0.006629
Other	45,904	0.005653
DNA	40,982	0.005046
DNA/MuDR	36,393	0.004481
DNA/hAT	34,576	0.004258
LINE	21,923	0.002700
Satellite	9,917	0.001221
DNA/Harbinger	8,519	0.001049
tRNA	7,049	0.000868
DNA/TcMar	6,118	0.000753
DNA/Mite	3,643	0.000449
RC/Helitron	1,874	0.000231
SINE	883	0.000109
DNA/hAT-Ac	815	0.000100
DNA/Stowaway	344	0.000042
DNA/Tourist	55	0.000007
Other/Centromeric	52	0.000006
DNA/TcMar-Pogo	6	0.000001
Repetitive element total	81755957	10.07
Genome uncharacterised	609297428	75.03

6.2.2. *De novo* assembly and linkage map integration

Following this analysis of trimmed read data, ABySS was used to perform a *de novo* genome assembly of short reads. This resulted in the generation of 361,137,728 contigs, which varied in length from 50 bp to in excess of 5 kb (Figure 6.2.2-1 A, B).

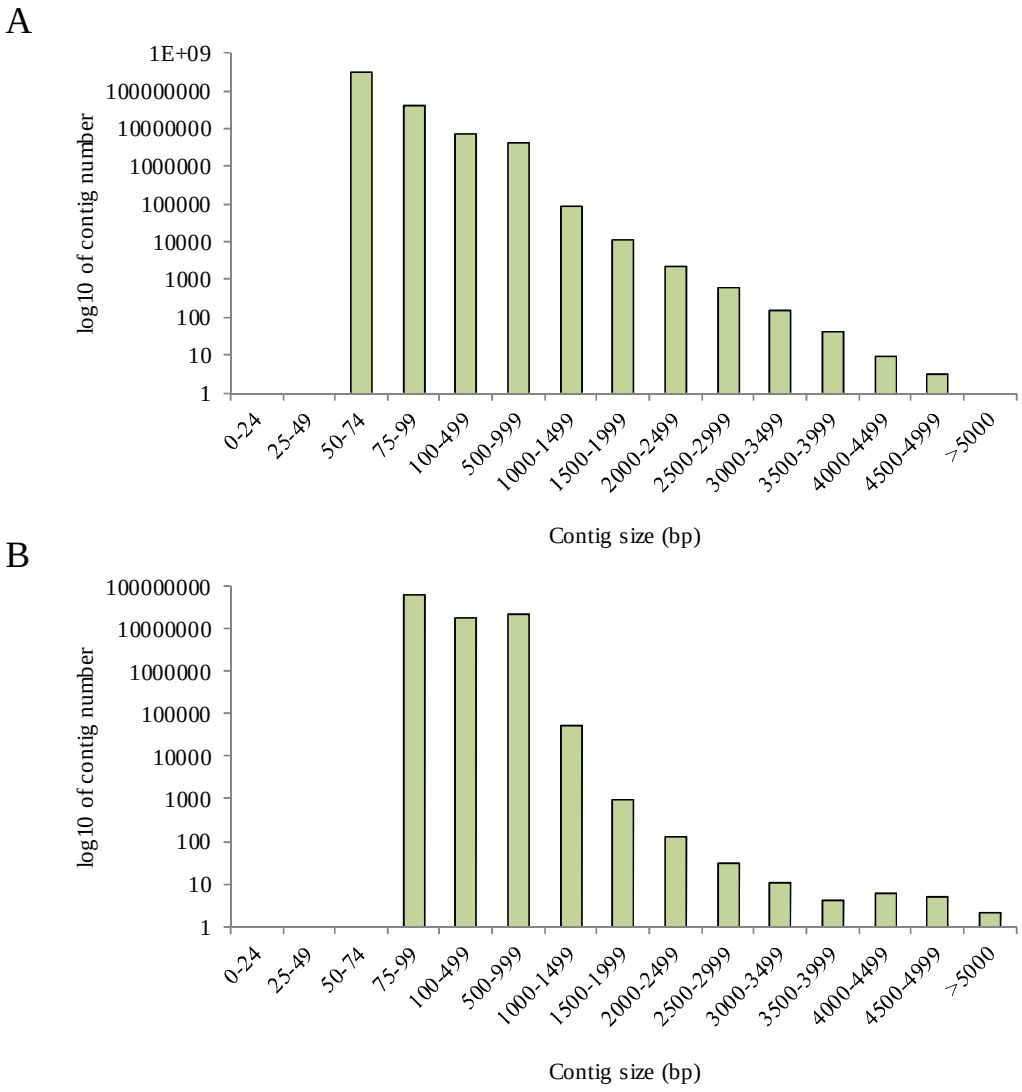

Figure 6.2.2-1: A) The $\log_{10}$ contig abundance over a range of contig sizes, produced from 32 bp kmers; B) The $\log_{10}$ contig abundance over a range of contig sizes, produced from 64 bp kmers.

The abundance of contigs that were generated was highly dependent on kmer size (Figure 6.2.2-1 A) with 32 bp kmers showing a wider range of contig sizes, together with a higher number of contigs compared to those produced using a kmer size of 64 bp (Figure 6.2.2-1 B).

The contigs shown in Figure 6.2.2-1 were used to enhance sections of the synteny-based SNP linkage map produced by Webb et al., (2016). A complete list of the searched syntenic markers used can be found in the Appendix II.

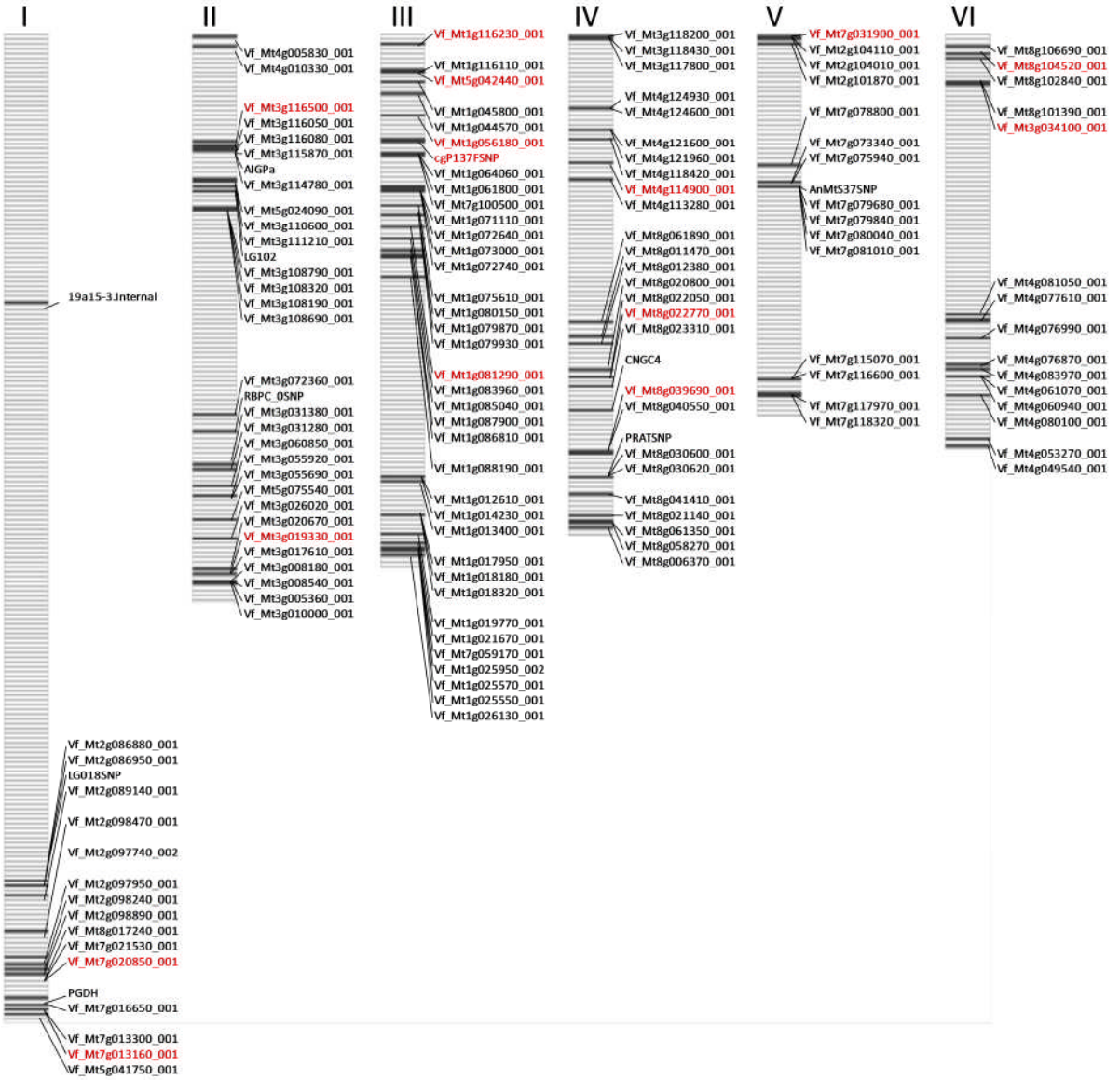

Figure 6.2.2-2: Enhanced synteny based SNP map of *V. faba*, showing the grouping of *M. truncatula* orthologous into 6 linkage groups, corresponding to each of the six *V. faba* chromosomes (as described by Webb et al. (2016). SNP markers are shown in black and have had their associated *V. faba* sequences extended by a minimum of 300bp through genomic read alignment. Markers shown in red have had their associated sequences extended by a minimum of 1500 bp.

For the SNP based linkage marker sequences shown in Figure 6.2.2-2, the published sequence lengths were increased at 147 chromosomal loci, with a minimum of 2 SNP markers per chromosome being increased in sequence length by >1500bp (Tables 2-7). The data presented in Tables 2-7 show the range of chromosomal loci at which genomic contigs were mapped.

Table 8: Lengths and identities of SNP based synteny markers on *Vicia faba* chromosome 1 and the increase in loci sequence length through contig mapping. Data presented show SNP based linkage marker ID, the length of the SNP based linkage marker, the length of the mapped contig and the subsequent increase in marker length at the identified loci.

SNP marker loci	Original marker length (bp)	Mapped contig length (bp)	Length increase (bp)
Vf_Mt7g020850_001	143	2043	1900
Vf_Mt7g013160_001	198	1782	1584
Vf_Mt2g098240_001	31	1494	1463
Vf_Mt2g086950_001	151	1477	1326
Vf_Mt2g098890_001	185	1432	1247
Vf_Mt2g086880_001	168	1429	1261
Vf_Mt5g041750_001	189	1362	1173
Vf_Mt2g098470_001	172	1256	1084
Vf_Mt7g013300_001	149	1243	1094
Vf_Mt7g016650_001	135	1007	872
Vf_Mt2g097740_002	31	840	809
Vf_Mt2g089140_001	200	737	537
LG018SNP	31	674	643
PGDH	17	636	619
19a15-3.Internal	19	591	572
Vf_Mt8g017240_001	196	583	387
Vf_Mt7g021530_001	196	583	387
Vf_Mt2g097950_001	149	571	422

Table 9: Lengths and identities of SNP based synteny markers on *Vicia faba* chromosome 2 and the increase in loci sequence length through contig mapping. Data presented show SNP based linkage marker ID, the length of the SNP based linkage marker, the length of the mapped contig and the subsequent increase in marker length at the identified loci.

SNP Marker loci	Original marker length	Mapped contig length	Length increase (bp)
Vf_Mt3g019330_001	176	3310	3134
LG102	19	2041	2022
Vf_Mt3g116500_001	201	1997	1796
Vf_Mt3g108320_001	31	1419	1388
Vf_Mt3g115870_001	31	1391	1360
Vf_Mt3g008540_001	198	1200	1002
Vf_Mt3g005360_001	201	1158	957
Vf_Mt3g055690_001	202	1128	926
AIGPa	19	1088	1069
Vf_Mt3g111210_001	31	1085	1054
Vf_Mt3g055920_001	189	1020	831
Vf_Mt3g008180_001	31	996	965
Vf_Mt5g075540_001	31	992	961
Vf_Mt4g010330_001	31	945	914
Vf_Mt3g020670_001	194	931	737
Vf_Mt3g108190_001	151	882	731
Vf_Mt3g110600_001	118	846	728
Vf_Mt3g010000_001	190	841	651
Vf_Mt3g116050_001	201	811	610
Vf_Mt3g060850_001	31	797	766
RBPC_0SNP	31	705	674
Vf_Mt3g017610_001	146	689	543
Vf_Mt3g108690_001	31	654	623
Vf_Mt3g116080_001	31	639	608
Vf_Mt4g005830_001	193	632	439
Vf_Mt3g114780_001	31	620	589
Vf_Mt3g031280_001	31	618	587
Vf_Mt3g072360_001	156	617	461
Vf_Mt3g026020_001	31	615	584
Vf_Mt5g024090_001	31	591	560
Vf_Mt3g031380_001	169	538	369
Vf_Mt3g108790_001	199	533	334

Table 10: Lengths and identities of SNP based synteny markers on *Vicia faba* chromosome 3 and the increase in loci sequence length through contig mapping. Data presented show SNP based linkage marker ID, the length of the SNP based linkage marker, the length of the mapped contig and the subsequent increase in marker length at the identified loci.

SNP Marker loci	Original marker length	Mapped contig length	Length increase (bp)
Vf_Mt1g116230_001	31	2472	2441
Vf_Mt5g042440_001	176	1763	1587
cgP137FSNP	31	1611	1580
Vf_Mt1g056180_001	185	1611	1426
Vf_Mt1g081290_001	139	1575	1436
Vf_Mt1g079930_001	194	1407	1213
Vf_Mt1g072740_001	201	1353	1152
Vf_Mt7g100500_001	138	1281	1143
Vf_Mt1g021670_001	162	1203	1041
Vf_Mt1g019770_001	196	1184	988
Vf_Mt7g059170_001	185	1169	984
Vf_Mt1g075610_001	153	1135	982
Vf_Mt1g012610_001	31	1084	1053
Vf_Mt1g017950_001	200	1019	819
Vf_Mt1g083960_001	184	970	786
Vf_Mt1g088190_001	31	964	933
Vf_Mt1g045800_001	202	945	743
Vf_Mt1g025570_001	182	944	762
Vf_Mt1g072640_001	31	860	829
Vf_Mt1g087900_001	155	827	672
Vf_Mt1g079870_001	31	805	774
Vf_Mt1g018180_001	31	780	749
Vf_Mt1g014230_001	31	777	746
Vf_Mt1g071110_001	31	767	736
Vf_Mt1g026130_001	199	763	564
Vf_Mt1g018320_001	190	724	534
Vf_Mt1g085040_001	31	718	687
Vf_Mt1g044570_001	31	713	682
Vf_Mt1g025950_002	31	669	638
Vf_Mt1g013400_001	31	639	608
Vf_Mt1g061800_001	31	632	601
Vf_Mt1g080150_001	163	594	431
Vf_Mt1g073000_001	119	565	446
Vf_Mt1g086810_001	31	556	525
Vf_Mt1g025550_001	143	538	395
Vf_Mt1g116110_001	31	513	482
Vf_Mt1g064060_001	158	511	353

Table 11: Lengths and identities of SNP based synteny markers on *Vicia faba* chromosome 4 and the increase in loci sequence length through contig mapping. Data presented show SNP based linkage marker ID, the length of the SNP based linkage marker, the length of the mapped contig and the subsequent increase in marker length at the identified loci.

SNP Marker loci	Original marker length	Mapped contig length	Length increase (bp)
Vf_Mt4g114900_001	201	1733	1532
Vf_Mt8g022770_001	170	1579	1409
Vf_Mt8g039690_001	201	1565	1364
PRATSNP	31	1456	1425
Vf_Mt8g020800_001	31	1451	1420
Vf_Mt8g022050_001	147	1451	1304
Vf_Mt4g121960_001	31	1397	1366
CNGC4	31	1384	1353
Vf_Mt8g021140_001	176	1315	1139
Vf_Mt8g061890_001	31	1293	1262
Vf_Mt8g012380_001	134	1239	1105
Vf_Mt4g124600_001	167	1222	1055
Vf_Mt3g117800_001	31	1180	1149
Vf_Mt8g006370_001	184	1162	978
Vf_Mt8g023310_001	164	1027	863
Vf_Mt4g113280_001	151	923	772
Vf_Mt8g030600_001	169	866	697
Vf_Mt4g121600_001	172	865	693
Vf_Mt8g030620_001	175	863	688
Vf_Mt8g058270_001	201	797	596
Vf_Mt8g041410_001	185	784	599
Vf_Mt4g118420_001	198	754	556
Vf_Mt8g011470_001	31	752	721
Vf_Mt3g118200_001	31	739	708
Vf_Mt4g124930_001	31	712	681
Vf_Mt3g118430_001	31	698	667
Vf_Mt8g061350_001	31	648	617
Vf_Mt8g040550_001	160	525	365

Table 12: Lengths and identities of SNP based synteny markers on *Vicia faba* chromosome 5 and the increase in loci sequence length through contig mapping. Data presented show SNP based linkage marker ID, the length of the SNP based linkage marker, the length of the mapped contig and the subsequent increase in marker length at the identified loci.

SNP Marker loci	Original marker length	Mapped contig length	Length increase (bp)
Vf_Mt7g031900_001	169	3412	3243
Vf_Mt7g080040_001	196	1417	1221
Vf_Mt7g079680_001	200	1368	1168
Vf_Mt7g116600_001	31	1257	1226
AnMtS37SNP	31	1229	1198
Vf_Mt2g104010_001	180	1150	970
Vf_Mt7g115070_001	201	937	736
Vf_Mt7g081010_001	132	852	720
Vf_Mt2g101870_001	31	817	786
Vf_Mt7g073340_001	191	692	501
Vf_Mt7g075940_001	184	686	502
Vf_Mt7g078800_001	31	637	606
Vf_Mt7g117970_001	196	605	409
Vf_Mt2g104110_001	188	551	363
Vf_Mt7g118320_001	31	527	496
Vf_Mt7g079840_001	193	520	327

Table 13: Lengths and identities of SNP based synteny markers on *Vicia faba* chromosome 6 and the increase in loci sequence length through contig mapping. Data presented show SNP based linkage marker ID, the length of the SNP based linkage marker, the length of the mapped contig and the subsequent increase in marker length at the identified loci.

SNP Marker loci	Original marker length	Mapped contig length	Length increase (bp)
Vf_Mt8g104520_001	31	1718	1687
Vf_Mt3g034100_001	196	1514	1318
Vf_Mt4g077610_001	179	1105	926
Vf_Mt4g081050_001	123	968	845
Vf_Mt4g053270_001	31	960	929
Vf_Mt4g076870_001	201	949	748
Vf_Mt8g102840_001	185	926	741
Vf_Mt4g080100_001	182	862	680
Vf_Mt4g076990_001	183	789	606
Vf_Mt4g083970_001	125	784	659
Vf_Mt8g101390_001	31	755	724
Vf_Mt8g106690_001	31	731	700
Vf_Mt4g060940_001	161	547	386
Vf_Mt4g049540_001	153	504	351
Vf_Mt4g061070_001	31	500	469

All mapped contigs shown in Tables 7-12 were compared against the *M. truncatula* genome database (Young et al., 2011). Gene orthologues for contigs that had an alignment length equal to or in excess of the query length with a percentage identity >85% are shown in Table 8. Out of a total of 271 BLAST hits obtained in this way, probable gene identities were obtained for 5 *V. faba* genes (Table 8). The putative gene identifications are: subunit 8 of the anaphase promoting complex; a pre-mRNA splicing factor; polyadenylate binding protein II; a zinc finger family protein and an arogenate/prephenate dehydratase (Table 14).

Table 14: The linkage map identities and corresponding mapped genomic contigs of *V. faba*. Contigs were identified through a BLAST search against the *M. truncatula* database to determine probable gene identity and function. Query length, alignment length and single nucleotide variation (SNV) and gap number are shown.

V. faba Linkage ID	*V. faba* contig ID	Gene function	M.t ID	Query length	Align length	ID %	SNV	Gaps
Vf_Mt8g021140_001	176862097131569442	anaphase promoting complex subunit 8	MTR_1g103750	1315	1323	89	130	6
Vf_Mt1g072740_001	115665543135372887	Pre-mRNA splicing factor	MTR_4g102520	1353	1377	89	130	8
Vf_Mt1g073000_001	2498106125652516	polyadenylate-binding protein II	MTR_1g073000	565	566	86	54	8
Vf_Mt3g111210_001	2850992881085417 7	zinc finger (C3HC4-type RING finger) family protein	MTR_3g111210	1085	1089	86	131	6
Vf_Mt4g061070_001	104720015001890	arogenate/prephenate dehydratase	MTR_4g061070	500	502	85	67	3

6.2.3. Single nucleotide polymorphisms in the organellar genomes of *Vicia faba*

To investigate species level variation within the organellar genomes of *V. faba* raw DNA sequence reads were mapped against the reference sequences for the chloroplast and mitochondria (Negruk, 2013; Sabir et al., 2014). The map shown in Figure 6.2.3-1 reveals the locations of gene-based variation within the *V. faba* chloroplast genome, obtained by aligning the raw DNA sequence reads to the faba bean chloroplast sequence published by Sabir et al. (2014).

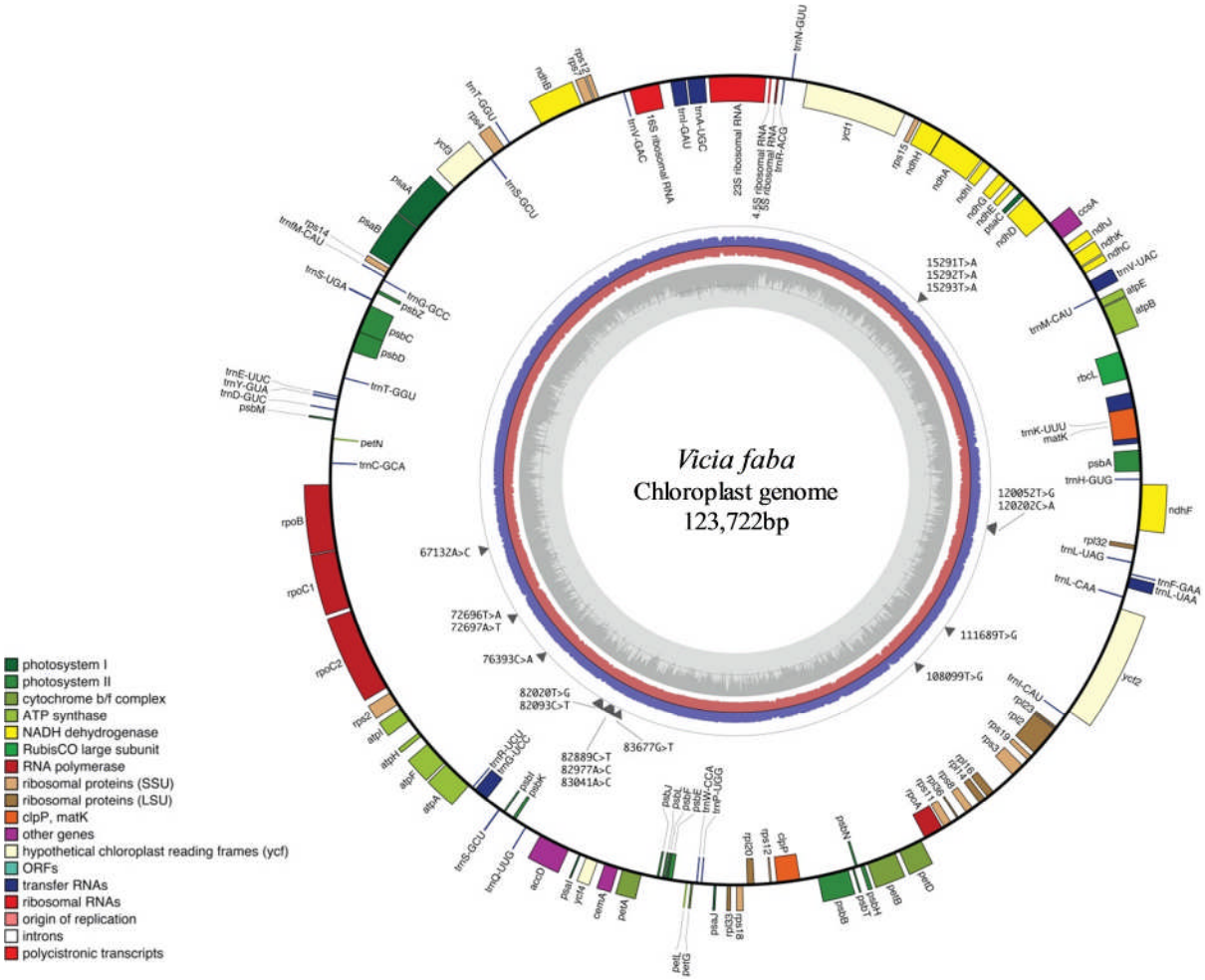

Figure 6.2.3-1: *Vicia faba* chloroplast genome map. Outermost circle shows gene identities and read direction with out-facing genes being in the positive direction and inward facing genes being in the negative direction. SNPs are denoted by grey triangles with the location and nature of polymorphism detailed. Read depth is shown for the forward reads (blue ring) and reverse reads (red ring). GC content (%) is shown by the innermost grey circle with 50% being denoted by the dark grey line. Gene mapping and annotation was performed in OGDRAW.

A high level of homology was found between the published reference sequence (Sabir et al., 2014) and the chloroplast genome of the Wizard cultivar. However, a number of single nucleotide polymorphisms were present (Table 15).

Table 15: Single nucleotide polymorphisms in the chloroplast genome of *Vicia faba*, comparing the Wizard cultivar to the reference sequence published by Sabir et al., (2014).

Map identifier	Gene identity	SNP position	Referenced base	Sequenced base
rpoC1	RNA polymerase β chain	67132	A	C
atpF	ATPase subunit I	76393	C	A
trnQ-UUG	tRNA	82093	G	A
accD	Acetyl-CoA carboxylase subunit	82977	A	C
accD	Acetyl-CoA carboxylase subunit	83041	A	C
accD	Acetyl-CoA carboxylase subunit	83677	G	T
rps3	Ribosomal protein S3	108099	T	G

Four genes encoding the RNA polymerase β chain, ATPase subunit I, tRNA Q and ribosomal protein S3 had a single polymorphism (Table 15). The gene encoding acetyl-CoA carboxylase subunit (accD) showed 3 single nucleotide polymorphisms.

The level of in-species variation for the mitochondrial genome that is depicted in Figure 6.2.3-2 shows high number of SNPs in the gene coding and the intergenic regions. This map is based on genomic read alignment to the faba bean mitochondrial genome reference, constructed for the cultivar Broad Windsor (Negruk, 2013).

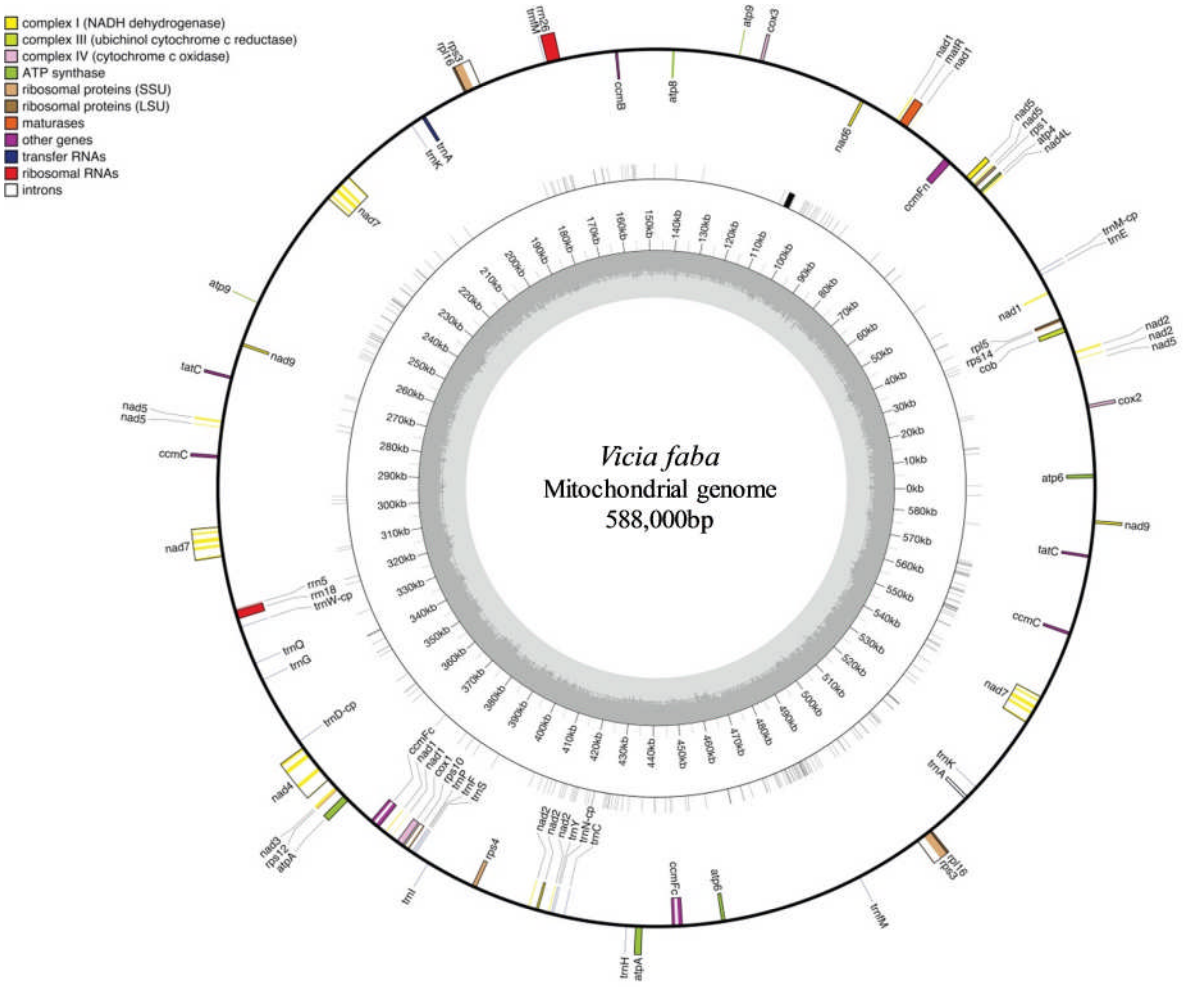

Figure 6.2.3-2: *Vicia faba* mitochondrial genome map. Outermost circle shows gene identities and read direction with out-facing genes being in the positive direction and inward facing genes being in the negative direction. SNPs are denoted by grey bars on the second concentric circle. Base pair positioning is detailed in the third circle. GC content (%) is shown by the innermost grey circle with 50% being demarked by the dark grey line. Legend details mitochondrial gene families. Gene mapping and annotation was performed in OGDRAW.

While a high level of homology was found between the gene space published by Negruk, (2013) and that assembled from raw genomic reads of the Wizard cultivar, 7 genes were found to have polymorphisms (Table 16).

Table 16: Single nucleotide polymorphisms in the mitochondrial genome of *Vicia faba*, comparing the Wizard cultivar to the reference sequence published by Negruk, (2013).

Map identifier	Gene identity	SNP position	Reference base	Sequenced base
rrn26.r01	26S ribosomal RNA	167803	T	A
rrn18.r01	18S ribosomal RNA	321111	T	G
rps14	ribosomal protein S14	36460	T	G
rps14	ribosomal protein S14	36461	C	G
rps14	ribosomal protein S14	36462	C	A
rps14	ribosomal protein S14	36463	A	T
rps14	ribosomal protein S14	36490	G	T
rps14	ribosomal protein S14	36616	A	G
nad6	NADH dehydrogenase subunit 6	101407	A	T
nad6	NADH dehydrogenase subunit 6	101508	G	T
nad4.CDS.3	NADH dehydrogenase subunit 4	361807	T	G
matR	Maturase R	90908	G	T
matR	Maturase R	92082	A	C
cox2.p01.CDS.1	cytochrome c oxidase subunit II	25588	C	A
cox2.p01.CDS.1	cytochrome c oxidase subunit II	25760	C	A
cox2.p01.CDS.1	cytochrome c oxidase subunit II	25862	T	A
cox2.p01.CDS.1	cytochrome c oxidase subunit II	25863	T	A
cox2.p01.CDS.1	cytochrome c oxidase subunit II	25588	C	A
cox2.p01.CDS.1	cytochrome c oxidase subunit II	25760	C	A

The number of polymorphisms present varied between genes, with the genes encoding 26S ribosomal RNA, 18S ribosomal RNA and NADH dehydrogenase subunit 4 having 1 SNP and the genes

encoding Maturase R and NADH dehydrogenase subunit 6 having 2 SNPs. The genes encoding ribosomal protein S14 and cytochrome c oxidase subunit II had 6 SNPs.

6.2.4. Comparison of legume organelle genome sequences

The coding regions of the faba bean chloroplast and mitochondrial chromosomes were compared to those of other legume organelle genomes that are available on the NCBI database (Benson et al., 2013).

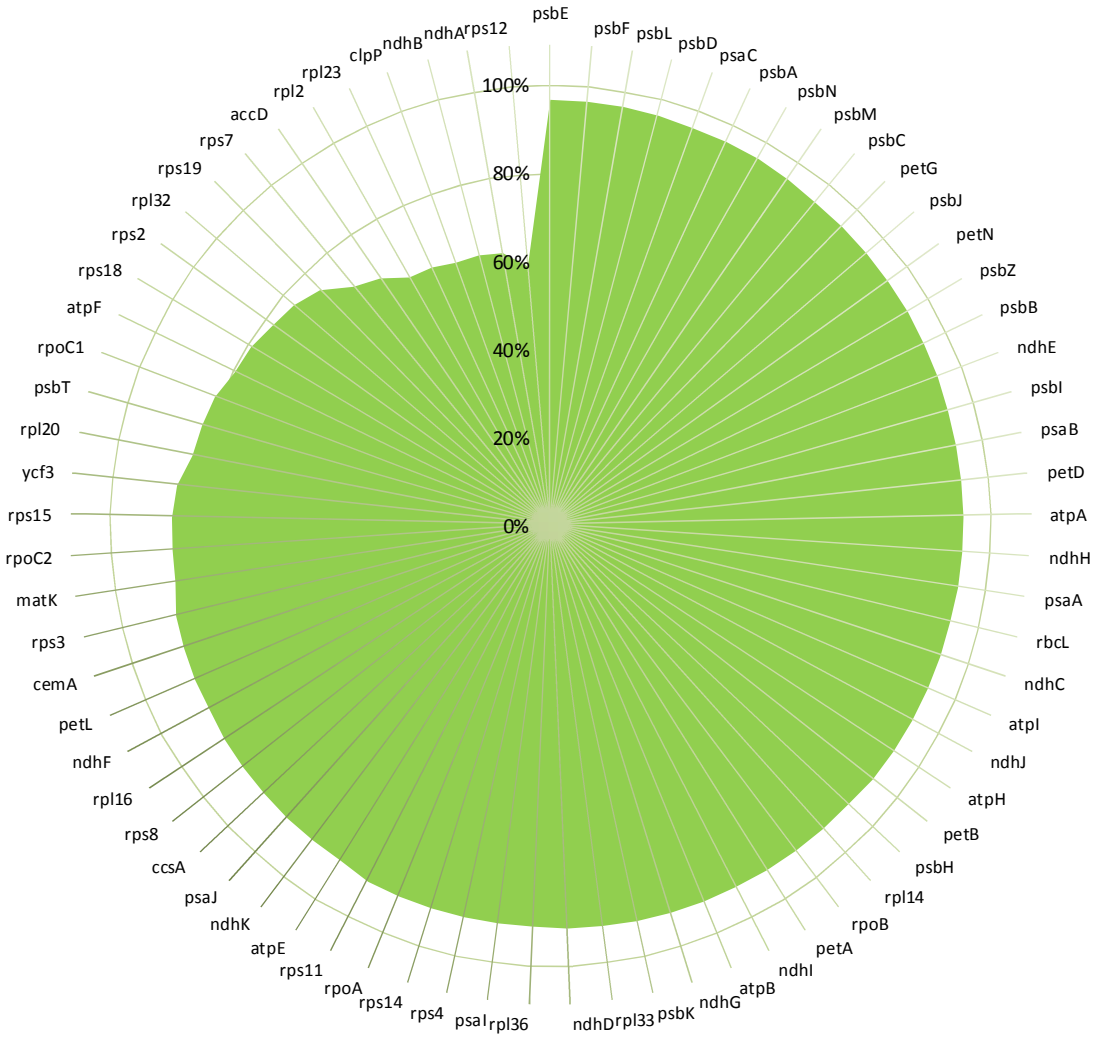

Figure 6.2.4-1: The percentage of homology for chloroplast encoded genes, showing the average data for a 55-way alignment for individual chloroplast genes of 11 species. Gene identities are given in the outermost circle. The scale shows the homology percentage (0-100%).

Genome sequence alignment of the 11 reference chloroplast sequences that are available for grain legumes (*Glycine max*; *Lotus japonicus*; *Vigna ungulicata*; *Lens culinaris*; *Cicer arietinum*; *Vigna radiata*; *Pisum sativum*; *Medicago truncatula*; *Arachis hypogaea*; *Phaseolus vulgaris*) allowed for the identification of a core set of chloroplast genes that are conserved across all legumes (Figure 6.2.4-1). The extent of homology between all 11 chloroplast sequences was well conserved. For example, the average sequence homology in the majority of genes encoding photosynthetic electron transport proteins was more than 80%. However, the percentage of homology was lower in genes encoding ribosomal proteins. Between the plastid genomes, the greatest sequence variations were found in *clpP*, *ndhA* and *rps12*, which showed less than 60% homology. The least variable genes were *psbE*, *psbF* and *psbD*, all of which had a homology greater than 95%.

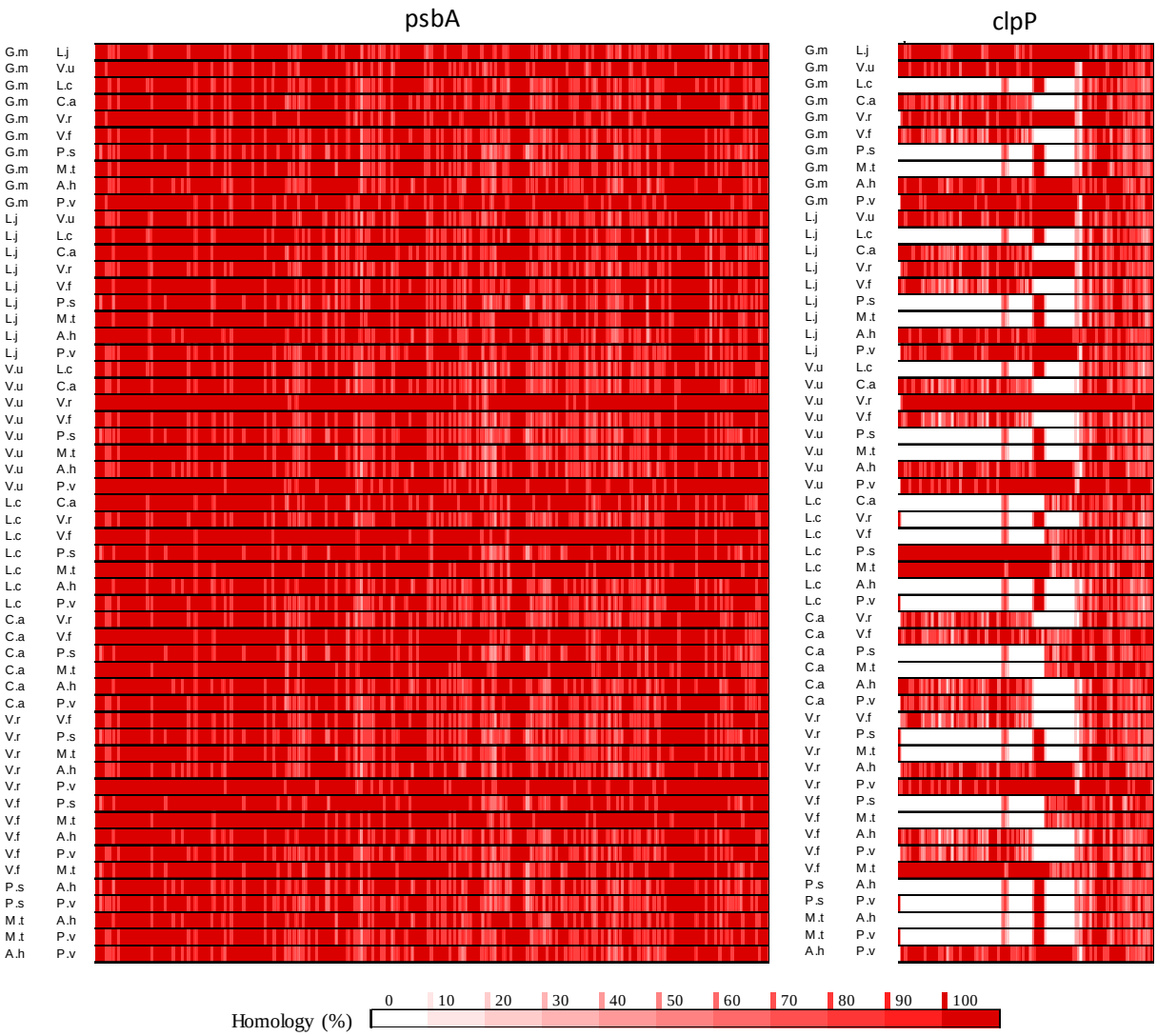

Figure 6.2.4-2: Representative examples of percentage homology maps drawn for the highly homologous *psaB* gene and the *clpP* gene with low homology. Maps were constructed from a multi-way homology comparison between 7 legume species; *Glycine max* (G.m); *Lotus japonicus* (L.j); *Vigna ungulicata* (V.u); *Lens culinaris* (L.c); *Cicer arietinum* (C.a); *Vigna radiata* (V.r); *Pisum sativum* (P.s); *Medicago truncatula* (M.t); *Arachis hypogaea* (A.h); *Phaseolus vulgaris* (P.v). High degrees of homology are shown in dark red whilst a lack of detectable matches is shown in white, as shown in the homology scale bar. Homology was determined across a 10 bp frame, i.e. a single polymorphism would give a 90% homology.

Chloroplast genome variation was further analysed in homology maps in a pairwise manner for each gene and species. However, for simplicity, representative examples are shown in Figure 6.2.4-2 for the *psbA* and *clpP* genes. While *psbA* shows a very high homology across all species, *clpP* shows far more inter species variation, with large regions being absent from the coding sequences of *L. culinaris*, *M. truncatula* and *P. sativum* (Figure 6.2.4-2).

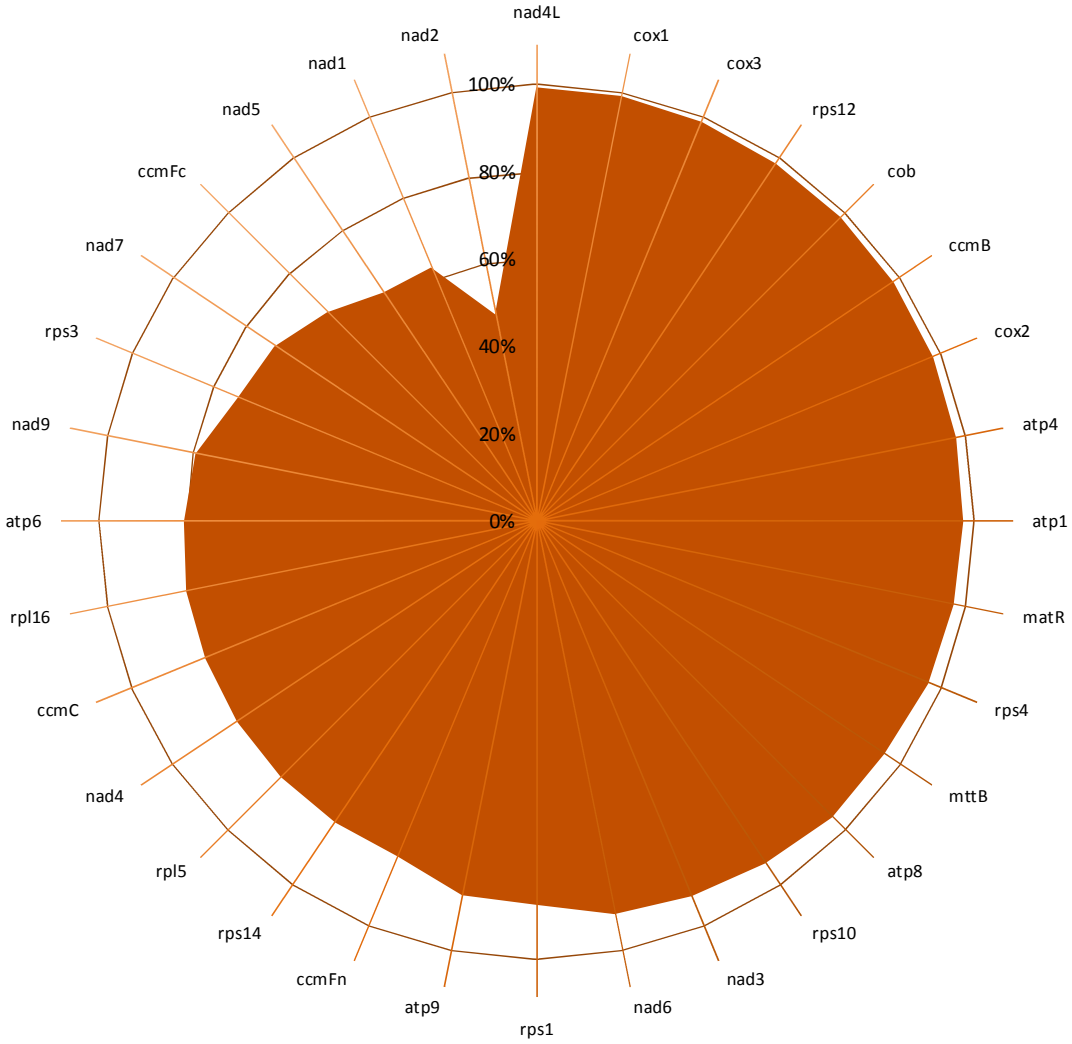

Figure 6.2.4-3: The percentage of homology for genes encoded in the mitochondrial genome. Average data for individual mitochondrial genes from 6 species were subjected to a 15-way alignment. Gene identities are given in the outermost circle. The scale shows the homology percentage (0-100%).

Reference mitochondrial genomes were available for 6 legume species on the NCBI database (Benson et al., 2013). These sequences were compared to define a core set of conserved mitochondrial genes. The extent of homology in mitochondrial genomes was well conserved, as shown in a multi-way comparison of the 6 genomes (Figure 6.2.4-3). All of the cytochrome-associated genes had an average sequence homology of more than 90%. However, genes encoding ribosomal proteins and the NADH dehydrogenase complex had a lower average sequence homology (Figure 6.2.4-3). The most variable genes across the mitochondrial genomes were *nad5*, *nad1* and *nad2* which showed less than 60% homology across the legume sequences analysed. The least variable genes were *nad4L*, *cox1* and *cox3*, all of which had a homology greater than 95%.

The mitochondrial genome variation homology maps were examined further in a pairwise manner for each gene and species. Representative examples are shown in Figure 6.2.4-4.

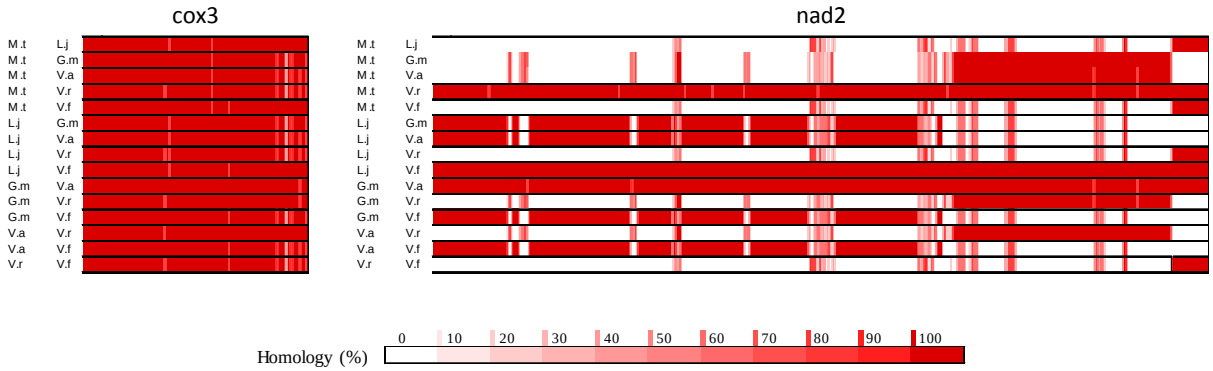

Figure 6.2.4-4: Percentage homology maps for *cox3* and *nad2*. Maps were constructed from a multi-way homology comparison of 7 legume species; *Medicago truncatula* (M.t); *Lotus japonicus* (L.j); *Glycine max* (G.m); *Vigna angularis* (V.a); *Vigna radiata* (V.r); *Vicia faba* (V.f). High degrees of homology are shown in dark red and a lack of detectable match is shown in white, with quantitation as shown in the scale bar.

A high degree of homology was observed in the *cox3* gene across species (Figure 6.2.4-4). In contrast, the extent of variation was high in the *nad2* gene across species. Crucially, large coding regions appear to have been lost between *M. trunctula* and *L. japonicus*, *G. max*, *V. angularis* and *V. faba* (Figure 6.2.4-4).

6.3. Discussion

Genetic improvement in faba bean requires a much deeper characterisation and understanding of the genome sequence and its regulation under optimal and stress conditions. The genes underpinning tolerance to stresses such as chilling and freezing can only be defined by the correct annotation of sequences. The data presented here lay the foundations for the generation of a draft nuclear genome sequence, together with the characterisation of polymorphic regions in the genomes housed in the chloroplast and mitochondria.

Previous studies on *V. faba* have suggested that chromosomal fusion has occurred particularly in chromosome I (Fuchs et al., 1998). However, the giant size of genome size at ~13 Gb is surprising given that *V. faba* is diploid (2n=12 chromosomes). While the majority of plants have small genomes (Kelly and Leitch, 2011) the data presented here confirm that faba bean belongs to those lineages that have giant genomes. As with other large genomes, genome size expansion can be accounted for by repetitive DNA sequences that consist of different types of transposable elements. However, in the case of *V. faba* only ~10% of reads could be identified in a repetitive element database (Bao et al., 2015). Larger plant nuclear genomes, such as maize, can contain 85% repetitive DNA made up of intact and simply organised RTs (Schnable et al., 2009). Many RTs that use element-encoded mRNAs as transposition intermediates can rapidly proliferate in copy number, resulting in large differences in genome sizes between related species. The action of these mobile elements can restructure the genome, resulting in a high level of genetic variability. Moreover these RT-induced mutations are usually stable and can be used as molecular tools to study gene tagging and functional analysis (Bennetzen, 2000). The gypsy and copia type RTs belong to the long terminal repeat (LTR) family and are referred to as Metaviridae and Pseudoviridae elements respectively (Grandbastien, 2015). LTR replication via an RNA template is reminiscent of retroviral proliferation, and interestingly these are the predominant RTs in plants. Genome fluidity arising from the activities of these mobile elements has long been recognised as an opportunity for the genome to evolve in response to environmental challenges (Wicker et al., 2007; Lisch, 2002). The expression of LTR RTs is important in host functional plasticity, with regulation being coordinated in response to a diverse array of external stresses. Transposable elements can act as dispersible regulatory modules that redirect stress responses to adjacent plant genes, an action that may be crucial for stress avoidance, escape or tolerance (Grandbastien, 2015). The activation of LTR retrotransposons results from interplay between the release of epigenetic silencing and the recruitment by LTRs of specific regulatory factors. While evidence for major mobilisations of LTR RTs is rare (Reichmann et al., 2012; Giordani et al., 2016), future sequencing of the faba bean genome will allow the identification of specific RTs and their movement in optimal and stress conditions.

The datasets obtained in the present study, combined with sequence data with linkage marker data (Webb et al., 2016) have facilitated an enhancement of linkage sequences at 141 chromosomal loci. While 272 BLAST hits were obtained for linkage-anchored contigs, only 5 of these had sufficient alignment length and identity to classify gene orthologues. However, this analysis has allowed resolution of the putative sequences of 5 *V. faba* genes, based on homology to *M. truncatula* (Webb et al., 2016). Since the majority of the *V. faba* genome consists of repetitive sequences, and >90% of the assembled contigs having no homology to the coding regions of *M. truncatula*, it is clear that a much more varied sequencing approach is required. Given the rapid advances in sequencing technologies, it is feasible that much more genome information can be rapidly gained within the next few years by an intense sequencing and bioinformatics approach.

Although the present characterisation of the nuclear genome proved to be challenging given the length and coverage of genomic reads, the mapping of the organellar genomes was much more informative. Relatively few differences in the coding regions of the faba bean chloroplast genome were identified in comparisons of genome reads to the chloroplast reference (Sabir et al., 2014). However, SNPs were identified in the genes encoding the RNA polymerase subunit C1 (*rpoC1*), the ATpase β subunit (*atpF*), glutamine tRNA (*trnQ-UUG*) and the β-carboxyl transferase subunit of acetyl co-A carboxylase (*accD*). Among these *accD* contained the most SNPs with 3 detectable polymorphisms. This finding might at first glance be surprising because the activity of the acetyl co-A carboxylase is essential for plastid functions and for fatty acid biosynthesis, with tobacco *accD* knockout mutants being lethal (Kode et al., 2005). However, the *accD* gene has previously been shown to be highly variable across 24 *M. truncatula* ecotypes (Csanad and Pal, 2014). Ecotype specific *accD* gene sequences ranging from 650-796 amino acids in length were reported (Csanad and Pal, 2014). Despite this variability a conserved carboxylase domain was always present and gene length expansion and contraction was attributed to repetitive sequence integration in intronic regions (Csanad and Pal, 2014). Moreover, despite the essential functions that *accD* plays in plants, it has been lost during evolution in a number of species (Rousseau-Gueutin et al., 2013). In these situations the gene either moves to the nuclear genome or is functionally replaced by a nuclear encoded analogue(Rousseau-Gueutin et al., 2013).

The high level of conservation of the plastid genome sequences between legumes is highlighted in the data presented here. The data show a low level of gene sequence variation amongst the 11 legumes analysed in this study. There were notable exceptions however, particularly in the *rps2, rpl32, rps19, rps7, accD, rpl2, rpl23, clpP, ndhB, ndhA* and *rps12* genes, which showed sequence homologies of only between 60-79%. These findings are consistent with the view that most photosynthesis-related genes are conserved to a higher level than ribosomal genes, with chloroplast genomes showing far

higher degrees of conservation than the nuclear and mitochondrial genomes (Xu et al., 2015). Interestingly, despite the high level of variation in the *rps12* gene, loss of *rps12* function might be predicted to lead to a loss of chloroplast translation capacity (Ramundo et al., 2013). Intra-species comparisons of faba bean chloroplast genes may form the basis for future cultivar genotyping.

The number of polymorphisms in the mitochondrial genome were greater than those detected in the chloroplast genome, with 6 genes showing single base pair mutations compared to the reference sequence (Negruk, 2013). Two SNPs were identified in NADH dehydrogenase subunit 6 and Maturase R, with Ribosomal protein S14 and cytochrome c-oxidase subunit II having 6 SNPs. While the relatively small number of polymorphisms in the coding regions is unlikely to have extensive functional repercussions, genes showing polymorphisms between faba bean cultivars are well conserved across the mitochondrial genomes of 6 other legume species. However, in comparison to the chloroplasts the mitochondria were shown to be more prone to the accumulation of mutations, though this was restricted to the intergenic spaces.

Plant mitochondrial genomes are characterised by their very large size, ranging from 200 to 2500 kb. They contain many introns and repeated elements, experiencing frequent gain/loss of genes, gene transfer and duplication and genome rearrangements (Kitazaki et al., 2010). Intriguingly, despite the affinity of plant mitochondrial genomes for rearrangement, their rate of nucleotide substitution is low. Moreover, mitochondrial genome variation within species is derived from double-stranded DNA breakage and repair, via highly efficient recombination of asymmetric sequences (Davila et al., 2011). Thus, while the genomes are prone to structural changes, the encoded content is well conserved. The mechanisms underpinning mitochondrial genome recombination are key to within- and between-species variation (Galtier, 2011).

Taken together, the data presented in this chapter provide new insights into the large and highly repetitive faba bean genome. Moreover, these data show the extent of species-level variation within the legume family and identify genes which are more prone to the accumulation of mutations. Interestingly, while the chloroplast genome is well conserved on an intraspecies level, the mitochondrial genome is more prone to sequence variation. Future studies of the type described here should provide enhanced genomic information in faba bean, allowing the generation of novel breeding tools. Unravelling the nuclear and organellar genomes of faba bean, their plasticity, and regulation in response to environmental challenges, will not only increase our understanding of how stress tolerance is regulated but it will also bring faba bean science into the 21st century and so accelerate breeding progress.

“There are three kinds of lies: lies, damned lies and statistics”

-Benjamin Disraeli

7. Transcriptomic analysis of *Vicia faba* cultivars differing in low temperature tolerance, following acclimatory growth and following exposure to dark-freezing

7.1. Introduction

Plants vary in their responses to cold stress, with cellular changes ranging from altered membrane and protein composition (Pearce, 2001; Kosová et al., 2011) to cryoprotectant production and changes in ROS scavenging activity (Apel and Hirt, 2004). Cold temperatures can also induce secondary metabolic pathways. Flavonoids in particular have been identified as a primary target of study in cold stress. This large family of metabolites has been linked to plant protection from the effects of chilling and freezing. Notably anthocyanin is thought to confer protection to the photosynthetic machinery and the water status of plants cells (Calzadilla et al., 2016; Chalker-Scott, 1999).

Cold stress responses are dependent on changes in gene expression, for which a number of transcription factors have been identified as central regulators (Chinnusamy et al., 2007). Of these the most well characterised is the Cold Binding Factor (CBF) regulon, which acts upstream of several genes that confer protection to chilling and freezing (Thomashow, 2001; Yamaguchi-Shinozaki and Shinozaki, 2006). While the specific activities of CBF regulated genes have not been elucidated in full, late embryogenesis abundance (LEA) proteins are thought to be central to CBF-depdendent cryoprotection, playing diverse roles in protein and membrane stabilisation (Sanghera et al., 2011).

Next-generation sequencing technologies have increased the knowledge of which genes and gene families underpin plant stress tolerance (Pang et al., 2013). However, research into the biochemical and genetic factors contributing to low temperature tolerance has predominantly focused on *A. thaliana* (Kaplan et al., 2007). Nevertheless, there is an emerging body of research into the cold stress responses of legumes. Amplified fragment length polymorphism (AFLP) studies in cold tolerant chickpea (*C. arietinum*) identified 77 transcripts that were upregulated in response to chilling. These were related to metabolism, signal transduction and transcription, with a further 22 transcripts having unknown function (Dinari et al., 2013). Moreover, in freezing sensitive and freezing tolerant cultivars of pea, microarray analysis allowed cold-induced global gene expression to be profiled. Chilling tolerance was related to genes downstream of the CBF regulon, with the chilling tolerant cultivar showing earlier expression of cold-inducible genes. These gene expression changes were paired with physical measurements of cellular osmotic stabilisation, photosynthesis modifications and antioxidant production (Lucau-Danila et al., 2012). The most in-depth study of cold acclimation in legumes was conducted on *L. japonicus* (Calzadilla et al., 2016). In these studies high throughput RNA sequencing

was used to identify 1077 differentially expressed genes, 713 of which were up-regulated in response to chilling and 364 which were down-regulated. Up-regulated genes were related to lipid, cell wall, phenylpropanoid, sugar and proline regulation (Calzadilla et al., 2016). Down-regulated genes affected photosynthetic processes and chloroplast development, and a total of 41 cold-inducible transcription factors were identified. These belonged to the APETALA 2/ethylene-responsive element binding factor (AP2/ERF), NAC (acronym derived from three genes discovered to contain the binding domain (Nuruzzaman et al., 2013), MYB (a conserved binding domain (Stracke et al., 2001), WRKY (named after a conserved N-terminus amino acid sequence) and DREB/CBF families.

Taken together these studies have been useful in the characterisation of chilling and freezing tolerance in legumes. However they have been limited, either by the depth of information provided or the breadth of the studies undertaken. As such there is still a tangible knowledge gap in the current understanding of legume tolerance to low temperatures, with particular regard to differences in gene regulation between cultivars of varying low temperature sensitivity, under both acclimation and freezing stress.

The results provided in chapter 5 identified 2 cultivars of *Vicia faba* with differing tolerance to both chilling and freezing stress. The Hiverna cultivar was shown to be chilling and freezing tolerant, while the Wizard cultivar was shown to be comparatively sensitive to low temperatures. The following study employed RNA sequencing to characterise the transcriptomes of both Hiverna and Wizard, under control conditions after low temperature exposure during their night cycle.

7.2. Results

In the following studies RNA was extracted from leaf discs, taken from the oldest leaves of the Hiverna and Wizard cultivars. Plants had been subjected to one of four growth regimes: maintained growth under control conditions for 24 days (control); maintained growth under control conditions for 24 days with subjection to a 30 minute freezing period during the final hour of the last night cycle (control, frozen), maintained growth under control conditions for 14 days and grown under acclimatory conditions for a further 10 days (acclimated) and maintained growth under control conditions for 14 days and growth under acclimatory conditions for a further 10 days with subjection to a 30 minute freezing period during the final hour of the last night cycle (acclimated, frozen).

RNA samples consisted of RNA extracted from the leaf tissue of 3 pooled biological replicates. 3 experimental replicates were produced per genotype and conditions, totalling 24 RNA samples (Figure 7.2-1).

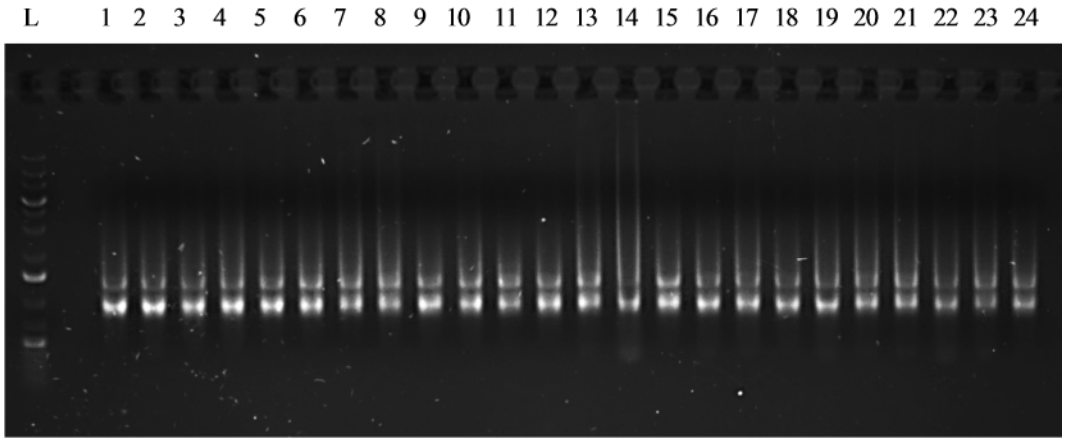

Figure 7.2-1: Agarose gel electrophoresis of RNA extracted from Hiverna and Wizard cultivars grown under control conditions, acclimatory conditions, control conditions followed by freezing or acclimatory conditions followed by freezing. All numbered lanes contain 5 µl of RNA sample. Lanes 1-3: Wizard control. Lanes 4-6: Hiverna control. Lanes 7-9: Wizard control and freezing. Lanes 10-12: Hiverna control and freezing. Lanes 13-15: Wizard acclimated. Lanes 16-18: Hiverna acclimated. Lanes 19-21: Wizard acclimated freezing. Lanes 22-24: Hiverna acclimated freezing. Lane L contained 3 µl of 1 kb plus GeneRule DNA ladder. Gel was 1 % agarose stained with SYBR Safe ®, run for 1 hour at 80 V.

Extracted RNA was sent to the Institute of Molecular Medicine at St James' Hospital, University of Leeds. RNA quantification and quality control nuclear DNA depletion were performed, before high throughput sequencing was conducted on an Illumina HiSeq 2500 platform using paired end 150 bp sequencing of polyadenylated transcripts. Sequence data was then analysed.

7.2.1. Read data and cultivar comparison under control conditions

A total of 24 samples were sequenced, producing 3,066,773,157 paired end reads. Of these, 2,738,047,391 could be mapped to the *V. faba* RefTrans.v1 unigene transcriptome at the cool season food legume database – a web based resource containing gene identities for multiple grain legume species (Humann et al., 2016). Based on the number of reads that could be identified against this database, 23,796 transcripts were determined across all 24 RNA sample libraries. Of these, 16,687 showed significant transcription (Table 17).

Table 17: Total number of reads resulting from RNA sequencing of 24 samples, and the number of reads that could be mapped to transcriptomic databases to produce a reference transcriptome. Of the 69,784 transcripts that comprised the reference transcriptome, 16,687 showed evidence of transcription in at least 1 time point or genotype.

	Number of paired reads	Number of paired reads mapped to CSFL	Genes in reference transcriptome
24 samples	3,066,773,157	2,738,047,391	16,687*

Using the list of 16,687 genes that were transcribed at significant levels, the transcription profiles of the Wizard and Hiverna cultivar were compared under control conditions. While the majority of the 14,883 transcripts did not significantly differ in their level of transcription, 361 genes were shown to be differentially regulated between cultivars (Figure 7.2.1-1).

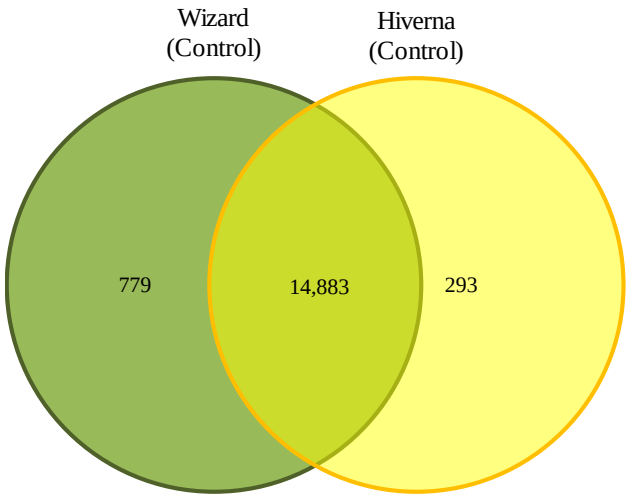

Figure 7.2.1-1 The total number of transcripts expressed in the Wizard and the Hiverna cultivars when grown under control conditions. Overlapping region shows the number of transcripts that common between the cultivars, under control conditions (counts >= 100). Note that changed genes may not be significantly different between cultivars.

A gene ontology analysis of these transcripts showed several families to be differentially regulated between Wizard and Hiverna (Figure 7.2.1-2). More genes related to cellular responses to nitrogen compounds were expressed in Hiverna compared to Wizard, incorporating genes acting to regulate movement, secretion, enzyme production and gene expression. Genes related to isoprenoid metabolic processes (the metabolism of isoprenoid compounds) were more highly expressed in Wizard compared to Hiverna. Coenzyme metabolic processes had a higher number of underpinning genes expressed in the Wizard cultivar than the Hiverna cultivar. There were more genes related to responses to organonitrogen expressed in Hiverna than Wizard, however isopentyl diphosphate biosynthetic process genes were only expressed in Wizard and not Hiverna. Genes linked to the isopentyl diphosphate pathway are not inclusive of the mevalonate/MEP pathway. Genes involving the cellular response to chitin (movement, secretion, enzyme production and gene expression) were expressed in higher numbers in Hiverna compared to Wizard.

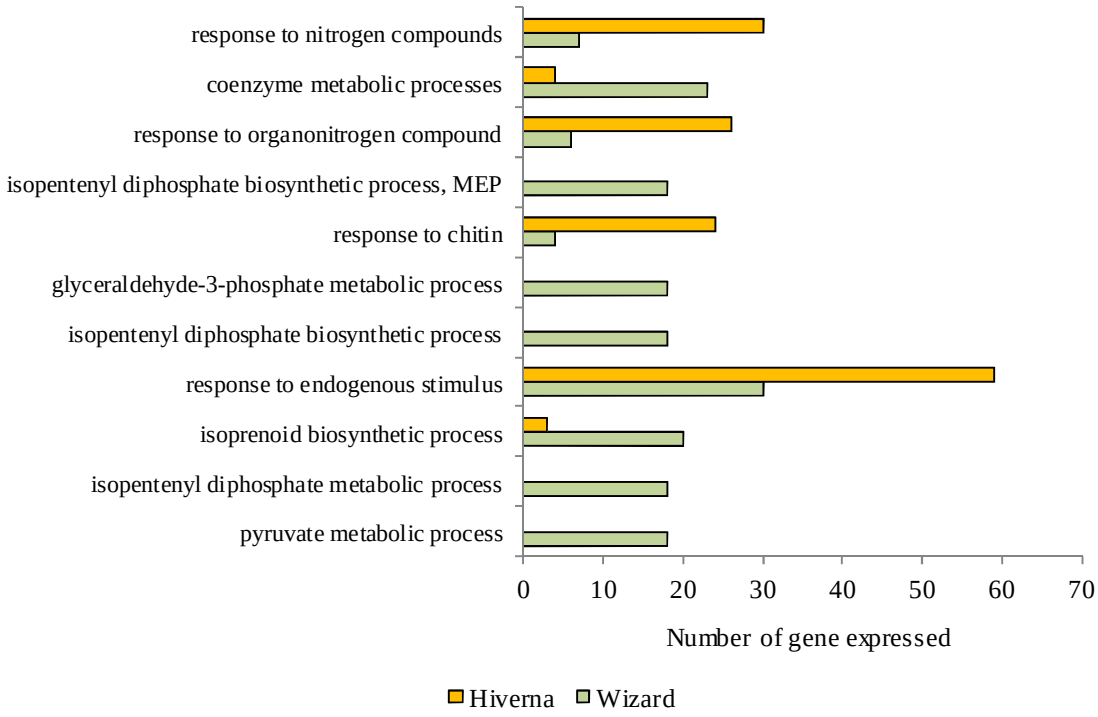

Figure 7.2.1-2: Metabolic process gene ontology showing the number of genes differentially expressed, and corresponding gene families, between the Wizard and Hiverna cultivars under control conditions.

Interestingly, genes involved in glyceraldehyde-3-phosphate metabolism (glycolysis) were expressed in Wizard but not Hiverna, under control conditions. Similarly genes involved in isopentyl diphosphate biosynthesis were expressed in Wizard but not Hiverna. Conversely, Hiverna had a higher number of genes expressed that were related to responses to endogenous stimuli, than did Wizard. Genes related to isoprenoid biosynthetic processes were more abundant in Wizard than

Hiverna, while Hiverna did not express any genes related to isopentyl diphosphate metabolism or pyruvate metabolism (Figure 7.2.1-2).

7.2.2. Principal component analysis

A principal component analysis (PCA) was performed, combining the 24 transcriptomic data sets to determine which factors contributed the highest level of variance in gene expression (Figure 7.2.2-1).

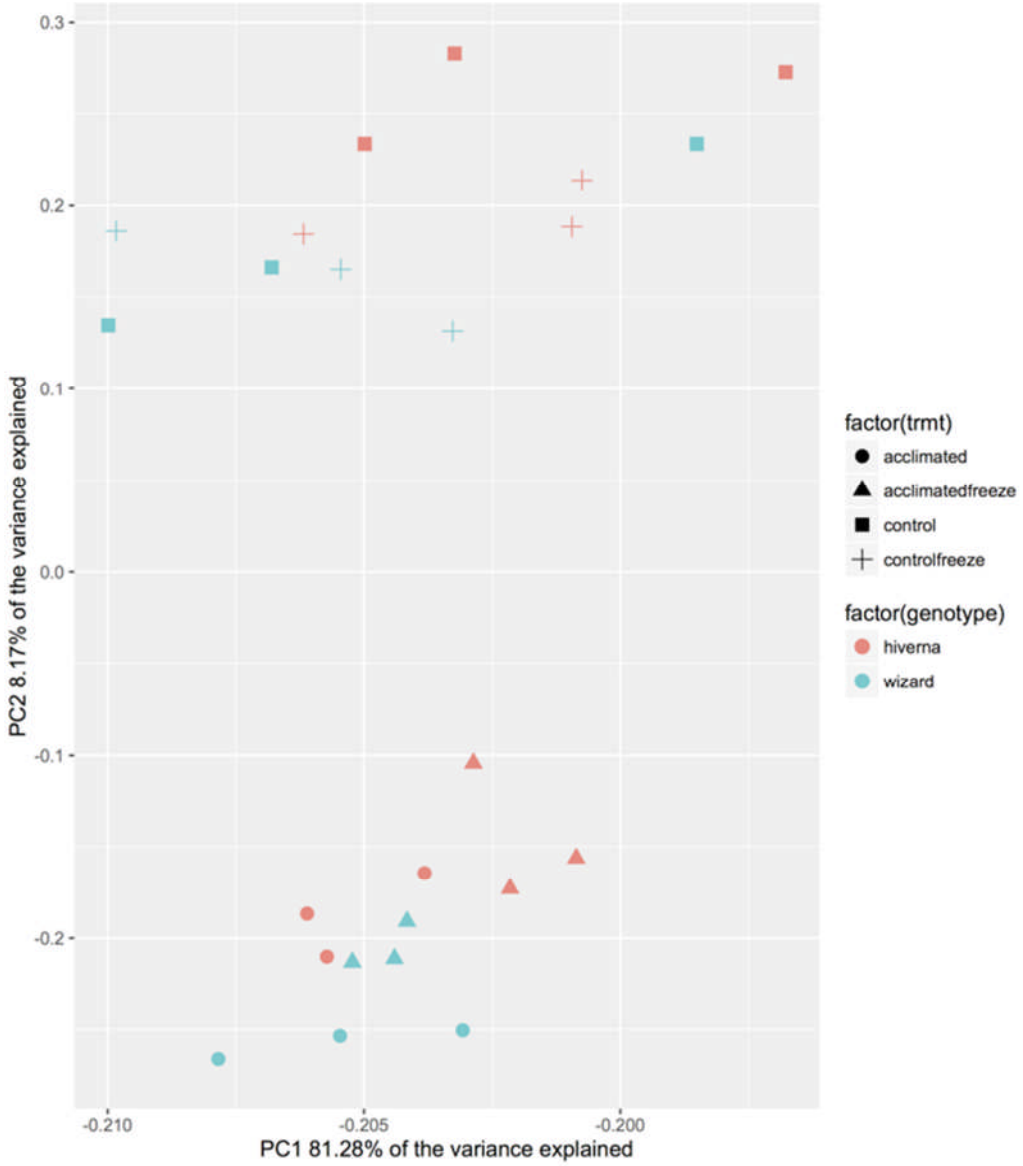

Figure 7.2.2-1: Principal component analysis of transcriptomic data sets, showing 3 repeats for both the Hiverna and Wizard cultivars that had been: maintained under control conditions for 24 days; grown for 14 days under control conditions and subjected to acclimatory night temperatures for 10 consecutive nights; maintained under control conditions for 24 days, culminating in a 30 minute freezing period on the 24th night; grown for 14 days under control conditions followed by 10 consecutive nights of growth under acclimatory conditions, culminating in a 30 minute freezing period on the 10th night of acclimation.

The PCA analysis assessed 5 factors; genotype (Hiverna/Wizard) and the four treatment conditions. Grouping could be seen for both genotypes that had been subjected to acclimation conditions, and acclimation conditions followed by a freezing period (Figure 7.2.2-1, lower middle). A lesser degree of grouping could be seen for both genotypes that had been maintained under control conditions, and maintained under control conditions followed by freezing exposure (Figure 7.2.2-1,upper). Moreover, the variation in the transcriptome profiles of plants that had been subjected to control and freezing conditions was grouped to a lesser extent than samples that had undergone acclimation (Figure 7.2.2-1).

7.2.3. Differential gene expression between genotypes under acclimation

The quantification and subsequent PCA identified a set of 16,687 genes that demonstrated a significant level of differential expression, when comparing any 2 factors. A significance boundary of P=<0.05 was introduced with a log fold change value of =>1 for up-regulated genes and =<-1 for down-regulated genes. This set was then used to compare gene expression between both Wizard and Hiverna under control and acclimatory conditions (Figure 7.2.3-1).

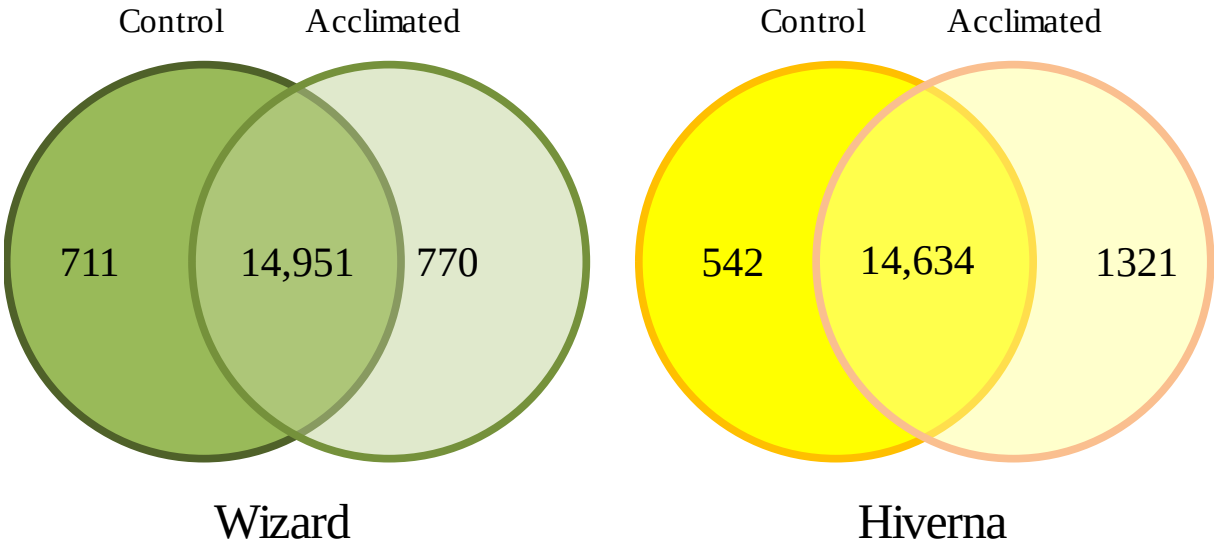

Figure 7.2.3-1 The total number of transcripts differentially expressed in the Wizard and the Hiverna cultivars, comparing control conditions to acclimatory conditions. Overlapping region shows the number of transcripts that are commonly expressed between the conditions.

In the Wizard cultivar 770 genes were found to be differentially regulated when plants were subjected to acclimatory conditions. In the Hiverna cultivar 1321 genes were differentially regulated under acclimation (Figure 7.2.3-1).

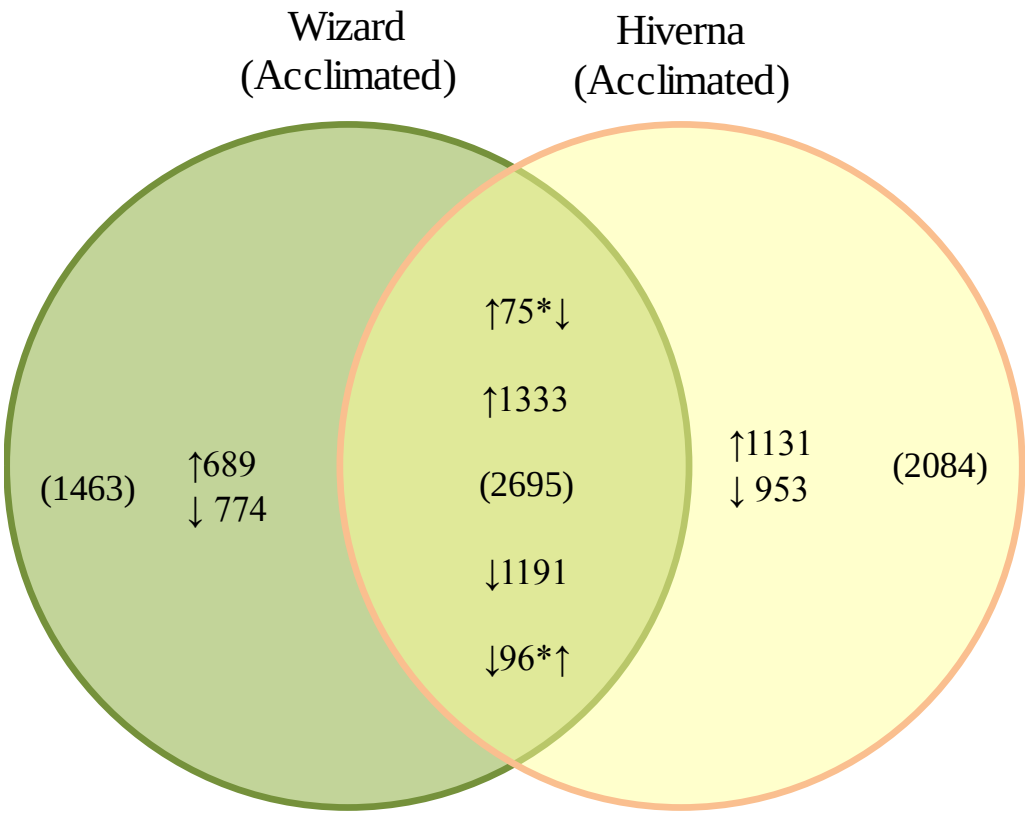

Number of transcripts	Expression in response to acclimation
1191	Down in both
953	Down in Hiverna
774	Down in Wizard
96	Up in Hiverna, Down in Wizard
75	Down in Hiverna, Up in Wizard
10445	No change in either
1131	Up in Hiverna
689	Up in Wizard
1333	Up in both

Figure 7.2.3-2 Venn diagram to show the set of differentially regulated transcripts between acclimation and control in both genotypes. The overlapping segment shows transcripts which are shared in the acclimation response of Wizard and Hiverna. The numbers represented by a star (*) are shared between Wizard and Hiverna, but respond in a different manner, indicated by the left hand arrow (Wizard) and right hand arrow (Hiverna). Numbers in non-overlapping segments are specific in the acclimation response for the cultivar. Bracketed numbers show the total number of transcripts that are specific to either Wizard or Hiverna. Table gives an alternate presentation of Venn diagram data.

A between-cultivar comparison of the genes differentially expressed under acclimatory conditions showed 284 genes to be expressed differently between Wizard and Hiverna under acclimatory conditions (Figure 7.2.3-3).

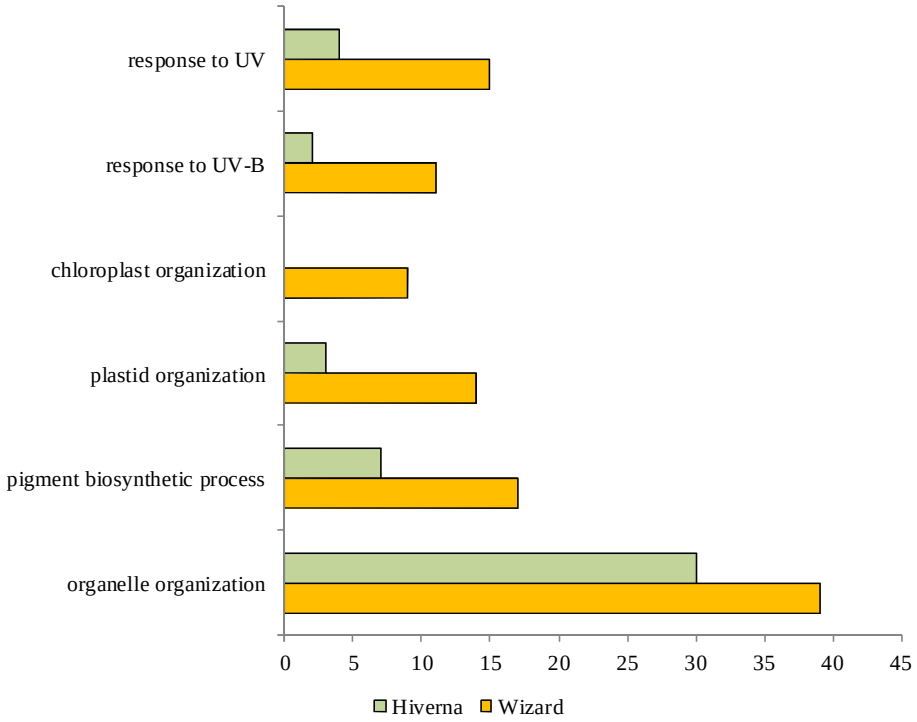

Figure 7.2.3-3: Metabolic process gene ontology showing the number of genes, and corresponding gene families, of differentially expressed between the Wizard and Hiverna cultivars under acclimatory conditions.

A gene ontology analysis showed that the differentially expressed genes belonged to 6 metabolic families (Figure 7.2.3-3). Fewer genes relating to ultraviolet radiation (UV) and UV-B were differentially expressed in Hiverna compared to Wizard. Interestingly, while no genes relating to chloroplast organisation were differentially expressed in Hiverna, 14 were differentially regulated in Wizard. Hiverna also had lower levels of differential gene expression for the metabolic processes underpinning plastid organisation, pigment biosynthesis and organelle organisation (Figure 7.2.3-3).

When searching the 284 differentially regulated genes for transcription factors, 12 were shown to be differentially regulated between Wizard and Hiverna (Table 18). Of these, 2 were GRAS family transcription factors, 3 were NAC family transcription factors and the remainder were a BEL-1 domain like transcription factor, a MYB like transcription factor, an E2F transcription factor, a PLATZ family transcription factor and a transcription factor jumonji domain protein. A plastid transcriptionally active protein and a putative transcription co-factor were also differentially expressed (Table 18). All of these transcription factors were less expressed in Wizard than Hiverna,

with the exception of the plastid transcriptionally active protein and the putative transcription co-factor.

Table 18: Transcription factors differentially regulated between the Wizard and Hiverna cultivars under acclimatory conditions. Log fold changes show the difference in gene expression in Wizard, compared to Hiverna, thus a negative values show gene down-regulation in Wizard and positive values show up-regulation. Conversely, if a gene is down-regulated in Wizard it will be up-regulated in Hiverna.

Transcript ID	Homologous element, species and gene ID	log fold change	P value
vf_0024348	GRAS family transcription (Medicago truncatula MTR_2g082090)	-1.93	0.00303
vf_0056807	GRAS family transcription factor (Medicago truncatula MTR_2g097463)	-1.72	0.04826
vf_0023632	BEL1-like homeodomain transcription factor (Trifolium pratense)	-1.40	0.00003
vf_0008457	MYB-like transcription factor family protein (Medicago truncatula MTR_2g100930)	-1.29	0.02549
vf_0024415	NAC transcription factor-like protein (Medicago truncatula MTR_2g079990)	-1.20	0.00483
vf_0023048	E2F transcription factor (Medicago truncatulaMTR_4g052000)	-1.20	0.00003
vf_0041085	Transcription factor jumonji (JmjC) domain protein (Medicago truncatula MTR_7g117445)	-1.18	0.00025
vf_0033376	NAC transcription factor-like protein (Medicago truncatula MTR_4g075980)	-1.12	0.04197
vf_0042236	PLATZ transcription factor family protein (Medicago truncatula MTR_8g066820)	-1.05	0.00409
vf_0043576	NAC-like transcription factor (Medicago truncatula MTR_3g096920)	-1.02	0.00409
vf_0065067	Plastid transcriptionally active protein (Medicago truncatula MTR_4g064750)	1.46	0.03578
vf_0060938	Transcription cofactor, putative (Medicago truncatulaMTR_2g104400)	1.63	0.01841

Table 19: Repetitive element identities and corresponding faba bean transcripts, determined by repetitive element database BLAST of uncharacterised sequences differentially expressed between genotypes under acclimatory conditions.

Transcript ID	Repetitive element ID and species	Identity (%)
v.faba_csfl_reftransV1_0022101	RLX_72950 G. max LTR	87.5
v.faba_csfl_reftransV1_0022101	RLC_167431 Gossypium LTR/Copia	90.323
v.faba_csfl_reftransV1_0039937	RLX_76673 Medicago LTR	71.5
v.faba_csfl_reftransV1_0039937	MTIS112A	69.149
v.faba_csfl_reftransV1_0040437	RLG_158021 Hordeum LTR/Gypsy	79.63
v.faba_csfl_reftransV1_0040437	RLX_160954 Hordeum LTR	80
v.faba_csfl_reftransV1_0010268	RLG_43598 Zea mays LTR/Gypsy	96.296
v.faba_csfl_reftransV1_0010268	RLC_124140 Lycopersicon LTR/Copia	87.5
v.faba_csfl_reftransV1_0010268	RLC_124140 Lycopersicon LTR/Copia	96.154
v.faba_csfl_reftransV1_0025006	RLX_163326 Gossypium LTR	82.979
v.faba_csfl_reftransV1_0025006	RLX_163326 Gossypium LTR	83.333
v.faba_csfl_reftransV1_0025006	RLX_70522 Glycine LTR	85
v.faba_csfl_reftransV1_0009781	RLG_76427 Medicago LTR	69.784
v.faba_csfl_reftransV1_0009781	RLG_76422 Medicago LTR	69.784
v.faba_csfl_reftransV1_0011950	RLX_75637 Lotus LTR	91.667
v.faba_csfl_reftransV1_0011950	TXX_169408 Gossypium Mobile element	96
v.faba_csfl_reftransV1_0035145	RLX_123952 Lycopersicon LTR	96
v.faba_csfl_reftransV1_0035145	Copia-8_ATr-I	96
v.faba_csfl_reftransV1_0020813	RLX_39536 Sorghum LTR	86.047
v.faba_csfl_reftransV1_0020813	RLX_76648 Medicago LTR	87.805
v.faba_csfl_reftransV1_0020813	RLX_76648 Medicago LTR	65.806
v.faba_csfl_reftransV1_0026937	RLX_123398 Lycopersicon LTR	80.952
v.faba_csfl_reftransV1_0026937	RLX_164440 Gossypium LTR	77.778
v.faba_csfl_reftransV1_0012615	RLX_122977 Solanum LTR	81.818
v.faba_csfl_reftransV1_0012615	RLG_163287 Gossypium LTR	95.833
v.faba_csfl_reftransV1_0044038	RLX_70727 Glycine LTR	87.5
v.faba_csfl_reftransV1_0044038	RLX_70727 Glycine LTR	84.375
v.faba_csfl_reftransV1_0044038	RLX_76542 Medicago LTR	82.5
v.faba_csfl_reftransV1_0044038	RLX_76542 Medicago LTR	78.571
v.faba_csfl_reftransV1_0027409	RLX_70164 Glycine LTR	93.333
v.faba_csfl_reftransV1_0027409	RLX_55442 Arabidopsis LTR	89.189
v.faba_csfl_reftransV1_0026277	Gypsy4-VV_I	93.103
v.faba_csfl_reftransV1_0026277	RLX_72063 Glycine LTR	86.111
v.faba_csfl_reftransV1_0004886	RLG_72410 Glycine LTR	87.5
v.faba_csfl_reftransV1_0004886	RLX_51444 Zea LTR	81.579

Of the transcripts that were significantly differentially regulated, 36 had no identifying homologue in the cool season food legume database. When comparing these transcript sequences to the known sequences of repetitive elements, significant homology was found. These repetitive elements consisted predominantly of LTR retrotransposons (31), with the remaining elements being gypsy, copia or uncharacterised mobile genetic elements (Table 19).

7.3. Discussion

In the present study the transcriptome profiles of 2 faba bean cultivars, Hiverna and Wizard were characterised under control and acclimatory conditions. As few studies have been conducted on the regulation of gene expression under low temperatures in legumes (Calzadilla et al., 2016), this study provides novel information on the genetic differences underpinning chilling and freezing tolerance in legumes. Moreover, the depth of the data generated will assist greatly in the characterisation of the faba bean gene space. In this study Wizard was found to have a higher number of differentially expressed genes than Hiverna under control conditions. However, Hiverna had more differentially expressed genes than Wizard under acclimatory conditions.

Ontology analysis of differentially regulated genes under control conditions showed that the principle metabolic families were involved with energy metabolism and the biosynthesis of isoprenoid compounds. Isoprenoids have previously been linked to enhanced abiotic stress tolerance, acting as ROS scavengers (Vickers et al., 2009). Moreover, isoprenoid compounds provide the chemical precursors to chlorophyll, carotenoids and their derivatives, thus presenting the most diverse group of plant metabolites (Vranová et al., 2012). There are few resources in the literature which elaborate on the potential reasons for differences in isoprenoid pathway transcription. Indeed, as such a diverse group of metabolites, much remains to be elucidated about isoprenoid regulation (Vranová et al., 2011).

While detailed transcriptome comparisons have not been performed on contrasting legume cultivars, studies have been conducted in rice (Shankar et al., 2016). In comparisons of the drought tolerant cultivar Nagina 22 and the drought sensitive cultivar IR64 grown under control conditions, 1076 transcripts were found to be differentially regulated (674 + 402), however these studies did not detail the gene family differences between cultivars (Shankar et al., 2016). Interestingly the number of differentially expressed genes in rice was comparable to faba bean, for which 1072 (779+293) transcripts were differentially expressed between cultivars under control conditions.

Little is known about the regulation of gene expression in legume acclimation to low temperatures. Of the studies conducted, the majority have utilised array technologies, thus the identification of novel genes has not been possible (Lucau-Danila et al., 2012). The most in depth study to date was conducted on *L. japonicus* (Calzadilla et al., 2016). Through analysing the transcript profile of cold-exposed plants over a 24 hour period a total of 1077 differentially expressed genes were identified. These were related to lipid synthesis, cell wall regulation and chloroplast development. Moreover, 41 transcription factors were identified from several families (Calzadilla et al., 2016).

Legume genomes encode upwards of 2000 transcription factors, but less than 1% of these have been genetically characterised in model species (Udvardi et al., 2007). Transcription factors act as molecular switches for the regulation of gene expression and are usually composed of at least four domains: a DNA-binding domain, a nuclear-localisation signal, a transcription-activation domain, and an oligomerisation site (Reichmann et al., 2012). In the present study 12 transcription factors were shown to be differentially regulated in response to dark-chilling. The low-temperature tolerant Hiverna cultivar expressed 10 transcription factors to a higher level than the sensitive Wizard cultivar. These are discussed in turn.

Two GRAS proteins were found to be differentially regulated between Wizard and Hiverna under acclimatory conditions. GRAS proteins are plant-specific and their name is derived from the first three members; GIBBERELIC-ACID INSENSITIVE (GAI), REPRESSOR OF GAI (RGA) and SCARECROW (SCR; Hirsch and Oldroyd, 2009). They play diverse roles in gibberellic acid (GA) signalling, shoot development and phytochrome-A signal transduction (Bolle, 2004). In the model legumes *M. truncatula* and *Lotus japonicus* GRAS proteins are required for nodule morphogenesis (Heckmann et al., 2006). Moreover, their role as transcription factors has recently become established, particularly in the control of arbuscule development (Xue et al., 2015).

Under acclimatory conditions 3 NAC-like transcription factors were found to be upregulated in Hiverna compared to Wizard. The NAC transcription factor family is named after the three genes that were initially discovered to contain the NAC domain: NAM (no apical meristem), ATAF1 and -2 and CUC2 (cup-shaped cotyledon; Souer et al., 1996; Aida et al., 1997; Nuruzzaman et al., 2013). NAC transcription factors play central roles in regulating plant growth and development processes, including responses to abiotic stresses (Shao et al., 2015). However, the precise downstream targets of NAC transcription factors are still unknown (Shao et al., 2015).

BEL1-like homeodomain transcription factors are members of the three-amino-acid-loop-extension (TALE) class of homeoproteins, which constitute the major regulators of meristematic activity (Arnaud and Pautot, 2014). BEL1-like transcription factors may function as heterodimers with KNOTTED-like (KNOX) proteins, arranging in many conformations to regulate distinct aspects of plant morphogenesis (Arnaud and Pautot, 2014). They have been shown to act as long-distance signals, being detected in the phloem sap of solanaceous species (Campbell et al., 2008) and have been shown to have differential expression in Arabidopsis leaves, resulting in differences to leaf phenotype (Kumar et al., 2007). However, while the roles of BEL1-like transcription factors have been explored in plant development, there are no known references to their regulation or function under stress conditions.

One MYB-like transcription factor was more highly expressed in Hiverna than Wizard under acclimatory conditions. The MYB superfamily constitutes one of the most abundant groups of transcription factors in plants (Du et al., 2012), acting to regulate numerous metabolic functions such as phenylpropanoid biosynthesis, cell morphogenesis and the cell cycle (Roy, 2016; Weisshaar and Jenkins, 1998). In particular the R2R3-type MYB family members have been linked to abiotic stress tolerance in *A. thaliana*, a result of their interaction with genes of phenylpropanoid pathway and the consequent effects on sinapate ester and flavonoid abundance (Roy, 2016). These metabolites are essential in UV-B absorption, thus up regulation of MYB transcription factors could reasonably be attributed to enhanced UV-B tolerance (Bieza and Lois, 2001).

E2F transcription factors are crucial in the regulation of genes required for G1/S cell cycle transition and S-phase progression (Trimarchi and Lees, 2002). A single E2F transcription factor was found to be more highly expressed in Hiverna than Wizard. However, the mechanisms of E2F function are not fully understood (Ramirez-Parra et al., 2003). Roles have been identified for the E2F family in the mediation of *A. thaliana* responses to non-stress temperatures, however its wider roles in abiotic stress tolerance remain to be characterised (Zhou et al., 2014).

PLATZ is an AT-rich sequence and zinc-binding protein family, the members of which act as transcription factors in plants (Nagano et al., 2001). A single PLATZ gene transcript was found to be more highly expressed in Hiverna than Wizard. In the initial identification of the PLATZ transcription factor it was found to have a conserved binding domain that targeted AT-rich regions and appeared to have specific regulatory functions in plastid gene expression (Nagano et al., 2001). In soybean PLATZ was shown to be responsive to ABA, drought and high salinity, and was implied in developmental processes such as germination under osmotic stress (So et al., 2015). To date, functional characterisation of PLATZ factors has focused on legume species

Transcription factor jumonji (JmjC) belongs to a class of transcription factors that regulate histone methylation (Klose et al., 2006). A conserved class of proteins within higher eukaryotes, jumonji domain-containing proteins are linked to the epigenetic regulation of gene expression (Hu et al., 2015). Thus the differential expression of JMJC in Hiverna presents an interesting target for the investigation of potential epigenetic factors that contribute to low temperature tolerance.

In addition to the differential expression of transcription factors, a number of mobile genetic elements were identified. Mobile genetic elements, in particular retrotransposons of the long terminal repeat family (LTR) class, are capable of propagating in the plant genome via a “copy and paste” mechanism. However, evidence has suggested that they play roles in the regulation of gene expression (Grandbastien, 2015). As such, an analysis of the differential expression of transposable

genetic elements would be an interesting step to take in the elucidation of low temperature defence mechanisms in plants.

Plant responses to abiotic stress require rapid and coordinated changes at the transcriptional level. Through characterising those transcription factors that are differentially regulated between sensitive and tolerant cultivars under chilling stress, specific gene targets may be identified for the further exploration of low temperature tolerance traits in faba bean. The data presented in the present study enhance current knowledge of the faba bean genome and its regulation in response to cold temperatures. However, a more comprehensive approach needs to be taken, including the construction of a *de novo* reference transcriptome which may be used as a foundation for the identification of novel genes.

"If I have seen further, it is by standing on the shoulders of giants."

-Isaac Newton

8. General Discussion

The hypothesis upon which this thesis was based is that low temperature tolerance is influenced by phytocystatin expression and the strigolactone pathway. The specific objectives of the work were:

- To characterise the effects of OCI expression on dark-chilling tolerance in soybean.
- To characterise the effects of the strigolactone (SL) pathway on the dark chilling tolerance of pea and *A. thaliana.*
- To physiologically and genetically characterise low temperature tolerance in faba bean, for the development of tolerance markers.

The studies reported in this thesis have explored the effects of low temperatures on photosynthesis and biomass production in 4 species; the legumes soybean, pea and faba bean, and the model plant *A. thaliana*. Moreover, the specific objectives of the work have been met. Chilling temperatures were found to inhibit photosynthesis in Wt soybean, a tropical legume. However photosynthesis was not affected in the Wt of other species, which were of temperate origin. The inhibition of photosynthesis and biomass accumulation was decreased in OCI expressing soybean compared to Wt. Moreover, chilling sensitivity in soybean, pea and *A. thaliana* was linked to SL. Increased abundance of SL synthesis transcripts in OCI expressing soybean was linked to enhanced chilling tolerance. Additionally, the impaired synthesis or signalling of SL in pea and *A. thaliana* increased sensitivity to low temperatures. Crucially, high resolution genomic information on faba bean was produced in these studies, together with transcriptome profiles of sensitive and tolerant cultivars under chilling and freezing stress. Taken together the data presented in this thesis provide physiological, metabolic and genetic information that can be used to develop markers for the accelerated breeding of low temperature tolerance in faba bean, as discussed below.

8.1. The importance of legumes in a changing world

Legumes, such as soybean, pea and faba bean will be central components of crop production, underpinning future food security (Foyer et al., 2016). Legumes are integral to sustainable farming systems (Lassaletta et al., 2014; Barton et al., 2014) and comprise the majority of the world's dietary protein (Graham and Vance, 2003). Moreover, they have numerous proven health benefits. However, the growth and productivity of legumes is currently limited by abiotic stress factors, in particular chilling and freezing temperatures (Maqbool et al., 2010). The incidence of extreme low temperature events is predicted to increase in the next 50 years (Olesen et al., 2011). Additionally, with the current

rate of population growth, the increased production of nutritionally beneficial crops is essential. Thus the development of legume cultivars that are more tolerant to low temperatures is a key concern in food security.

Changes to the world's climate are characterised by: rising temperatures, an increase in atmospheric CO_2 concentration, and an increase in the incidence of extreme weather events (Vitousek, 1994). These changes are partly due to an expanding global population, with an associated increase in greenhouse gas emissions being the driving factor for global warming. Indeed global average temperatures have risen by approximately 0.13ºC per decade since 1950 (Lobell et al., 2011). However, an underappreciated aspect of global warming is the increase in frequency of extreme cold weather events despite rising temperatures (Jones and Moberg, 2003; Olesen et al., 2011).

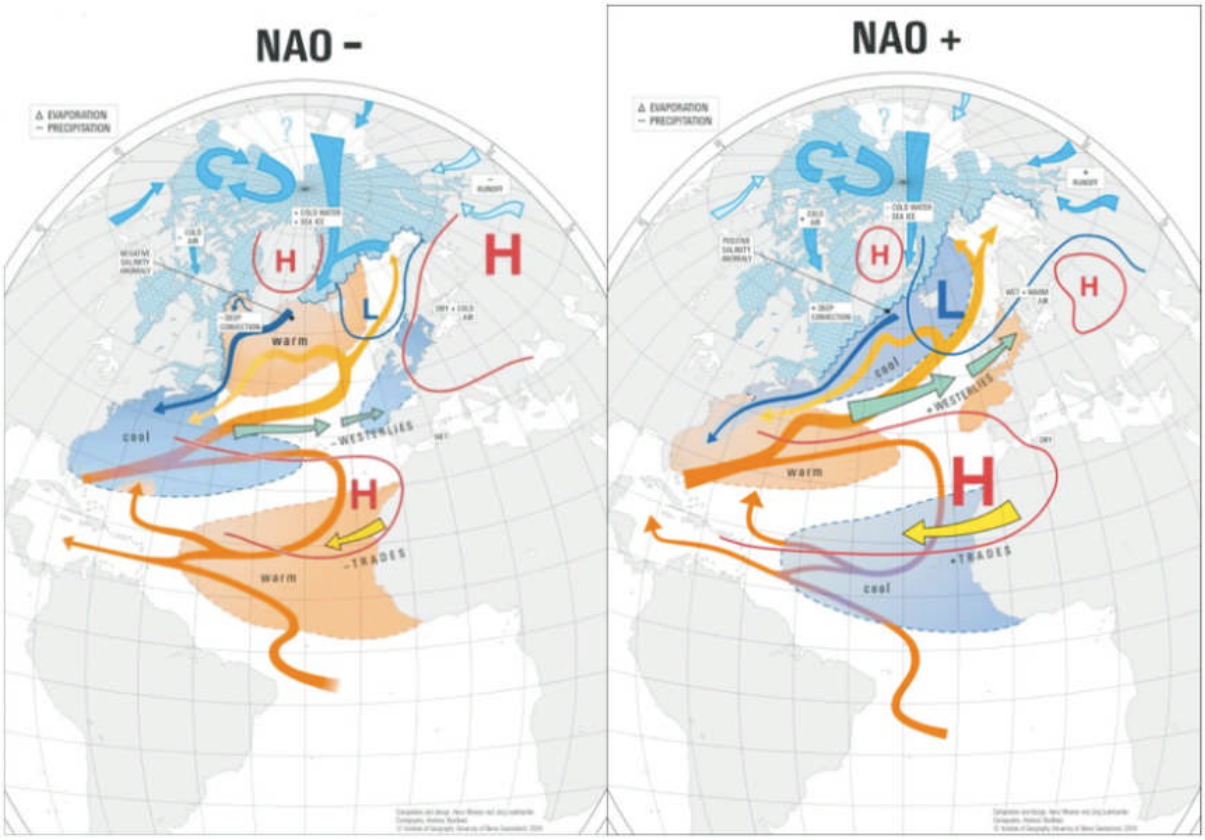

Figure 8.1-1: A graphical representation of the two states of the NAO, drawn from consensus data. In the negative phase (NAO-) cold air is drawn into Europe from the Siberian and Arctic regions. In the positive phase (NAO+) warm air is drawn into Europe from Central and Northern America. Geographical features are shown in grey, cold air in blue and warm air in orange. Figure adapted from Wanner et al (2001).

While extreme cold events are localised in nature, their induction is a result of large scale changes in hemispheric air circulation patterns, caused by global warming (Zhang et al., 2012). In Eurasia, for

example, the past decade has seen an increase in the incidence of extreme cold weather events, resulting from changes in the position of the North-Atlantic Oscillation (NAO). The NAO is a meteorological phenomenon comprising two interacting areas of atmospheric pressure; the Icelandic low and the Azores high. A large difference in pressure between these two regions (NAO+) leads to an increase in wind drawn from the warm, humid regions of America. However, a low difference in pressure (NAO-) causes colder winds to be drawn into Europe from Siberia (Figure 8.1-1; Wanner et al., 2001).

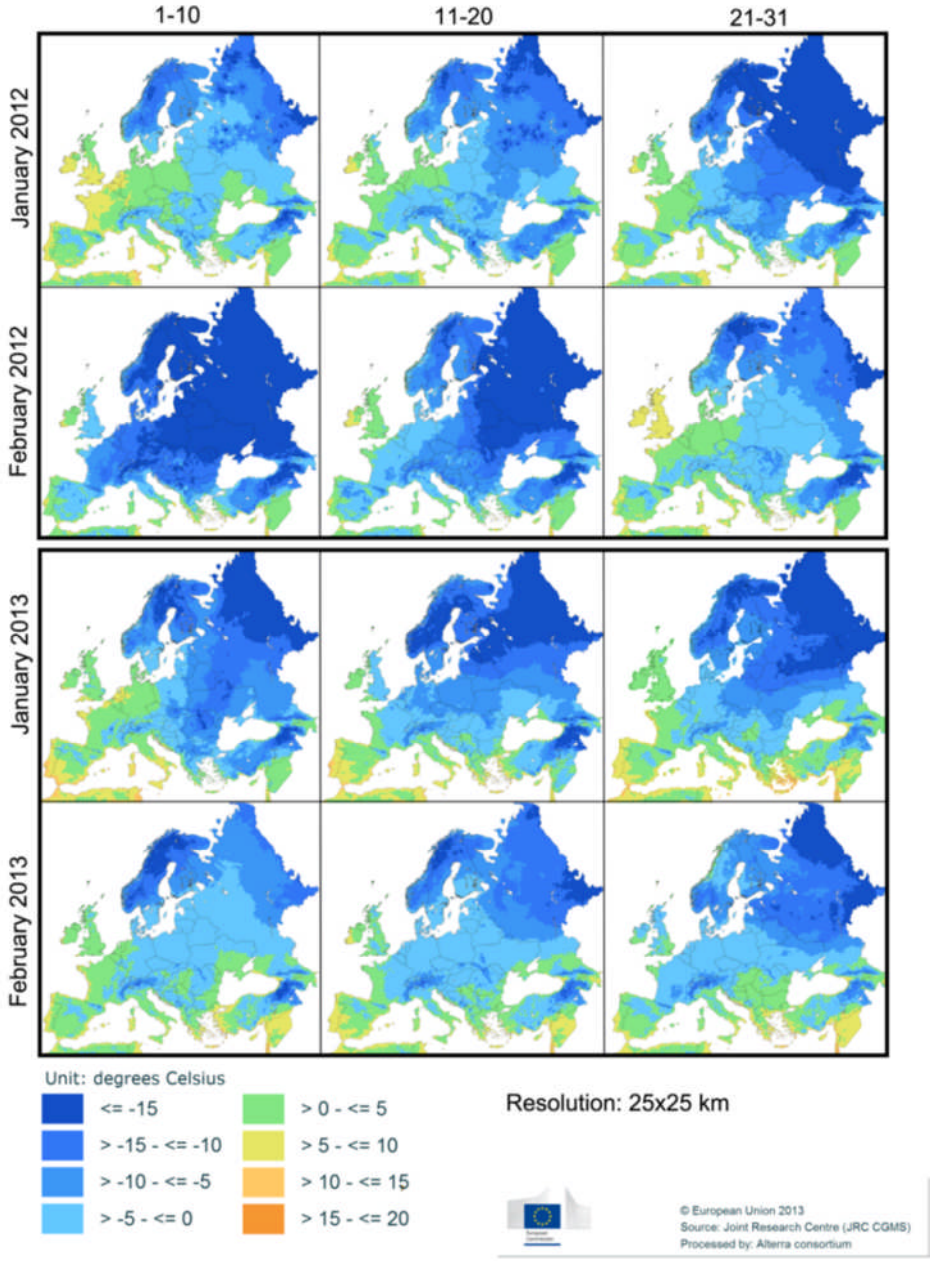

Figure 8.1-2: Average minimum daily temperatures for the months of January and February, years 2012 and 2013. Each panel represents a 9-10 day period. Figure constructed using resources from the European Commission's Monitoring Agricultural Resources Agri4Cast web page (European Comission Joint Research Centre, 2011).

Severe cold weather events have a detrimental effect on agricultural productivity, with different crops and agro-environmental strata being influenced to differing degrees (Olesen and Bindi, 2002). Recent years have seen European winters with freezing temperatures that may be considered extreme (below -15 °C; Figure 8.1-2). Moreover the current intergovernmental Panel on Climate Change report stated that future weather will consist of frequently high temperatures, corresponding dry spells and the continued occurrence of occasional cold temperature extremes (IPCC, 2014). This is a particular danger for overwintering crops which are autumn sown and establish during the winter months, and which can be killed by exposure to extreme low temperatures. The need for the development of cold tolerant legumes is two-fold, stemming from the need to mitigate the impact of future climatic variability, but also to increase the current area upon which crops can be grown.

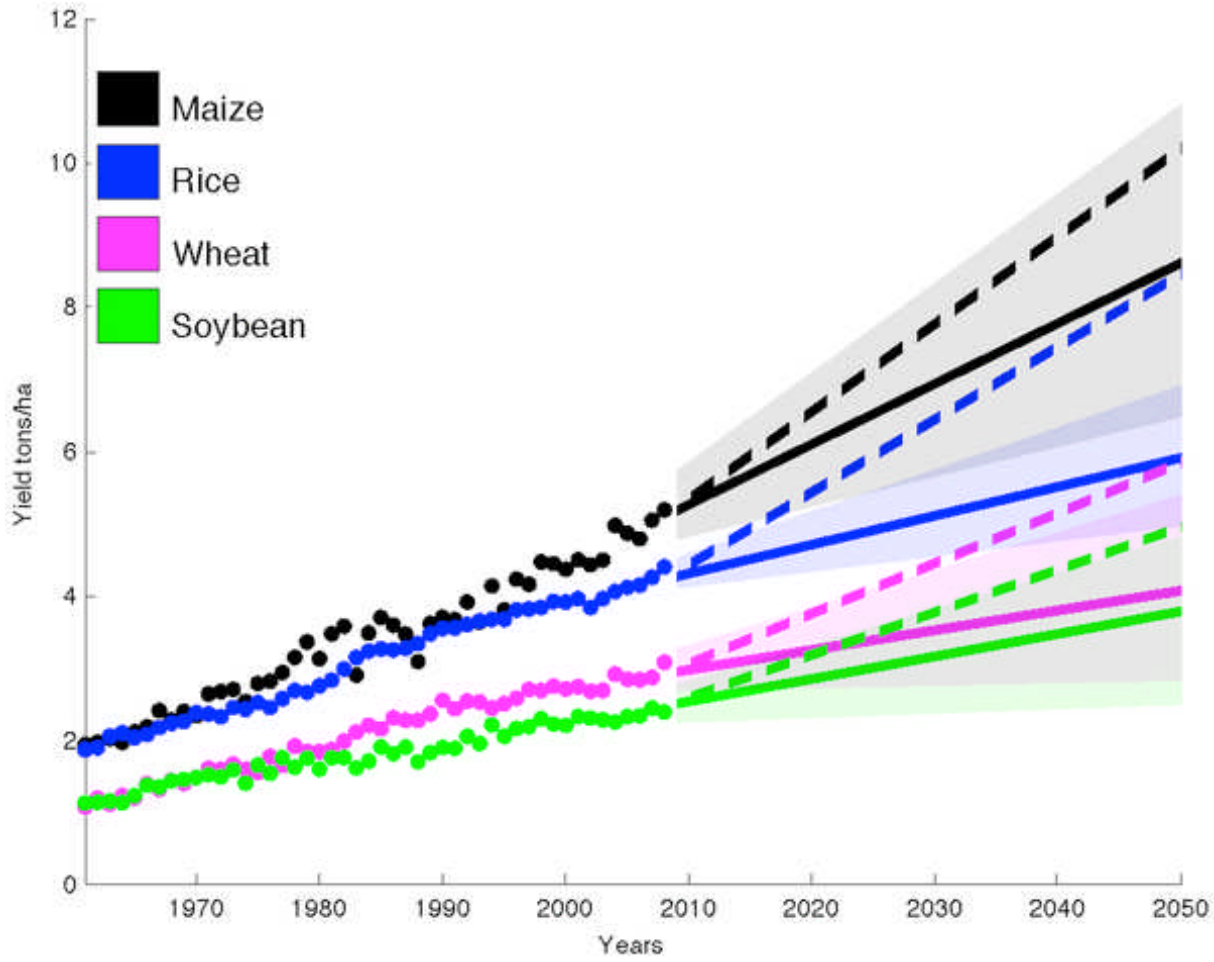

Figure 8.1-3: Annual global yield averages in dry metric tons per hectare for each year from 1961 to 2008 for maize, rice, wheat and soybean. Solid lines show projected yields to 2050. Dashed line shows the trend of the ~2.4% yield improvement required each year to double the production of these crops by 2050 without cultivating additional land. Taken from Ray et al., (2013).

Agriculture occupies approximately 38% of the Earths terrestrial surface constituting the largest use of land on the planet (Foley et al., 2011). However despite the comparatively large area dedicated to agriculture, food security remains a pressing concern – particularly in the context of population growth (Godfray and Garnett, 2014). The global population is growing at a rate of 1.8% per year and is estimated to reach approximately 9.7 billion by 2050 (United Nations Department of Economic and Social Affairs Population Division, 2015).

Current projections of crop yields show a large gap between the world's future needs and what can be provided by current improvement rates (Figure 8.1-3; Ray et al., 2013). As such, the threats to global food security are multifaceted with major challenges coming from climate change and land use competition. The latter is a result of various industrial demands, for example animal feed and biofuels (Baldos and Hertel, 2014). Furthermore, to portray global food needs in the context of caloric provision alone is inadequate. Malnutrition is a widespread phenomenon, thus the provision of sufficiently nutritious food for the growing population is an equally pressing concern (Godfray et al., 2010).

Threats to food security are multifaceted, comprising population expansion, climate change and land use competition. Legumes are well suited to meet the dietary needs of the world's population, being rich in proteins and other essential dietary components (Foyer et al., 2016). However, more extensive research must be conducted into the factors that limit legumes, in particular low temperature stresses. In order to mitigate the influence of chilling and freezing stress on legume productivity, a multidisciplinary approach is needed. The pairing of mathematical modelling with a thorough understanding of the biological mechanisms underpinning stress tolerance traits will help to reduce threats to the global food network (Prasad et al., 2010). Moreover, through understanding low temperature tolerance traits in legumes, the agricultural land available for their growth may be expanded. However, in order to breed more tolerant legume crops, the processes that regulate acclimation to low temperatures must be understood.

8.2. Proteases and protease inhibitors as targets for crop improvement

Acclimation to chilling and freezing requires substantial turnover of proteins, so that the leaf proteome is appropriate to the metabolic conditions pertaining under chilling and freezing stress (Kosová et al., 2011). The results presented in chapter 3 showed that constitutive expression of OCI conferred protection to the chilling-induced inhibition of photosynthesis in soybean. Constitutive

expression of protease inhibitors has previously been shown to enhance plant tolerance to biotic stresses, such as nematode infection and coleopteran herbivory (Liang et al., 1991; Zhang et al., 2012a). However, the impact of protease inhibitors on abiotic stress tolerance has been relatively unexplored (Kunert et al., 2015).

Protein breakdown resulting from stress exposure involves many proteases, regulators, and dynamic protein trafficking processes which ensure the complete transformation of proteins into transportable and useful products (Diaz-mendoza et al., 2016). Through inhibiting the activity of proteases, the protein restructuring of cells in response to stress is modified (Kunert et al., 2015). A model has previously been shown whereby the transgenic expression of OCI prevents the breakdown of the key photosynthetic enzyme, RuBisCo (Prins et al., 2008). Additional research has shown that the expression of phytocystatins in broccoli delays the onset of post-harvest senescence (Eason et al., 2014). Thus, the expression of protease inhibitors appears to have pleiotropic effects. However, while the precise mechanisms of cystatin-protease interactions in abiotic tolerance need to be explored, their use in the development of agronomically favourable crop traits is promising (Kunert et al., 2015).

Many plant encoded cystatins contain a DRE/CRT transcription factor binding element (Seki et al., 2002). The role of DRE binding factors in the regulation of cystatin expression is exemplified by the *A. thaliana* cystatin, AtCYSa (Zhang et al., 2008). Interestingly while the DRE/CBF family is conserved in soybean, chilling sensitivity in still displayed (Kidokoro et al., 2015). In the present studies constitutive OCI expression was shown to confer protection to the chilling-dependent inhibition of photosynthesis in soybean. The interacting partners of DRE/CRT binding factor elements in soybean would therefore be interesting to explore, as studies show that DREB family members have highly specific functions in response to abiotic stresses (Li et al., 2005). Therefore it is possible that the transcriptional networks acting to protect tolerant plant species from low temperature stress are not present in soybean, despite members of the transcription factor family being conserved. With the advent of gene editing technologies such as CRISPR/CAS9, the activities of transcription factors may be modified so that their downstream genes functioned to protect against low temperature as well as other abiotic stresses (Bortesi and Fischer, 2015).

The effect of OCI expression on the abundance of SL synthesis enzyme transcripts has been reported previously (Quain et al., 2014). However the precise interaction between cysteine proteases and SL pathway proteins is currently unknown. SL is known to regulate a wide range of processes, including natural and stress-induced senescence (Hye et al., 2004; Woo et al., 2001). Thus SL presents an interesting target for the development of stress tolerance. Moreover, the interaction between proteases, inhibitors and the SL pathway should be explored further.

8.3. The strigolactone pathway as a mediator of stress tolerance

In addition to the protective effect of OCI expression against the chilling-dependent inhibition of photosynthesis in soybean, low temperature sensitivity was also linked to SL in all of the species studied. Previous studies have reported a link between SL synthesis and signalling, and the tolerance of plants to drought stress (van Ha et al., 2014). This is interesting as the regulatory factors underpinning tolerance to drought and chilling are often conserved (Thomashow, 1999). The work presented in chapter 4 showed that SL synthesis and signalling mutants of pea and *A. thaliana* had a lower tolerance to chilling stress than the respective wild types. However, when *A. thaliana* Wt and mutants were grown on plates in the presence of 2 µM GR24, sensitivity to chilling temperatures was increased. Relatively few studies have been conducted on the role of SL in abiotic stress tolerance. However, SL deficiency has been linked to increased drought and salt sensitivity (van Ha et al., 2014; Pandey et al., 2016), and a delay in senescence (Woo et al., 2001). While the mechanisms underpinning the effect of SL on abiotic stress tolerance are not yet clear, SL levels have been shown to be responsive to abscisic acid (ABA; López-Ráez et al., 2010). Moreover, research suggests that the concentration of SL is integral to its effect on plant physiology and metabolism. Thus, future studies should aim to characterise the effects of SL concentration on plant physiology and stress tolerance (Cheng et al., 2013). Moreover, the interactions between SL and other plant hormones should be explored.

SL signalling is essential to the composition of the plants microbiome, with low concentrations of SL inducing the growth of arbuscular mycorrhizal (AM) fungi in legumes (Besserer et al., 2006). Interactions with the rhizosphere have been shown to have direct effects on plant health, both during development and in response to stress (Philippot et al., 2013). The composition of the rhizosphere is dependent on plant-microbe and microbe-microbe interactions. As such, while the diversity of organisms in the soil is the key factor in microbiome constitution, the host genotype also has a strong influence on microbial community composition (Lareen et al., 2016). While the link between plants and their symbiotic microorganisms has long been recognised, the importance of this interaction has only recently become a research focus. Indeed, the root microbiome is considered by some to act as a "secondary genome", providing host plants with a range of beneficial metabolites (Lareen et al., 2016; Rout and Southworth, 2013; Berendsen et al., 2012).

The potential benefit of the soil microbiome has been exemplified in work conducted on *A. thaliana*. When plants were grown in soil having a history of exposure to *A. thaliana* (sympatric), plant

biomass accumulation was significantly increased when compared to plants grown on non-sympatric soils (Zolla et al., 2013). In addition, AM symbiosis has been shown to induce SL biosynthesis under drought conditions in lettuce and tomato, resulting in enhanced drought tolerance and increased AM proliferation (Ruiz-Lozano et al., 2016). Moreover the presence of AM communities has been shown to protect *P. vulgaris* from reduced root-water uptake in response to chilling stress (Aroca et al., 2007). Taken together these studies could, in part, explain why soil grown SL mutants of *A. thaliana* performed differently to those grown on plates (Chapter 4). Crop species need to be considered in the broader context of the ecological niche that they inhabit. Biotechnological approaches to crop improvement would benefit from recognising the diverse community of microorganisms that contribute to plant development and environmental stress tolerance traits (Coleman-Derr and Tringe, 2014). As such SL research should not be considered in the context of the plant alone, but also the environment that it inhabits. The link between plants, their microbiome and stress tolerance traits is particularly interesting in the context of legumes, which are characterised by their symbiotic interactions. However, in order to fully understand the dynamic processes underpinning legume responses to abiotic stresses, more comprehensive genetic resources must be developed.

8.4. Enhancing low temperature tolerance in *Vicia faba*

Faba bean is a globally important legume, the growth of which is restricted in Europe by the incidence of extreme freezing (Herzog, 1987; Link et al., 2010). However, while classical genetic approaches have gone some way toward the development of improved faba bean cultivars, a lack of in-depth sequence information (O'Sullivan and Angra, 2016) has hindered modern breeding approaches, such as marker assisted selection. As such, the studies undertaken in this thesis characterised the low temperature tolerance of 5 faba bean cultivars and transcriptomic analysis was performed on the most sensitive and tolerant of these. Additionally, genetic resources were enhanced for *V. faba* through the genome sequencing of the Wizard cultivar. Thus, these studies have increased the physiological understanding of low temperature tolerance in faba bean, but crucially they have significantly contributed to the currently available genetic data.

The results presented in chapter 6 showed the faba bean genome to be large and highly repetitive, with some polymorphisms being present in the coding regions of chloroplast and mitochondrial genomes. The nuclear genome of faba bean is fascinating, not least because it is very large for a diploid species (~13 Gb), with a largely repetitive composition and a high number of retrotransposons (RT). RTs are considered to be the raw material for evolutionary innovation in plant genomes (Grandbastien, 2015), allowing the inclusion of new genes, regulating gene expression and contributing to histone modification and DNA methylation (Cavrak et al., 2014). However, the

relative organization of these retroelements in complex plant genomes and their regulation during environmental stress remains poorly understood. The results presented in chapter 7 showed a number of transcription factors to be up-regulated in the cold tolerant cultivar, Hiverna, as compared to Wizard. Among these was transcription factor jumonji, which is linked to histone methylation and the epigenetic regulation of gene expression (Hu et al., 2015). Moreover, 36 repetitive elements were identified as being actively transcribed under acclimatory conditions. As such, the epigenetic factors contributing to low temperature tolerance would be an interesting target for future work. The establishment and application of retrotransposon and single nucleotide polymorphism marker systems should be explored, together with the characterisation of genome methylation patterns and retrotransposon activation in response to alterations in cellular redox state resulting from exposure to chilling (Peng and Zhang, 2009; Cavrak et al., 2014; Alzohairy et al., 2014). However, such investigations would be contingent on the availability of a comprehensive reference genome.

In the low temperature acclimation transcriptome presented in chapter 7, 12 transcription factors were shown to be more highly expressed in Hiverna than Wizard. Transcription factors have been proposed as selection markers in their own right for the accelerated breeding of favourable agronomic traits (Han et al., 2010; Bianchi et al., 2015; Pandey et al., 2016). Thus these studies present interesting targets for further investigation. Moreover, the sequence data generated in these studies may assist in the identification of novel genes, specific to faba bean. However, efforts must be made to fully characterise the transcriptomic data generated, with particular regard to the generation of a comprehensive reference transcriptome, for which current annotations remain inadequate (Humann et al., 2016). Furthermore, the data arising from these studies can be utilised to understand the differences in gene expression between chilling and freezing stresses in faba bean.

Subsequent studies in faba bean genetics should aim to define the gene space of faba bean by whole genome sequencing, and to order these genes into physical and genetic maps using methods such as optical mapping (Tang et al., 2015). Through combining molecular genetics, bioinformatics, whole plant physiology, and biochemistry; new fundamental information concerning the evolution and regulation of the faba bean genome may be provided. The adoption of next-generation sequencing approaches in faba bean research will facilitate the identification of new stress tolerance markers, that will accelerate breeding programs (Paszkowski, 2015).

8.5. Conclusions

The studies presented in this thesis have highlighted the effect of phytocystatins and strigolactones on low temperature tolerance in legume species. The development of chilling and freezing tolerant legumes is an essential step in the protection of global food security. However, few comprehensive genetic resources exist for important legume crops, such as faba bean. Thus to date, cultivar development has not kept pace with cereal crops. These studies have generated genetic and transcriptomic data for faba bean. Through combining transcriptomic data analysis with experimental approaches, based on the findings in pea, soybean and Arabidopsis, markers may be identified for the accelerated breeding of low temperature tolerance in this crop. Moreover, the depth of the gene based data will allow for the construction of genomic and transcriptomic resources that will be integral to further research in the field of faba bean biology.

9. References

Abe, K., Kondo, H., and Arai, S. (1987). Purification and characterization of a rice cysteine proteinase inhibitor. Agric. Biol. Chem **51**: 2763–2768.

Abe, M., Kobayashi, Y., Yamamoto, S., Daimon, Y., Yamaguchi, A., Ikeda, Y., Ichinoki, H., Notaguchi, M., Goto, K., and Araki, T. (2005). FD, a bZIP protein mediating signals from the floral pathway integrator FT at the shoot apex. Science **309**: 1052–1056.

Achard, P., Gong, F., Cheminant, S., Alioua, M., Hedden, P., and Genschik, P. (2008). The cold-inducible CBF1 factor-dependent signaling pathway modulates the accumulation of the growth-repressing DELLA proteins via its effect on gibberellin metabolism. Plant Cell **20**: 2117–29.

Aida, M., Ishida, T., Fukaki, H., Fujisawa, H., and Tasaka, M. (1997). Genes involved in organ separation in *Arabidopsis*: . An analysis of the cup-shaped cotyledon mutant. Plant Cell Am. Soc. Plant Physiol. **9**: 841–857.

Al-Babili, S. and Bouwmeester, H.J. (2015). Strigolactones, a novel carotenoid-derived plant hormone. Annu. Rev. Plant Biol. **66**: 161–86.

Al-Shahrour, F., Díaz-Uriarte, R., and Dopazo, J. (2004). FatiGO: A web tool for finding significant associations of gene ontology terms with groups of genes. Bioinformatics **20**: 578–580.

Alzohairy, A.M., Sabir, J.S.M., Gyulai, G., Younis, R.A.A., Jansen, R.K., and Bahieldin, A. (2014). Environmental stress activation of plant long-terminal repeat retrotransposons. Funct. Plant Biol. **41**: 557–567.

Amid, A., Lytovchenko, A., Fernie, A.R., Warren, G., and Thorlby, G.J. (2012). The sensitive to freezing3 mutation of *Arabidopsis thaliana* is a cold-sensitive allele of homomeric acetyl-CoA carboxylase that results in cold-induced cuticle deficiencies. J. Exp. Bot. **63**: 5289–5299.

Andrews, S. (2015). Babraham Bioinformatics - Trim Galore! Trim Galore! wrapper Scr. Autom. Qual. Adapt. trimming Qual. Control.

Andrews, S. (2010). FastQC: A quality control tool for high throughput sequence data. Bioinformatics: 1.

Apel, K. and Hirt, H. (2004). Reactive oxygen species: metabolism, oxidative stress, and signal transduction. Annu. Rev. Plant Biol. **55**: 373–99.

Arai, S., Watanabe, H., Kondo, H., Emori, Y., and Abe, K. (1991). Papain-inhibitory activity of oryzacystatin, a rice seed cysteine proteinase inhibitor, depends on the central Gln-Val-Val-Ala-Gly region conserved among cystatin superfamily members. J. Biochem. **109**: 294–8.

Arbaoui, M. and Link, W. (2008). Effect of hardening on frost tolerance and fatty acid composition of leaves and stems of a set of faba bean (Vicia faba L.) genotypes. Euphytica **162**: 211–219.

Arite, T., Umehara, M., Ishikawa, S., Hanada, A., Maekawa, M., Yamaguchi, S., and Kyozuka, J. (2009). D14, a strigolactone-insensitive mutant of rice, shows an accelerated outgrowth of tillers. Plant Cell Physiol. **50**: 1416–1424.

Arnaud, N. and Pautot, V. (2014). Ring the BELL and tie the KNOX: roles for TALEs in gynoecium development. Front. Plant Sci. **5**: 93.

Aroca, R., Porcel, R., and Ruiz-Lozano, J.M. (2007). How does arbuscular mycorrhizal symbiosis regulate root hydraulic properties and plasma membrane aquaporins in Phaseolus vulgaris under drought, cold or salinity stresses? New Phytol. **173**: 808–816.

Artus, N.N., Uemura, M., Steponkus, P.L., Gilmour, S.J., Lin, C., and Thomashow, M.F. (1996). Constitutive expression of the cold-regulated Arabidopsis thaliana COR15a gene affects both chloroplast and protoplast freezing tolerance. Proc. Natl. Acad. Sci. U. S. A. **93**: 13404–13409.

Arun-Chinnappa, K.S. and McCurdy, D.W. (2015). De novo assembly of a genome-wide transcriptome map of Vicia faba (L.) for transfer cell research. Front. Plant Sci. **6**: 217.

Atkins, C.A. (1987). Metabolism and translocation of fixed nitrogen in the nodulated legume. Plant Soil **100**: 157–169.

Atkinson, N.J. and Urwin, P.E. (2012). The interaction of plant biotic and abiotic stresses: from genes to the field. J. Exp. Bot. **63**: 3523–3543.

Baldos, U.L.C. and Hertel, T.W. (2014). Global food security in 2050: the role of agricultural productivity and climate change. Aust. J. Agric. Resour. Econ. **58**: 554–570.

Bao, W., Kojima, K.K., and Kohany, O. (2015). Repbase update, a database of repetitive elements in eukaryotic genomes. Mob. DNA **6**: 11.

Barton, L., Thamo, T., Engelbrecht, D., and Biswas, W.K. (2014). Does growing grain legumes or applying lime cost effectively lower greenhouse gas emissions from wheat production in a semi-arid climate? J. Clean. Prod. **83**: 194–203.

Baxter, A., Mittler, R., and Suzuki, N. (2014). ROS as key players in plant stress signalling. J. Exp. Bot. **65**: 1229–1240.

Beers, E.P., Woffenden, B.J., and Zhao, C. (2000). Plant proteolytic enzymes: Possible roles during programmed cell death. Plant Mol. Biol. **44**: 399–415.

Belenghi, B., Acconcia, F., Trovato, M., Perazzolli, M., Bocedi, A., Polticelli, F., Ascenzi, P., and Delledonne, M. (2003). AtCYS1, a cystatin from *Arabidopsis thaliana*, suppresses hypersensitive cell death. Eur. J. Biochem. **270**: 2593–2604.

Benchabane, M., Schluter, U., Vorster, J., Goulet, M.C., and Michaud, D. (2010). Plant cystatins. Biochimie **92**: 1657–1666.

Bennett, T., Sieberer, T., Willett, B., Booker, J., Luschnig, C., and Leyser, O. (2006). The Arabidopsis MAX pathway controls shoot branching by regulating auxin transport. Curr. Biol. **16**: 553–563.

Bennetzen, J.L. (2000). Transposable element contributions to plant gene and genome evolution. Plant Mol. Biol. **42**: 251–269.

Benson, D.A., Cavanaugh, M., Clark, K., Karsch-Mizrachi, I., Lipman, D.J., Ostell, J., and Sayers, E.W. (2013). GenBank. Nucleic Acids Res. **41**.

Berendsen, R.L., Pieterse, C.M.J., and Bakker, P.A.H.M. (2012). The rhizosphere microbiome and plant health. Trends Plant Sci. **17**: 478–486.

Bertioli, D.J. et al. (2016). The genome sequences of *Arachis duranensis* and *Arachis ipaensis*, the diploid ancestors of cultivated peanut. Nat Genet **48**: 438–446.

Bertrand, A., Bipfubusa, M., Castonguay, Y., Rocher, S., Szopinska-Morawska, A., Papadopoulos, Y., and Renaut, J. (2016). A proteome analysis of freezing tolerance in red clover (*Trifolium pratense* L.). BMC Plant Biol. **16**: 65.

Besserer, A., Puech-Pagès, V., Kiefer, P., Gomez-Roldan, V., Jauneau, A., Roy, S., Portais, J.C., Roux, C., Bécard, G., and Séjalon-Delmas, N. (2006). Strigolactones stimulate arbuscular

mycorrhizal fungi by activating mitochondria. PLoS Biol. **4**: 1239–1247.

Beveridge, C. a, Dun, E. A, and Rameau, C. (2009). Pea has its tendrils in branching discoveries spanning a century from auxin to strigolactones. Plant Physiol. **151**: 985–990.

Bhalerao, R., Keskitalo, J., Sterky, F., Erlandsson, R., Björkbacka, H., Birve, S.J., Karlsson, J., Gardeström, P., Gustafsson, P., Lundeberg, J., and Jansson, S. (2003). Gene expression in autumn leaves. Plant Physiol. **131**: 430–342.

Bianchi, V.J., Rubio, M., Trainotti, L., Verde, I., Bonghi, C., and Martínez-Gómez, P. (2015). Prunus transcription factors: breeding perspectives. Front. Plant Sci. **6**: 443.

Bieza, K. and Lois, R. (2001). An *Arabidopsis* mutant tolerant to lethal ultraviolet-B levels shows constitutively elevated accumulation of flavonoids and other phenolics. Plant Physiol. **126**: 1105–1115.

Bolle, C. (2004). The role of GRAS proteins in plant signal transduction and development. Planta **218**: 683–692.

Bond, D.A. and Crofton, G.R.A. (1999). History of winter beans (*Vicia faba*) in the UK. J. R. Agric. Soc. Engl. **160**: 200–209.

Bond, D.A. and Toynbee-clarke, G. (1968). Protein content of spring and winter varieties of field beans (Vicia faba L .) sown and harvested on the same dates. J. Agric. Sci. Cambridge **70**: 403–404.

Bortesi, L. and Fischer, R. (2015). The CRISPR/Cas9 system for plant genome editing and beyond. Biotechnol. Adv. **33**: 41–52.

Bowler, C., Montagu, M. V, and Inze, D. (1992). Superoxide dismutase and stress tolerance. Annu. Rev. Plant Physiol. Plant Mol. Biol. **43**: 83–116.

Boye, J., Zare, F., and Pletch, A. (2010). Pulse proteins: Processing, characterization, functional properties and applications in food and feed. Food Res. Int. **43**: 414–431.

Boyer, J.S. (1982). Plant productivity and environment. Science (80-.). **218**: 443–448.

Braun, N. et al. (2012). The pea TCP transcription factor PsBRC1 acts downstream of Strigolactones to control shoot branching. Plant Physiol. **158**: 225–38.

Bu, Q., Lv, T., Shen, H., Luong, P., Wang, J., Wang, Z., Huang, Z., Xiao, L., Engineer, C., Kim, T.H., Schroeder, J.I., and Huq, E. (2014). Regulation of drought tolerance by the F-box protein MAX2 in arabidopsis. Plant Physiol. **164**: 424–39.

Calzadilla, P.I., Maiale, S.J., Ruiz, O.A., and Escaray, F.J. (2016). Transcriptome response mediated by cold stress in *Lotus japonicus*. Front. Plant Sci. **7**: 347.

Campbell, B.A., Hallengren, J., and Hannapel, D.J. (2008). Accumulation of BEL1-like transcripts in solanaceous species. Planta **228**: 897–906.

Carpaneto, A., Ivashikina, N., Levchenko, V., Krol, E., Jeworutzki, E., Zhu, J.-K., and Hedrich, R. (2007). Cold transiently activates calcium-permeable channels in Arabidopsis mesophyll cells. Plant Physiol. **143**: 487–494.

Carrión, C., Martínez, D., Costa, M., and Guiamet, J. (2014). Senescence-associated vacuoles, a specific lytic compartment for degradation of chloroplast proteins? Plants **3**: 498–512.

Catala, R., Lopez-Cobollo, R., Mar Castellano, M., Angosto, T., Alonso, J.M., Ecker, J.R., and

Salinas, J. (2014). The *Arabidopsis* 14-3-3 Protein RARE COLD INDUCIBLE 1A Links Low-Temperature Response and Ethylene Biosynthesis to Regulate Freezing Tolerance and Cold Acclimation. Plant Cell **26**: 1–18.

Cavrak, V. V., Lettner, N., Jamge, S., Kosarewicz, A., Bayer, L.M., and Mittelsten Scheid, O. (2014). How a retrotransposon exploits the plant's heat stress response for its activation. PLoS Genet. **10**.

Chalker-Scott, L. (1999). Environmental significance of anthocyanins in plant stress responses. Photochem. Photobiol. **70**: 1–9.

Chang, W.C., Wahlqvist, M.L., Chang, H.Y., Hsu, C.C., Lee, M.S., Wang, W.S., and Hsiung, C.A. (2012). A bean-free diet increases the risk of all-cause mortality among Taiwanese women: the role of the metabolic syndrome. Public Health Nutr. **15**: 663–672.

Chen, C.C., Liang, C.S., Kao, A.L., and Yang, C.C. (2010). HHP1, a novel signalling component in the cross-talk between the cold and osmotic signalling pathways in Arabidopsis. J. Exp. Bot. **61**: 3305–3320.

Chen, Z., Zheng, Z., Huang, J., Lai, Z., and Fan, B. (2009). Biosynthesis of salicylic acid in plants. Plant Signal. Behav. **4**: 493–496.

Cheng, L., Gao, X., Li, S., Shi, M., Javeed, H., Jing, X., Yang, G., and He, G. (2010). Proteomic analysis of soybean [*Glycine max* (L.) Meer.] seeds during imbibition at chilling temperature. Mol. Breed. **26**: 1–17.

Cheng, X., Ruyter-Spira, C., and Bouwmeester, H. (2013). The interaction between strigolactones and other plant hormones in the regulation of plant development. Front. Plant Sci. **4**: 199.

Chinnusamy, V., Ohta, M., Kanrar, S., Lee, B. ha, Hong, X., Agarwal, M., and Zhu, J.K. (2003). ICE1: A regulator of cold-induced transcriptome and freezing tolerance in arabidopsis. Genes Dev. **17**: 1043–1054.

Chinnusamy, V., Zhu, J., and Zhu, J.-K. (2007). Cold stress regulation of gene expression in plants. Trends Plant Sci. **12**: 444–51.

Chu, M.H., Liu, K.L., Wu, H.Y., Yeh, K.W., and Cheng, Y.S. (2011). Crystal structure of tarocystatin-papain complex: Implications for the inhibition property of group-2 phytocystatins. Planta **234**: 243–254.

Ciardi, J.A., Deikman, J., and Orzolek, M.D. (1997). Increased ethylene synthesis enhances chilling tolerance in tomato. Physiol. Plant. **101**: 333–340.

Coleman-Derr, D. and Tringe, S.G. (2014). Building the crops of tomorrow: Advantages of symbiont-based approaches to improving abiotic stress tolerance. Front. Microbiol. **5**.

Cook, C.E., Whichard, L.P., Wall, M., Egley, G.H., Coggon, P., Luhan, P. A., and McPhail, A. T. (1972). Germination stimulants. II. Structure of strigol, a potent seed germination stimulant for witchweed (*Striga lutea*). J. Am. Chem. Soc. **94**: 6198–6199.

Crawford, A.J., McLachlan, D.H., Hetherington, A.M., and Franklin, K.A. (2012). High temperature exposure increases plant cooling capacity. Curr. Biol. **22**.

Csanad, G. and Pal, M. (2014). Two distinct plastid genome configurations and unprecedented intraspecies length variation in the accD coding region in *Medicago truncatula*. DNA Res. **21**: 417–427.

Cubero, J.I. (1974). On the Evolution of *Vicia faba* L . Theor Appl Genet **45**: 47–51.

De Cuyper, C., Fromentin, J., Yocgo, R.E., De Keyser, A., Guillotin, B., Kunert, K., Boyer, F.D., and Goormachtig, S. (2015). From lateral root density to nodule number, the strigolactone analogue GR24 shapes the root architecture of *Medicago truncatula*. J. Exp. Bot. **66**: 137–146.

Dash, S. et al. (2015). Legume information system (LegumeInfo.org): a key component of a set of federated data resources for the legume family. Nucleic Acids Res. **44**: gkv1159.

Davila, J.I., Arrieta-Montiel, M.P., Wamboldt, Y., Cao, J., Hagmann, J., Shedge, V., Xu, Y.-Z., Weigel, D., and Mackenzie, S.A. (2011). Double-strand break repair processes drive evolution of the mitochondrial genome in *Arabidopsis*. BMC Biol. **9**: 64.

Desbrosses, G.J. and Stougaard, J. (2011). Root nodulation: A paradigm for how plant-microbe symbiosis influences host developmental pathways. Cell Host Microbe **10**: 348–358.

Diaz-mendoza, M., Velasco-arroyo, B., Santamaria, M.E., González-melendi, P., Martinez, M., and Diaz, I. (2016). Plant senescence and proteolysis : two processes with one destiny. Genet. Mol. Biol. **39**: 329–338.

Dinari, A., Niazi, A., Afsharifar, A.R., and Ramezani, A. (2013). Identification of upregulated genes under cold stress in cold-tolerant chickpea using the cDNA-AFLP approach. PLoS One **8**.

Dita, M.A., Rispail, N., Prats, E., Rubiales, D., and Singh, K.B. (2006). Biotechnology approaches to overcome biotic and abiotic stress constraints in legumes. Euphytica **147**: 1–24.

Divi, U.K. and Krishna, P. (2010). Overexpression of the brassinosteroid biosynthetic gene AtDWF4 in *Arabidopsis* seeds overcomes abscisic acid-induced inhibition of germination and increases cold tolerance in transgenic seedlings. J. Plant Growth Regul. **29**: 385–393.

Dong, C.-J., Li, L., Shang, Q.-M., Liu, X.-Y., and Zhang, Z.-G. (2014). Endogenous salicylic acid accumulation is required for chilling tolerance in cucumber (*Cucumis sativus* L.) seedlings. Planta **240**: 687–700.

Dong, Y. et al. (2012). Sequencing and automated whole-genome optical mapping of the genome of a domestic goat (*Capra hircus*). Nat. Biotechnol. **31**: 135–141.

Van Doorn, W.G. and Woltering, E.J. (2004). Senescence and programmed cell death: Substance or semantics? J. Exp. Bot. **55**: 2147–2153.

Dor, E., Joel, D.M., Kapulnik, Y., Koltai, H., and Hershenhorn, J. (2011). The synthetic strigolactone GR24 influences the growth pattern of phytopathogenic fungi. Planta **234**: 419–427.

Drummond, R.S.M., Sheehan, H., Simons, J.L., Martínez-Sánchez, N.M., Turner, R.M., Putterill, J., and Snowden, K.C. (2011). The expression of petunia strigolactone pathway genes is altered as part of the endogenous developmental program. Front. Plant Sci. **2**: 115.

Du, H., Liu, H., and Xiong, L. (2013). Endogenous auxin and jasmonic acid levels are differentially modulated by abiotic stresses in rice. Front. Plant Sci. **4**: 397.

Du, H., Yang, S.-S., Liang, Z., Feng, B.-R., Liu, L., Huang, Y.-B., and Tang, Y.-X. (2012). Genome-wide analysis of the MYB transcription factor superfamily in soybean. BMC Plant Biol. **12**: 106.

Du, Y.C., Nose, A., and Wasano, K. (1999). Effects of chilling temperature on photosynthetic rates, photosynthetic enzyme activities and metabolite levels in leaves of three sugarcane species. Plant, Cell Environ. **22**: 317–324.

Duc, G., Bao, S., Baum, M., Redden, B., Sadiki, M., Suso, M.J., Vishniakova, M., and Zong, X. (2010). Diversity maintenance and use of *Vicia faba* L. genetic resources. F. Crop. Res. **115**: 270–278.

Duc, G., Moussy, F., Zong, X., and Ding, G. (1999). Single gene mutation for green cotyledons as a marker for the embryonic genotype in faba bean, *Vicia faba*. Plant Breed. **118**: 577–578.

Duc, G. and Picard, J. (1986). Note on the presence of the Sym-1 gene in *Vicia faba* hampering its symbiosis with *Rhizobium leguminosarum*. Euphytica **35**: 61–64.

Dun, E.A., Brewer, P.B., and Beveridge, C.A. (2009). Strigolactones: discovery of the elusive shoot branching hormone. Trends Plant Sci. **14**: 364–372.

Van Durme, M. and Nowack, M.K. (2016). Mechanisms of developmentally controlled cell death in plants. Curr. Opin. Plant Biol. **29**: 29–37.

Eason, J.R., West, P.J., Brummell, D.A., Watson, L.M., Somerfield, S.D., and McLachlan, A.R.G. (2014). Overexpression of the protease inhibitor BoCPI-1 in broccoli delays chlorophyll loss after harvest and causes down-regulation of cysteine protease gene expression. Postharvest Biol. Technol. **97**: 23–31.

Ellwood, S.R., Phan, H.T.T., Jordan, M., Hane, J., Torres, A.M., Avila, C.M., Cruz-Izquierdo, S., and Oliver, R.P. (2008). Construction of a comparative genetic map in faba bean (Vicia faba L.); conservation of genome structure with Lens culinaris. BMC Genomics **9**: 380.

Enneking, D. (1994). The toxicity of *Vicia* species and their utilisation as grain legumes (The University of Adelaide, AUS, Thesis).

Eremina, M., Rozhon, W., and Poppenberger, B. (2016). Hormonal control of cold stress responses in plants. Cell. Mol. Life Sci. **73**: 797–810.

Erith, A.G. (1930). The inheritance of colour, size and form of seeds, and of flower colour in Vicia faba L. Genetica **12**: 477–510.

European Comission Joint Research Centre (2011). Monitoring of agricultural resources. **2016**.

FAOSTAT (2016). United Nations Food and Agriculture Organisation Website. **2016**.

Ferguson, B.J., Indrasumunar, A., Hayashi, S., Lin, M.H., Lin, Y.H., Reid, D.E., and Gresshoff, P.M. (2010). Molecular analysis of legume nodule development and autoregulation. J. Integr. Plant Biol. **52**: 61–76.

Foley, J.A. et al. (2011). Solutions for a cultivated planet. Nature **478**: 337–342.

Foo, E. and Davies, N.W. (2011). Strigolactones promote nodulation in pea. Planta **234**: 1073–1081.

Foyer, C.H. et al. (2016). Neglecting legumes has compromised human health and sustainable food production. Nat. Plants **2**: 1–10.

Franklin, K.A. (2009). Light and temperature signal crosstalk in plant development. Curr. Opin. Plant Biol. **12**: 63–68.

Franks, F. (1985). Biophysics and biochemistry at low temperatures (Cambridge University Press: Cambridge).

Fuchs, J., Strehl, S., Brandes, A., Schweizer, D., and Schubert, I. (1998). Molecular-cytogenetic characterization of the *Vicia faba* genome - Heterochromatin differentiation, replication patterns and sequence localization. Chromosom. Res. **6**: 219–230.

Galtier, N. (2011). The intriguing evolutionary dynamics of plant mitochondrial DNA. BMC Biol. **9**: 61.

Garg, N. and Geetanjali (2007). Symbiotic nitrogen fixation in legume nodules: process and signaling. A review. Agron. Sustain. Dev. **27**: 59–68.

Gass, T., Schori, A., Fossati, A., Soldati, A., and Stamp, P. (1996). Cold tolerance of soybean (*Glycine max* (L.) Merr.) during the reproductive phase. Eur. J. Agron. **5**: 71–88.

Gaveliene, V., Novickiene, L., and Pakalniškyte, L. (2013). Effect of auxin physiological analogues on rapeseed (*Brassica napus*) cold hardening, seed yield and quality. J. Plant Res. **126**: 283–292.

Gill, S.S. and Tuteja, N. (2010). Reactive oxygen species and antioxidant machinery in abiotic stress tolerance in crop plants. Plant Physiol. Biochem. **48**: 909–930.

Giordani, T., Cossu, R.M., Mascagni, F., Marroni, F., Morgante, M., Cavallini, A., and Natali, L. (2016). Genome-wide analysis of LTR-retrotransposon expression in leaves of *Populus* × *canadensis* water-deprived plants. Tree Genet. Genomes **12**: 75.

Godfray, H.C.J., Beddington, J.R., Crute, I.R., Haddad, L., Lawrence, D., Muir, J.F., Pretty, J., Robinson, S., Thomas, S.M., and Toulmin, C. (2010). Food Security: The challenge of feeding 9 billion people. Science (80-.). **327**: 812–818.

Godfray, H.C.J. and Garnett, T. (2014). Food security and sustainable intensification. Philos. Trans. R. Soc. B-Biological Sci. **369**.

Goldberg, I., Nadler, V., and Hochman, A. (1987). Mechanism of nitrogenase switch-off by oxygen. J. Bacteriol. **169**: 874–879.

González-Rábade, N., Badillo-Corona, J.A., Aranda-Barradas, J.S., and Oliver-Salvador, M.D.C. (2011). Production of plant proteases in vivo and in vitro--a review. Biotechnol. Adv. **29**: 983–96.

Goodstein, D.M., Shu, S., Howson, R., Neupane, R., Hayes, R.D., Fazo, J., Mitros, T., Dirks, W., Hellsten, U., Putnam, N., and Rokhsar, D.S. (2012). Phytozome: A comparative platform for green plant genomics. Nucleic Acids Res. **40**.

Graham, P.H. and Vance, C.P. (2003). Legumes: Importance and constraints to greater use. Plant Physiol. **131**: 872–877.

Grandbastien, M.A. (2015). LTR retrotransposons, handy hitchhikers of plant regulation and stress response. Biochim. Biophys. Acta - Gene Regul. Mech. **1849**: 403–416.

Guo, Y. (2013). Towards systems biological understanding of leaf senescence. Plant Mol. Biol. **82**: 519–528.

Guo, Z., Tan, J., Zhuo, C., Wang, C., Xiang, B., and Wang, Z. (2014). Abscisic acid, H2O2 and nitric oxide interactions mediated cold-induced S-adenosylmethionine synthetase in *Medicago sativa* subsp. Falcata that confers cold tolerance through up-regulating polyamine oxidation. Plant Biotechnol. J. **12**: 601–612.

van Ha, C. et al. (2014). Positive regulatory role of strigolactone in plant responses to drought and salt stress. Proc. Natl. Acad. Sci. U. S. A. **111**: 851–6.

Hakam, N., Khanizadeh, S., DeEll, J.R., and Richer, C. (2000). Assessing chilling tolerance in roses using chlorophyll fluorescence. HortScience **35**: 184–186.

Han, Y.H., Khu, D.M., Torres-Jerez, I., Udvardi, M., and Monteros, M.J. (2010). Plant transcription factors as novel molecular markers for legumes. Sustain. Use Genet. Divers. Forage Turf Breed.: 421–425\n572.

Hannah, M.A., Heyer, A.G., and Hincha, D.K. (2005). A global survey of gene regulation during cold acclimation in *Arabidopsis thaliana*. PLoS Genet. **1**: 0179–0196.

Harrak, H., Azelmat, S., Baker, E.N., and Tabaeizadeh, Z. (2001). Isolation and characterization of a gene encoding a drought-induced cysteine protease in tomato (*Lycopersicon esculentum*). Genome **44**: 368–374.

Hartman, G.L., West, E.D., and Herman, T.K. (2011). Crops that feed the World 2. Soybean-worldwide production, use, and constraints caused by pathogens and pests. Food Secur. **3**: 5–17.

Hasanuzzaman, M., Nahar, K., and Fujita, M. (2009). Extreme temperature responses , oxidative stress and antioxidant defense in plants. In Abiotic Stress - Plant Responses and Applications in Agriculture, pp. 169–205.

Hecht, V., Knowles, C.L., Vander Schoor, J.K., Liew, L.C., Jones, S.E., Lambert, M.J.M., and Weller, J.L. (2007). Pea LATE BLOOMER1 is a GIGANTEA ortholog with roles in photoperiodic flowering, deetiolation, and transcriptional regulation of circadian clock gene homologs. Plant Physiol. **144**: 648–61.

Heckmann, A.B., Lombardo, F., Miwa, H., Perry, J.A., Bunnewell, S., Parniske, M., Wang, T.L., and Downie, J.A. (2006). *Lotus japonicus* nodulation requires two GRAS domain regulators, one of which is functionally conserved in a non-legume. Plant Physiol **142**: 1739–1750.

Hedden, P. and Thomas, S.G. (2012). Gibberellin biosynthesis and its regulation. Biochem. J. **444**: 11–25.

Van Heerden, P.D.R., Kiddle, G., Pellny, T.K., Mokwala, P.W., Jordaan, A., Strauss, A.J., de Beer, M., Schlüter, U., Kunert, K.J., and Foyer, C.H. (2008). Regulation of respiration and the oxygen diffusion barrier in soybean protect symbiotic nitrogen fixation from chilling-induced inhibition and shoots from premature senescence. Plant Physiol. **148**: 316–327.

Van Heerden, P.D.R., Kruger, G.H.J., Loveland, J.E., Parry, M.A.J., and Foyer, C.H. (2003). Dark chilling imposes metabolic restrictions on photosynthesis in soybean. Plant Cell Environ. **26**: 323–337.

Van Heerden, P.D.R., Strasser, R.J., and Krüger, G.H.J. (2004a). Reduction of dark chilling stress in N2-fixing soybean by nitrate as indicated by chlorophyll α fluorescence kinetics. Physiol. Plant. **121**: 239–249.

Van Heerden, P.D.R., Viljoen, M.M., De Villiers, M.F., and Krüger, G.H.J. (2004b). Limitation of photosynthetic carbon metabolism by dark chilling in temperate and tropical soybean genotypes. Plant Physiol. Biochem. **42**: 117–124.

Hekneby, M., Antolín, M.C., and Sánchez-Díaz, M. (2006). Frost resistance and biochemical changes during cold acclimation in different annual legumes. Environ. Exp. Bot. **55**: 305–314.

Herzog, H. (1987). Freezing resistance and development of faba beans as affected by ambient temperatures, soil moisture and variety. J. Agron. Crop Sci. **159**: 90–100.

Herzog, H. (1989). Influence of pre-hardening duration and dehardening temperatures on varietal freezing resistance in faba beans (Vicia faba L.). Agronomie **9**: 55–61.

Hetherington, A.M. and Brownlee, C. (2004). The generation of Ca(2+) signals in plants. Annu.

Rev. Plant Biol. **55**: 401–27.

Hirsch, S. and Oldroyd, G.E.D. (2009). GRAS-domain transcription factors that regulate plant development. Plant Signal. Behav. **4**: 698–700.

Hoagland, D.R. and Arnon, D.I. (1950). The water-culture method for growing plants without soil. Calif. Agric. Exp. Stn. **Circular 3**: 30–32.

van der Hoorn, R. A. (2008). Plant proteases: from phenotypes to molecular mechanisms. Annu. Rev. Plant Biol. **59**: 191–223.

Hu, Y., Jiang, L., Wang, F., and Yu, D. (2013). Jasmonate regulates the inducer of cbf expression-C-repeat binding factor/DRE binding factor1 cascade and freezing tolerance in *Arabidopsis*. Plant Cell **25**: 2907–24.

Hu, Y.-J., Belaghzal, H., Hsiao, W.-Y., Qi, J., Bradner, J.E., Guertin, D.A., Sif, S., and Imbalzano, A.N. (2015). Transcriptional and post-transcriptional control of adipocyte differentiation by Jumonji domain-containing protein 6. Nucleic Acids Res. **43**: 7790–804.

Huang, X., Li, J., Bao, F., Zhang, X., and Yang, S. (2010). A gain-of-function mutation in the *Arabidopsis* disease resistance gene RPP4 confers sensitivity to low temperature. Plant Physiol. **154**: 796–809.

Huber, W. et al. (2015). Orchestrating high-throughput genomic analysis with Bioconductor. Nat Methods **12**: 115–121.

Humann, J.L. et al. (2016). Cool Season Food Legume Genome Database: An up-to-date resource enabling genetics, genomics and breeding research in pea, lentil, faba bean and chickpea. In Proceedings of the International Plant and Animal Genome Conference (San Diego, CA, USA).

Hume, D.J. and Jackson, A.K.H. (1981). Frost Tolerance in Soybeans. Crop Sci. **21**: 689–692.

Huston, A.L., Krieger-Brockett, B.B., and Deming, J.W. (2000). Remarkably low temperature optima for extracellular enzyme activity from Arctic bacteria and sea ice. Environ. Microbiol. **2**: 383–388.

Hye, R.W., Jin, H.K., Hong, G.N., and Pyung, O.L. (2004). The delayed leaf senescence mutants of Arabidopsis, ore1, ore3, and ore9 are tolerant to oxidative stress. Plant Cell Physiol. **45**: 923–932.

Illumina (2014). Sequencing Methods Review (A review of publications featuring Illumina Technology). Illumina Protoc. **199**: 27.

Inci, N.E. and Toker, C. (2011). Screening and selection of faba beans (Vicia faba L.) for cold tolerance and comparison to wild relatives. Genet. Resour. Crop Evol. **58**: 1169–1175.

IPCC (2014). Summary for Policymakers.

Irving, L.J. and Robinson, D. (2006). A dynamic model of Rubisco turnover in cereal leaves. New Phytol. **169**: 493–504.

Jaglo, K.R., Kleff, S., Amundsen, K.L., Zhang, X., Haake, V., Zhang, J.Z., Deits, T., and Thomashow, M.F. (2001). Components of the *Arabidopsis* C-repeat/dehydration-responsive element binding factor cold-response pathway are conserved in *Brassica napus* and other plant species. Plant Physiol. **127**: 910–7.

Jain, M. and Khurana, J.P. (2009). Transcript profiling reveals diverse roles of auxin-responsive genes during reproductive development and abiotic stress in rice. FEBS J. **276**: 3148–3162.

Jaleel, C.A., Riadh, K., Gopi, R., Manivannan, P., Inès, J., Al-Juburi, H.J., Chang-Xing, Z., Hong-Bo, S., and Panneerselvam, R. (2009). Antioxidant defense responses: Physiological plasticity in higher plants under abiotic constraints. Acta Physiol. Plant. **31**: 427–436.

Jarillo, J.A., Leyva, A., Salinas, J., and Martinez-Zapater, J.M. (1993). Low temperature induces the accumulation of alcohol dehydrogenase mRNA in *Arabidopsis thaliana*, a chilling-tolerant Plant. Plant Physiol **101**: 833–837.

Jeon, J., Kim, N.Y., Kim, S., Kang, N.Y., Novák, O., Ku, S.J., Cho, C., Lee, D.J., Lee, E.J., Strnad, M., and Kim, J. (2010). A subset of cytokinin two-component signaling system plays a role in cold temperature stress response in Arabidopsis. J. Biol. Chem. **285**: 23371–23386.

Jiang, Y.P., Huang, L.F., Cheng, F., Zhou, Y.H., Xia, X.J., Mao, W.H., Shi, K., and Yu, J.Q. (2013). Brassinosteroids accelerate recovery of photosynthetic apparatus from cold stress by balancing the electron partitioning, carboxylation and redox homeostasis in cucumber. Physiol. Plant. **148**: 133–145.

Johnson, X., Brcich, T., Dun, E.A., Goussot, M., Haurogné, K., Beveridge, C.A., and Rameau, C. (2006). Branching genes are conserved across species. Genes controlling a novel signal in pea are coregulated by other long-distance signals. Plant Physiol. **142**: 1014–26.

Jones, P.D. and Moberg, A. (2003). Hemispheric and large-scale surface air temperature variations: An extensive revision and an update to 2001. J. Clim. **16**: 206–223.

Kagale, S., Divi, U.K., Krochko, J.E., Keller, W.A., and Krishna, P. (2007). Brassinosteroid confers tolerance in *Arabidopsis thaliana* and *Brassica napus* to a range of abiotic stresses. Planta **225**: 353–364.

Kang, Y.J. et al. (2015). Draft genome sequence of adzuki bean, Vigna angularis. Sci. Rep. **5**: 8069.

Kang, Y.J. et al. (2014). Genome sequence of mungbean and insights into evolution within Vigna species. Nat. Commun. **5**: 5443.

Kaplan, F., Kopka, J., Sung, D.Y., Zhao, W., Popp, M., Porat, R., and Guy, C.L. (2007). Transcript and metabolite profiling during cold acclimation of *Arabidopsis* reveals an intricate relationship of cold-regulated gene expression with modifications in metabolite content. Plant J. **50**: 967–981.

Kasuga, M., Liu, Q., Miura, S., Yamaguchi-Shinozaki, K., and Shinozaki, K. (1999). Improving plant drought, salt, and freezing tolerance by gene transfer of a\nsingle stress-inducible transcription factor. Nat. Biotechnol. **17**: 287–291.

Kato, Y., Murakami, S., Yamamoto, Y., Chatani, H., Kondo, Y., Nakano, T., Yokota, A., and Sato, F. (2004). The DNA-binding protease, CND41, and the degradation of ribulose-1,5-bisphosphate carboxylase/oxygenase in senescent leaves of tobacco. Planta **220**: 97–104.

Kaur, S., Pembleton, L.W., Cogan, N.O., Savin, K.W., Leonforte, T., Paull, J., Materne, M., and Forster, J.W. (2012). Transcriptome sequencing of field pea and faba bean for discovery and validation of SSR genetic markers. BMC Genomics **13**: 104.

Kelly, L.J. and Leitch, I.J. (2011). Exploring giant plant genomes with next-generation sequencing technology. Chromosom. Res. **19**: 939–953.

Kidokoro, S., Watanabe, K., Ohori, T., Moriwaki, T., Maruyama, K., Mizoi, J., Myint Phyu Sin Htwe, N., Fujita, Y., Sekita, S., Shinozaki, K., and Yamaguchi-Shinozaki, K. (2015). Soybean DREB1/CBF-type transcription factors function in heat and drought as well as cold stress-responsive gene expression. Plant J. **81**: 505–518.

Kiggundu, A. (2008). Engineering plant cysteine protease inhibitors for the transgenic control of banana weevil, *Cosmopolites sordidus* (Germar) (Coleoptera: Curculionidae) and other coleopteran insects in transgenic plants. (University of Pretoria, SA, Thesis).

Kim, D.-H., Doyle, M.R., Sung, S., and Amasino, R.M. (2009). Vernalization: winter and the timing of flowering in plants. Annu. Rev. Cell Dev. Biol. **25**: 277–299.

Kim, S.Y. and Nam, K.H. (2010). Physiological roles of ERD10 in abiotic stresses and seed germination of *Arabidopsis*. Plant Cell Rep. **29**: 203–209.

Kim, Y., Park, S., Gilmour, S.J., and Thomashow, M.F. (2013). Roles of CAMTA transcription factors and salicylic acid in configuring the low-temperature transcriptome and freezing tolerance of *Arabidopsis*. Plant J. **75**: 364–376.

Kingston-Smith, A.H., Harbinson, J., Williams, J., and Foyer, C.H. (1997). Effect of chilling on carbon assimilation, enzyme activation, and photosynthetic electron transport in the absence of photoinhibition in maize leaves. Plant Physiol. **114**: 1039–1046.

Kitazaki, K., Kubo, T., Kitazaki, K., and Kubo, T. (2010). Cost of having the largest mitochondrial genome: Evolutionary mechanism of plant mitochondrial genome. J. Bot. **2010**: 1–12.

Klein, A., Houtin, H., Rond, C., Marget, P., Jacquin, F., Boucherot, K., Huart, M., Rivière, N., Boutet, G., Lejeune-Hénaut, I., and Burstin, J. (2014). QTL analysis of frost damage in pea suggests different mechanisms involved in frost tolerance. Theor. Appl. Genet. **127**: 1319–1330.

Klose, R.J., Kallin, E.M., and Zhang, Y. (2006). JmjC-domain-containing proteins and histone demethylation. Nat. Rev. Genet. **7**: 715–27.

Knight, H., Trewavas, A.J., and Knight, M.R. (1996). Cold calcium signaling in *Arabidopsis* involves two cellular pools and a change in calcium signature after acclimation. Plant Cell **8**: 489–503.

Knott, C.M., Biddle, A.J., and McKeown, B.M. (1994). Field Bean Handbook (The PGRO: Peterborough, UK).

Kode, V., Mudd, E.A., Iamtham, S., and Day, A. (2005). The tobacco plastid accD gene is essential and is required for leaf development. Plant J. **44**: 237–244.

Kosová, K. et al. (2012). Complex phytohormone responses during the cold acclimation of two wheat cultivars differing in cold tolerance, winter Samanta and spring Sandra. J. Plant Physiol. **169**: 567–576.

Kosová, K., Vítámvás, P., Prášil, I.T., and Renaut, J. (2011). Plant proteome changes under abiotic stress - Contribution of proteomics studies to understanding plant stress response. J. Proteomics **74**: 1301–1322.

Kranner, I., Minibayeva, F. V, Beckett, R.P., and Seal, C.E. (2010). What is stress? Concepts, definitions and applications in seed science. New Phytol. **188**: 655–673.

Krüger, G.H.J., De Villiers, M.F., Strauss, A.J., de Beer, M., van Heerden, P.D.R., Maldonado, R., and Strasser, R.J. (2014). Inhibition of photosystem II activities in soybean (*Glycine max*) genotypes differing in chilling sensitivity. South African J. Bot. **95**: 85–96.

Kumar, R., Kushalappa, K., Godt, D., Pidkowich, M.S., Pastorelli, S., Hepworth, S.R., and Haughn, G.W. (2007). The Arabidopsis BEL1-LIKE HOMEODOMAIN proteins SAW1 and SAW2 act redundantly to regulate KNOX expression spatially in leaf margins. Plant Cell **19**: 2719–2735.

Kunert, K.J., Vorster, B.J., Fenta, B.A., Kibido, T., Dionisio, G., and Foyer, C.H. (2016). Drought Stress Responses in Soybean Roots and Nodules. Front. Plant Sci. **7**: 1–7.

Kunert, K.J., Van Wyk, S.G., Cullis, C.A., Vorster, B.J., and Foyer, C.H. (2015). Potential use of phytocystatins in crop improvement, with a particular focus on legumes. J. Exp. Bot. **66**: 3559–3570.

de la Vega, M.P., Torres, A.M., Cubero, J.I., and Kole, C. (2012). Genetics, genomics and breeding of cool season grain legumes C. Kole, ed (Science Publishers: Enfield, New Hampshire, USA).

Langmead, B. and Salzberg, S.L. (2012). Fast gapped-read alignment with Bowtie 2. Nat Methods **9**: 357–359.

Lareen, A., Burton, F., and Schäfer, P. (2016). Plant root-microbe communication in shaping root microbiomes. Plant Mol. Biol. **90**: 575–587.

Lassaletta, L., Billen, G., Grizzetti, B., Anglade, J., and Garnier, J. (2014). 50 year trends in nitrogen use efficiency of world cropping systems: the relationship between yield and nitrogen input to cropland. Environ. Res. Lett. **9**.

Lee, D.H. and Lee, C.B. (2000). Chilling stress-induced changes of antioxidant enzymes in the leaves of cucumber: In gel enzyme activity assays. Plant Sci. **159**: 75–85.

Lee, H.G. and Seo, P.J. (2015). The MYB96-HHP module integrates cold and abscisic acid signaling to activate the CBF-COR pathway in Arabidopsis. Plant J.: 962–977.

Levine, A., Belinghi, B., Solomon, M., and Delledonne, M. (1999). Regulation of programmed cell death in cultured soybean cells by a cysteine protease inhibitor. In Plant Biotechnology and In Vitro Biology in the 21st Century, A. Altman, M. Ziv, and S. Izhar, eds (Kluwer Academic Publishers: Jerusalem, Israel), pp. 421–424.

Li, H. (2011). A statistical framework for SNP calling, mutation discovery, association mapping and population genetical parameter estimation from sequencing data. Bioinformatics **27**: 2987–2993.

Li, X.P., Tian, A.G., Luo, G.Z., Gong, Z.Z., Zhang, J.S., and Chen, S.Y. (2005). Soybean DRE-binding transcription factors that are responsive to abiotic stresses. Theor. Appl. Genet. **110**: 1355–1362.

Liang, C., Brookhart, G., Feng, G.H., Reeck, G.R., and Kramer, K.J. (1991). Inhibition of digestive proteinases of stored grain Coleoptera by oryzacystatin, a cysteine proteinase inhibitor from rice seed. FEBS Lett. **278**: 139–142.

Lichtenthaler, H.K. (1987). Chlorophylls and carotenoids: Pigments of photosynthetic biomembranes. Methods Enzymol. **148**: 350–382.

Link, W., Balko, C., and Stoddard, F.L. (2010). Winter hardiness in faba bean: Physiology and breeding. F. Crop. Res. **115**: 287–296.

Lisch, D. (2002). Mutator transposons. Trends Plant Sci. **7**: 498–504.

Lobell, D.B., Schlenker, W., and Costa-Roberts, J. (2011). Climate trends and global crop production since 1980. Science (80-.). **333**: 616–620.

Long, N.V., Dolstra, O., Malosetti, M., Kilian, B., Graner, A., Visser, R.G.F., and van der Linden, C.G. (2013). Association mapping of salt tolerance in barley (*Hordeum vulgare* L.). Theor. Appl. Genet. **126**: 2335–2351.

López-González, L., Mouriz, A., Narro-Diego, L., Bustos, R., Martínez-Zapater, J.M., Jarillo, J. a, and Piñeiro, M. (2014). Chromatin-dependent repression of the *Arabidopsis* floral integrator genes involves plant specific PHD-containing proteins. Plant Cell **26**: 3922–38.

Lopez-Obando, M., Ligerot, Y., Bonhomme, S., Boyer, F.-D., and Rameau, C. (2015). Strigolactone biosynthesis and signaling in plant development. Development **142**: 3615–9.

López-Ráez, J.A., Kohlen, W., Charnikhova, T., Mulder, P., Undas, A.K., Sergeant, M.J., Verstappen, F., Bugg, T.D.H., Thompson, A.J., Ruyter-Spira, C., and Bouwmeester, H. (2010). Does abscisic acid affect strigolactone biosynthesis? New Phytol. **187**: 343–354.

Los, D.A. and Murata, N. (2004). Membrane fluidity and its roles in the perception of environmental signals. Biochim. Biophys. Acta - Biomembr. **1666**: 142–157.

Lucau-Danila, A., Toitot, C., Goulas, E., Blervacq, A.S., Hot, D., Bahrman, N., Sellier, H., Lejeune-Henaut, I., and Delbreil, B. (2012). Transcriptome analysis in pea allows to distinguish chilling and acclimation mechanisms. Plant Physiol. Biochem. **58**: 236–244.

Lukatkin, A.S., Brazaityte, A., Bobinas, C., and Duchovskis, P. (2012). Chilling injury in chilling-sensitive plants: a review. Agriculture **99**: 111–124.

Lukatkin, A.S. (2005). Initiation and development of chilling injury in leaves of chilling-sensitive plants. Russ. J. Plant Physiol. **52**: 542–546.

Lyons, J.M. (1973). Chilling injury in plants. Annu. Rev. Plant Physiol. **24**: 445–466.

Macas, J., Neumann, P., and Navrátilová, A. (2007). Repetitive DNA in the pea (*Pisum sativum* L.) genome: comprehensive characterization using 454 sequencing and comparison to soybean and *Medicago truncatula*. BMC Genomics **8**: 427.

Mahajan, S., Mahajan, S., Tuteja, N., and Tuteja, N. (2005). Cold, salinity and drought stresses: an overview. Arch. Biochem. Biophys. **444**: 139–58.

Mahajan, S. and Tuteja, N. (2005). Cold, salinity and drought stresses: An overview. Arch. Biochem. Biophys. **444**: 139–158.

Maqbool, A., Shafiq, S., and Lake, L. (2010). Radiant frost tolerance in pulse crops-a review. Euphytica **172**: 1–12.

Martínez, D.E., Costa, M.L., Gomez, F.M., Otegui, M.S., and Guiamet, J.J. (2008). "Senescence-associated vacuoles" are involved in the degradation of chloroplast proteins in tobacco leaves. Plant J. **56**: 196–206.

Maruyama, K., Urano, K., Yoshiwara, K., Morishita, Y., Sakurai, N., Suzuki, H., Kojima, M., Sakakibara, H., Shibata, D., Saito, K., Shinozaki, K., and Yamaguchi-Shinozaki, K. (2014). Integrated analysis of the effects of cold and dehydration on rice metabolites, phytohormones, and gene transcripts. Plant Physiol. **164**: 1759–71.

Mashiguchi, K. et al. (2011). The main auxin biosynthesis pathway in *Arabidopsis*. Proc. Natl. Acad. Sci. **108**: 18512–18517.

Masoud, S. A., Johnson, L.B., White, F.F., and Reeck, G.R. (1993). Expression of a cysteine proteinase inhibitor (oryzacystatin-I) in transgenic tobacco plants. Plant Mol. Biol. **21**: 655–63.

Massonneau, A., Condamine, P., Wisniewski, J.P., Zivy, M., and Rogowsky, P.M. (2005). Maize cystatins respond to developmental cues, cold stress and drought. Biochim. Biophys. Acta - Gene Struct. Expr. **1729**: 186–199.

Mickelbart, M. V., Hasegawa, P.M., and Bailey-Serres, J. (2015). Genetic mechanisms of abiotic stress tolerance that translate to crop yield stability. Nat. Rev. Genet. **16**: 237–251.

Mittler, R. (2002). Oxidative stress, antioxidants and stress tolerance. Trends Plant Sci. **7**: 405–410.

Mittler, R., Vanderauwera, S., Gollery, M., and Van Breusegem, F. (2004). Reactive oxygen gene network of plants. Trends Plant Sci. **9**: 490–498.

Mok, D.W.S. and Mok, M.C. (2001). Cytokinin metabolism and action. Annu. Rev. Plant Physiol. nad Plant Mol. Biol. **52**: 89–118.

Monroy, A.F., Sangwan, V., and Dhindsa, R.S. (1998). Low temperature signal transduction during cold acclimation: Protein phosphatase 2A as an early target for cold-inactivation. Plant J. **13**: 653–660.

Moreno, J., Garcia-Murria, M.J., and Marin-Navarro, J. (2008). Redox modulation of Rubisco conformation and activity through its cysteine residues. In Journal of Experimental Botany, pp. 1605–1614.

Murata, N. and Los, D. A. (1997). Membrane fluidity and temperature perception. Plant Physiol. **115**: 875–879.

Nagano, Y., Furuhashi, H., Inaba, T., and Sasaki, Y. (2001). A novel class of plant-specific zinc-dependent DNA-binding protein that binds to A/T-rich DNA sequences. Nucleic Acids Res. **29**: 4097–105.

Nagata, K., Kudo, N., Keiko, A., Arai, S., and Tanokura, M. (2000). Three-dimensional solution structure of oryzacystatin-I , a cysteine proteinase. Biochemistry **39**: 14753–14760.

Nair, J.S. and Ramaswamy, N.K. (2004). Chloroplast Proteases. Biol. Plant. **48**: 321–326.

Nakashima, K., Yamaguchi-Shinozaki, K., and Shinozaki, K. (2014). The transcriptional regulatory network in the drought response and its crosstalk in abiotic stress responses including drought, cold, and heat. Front. Plant Sci. **5**: 170.

Naya, L., Ladrera, R., Ramos, J., González, E.M., Arrese-Igor, C., Minchin, F.R., and Becana, M. (2007). The response of carbon metabolism and antioxidant defenses of alfalfa nodules to drought stress and to the subsequent recovery of plants. Plant Physiol. **144**: 1104–1114.

Negruk, V. (2013). Mitochondrial genome sequence of the legume *Vicia faba*. Front. Plant Sci. **4**: 128.

Nothlings, U. et al. (2008). Intake of vegetables, legumes, and fruit, and risk for all-cause, cardiovascular, and cancer mortality in a European diabetic population. J. Nutr. **138**: 775–781.

Nuruzzaman, M., Sharoni, A.M., and Kikuchi, S. (2013). Roles of NAC transcription factors in the regulation of biotic and abiotic stress responses in plants. Front. Microbiol. **4**.

O'Sullivan, D.M. and Angra, D. (2016). Advances in faba bean genetics and genomics. Front. Genet. **7**: 1–12.

Olesen, J.E. and Bindi, M. (2002). Consequences of climate change for European agricultural productivity, land use and policy. Eur. J. Agron. **16**: 239–262.

Olesen, J.E., Trnka, M., Kersebaum, K.C., Skjelvag, A.O., Seguin, B., Peltonen-Sainio, P., Rossi, F., Kozyra, J., and Micale, F. (2011). Impacts and adaptation of European crop production systems to climate change. Eur. J. Agron. **34**: 96–112.

Osmond, C.B., Austin, M.P., Berry, J.A., Billings, W.D., Boyer, J.S., Dacey, J.W.H., Nobel, P.S., Smith, S.D., and Winner, W.E. (1987). Stress physiology and the distribution of plants. Bioscience **37**: 38–48.

Otegui, M.S., Noh, Y.S., Martínez, D.E., Vila Petroff, M.G., Staehelin, L.A., Amasino, R.M., and Guiamet, J.J. (2005). Senescence-associated vacuoles with intense proteolytic activity develop in leaves of *Arabidopsis* and soybean. Plant J. **41**: 831–844.

Palma, J.M., Sandalio, L.M., Javier Corpas, F., Romero-Puertas, M.C., McCarthy, I., and Del Rio, L.A. (2002). Plant proteases, protein degradation, and oxidative stress: Role of peroxisomes. In Plant Physiology and Biochemistry, pp. 521–530.

Pandey, A., Sharma, M., and Pandey, G.K. (2016). Emerging roles of strigolactones in plant responses to stress and development. Front. Plant Sci. **7**: 1–17.

Pang, T., Ye, C.-Y., Xia, X., and Yin, W. (2013). *De novo* sequencing and transcriptome analysis of the desert shrub, *Ammopiptanthus mongolicus*, during cold acclimation using Illumina/Solexa. BMC Genomics **14**: 488.

Parniske, M. (2008). Arbuscular mycorrhiza: the mother of plant root endosymbioses. Nat. Rev. Microbiol. **6**: 763–75.

Parween, S., Nawaz, K., Roy, R., Pole, A.K., Venkata Suresh, B., Misra, G., Jain, M., Yadav, G., Parida, S.K., Tyagi, A.K., Bhatia, S., and Chattopadhyay, D. (2015). An advanced draft genome assembly of a desi type chickpea (*Cicer arietinum* L.). Sci. Rep. **5**: 12806.

Paszkowski, J. (2015). Controlled activation of retrotransposition for plant breeding. Curr. Opin. Biotechnol. **32**: 200–206.

Patro, R., Duggal, G., and Kingsford, C. (2015). Salmon: Accurate, versatile and ultrafast quantification from RNA-seq data using lightweight-alignment. bioRxiv: 21592.

Patto, M.C. V., Torres, A.M., Koblizkova, A., Macas, J., and Cubero, J.I. (1999). Development of a genetic composite map of Vicia faba using F2 populations derived from trisomic plants. Theor. Appl. Genet. **98**: 736–743.

Pearce, R. (2001). Plant freezing and damage. Ann. Bot. **87**: 417–424.

Penfield, S. (2008). Temperature perception and signal transduction in plants. New Phytol. **179**: 615–628.

Peng, H. and Zhang, J. (2009). Plant genomic DNA methylation in response to stresses: Potential applications and challenges in plant breeding. Prog. Nat. Sci. **19**: 1037–1045.

Philippot, L., Raaijmakers, J.M., Lemanceau, P., and van der Putten, W.H. (2013). Going back to the roots: the microbial ecology of the rhizosphere. Nat. Rev. Microbiol. **11**: 789–799.

Prasad, D.H., Wibig, J., and Rzepa, M. (2010). Numerical modeling of the severe cold weather event over central Europe (January 2006). Adv. Meteorol.

Prins, A., van Heerden, P.D.R., Olmos, E., Kunert, K.J., and Foyer, C.H. (2008). Cysteine proteinases regulate chloroplast protein content and composition in tobacco leaves: a model for dynamic interactions with ribulose-1,5-bisphosphate carboxylase/oxygenase (Rubisco) vesicular bodies. J. Exp. Bot. **59**: 1935–50.

Qin, F., Shinozaki, K., and Yamaguchi-Shinozaki, K. (2011). Achievements and challenges in understanding plant abiotic stress responses and tolerance. Plant Cell Physiol. **52**: 1569–1582.

Quain, M.D., Makgopa, M.E., Cooper, J.W., Kunert, K.J., and Foyer, C.H. (2015). Ectopic phytocystatin expression increases nodule numbers and influences the responses of soybean (*Glycine max*) to nitrogen deficiency. Phytochemistry **112**: 179–187.

Quain, M.D., Makgopa, M.E., Márquez-Garcáa, B., Comadira, G., Fernandez-Garcia, N., Olmos, E., Schnaubelt, D., Kunert, K.J., and Foyer, C.H. (2014). Ectopic phytocystatin expression leads to enhanced drought stress tolerance in soybean (*Glycine max*) and *Arabidopsis thaliana* through effects on strigolactone pathways and can also result in improved seed traits. Plant Biotechnol. J. **12**: 903–913.

R Core Team (2015). R: A Language and Environment for Statistical Computing. R Found. Stat. Comput. Vienna Austria **0**: {ISBN} 3-900051-07-0.

Ramirez-Parra, E., Fründt, C., and Gutierrez, C. (2003). A genome-wide identification of E2F-regulated genes in Arabidopsis. Plant J. **33**: 801–811.

Ramsay, G. (1997). Inheritance and linkage of a gene for testa-imposed seed dormancy in faba bean (Vicia faba L.). Plant Breed. **116**: 287–289.

Ramundo, S., Rahire, M., Schaad, O., and Rochaix, J.-D. (2013). Repression of essential chloroplast genes reveals new signaling pathways and regulatory feedback loops in chlamydomonas. Plant Cell **25**: 167–86.

Rasband, W. (2015). ImageJ [Software]. U. S. Natl. Institutes Heal. Bethesda, Maryland, USA: //imagej.nih.gov/ij/.

Ray, D.K., Mueller, N.D., West, P.C., and Foley, J.A. (2013). Yield trends are insufficient to double global crop production by 2050. PLoS One **8**.

Ray, H. and Georges, F. (2010). A genomic approach to nutritional, pharmacological and genetic issues of faba bean (Vicia faba): Prospects for genetic modifications. GM Crops **1**: 99–106.

Reichmann, J., Crichton, J.H., Madej, M.J., Taggart, M., Gautier, P., Garcia-Perez, J.L., Meehan, R.R., and Adams, I.R. (2012). Microarray analysis of LTR retrotransposon silencing identifies Hdac1 as a regulator of retrotransposon expression in mouse embryonic stem cells. PLoS Comput. Biol. **8**.

Rhodes, D., Sims, A.P., and Folkes, B.F. (1980). Pathway of ammonia assimilation in illuminated Lemna minor. Phytochemistry **19**: 357–365.

Richards, R.A. (2000). Selectable traits to increase crop photosynthesis and yield of grain crops. J. Exp. Bot. **51**: 447–58.

Riechmann, J.L. et al. (2000). Arabidopsis transcription factors: genome-wide comparative analysis among eukaryotes. Science **290**: 2105–2110.

Ritchie, M.E., Phipson, B., Wu, D., Hu, Y., Law, C.W., Shi, W., and Smyth, G.K. (2015). Limma powers differential expression analyses for RNA-sequencing and microarray studies. Nucleic Acids Res. **43**: e47.

Rivas-San Vicente, M. and Plasencia, J. (2011). Salicylic acid beyond defence: Its role in plant growth and development. J. Exp. Bot. **62**: 3321–3338.

Robinson, M.D., McCarthy, D.J., and Smyth, G.K. (2010). edgeR: A bioconductor package for differential expression analysis of digital gene expression data. Bioinformatics **26**: 139–40.

Rousseau-Gueutin, M., Huang, X., Higginson, E., Ayliffe, M., Day, A., and Timmis, J.N. (2013). Potential functional replacement of the plastidic acetyl-CoA carboxylase subunit (*acc*D) gene by

recent transfers to the nucleus in some angiosperm lineages. Plant Physiol. **161**: 1918–29.

Rout, M.E. and Southworth, D. (2013). The root microbiome influences scales from molecules to ecosystems: The unseen majority. Am. J. Bot. **100**: 1689–1691.

Roy, S. (2016). Function of MYB domain transcription factors in abiotic stress and epigenetic control of stress response in plant genome. Plant Signal. Behav. **11**: e1117723.

Ruelland, E. and Zachowski, A. (2010). How plants sense temperature. Environ. Exp. Bot. **69**: 225–232.

Ruiz-Lozano, J.M., Aroca, R., Zamarreno, A.M., Molina, S., Andreo-Jimenez, B., Porcel, R., Garcia-Mina, J.M., Ruyter-Spira, C., and Lopez-Raez, J.A. (2016). Arbuscular mycorrhizal symbiosis induces strigolactone biosynthesis under drought and improves drought tolerance in lettuce and tomato. Plant, Cell Environ. **39**: 441–452.

Ruyter-Spira, C., Kohlen, W., Charnikhova, T., van Zeijl, A., van Bezouwen, L., de Ruijter, N., Cardoso, C., Lopez-Raez, J.A., Matusova, R., Bours, R., Verstappen, F., and Bouwmeester, H. (2011). Physiological effects of the synthetic strigolactone analog GR24 on root system architecture in *Arabidopsis*: another belowground role for strigolactones? Plant Physiol **155**: 721–34.

Sabir, J., Schwarz, E., Ellison, N., Zhang, J., Baeshen, N.A., Mutwakil, M., Jansen, R., and Ruhlman, T. (2014). Evolutionary and biotechnology implications of plastid genome variation in the inverted-repeat-lacking clade of legumes. Plant Biotechnol. J. **12**: 743–754.

Sakakibara, H. (2006). Cytokinins: activity, biosynthesis, and translocation. Annu. Rev. Plant Biol. **57**: 431–449.

Sallam, A. and Martsch, R. (2015). Association mapping for frost tolerance using multi-parent advanced generation inter-cross (MAGIC) population in faba bean (Vicia faba L.). Genetica **143**: 501–514.

Sanders, D., Pelloux, J., Brownlee, C., and Harper, J.F. (2002). Calcium at the crossroads of signaling. Plant Cell **14 Suppl**: S401–S417.

Sanghera, G.S., Wani, S.H., Hussain, W., and Singh, N.B. (2011). Engineering cold stress tolerance in crop plants. Curr. Genomics **12**: 30–43.

Sasse, J.M. (2003). Physiological actions of brassinosteroids: An update. J. Plant Growth Regul. **22**: 276–288.

Sato, S. et al. (2008). Genome structure of the legume, *Lotus japonicus*. DNA Res. **15**: 227–239.

Schmidt, A. and Kunert, K.J. (1986). Lipid peroxidation in higher plants : The role of glutathione reductase. Plant Physiol. **82**: 700–702.

Schmittgen, T.D. and Livak, K.J. (2008). Analyzing real-time PCR data by the comparative CT method. Nat. Protoc. **3**: 1101–1108.

Schmutz, J. et al. (2014). A reference genome for common bean and genome-wide analysis of dual domestications. Nat. Genet. **46**: 707–13.

Schmutz, J. et al. (2010). Genome sequence of the palaeopolyploid soybean. Nature **463**: 178–83.

Schnable, P.S. et al. (2009). The B73 maize genome: complexity, diversity, and dynamics. Science **326**: 1112–5.

Schwechheimer, C. (2012). Gibberellin signaling in plants – The extended version. Front. Plant Sci. **2**: 1–7.

Scott, I.M., Clarke, S.M., Wood, J.E., and Mur, L. a J. (2004). Salicylate accumulation inhibits growth at chilling temperature in *Arabidopsis*. Plant Physiol. **135**: 1040–1049.

Seki, M. et al. (2002). Monitoring the expression profiles of 7000 *Arabidopsis* genes under drought, cold and high-salinity stresses using a full-length cDNA microarray. Plant J. **31**: 279–292.

Shankar, R., Bhattacharjee, A., and Jain, M. (2016). Transcriptome analysis in different rice cultivars provides novel insights into desiccation and salinity stress responses. Sci. Rep. **6**: 23719.

Shao, H., Wang, H., and Tang, X. (2015). NAC transcription factors in plant multiple abiotic stress responses: progress and prospects. Front. Plant Sci. **6**: 902.

Sheldon, C.C., Rouse, D.T., Finnegan, E.J., Peacock, W.J., and Dennis, E.S. (2000). The molecular basis of vernalization: the central role of FLOWERING LOCUS C (FLC). Proc. Natl. Acad. Sci. U. S. A. **97**: 3753–3758.

Shi, H., Ye, T., Zhong, B., Liu, X., Jin, R., and Chan, Z. (2014). AtHAP5A modulates freezing stress resistance in *Arabidopsis* through binding to CCAAT motif of AtXTH21. New Phytol. **203**: 554–567.

Shi, Y., Tian, S., Hou, L., Huang, X., Zhang, X., Guo, H., and Yang, S. (2012). Ethylene signaling negatively regulates freezing tolerance by repressing expression of CBF and type-A ARR genes in *Arabidopsis*. Plant Cell **24**: 2578–2595.

Shibasaki, K., Uemura, M., Tsurumi, S., and Rahman, A. (2009). Auxin response in *Arabidopsis* under cold stress: underlying molecular mechanisms. Plant Cell **21**: 3823–38.

Siddique, K.H.M., Johansen, C., Turner, N.C., Jeuffroy, M.H., Hashem, A., Sakar, D., Gan, Y.T., and Alghamdi, S.S. (2012). Innovations in agronomy for food legumes. A review. Agron. Sustain. Dev. **32**: 45–64.

Simpson, J.T., Wong, K., Jackman, S.D., Schein, J.E., Jones, S.J.M., and Birol, I. (2009). ABySS: A parallel assembler for short read sequence data. Genome Res. **19**: 1117–1123.

Singh, K.B., Malhotra, R.S., and Saxena, M.C. (1993). Relationship between cold severity and yield loss in chickpea (*Cicer Arietinum* L). J. Agron. Crop Sci. **170**: 121–127.

Sinha, A.K., Jaggi, M., Raghuram, B., and Tuteja, N. (2011). Mitogen-activated protein kinase signaling in plants under abiotic stress. Plant Signal. Behav. **6**: 196–203.

Sjodin, J. (1970). Induced asynaptic mutants in Vicia faba L. Hereditas **66**: 215–232.

Sjodin, J. (1971). Induced morphological variation in Vicia faba L. Hereditas **67**: 155–180.

Smaczniak, C., Immink, R.G.H., Angenent, G.C., and Kaufmann, K. (2012). Developmental and evolutionary diversity of plant MADS-domain factors: insights from recent studies. Development **139**: 3081–3098.

So, H.-A., Choi, S.J., Chung, E., and Lee, J.H. (2015). Molecular characterization of stress-inducible PLATZ gene from soybean (*Glycine max* L.). Plant Omics **8**: 479–484.

Soares, A.S., Driscoll, S.P., Olmos, E., Harbinson, J., Arrabaça, M.C., and Foyer, C.H. (2008). Adaxial/abaxial specification in the regulation of photosynthesis and stomatal opening with respect to light orientation and growth with CO2 enrichment in the C4 species *Paspalum*

dilatatum. New Phytol. **177**: 186–198.

Solomon, M., Belenghi, B., Delledonne, M., Menachem, E., and Levine, A. (1999). The involvement of cysteine proteases and protease inhibitor genes in the regulation of programmed cell death in plants. Plant Cell **11**: 431–44.

Soneson, C., Love, M.I., and Robinson, M.D. (2015). Differential analyses for RNA-seq: transcript-level estimates improve gene-level inferences. F1000Research **4**: 1521.

Souer, E., Van Houwelingen, A., Kloos, D., Mol, J., and Koes, R. (1996). The no apical meristem gene of petunia is required for pattern formation in embryos and flowers and is expressed at meristem and primordia boundaries. Cell **85**: 159–170.

Spaink, H.P. (2000). Root nodulation and infection factors produced by rhizobial bacteria. Annu. Rev. Microbiol. **54**: 257–288.

Sprent, J.I., Ardley, J.K., and James, E.K. (2013). From north to south: A latitudinal look at legume nodulation processes. South African J. Bot. **89**: 31–41.

Sprent, J.I. and James, E.K. (2007). Legume evolution: Where do nodules and mycorrhizas fit in? Plant Physiol. **144**: 575–581.

Stacklies, W., Redestig, H., Scholz, M., Walther, D., and Selbig, J. (2007). pcaMethods - A bioconductor package providing PCA methods for incomplete data. Bioinformatics **23**: 1164–1167.

Steinkellner, S., Lendzemo, V., Langer, I., Schweiger, P., Khaosaad, T., Toussaint, J.P., and Vierheilig, H. (2007). Flavonoids and strigolactones in root exudates as signals in symbiotic and pathogenic plant-fungus interactions. Molecules **12**: 1290–1306.

Stewart Lilley, J.L., Gan, Y., Graham, I.A., and Nemhauser, J.L. (2013). The effects of DELLAs on growth change with developmental stage and brassinosteroid levels. Plant J. **76**: 165–173.

Stracke, R., Werber, M., and Weisshaar, B. (2001). The R2R3-MYB gene family in Arabidopsis thaliana. Curr. Opin. Plant Biol. **4**: 447–456.

Strauss, A.J., Krüger, G.H.J., Strasser, R.J., and Heerden, P.D.R. Van (2006). Ranking of dark chilling tolerance in soybean genotypes probed by the chlorophyll a fluorescence transient O-J-I-P. Environ. Exp. Bot. **56**: 147–157.

Strauss, A.J., Krüger, G.H.J., Strasser, R.J., and Van Heerden, P.D.R. (2007). The role of low soil temperature in the inhibition of growth and PSII function during dark chilling in soybean genotypes of contrasting tolerance. Physiol. Plant. **131**: 89–105.

Subramanian, P., Kim, K., Krishnamoorthy, R., Mageswari, A., Selvakumar, G., and Sa, T. (2016). Cold stress tolerance in psychrotolerant soil bacteria and their conferred chilling resistance in tomato (*Solanum lycopersicum* Mill.) under low temperatures. PLoS One **11**: e0161592.

Suzuki, N. and Mittler, R. (2006). Reactive oxygen species and temperature stresses: A delicate balance between signaling and destruction. Physiol. Plant. **126**: 45–51.

Tahara, E.B., Barros, M.H., Oliveira, G. a, Netto, L.E.S., and Kowaltowski, A.J. (2007). Dihydrolipoyl dehydrogenase as a source of reactive oxygen species inhibited by caloric restriction and involved in Saccharomyces cerevisiae aging. FASEB J. **21**: 274–283.

Tan, Y., Qin, Y., Li, Y., Li, M., and Ma, F. (2014). Overexpression of MpGR-RBP1, a glycine-rich RNA-binding protein gene from *Malus prunifolia* (Willd.) Borkh., confers salt stress tolerance

and protects against oxidative stress in *Arabidopsis*. Plant Cell. Tissue Organ Cult. **119**: 635–646.

Tang, H., Lyons, E., and Town, C.D. (2015). Optical mapping in plant comparative genomics. Gigascience **4**: 3.

Tausz, M., Šircelj, H., and Grill, D. (2004). The glutathione system as a stress marker in plant ecophysiology: Is a stress-response concept valid? In Journal of Experimental Botany, pp. 1955–1962.

Thomashow, M.F. (1999). Plant cold acclimation: Freezing tolerance genes and regulatory mechanisms. Annu. Rev. Plant Physiol. Plant Mol. Biol. **50**: 571–599.

Thomashow, M.F. (2001). So what's new in the field of plant cold acclimation? Lots! Plant Physiol. **125**: 89–93.

Thorlby, G., Fourrier, N., and Warren, G. (2004). The SENSITIVE TO FREEZING2 gene, required for freezing tolerance in Arabidopsis thaliana, encodes a beta-glucosidase. Plant Cell **16**: 2192–2203.

Thorvaldsdóttir, H., Robinson, J.T., and Mesirov, J.P. (2013). Integrative Genomics Viewer (IGV): High-performance genomics data visualization and exploration. Brief. Bioinform. **14**: 178–192.

Tian, Y., Zhang, H., Pan, X., Chen, X., Zhang, Z., Lu, X., and Huang, R. (2011). Overexpression of ethylene response factor TERF2 confers cold tolerance in rice seedlings. Transgenic Res. **20**: 857–866.

Torres, A.M., Avila, C.M., Gutierrez, N., Palomino, C., Moreno, M.T., and Cubero, J.I. (2010). Marker-assisted selection in faba bean (Vicia faba L.). F. Crop. Res. **115**: 243–252.

Torres, A.M., Weeden, N.F., and Martín, A. (1993). Linkage among isozyme, RFLP and RAPD markers in Vicia faba. Theor. Appl. Genet. **85**: 937–945.

Toyooka, K., Okamoto, T., and Minamikawa, T. (2000). Mass transport of proform of a KDEL-tailed cysteine proteinase (SH-EP) to protein storage vacuoles by endoplasmic reticulum-derived vesicle is involved in protein mobilization in germinating seeds. J. Cell Biol. **148**: 453–463.

Treangen, T.J. and Salzberg, S.L. (2012). Repetitive DNA and next-generation sequencing: Computational challenges and solutions. Nat. Rev. Genet. **13**: 36–46.

Trimarchi, J.M. and Lees, J. a (2002). Sibling rivalry in the E2F family. Nat. Rev. Mol. Cell Biol. **3**: 11–20.

Trinidad, T.P., Mallillin, A.C., Loyola, A.S., Sagum, R.S., and Encabo, R.R. (2010). The potential health benefits of legumes as a good source of dietary fibre. Br. J. Nutr. **103**: 569–574.

Udvardi, M.K., Kakar, K., Wandrey, M., Montanari, O., Murray, J., Andriankaja, A., Zhang, J.-Y., Benedito, V., Hofer, J.M.I., Chueng, F., and Town, C.D. (2007). Legume Transcription Factors: Global Regulators of Plant Development and Response to the Environment. Plant Physiol. **144**: 538–549.

United Nations Department of Economic and Social Affairs Population Division (2015). World population prospects: The 2015 revision, key findings and advance tables.

Unterholzner, S.J., Rozhon, W., Papacek, M., Ciomas, J., Lange, T., Kugler, K.G., Mayer, K.F., Sieberer, T., and Poppenberger, B. (2015). brassinosteroids are master regulators of

gibberellin biosynthesis in *Arabidopsis*. Plant Cell: 1–13.

Varshney, R.K. et al. (2013). Draft genome sequence of chickpea (*Cicer arietinum*) provides a resource for trait improvement. Nat Biotechnol **31**: 240–246.

Varshney, R.K. et al. (2011). Draft genome sequence of pigeonpea (*Cajanus cajan*), an orphan legume crop of resource-poor farmers. Nat. Biotechnol. **30**: 83–89.

De Vega, J.J. et al. (2015). Red clover (*Trifolium pratense* L.) draft genome provides a platform for trait improvement. Sci. Rep. **5**: 17394.

Vickers, C.E., Gershenzon, J., Lerdau, M.T., and Loreto, F. (2009). A unified mechanism of action for volatile isoprenoids in plant abiotic stress. Nat. Chem. Biol. **5**: 283–291.

Vierstra, R.D. (1996). Proteolysis in plants: mechanisms and functions. Plant Mol. Biol. **32**: 275–302.

Vigh, L., Horvàth, I., van Hasselt, P.R., and Kuiper, P.J. (1985). Effect of frost hardening on lipid and fatty acid composition of chloroplast thylakoid membranes in two wheat varieties of contrasting hardiness. Plant Physiol. **79**: 756–9.

Vitousek, P.M. (1994). Beyond global warming - Ecology and global change. Ecology **75**: 1861–1876.

Vranová, E., Coman, D., and Gruissem, W. (2012). Structure and dynamics of the isoprenoid pathway network. In Molecular Plant, pp. 318–333.

Vranová, E., Hirsch-Hoffmann, M., and Gruissem, W. (2011). AtIPD: A curated database of *Arabidopsis* isoprenoid pathway models and genes for isoprenoid network analysis. Plant Physiol. **156**: 1655–1660.

Van der Vyver, C., Schneidereit, J., Driscoll, S., Turner, J., Kunert, K., and Foyer, C.H. (2003a). Oryzacystatin I expression in transformed tobacco produces a conditional growth phenotype and enhances chilling tolerance. Plant Biotechnol. J. **1**: 101–112.

Van der Vyver, C., Schneidereit, J., Driscoll, S., Turner, J., Kunert, K., and Foyer, C.H. (2003b). Oryzacystatin I expression in transformed tobacco produces a conditional growth phenotype and enhances chilling tolerance. Plant Biotechnol. J. **1**: 101–112.

Wang, W., Vinocur, B., and Altman, A. (2003). Plant responses to drought, salinity and extreme temperatures: Towards genetic engineering for stress tolerance. Planta **218**: 1–14.

Wang, Y., Yang, J., and Yi, J. (2012). Redox sensing by proteins: oxidative modifications on cysteines and the consequent events. Antioxid. Redox Signal. **16**: 649–57.

Wanner, H., Bronnimann, S., Casty, C., Gyalistras, D., Luterbacher, J., Schmutz, C., Stephenson, D.B., and Xoplaki, E. (2001). North Atlantic Oscillation - Concepts and studies. Surv. Geophys. **22**: 321–382.

Warren, G.J. (1998). Cold stress: Manipulating freezing tolerance in plants. Curr. Biol. **8**: R514–R516.

Wassink, E.C. and Stolwijk, J.A.J. (1956). Effects of light quality onplant growth. Annu. Rev. Plant Physiol. Plant Mol. Biol. **7**: 373–400.

Watling, J.R., Robinson, S. a, and Seymour, R.S. (2006). Contribution of the alternative pathway to respiration during thermogenesis in flowers of the sacred lotus. Plant Physiol. **140**: 1367–1373.

Webb, A. et al. (2016). A SNP-based consensus genetic map for synteny-based trait targeting in faba bean (Vicia faba L.). Plant Biotechnol. J. **14**: 177–185.

Weisshaar, B. and Jenkins, G.I. (1998). Phenylpropanoid biosynthesis and its regulation. Corresp. Gareth I Jenkins Curr. Opin. Plant Biol. **1**: 251–257.

Weller, J.L. and Ortega, R. (2015). Genetic control of flowering time in legumes. Front. Plant Sci. **6**: 207.

Wicker, T. et al. (2007). A unified classification system for eukaryotic transposable elements. Nat. Rev. Genet. **8**: 973–982.

Wickham, H. (2009). ggplot2: Elegant graphics for data analysis (New York).

Winfield, M.O., Lu, C.G., Wilson, I.D., Coghill, J.A., and Edwards, K.J. (2010). Plant responses to cold: transcriptome analysis of wheat. Plant Biotechnol. J. **8**: 749–771.

Wojciechowski, M.F., Lavin, M., and Sanderson, M.J. (2004). A phylogeny of legumes (Leguminosae) based on analysis of the plastid matK gene resolves many well-supported subclades within the family. Am. J. Bot. **91**: 1846–1862.

Woo, H.R., Chung, K.M., Park, J.H., Oh, S.A., Ahn, T., Hong, S.H., Jang, S.K., and Nam, H.G. (2001). ORE9, an F-box protein that regulates leaf senescence in Arabidopsis. Plant Cell **13**: 1779–1790.

Wood, D.E. and Salzberg, S.L. (2014). Kraken: ultrafast metagenomic sequence classification using exact alignments. Genome Biol. **15**: R46.

Xia, X.-J., Wang, Y.-J., Zhou, Y.-H., Tao, Y., Mao, W.-H., Shi, K., Asami, T., Chen, Z., and Yu, J.-Q. (2009). Reactive oxygen species are involved in brassinosteroid-induced stress tolerance in cucumber. Plant Physiol. **150**: 801–814.

Xin, Z. and Browse, J. (2000). Cold comfort farm: the acclimation of plants to freezing temperatures. Plant Cell Environ. **23**: 893–902.

Xin, Z. and Browse, J. (1998). Eskimo1 mutants of *Arabidopsis* are constitutively freezing-tolerant. Proc. Natl. Acad. Sci. U. S. A. **95**: 7799–7804.

Xu, J.H., Liu, Q., Hu, W., Wang, T., Xue, Q., and Messing, J. (2015). Dynamics of chloroplast genomes in green plants. Genomics **106**: 221–231.

Xue, L., Cui, H., Buer, B., Vijayakumar, V., Delaux, P.-M., Junkermann, S., and Bucher, M. (2015). Network of GRAS transcription factors involved in the control of arbuscule development in *Lotus japonicus*. Plant Physiol. **167**: 854–71.

Yamada, Y. and Umehara, M. (2015). Possible roles of strigolactones during leaf senescence. Plants **4**: 664–677.

Yamaguchi-Shinozaki, K. and Shinozaki, K. (2006). Transcriptional regulatory networks in cellular responses and tolerance to dehydration and cold stresses. Annu. Rev. Plant Biol. **57**: 781–803.

Yamasaki, Y. and Randall, S.K. (2016). Functionality of soybean CBF/DREB1 transcription factors. Plant Sci. **246**: 80–90.

Yamazaki, T., Kawamura, Y., and Uemura, M. (2009). Extracellular freezing-induced mechanical stress and surface area regulation on the plasma membrane in cold-acclimated plant cells. Plant Signal. Behav. **4**: 231–233.

Yang, D.H., Andersson, B., Aro, E.M., and Ohad, I. (2001). The redox state of the plastoquinone pool controls the level of the light-harvesting chlorophyll a/b binding protein complex II (LHC II) during photoacclimation: Cytochrome b6f deficient *Lemna perpusilla* plants are locked in a state of high-light acclimat. Photosynth. Res. **68**: 163–174.

Yang, H., Tao, Y., Zheng, Z., Zhang, Q., Zhou, G., Sweetingham, M.W., Howieson, J.G., and Li, C. (2013). Draft genome sequence, and a sequence-defined genetic linkage map of the legume crop species *Lupinus angustifolius* L. PLoS One **8**.

Yang, T., Bao, S., Ford, R., Jia, T., Guan, J., He, Y., Sun, X., Jiang, J., Hao, J., Zhang, X., and Zong, X. (2012). High-throughput novel microsatellite marker of faba bean via next generation sequencing. BMC Genomics **13**: 602.

Yang, T., Chaudhuri, S., Yang, L., Du, L., and Poovaiah, B.W. (2010). A calcium/calmodulin-regulated member of the receptor-like kinase family confers cold tolerance in plants. J. Biol. Chem. **285**: 7119–7126.

Yao, C. and Finlayson, S.A. (2015). Abscisic acid is a general negative regulator of *Arabidopsis* axillary bud growth. Plant Physiol. **169**: 611–26.

Young, N.D. et al. (2011). The *Medicago* genome provides insight into the evolution of rhizobial symbioses. Nature **480**: 520–524.

Young, N.D., Mudge, J., and Ellis, T.H.N. (2003). Legume genomes: More than peas in a pod. Curr. Opin. Plant Biol. **6**: 199–204.

Zhang, H., Mao, J., Liu, F., and Zeng, F. (2012a). Expression of a nematode symbiotic bacterium-derived protease inhibitor protein in tobacco enhanced tolerance against *Myzus persicae*. Plant Cell Rep. **31**: 1981–1989.

Zhang, H.-M., Wheeler, S., Xia, X., Radchuk, R., Weber, H., Offler, C.E., and Patrick, J.W. (2015). Differential transcriptional networks associated with key phases of ingrowth wall construction in trans-differentiating epidermal transfer cells of *Vicia faba* cotyledons. BMC Plant Biol. **15**: 103.

Zhang, K., Halitschke, R., Yin, C., Liu, C.-J., and Gan, S.-S. (2013). Salicylic acid 3-hydroxylase regulates Arabidopsis leaf longevity by mediating salicylic acid catabolism. Proc. Natl. Acad. Sci. U. S. A. **110**: 14807–12.

Zhang, X., Liu, S., and Takano, T. (2008). Two cysteine proteinase inhibitors from *Arabidopsis thaliana*, AtCYSa and AtCYSb, increasing the salt, drought, oxidation and cold tolerance. Plant Mol. Biol. **68**: 131–143.

Zhang, X.D., Lu, C.H., and Guan, Z.Y. (2012b). Weakened cyclones, intensified anticyclones and recent extreme cold winter weather events in Eurasia. Environ. Res. Lett. **7**.

Zhang, Z., Zhang, H., Quan, R., Wang, X.-C., and Huang, R. (2009). Transcriptional regulation of the ethylene response factor LeERF2 in the expression of ethylene biosynthesis genes controls ethylene production in tomato and tobacco. Plant Physiol. **150**: 365–377.

Zhao, M., Liu, W., Xia, X., Wang, T., and Zhang, W.H. (2014). Cold acclimation-induced freezing tolerance of *Medicago truncatula* seedlings is negatively regulated by ethylene. Physiol. Plant. **152**: 115–129.

Zhou, S., Sun, H., Zheng, B., Li, R., and Zhang, W. (2014). Cell cycle transcription factor E2F2 mediates non-stress temperature response of AtHSP70-4 in *Arabidopsis*. Biochem. Biophys. Res. Commun. **455**: 139–146.

Zhu, X.G., Long, S.P., and Ort, D.R. (2010). Improving photosynthetic efficiency for greater yield. Annu Rev Plant Biol **61**: 235–261.

Zolla, G., Badri, D. V., Bakker, M.G., Manter, D.K., and Vivanco, J.M. (2013). Soil microbiomes vary in their ability to confer drought tolerance to *Arabidopsis*. Appl. Soil Ecol. **68**: 1–9.

Appendices

Appendix 1

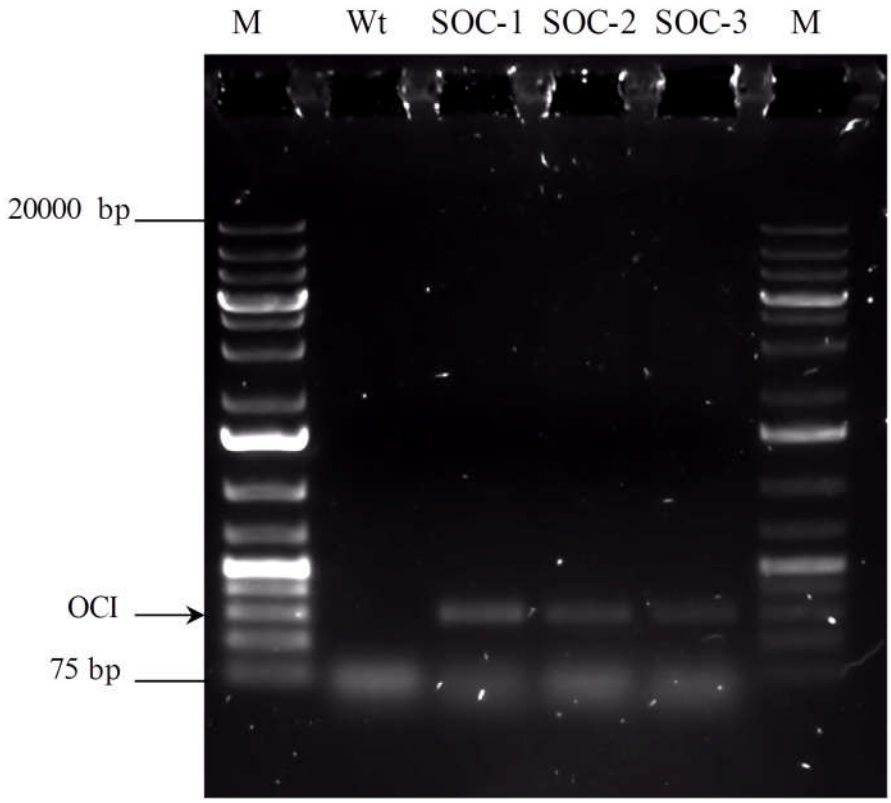

Agarose gel electrophoresis of products from a PCR amplification of OCI transgene in soybean. DNA was extracted from the leaf tissue of soybean Wt and 3 independent transgenic lines expressing the rice cysteine protease inhibitor oryzacystatin I: SOC-1, SOC-2, SOC-3. 5 µl of DNA was loaded per PCR reaction. Lane M contains ThermoScientific 1 kb+ gene ruler (6 µl, 1 µg/µl). Wt, SOC-1, SOC-2 and SOC-3 contains 6 µl of PCR mix. Gel consited of 1 % Agarose and was run at 80 V for 1h.

Appendix 2

List of SNP linkage markers used in genome sequence enrichment, chapter 6.

Chromosome I	Vf_Mt8g017240_001	**Chromosome II**	Vf_Mt5g024090_001
	Vf_Mt7g021530_001		Vf_Mt3g110630_001
19a15-3	Vf_Mt7g020850_001	AIGPa	Vf_Mt3g110600_001
LG018SNP	PGDH	LG102	Vf_Mt3g111210_001
Vf_Mt2g086560_001	Vf_Mt7g016650_001	RBPC_0SNP	Vf_Mt3g109330_001
Vf_Mt2g086880_001	Vf_Mt7g013300_001	AnMtL8	Vf_Mt3g109200_001
Vf_Mt2g086950_001	Vf_Mt7g010100_001	GLIP135	Vf_Mt3g108790_001
Vf_Mt2g089140_001	Vf_Mt7g013160_001	Vf_Mt3g116500_001	Vf_Mt3g108320_001
Vf_Mt2g093280_001	Vf_Mt7g080730_001	Vf_Mt3g116050_001	Vf_Mt3g108190_001
Vf_Mt2g098470_001	Vf_Mt5g041750_001	Vf_Mt3g115990_001	Vf_Mt3g108460_001
Vf_Mt2g097740_002	Vf_Mt2g088750_001	Vf_Mt3g116080_001	Vf_Mt3g108630_001
Vf_Mt2g097950_001	Vf_Mt5g039210_001	Vf_Mt3g115870_001	Vf_Mt3g108690_001
Vf_Mt2g098240_001	Vf_Mt5g039000_001	Vf_Mt3g114780_001	Vf_Mt3g108160_001
Vf_Mt2g098890_001		Vf_Mt3g114850_001	Vf_Mt3g107970_001

Vf_Mt3g072360_001

Vf_Mt3g072390_001

Vf_Mt3g072080_001

Vf_Mt3g071620_001

Vf_Mt3g070310_001

Vf_Mt3g065190_001

Vf_Mt3g064740_001

Vf_Mt3g031380_001

Vf_Mt3g031280_001

Vf_Mt3g061590_001

Vf_Mt3g031380_001

Vf_Mt3g031280_001

Vf_Mt3g061590_001

Vf_Mt3g061640_001

Vf_Mt3g060850_001

Vf_Mt3g055920_001

Vf_Mt3g055690_001

Vf_Mt3g052760_001

Vf_Mt3g051280_001

Vf_Mt5g075540_001

Vf_Mt5g075540_001

Vf_Mt3g026020_001

Vf_Mt3g020670_001

Vf_Mt3g019330_001

Vf_Mt3g017610_001

Vf_Mt3g008180_001

Vf_Mt3g008540_001

Vf_Mt3g010290_001

Vf_Mt3g010000_001

Vf_Mt3g005360_001

Vf_Mt3g005050_001

Vf_Mt4g006200_001

Vf_Mt4g005830_001

Vf_Mt4g007030_001

Vf_Mt4g009920_001

Vf_Mt4g010330_001

Chromosome III

cgP137FSNP

GLPSNP

LG038

REPSNP

BGALSNP

Vf_Mt1g116810_001

Vf_Mt1g116230_001

Vf_Mt1g050730_001

Vf_Mt1g116110_001

Vf_Mt1g114560_001

Vf_Mt5g042440_001

Vf_Mt1g045800_001

Vf_Mt1g044570_001

Vf_Mt4g080370_001

Vf_Mt1g056180_001

Vf_Mt1g064060_001

Vf_Mt1g061800_001

Vf_Mt7g100500_001

Vf_Mt1g071110_001

Vf_Mt1g072640_001

Vf_Mt1g072740_001

Vf_Mt1g073000_001

Vf_Mt1g075140_001

Vf_Mt1g075610_001

Vf_Mt7g035110_001

Vf_Mt1g079520_001

Vf_Mt1g080150_001

Vf_Mt1g079870_001

Vf_Mt1g079930_001

Vf_Mt1g081290_001

Vf_Mt1g082210_001

Vf_Mt1g083450_001

Vf_Mt1g083460_001

Vf_Mt1g083960_001

Vf_Mt1g085040_001

Vf_Mt1g087900_001

Vf_Mt1g086810_001

Vf_Mt1g088190_001
Vf_Mt1g089980_001
Vf_Mt1g094870_001
Vf_Mt1g012610_001
Vf_Mt1g014230_001
Vf_Mt1g013400_001
Vf_Mt1g016390_001
Vf_Mt1g017950_001
Vf_Mt1g018180_001
Vf_Mt1g018320_001
Vf_Mt1g018790_001
Vf_Mt1g019810_001
Vf_Mt1g019770_001
Vf_Mt1g021760_001
Vf_Mt1g021670_001
Vf_Mt7g059170_001
Vf_Mt1g025570_001
Vf_Mt1g025550_001
Vf_Mt1g025950_001

Vf_Mt1g025950_002
Vf_Mt1g026130_001

Chromosome IV

GLIP137
PPHSNP
13n10-1
CNGC4
PRATSNP
GLIP089
Vf_Mt4g133070_001
Vf_Mt3g118200_001
Vf_Mt3g118430_001
Vf_Mt3g117800_001
Vf_Mt3g118320_001
Vf_Mt4g124930_001
Vf_Mt4g124600_001
Vf_Mt4g124640_001

Vf_Mt4g124070_001
Vf_Mt4g122670_001
Vf_Mt4g121600_001
Vf_Mt4g121960_001
Vf_Mt4g118420_001
Vf_Mt4g114900_001
Vf_Mt4g113280_001
Vf_Mt3g077990_001
Vf_Mt4g095440_001
Vf_Mt8g066180_001
Vf_Mt8g073580_001
Vf_Mt8g074010_001
Vf_Mt8g061890_001
Vf_Mt7g070290_001
Vf_Mt8g011470_001
Vf_Mt8g012400_001
Vf_Mt8g012380_001
Vf_Mt8g014660_001
Vf_Mt8g018770_001

Vf_Mt8g020800_001
Vf_Mt8g022290_001
Vf_Mt8g022050_001
Vf_Mt8g022770_001
Vf_Mt8g023310_001
Vf_Mt4g090120_001
Vf_Mt8g087440_001
Vf_Mt7g038120_001
Vf_Mt8g030430_001
Vf_Mt7g076160_001
Vf_Mt8g038880_001
Vf_Mt8g039690_001
Vf_Mt8g040150_001
Vf_Mt8g040550_001
Vf_Mt8g030600_001
Vf_Mt8g030620_001
Vf_Mt8g032450_001
Vf_Mt8g041410_001
Vf_Mt8g043510_001

Vf_Mt8g061230_001
Vf_Mt8g021140_001
Vf_Mt8g061350_001
Vf_Mt8g058270_001
Vf_Mt8g008870_001
Vf_Mt8g006370_001

Chromosome V

AnMtS37
Vf_Mt2g101430_001
Vf_Mt7g031900_001
Vf_Mt2g104110_001
Vf_Mt2g104010_001
Vf_Mt2g101870_001
Vf_Mt7g108490_001
Vf_Mt7g078800_001
Vf_Mt7g073340_001
Vf_Mt7g073970_001
Vf_Mt7g075940_001
Vf_Mt7g078730_001
Vf_Mt7g079680_001
Vf_Mt7g079840_001
Vf_Mt7g080040_001
Vf_Mt7g080250_001
Vf_Mt7g081010_001
Vf_Mt7g114940_001
Vf_Mt7g115070_001
Vf_Mt7g116600_001
Vf_Mt7g117970_001
Vf_Mt7g118320_001

Chromosome VI

New_GLIP307SNP
HYPTE3SNP
Vf_Mt8g107140_001
Vf_Mt8g107640_001
Vf_Mt8g106690_001
Vf_Mt8g105250_001
Vf_Mt8g104520_001
Vf_Mt8g103840_001
Vf_Mt8g102840_001
Vf_Mt8g102920_001
Vf_Mt8g102770_001
Vf_Mt8g102250_001
Vf_Mt8g101390_001
Vf_Mt3g034100_001
Vf_Mt4g081050_001
Vf_Mt4g077840_001
Vf_Mt4g078200_001
Vf_Mt4g077610_001
Vf_Mt4g075200_001
Vf_Mt4g075050_001
Vf_Mt4g076990_001
Vf_Mt4g078660_001
Vf_Mt4g068010_001
Vf_Mt4g076870_001
Vf_Mt4g083970_001
Vf_Mt4g061670_001
Vf_Mt4g061070_001
Vf_Mt4g061010_001
Vf_Mt4g060940_001
Vf_Mt4g080100_001
Vf_Mt2g094640_001
Vf_Mt4g053880_001
Vf_Mt4g053270_001
Vf_Mt4g053250_001
Vf_Mt4g053520_001
Vf_Mt4g049540_001